University of Southampton

Faculty of Environmental and Life Sciences

School of Biological Sciences

The Antibacterial Efficacy of Disinfectants used for Infection Control

by

Daniel John Noel

ORCID ID: 0000-0001-8560-4441

Thesis submitted for the degree of Doctor of Philosophy

April 2023

Supervisors: Professor CW Keevil, Dr SA Wilks

University of Southampton

Abstract

Faculty of Environmental and Life Sciences

School of Biological Sciences

Thesis for the degree of Doctor of Philosophy

The Antibacterial Efficacy of Disinfectants used for Infection Control

By Daniel John Noel

Healthcare associated infections (HAIs) account for hundreds of millions of infections worldwide every year. Chemical disinfectants are relied upon globally as a primary method of infection control, with this dependence likely to be further reinforced with the continually rising prevalence of antimicrobial resistance. Mitigating the impact of HAIs will require making improvements to current infection control measures, which can only be made once potential limitations have been elucidated.

Concerns regarding the use of disinfectants have been raised in terms of bacterial tolerance development and the ability for bacteria to adopt various survival-related behavioural responses, such as the viable but nonculturable (VBNC) state. In addition, many commercial disinfectant products consist of formulations of multiple active antimicrobials, with the central axiom being that the presence of more mechanisms of action must enhance the efficacy of the product and mitigate bacterial tolerance development. However, little scientific research has been conducted interrogating these assumed beneficial interactions. This project aims to elucidate the aforementioned limitations associated with the use of chemical disinfectants that are commonly used as an infection control measure.

Synergistic interactions between disinfectants were found to be uncommon, species-dependant and on the threshold of the synergism classification, while *Klebsiella pneumoniae* was found to be able to develop tolerance to individual disinfectants and a combined disinfectant formulation through the acquisition of adaptations and induction into the VBNC state. Molecular mechanisms of tolerance to a range of common disinfectants were identified through a multi-omics approach, allowing the identification of novel mechanisms of disinfectant tolerance demonstrated by *K. pneumoniae*.

These data demonstrate that HAI-associated pathogenic bacteria are able to adapt to low-level disinfectant exposure, and disinfectant formulations provide minimal benefits over disinfectants used individually in terms of tolerance development and VBNC induction. These data highlight limitations regarding our understanding and attitudes towards the disinfectants which are relied upon heavily across the world every day.

Finally, this project marks the initial development of a novel methodology of direct VBNC quantification and isolation. Currently, VBNC research is limited and restricted by the highly flawed methods used, so further development of this promising novel methodology may provide new opportunities to expand our understanding of the VBNC state as a whole.

Contents

List of figures

List of tables

Declaration of authorship

I, Daniel John Noel, declare that this thesis and the work presented in it is my own and has been generated by me as the result of my own original research.

I confirm that:

1. This work was done wholly or mainly while in candidature for a research degree at this University;
2. Where any part of this thesis has previously been submitted for a degree or any other qualification at this University or any other institution, this has been clearly stated;
3. Where I have consulted the published work of others, this is always clearly attributed;
4. Where I have quoted from the work of others, the source is always given. With the exception of such quotations, this thesis is entirely my own work;
5. I have acknowledged all main sources of help;
6. Where the thesis is based on work done by myself jointly with others, I have made clear exactly what was done by others and what I have contributed myself;
7. Parts of this work have been published as:

   Noel DJ, Keevil CW, Wilks SA. 2021. Synergism versus Additivity: Defining the Interactions between Common Disinfectants. mBio. Vol. 12, Issue 5. DOI: https://doi.org/10.1128/mBio.02281-21

Signed:

Date: 13/04/2023

Acknowledgements

I would like to thank JVS Products Ltd and the National Institute for Health and Care Research for funding this work and making it possible.

I would also like to thank my supervisors Dr Sandra Wilks and Professor Bill Keevil for their endless guidance, advice, and feedback throughout the project. Additionally, thank you to Rob Scoones for his tireless enthusiasm towards the work, and for providing me with valuable insights into the commercial and regulatory side of chemical disinfectants.

I would like to express my gratitude to the many individuals that have contributed to the project by providing academic and technical expertise that enabled me to undertake a variety of techniques that otherwise would not have been possible. These individuals include Dr Anton Page, Dr Patricia Goggin and Dr Elizabeth Angus for their invaluable expertise and insights into the art of electron microscopy; Dr Rachel Owen and Dr Mark Willet for their knowledge and advice regarding flow cytometry and Dr Alistair Bailey, Dr Benjamin Nicholas, Mr Alex Lister, and Professor Paul Skipp for guiding me through the daunting field of proteomics. Each and every person listed has been incredibly patient, approachable, and kind.

Thank you to Dr Malissa Rahimi for her vital help minimising my workload in the lab during the stressful final months of writing.

A huge thank you to Dr Catherine Bryant and Dr Sandra Wilks for keeping me sane throughout my PhD. The project has been an incredibly enjoyable but challenging process, both academically and mentally. I thank them both for always being there throughout it all, putting up with me and constantly providing support. The project would not have been possible without their input. I cannot express how grateful I am.

I am incredibly lucky to have been able to undertake this process alongside dear friends. Thank you to Katie, Ben, and Michael for being there to celebrate the highs and commiserate the lows, and generally making the trials and tribulations of scientific research bearable. My overall experience has been a positive one, and that is in no small part because of them. May there be many more coffees, pints and dice rolls in the years to come.

Last, but not least, I would like to thank my family for their unwavering support every step of the way, and for doing a fantastic job of pretending to listen as I ramble on about bacteria (again). In particular I would like to thank my perfect wife Rachel for being there throughout it all. She inspires me every day, and I never would have made it through this without her.

List of abbreviations

Abbreviation	Definition
(p)ppGpp	Guanosine pentaphosphate
·OH	Hydroxyl free radicals
2-NBDG	2-Deoxy-2-[(7-nitro-2,1,3-benzoxadiazol-4-yl)amino]-D-glucose
A. baumannii	*Acinetobacter baumannii*
ADP	Adenosine 5'-diphosphate
AMP	Adenosine monophosphate
AMR	Antimicrobial resistance
AMRF	Antimicrobial Resistance Finder plus
ANNOVAR	Annotate Variation
ATP	Adenosine 5'-triphosphate
B. cereus	*Bacillus cereus*
BAC	Benzalkonium chloride
bp	Base pairs
BPR	Biocidal Products Regulations
Br	Bronopol-tolerant *Klebsiella pneumoniae* sample
BWA	Burrows-Wheeler Aligner
Bz	Benzalkonium chloride-tolerant *Klebsiella pneumoniae* sample
cAMP	Cyclic adenosine monophosphate
CASAVA	Consensus Assessment of Sequence And Variation
Cc	Chlorocresol-tolerant *Klebsiella pneumoniae* sample
CF	Carboxyfluorescein
CFDA	Carboxyfluorescein diacetate
CFSE	Carboxyfluorescein succinimidyl ester
CFU	Colony forming unit
CI	Confidence interval
CLSI	Clinical Laboratory Standards Institute
COVID-19	Coronavirus disease 2019
CPD	Cell Proliferation Dye eFluor 670
CTC	5-cyano-2,3-ditolyl tetrazolium chloride
Da	Daltons
DAPI	4',6-diamidino-2-phenylindole
DAVID	Database for Annotation, Visualization and Integrated Discovery
Dd	Didecyldimethylammonium chloride-tolerant *Klebsiella pneumoniae* sample
DDAB	Didecyldimethylammonium bromide
DDAC	Didecyldimethylammonium chloride
DEB	Dey-Engley neutralising broth
DMSO	Dimethyl sulphoxide
DNA	Deoxyribonucleic acid
DVC	Direct viable count
E. coli	*Escherichia coli*
E. faecalis	*Enterococcus faecalis*
EMA	Ethidium monoazide

EPA	Environmental Protection Agency
EPS	Extracellular polymeric substance
EUCAST	European Committee on Antimicrobial Susceptibility Testing
FACS	Fluorescence-activated cell sorting
FDA	Food and Drug Administration
FDR	False discovery rate
FIC	Fractional inhibitory concentration
FICI	Fractional inhibitory concentration index
FSC H	Forward scatter pulse height
GATK	Genome analysis toolkit
GMP	Guanosine monophosphate
GO	Gene ontology
GTP	Guanosine triphosphate
H_2O_2	Hydrogen peroxide
HAI	Healthcare associated infection
ICU	Intensive care unit
IMP	Inosine monophosphate
InDel	Insertion/deletion of ≤ 50 base pairs (bp) in length
K. pneumoniae	*Klebsiella pneumoniae*
KEGG	Kyoto Encyclopedia of Genes and Genomes
L. monocytogenes	*Listeria monocytogenes*
L-Ara4N	4-amino-4-deoxy-L- arabinose
live/dead	LIVE/DEAD™ BacLight™
LPS	Lipopolysaccharides
LTA	Lipoteichoic acid
MHA	Mueller Hinton agar
MHB	Mueller Hinton broth
MIC	Minimum inhibitory concentration
MOA	Mechanism of action
MRSA	Methicillin-resistant *Staphylococcus aureus*
NADH	Nicotinamide adenine dinucleotide
NADP	Nicotinamide adenine dinucleotide phosphate
NDM	New Delhi metallo-β-lactamases
NMR	Nuclear magnetic resonance
OD	Optical density
P. aeruginosa	*Pseudomonas aeruginosa*
pBLAST	protein Basic Local Alignment Search Tool
PBS	Phosphate-buffered saline
PCR	Polymerase chain reaction
PE	Proliferation exclusion
PG	Phosphatidylglycerol
Ph	Polyhexamethylene biguanide-tolerant *Klebsiella pneumoniae* sample
PHMB	Polyhexamethylene biguanide
PI	Propidium iodide
PIPES	Piperazine-N,N'-bis(2-ethanesulfonic acid)
PMA	Propidium monoazide

ppGpp	Guanosine tetraphosphate
PPK1	Polyphosphate kinase 1
QAC	Quaternary ammonium compound
qPCR	Quantitative polymerase chain reaction
RNA	Ribonucleic acid
RND	Resistance-nodulation-division
ROS	Reactive oxygen species
S. aureus	*Staphylococcus aureus*
S. enterica	*Salmonella enterica*
S. Typhimurium	*Salmonella enterica* serovar Typhimurium
SARS-CoV-2	Severe acute respiratory syndrome coronavirus 2
SASP	Small acid-soluble spore protein
SDS	Sodium dodecyl sulphate
SEM	Scanning electron microscopy
SNP	Single nucleotide polymorphism
spp.	Species
SQ	Disinfectant formulation "SQ53"-tolerant *Klebsiella pneumoniae* sample
SQ53	Disinfectant formulation "SQ53"
SSC A	Side scatter pulse area
SSC H	Side scatter pulse height
TEM	Transmission electron microscopy
TNT	2,4,6-trinitrotoluene
Tris	Tris(hydroxymethyl)aminomethane
UDP-L-Ara4FN	Uridine diphosphate-L-4-formamido-arabinose
UMP	Uridine monophosphate
VBNC	Viable but nonculturable
VCF	Variant call format
WHO	World Health Organisation

List of definitions

Term	Definition
Additivity	An antimicrobial interaction characterised by the activity of both components combined being no greater than the sum of the activities of each component individually.
Antagonism	An antimicrobial interaction characterised by the activity of both components combined being less than to the activity of the most active component individually.
Antibacterial	A substance or mixture that contains or generates active substances that destroy, deter, prevent the action of, or exert a controlling effect on bacteria.
Antibiotic	A substance (or a chemical derivative) that is produced by a microorganism that selectively inhibits or kills other microorganisms
Antimicrobial	A substance or mixture that contains or generates active substances that destroy, deter, prevent the action of, or exert a controlling effect on microorganisms.
Antiseptic	A substance that inactivates or destroys microorganisms on living tissue. A sub-category of antimicrobials.
Biocide	A substance or mixture that contains or generates active substances that destroy, deter, prevent the action of, or exert a controlling effect on any harmful organism.
Disinfectant	A substance or mixture that contains or generates active substances that destroy, deter, prevent the action of, or exert a controlling effect on microorganisms, excluding cleaning products that have an unintentional biocidal effect, such as washing up liquids.
Frameshift	Refers to a type of insertion/deletion (InDel) mutation, whereby the mutation leads to a shift in the open reading frame.
Healthcare associated infections (HAI)	Infections acquired by patients while receiving medical treatment.
Indifference	An antimicrobial interaction characterised by the activity of both components combined being equal to the activity of the most active component individually
Insertion/Deletion (InDel)	A mutation characterised by a sequence insertion or deletion that is ≤ 50 base pairs in length
Minimum inhibitory concentration (MIC)	The lowest concentration of antimicrobial that completely inhibited bacterial growth.
Non-frameshift	Refers to a type of insertion/deletion (InDel) mutation, whereby the mutation does not shift the open reading frame.
Non-synonymous	Refers to a type of single nucleotide polymorphism (SNP) mutation, whereby the substituted nucleotide leads to a change in the amino acid sequence.
Preservative	Substances that prevent the replication of microorganisms. Used in the food and medical industries to prevent microbial contamination of consumables and medicines.
Single nucleotide polymorphism (SNP)	A mutation characterised by the substitution of a single nucleotide for another.

Sterilising agent	Substances that completely destroy all microorganisms, including spores.
Stop gain/loss	A mutation that leads to the introduction or deletion of stop codon.
Synergy	An antimicrobial interaction characterised by the activity of both components combined being greater than the sum of the activities of each component individually.
Synonymous	Refers to a type of single nucleotide polymorphism (SNP) mutation, whereby the substituted nucleotide does not lead to a change in the amino acid sequence.
Tolerance	An increased ability for a given bacterial population or sample to survive a given antimicrobial.
Viable but nonculturable (VBNC)	Bacteria that are viable but unable to be cultured on routine bacteriological media.

1. Literature Review

1.1. Healthcare associated infections

Healthcare associated infections (HAIs) are infections acquired by patients while receiving medical treatment [1], [2]. This has superseded former terms such as "hospital-acquired infections" or "nosocomial infections" as the spread of HAIs occurs in all healthcare environments, not just hospitals [2]. HAIs are responsible for hundreds of millions of infections worldwide every year, and are the most common adverse event during the delivery of health care [2]. It is estimated that 30% of patients admitted into an intensive care unit (ICU) will acquire one or more HAI in more economically developed countries [3], while in developing countries the HAI frequency in ICUs is at least 2-3 fold higher [2]. The average HAI acquisition rate at any given time across all hospitalised patents in Europe is 7.1% [4], rising to 15.5% in developing countries [2].

The pathogens that cause HAIs can be bacteria, viruses or fungal parasites [5]. Relative prevalence levels of each pathogen vary depending on the region and patient population, however it has been estimated that viruses account for approximately 5% of all nosocomial infections [6], while bacteria are the underlying cause for the overwhelming majority of cases [5].

Various bacterial species are commonly associated with HAIs, with the most frequently reported HAIs in European ICUs being caused by *Staphylococcus aureus* (21.8%), enterobacteriaceae spp. (excluding *Escherichia coli*) (20.2%), *Pseudomonas* spp. (17.2%), enterococci (10.0%), *E. coli* (9.1%), and *Acinetobacter* spp. (5.1%) according to a World Health Organization (WHO) meta-analysis [2]. Estimates of HAI-causative bacterial species in USA hospitals follow a similar distribution [7], [8], while enterobacteriaceae spp. (excluding *E. coli*) and *Acinetobacter* spp. were found to be the most prevalent HAIs associated with high-risk patients in a meta-analysis of prevalence in developing countries, accounting for 20% and 19% of identified species respectively [9].

1.1.1. Characteristics of bacteria responsible for healthcare associated infections

Bacteria are single-celled prokaryotic microorganisms that form one of the three domains of life, and display immense genetic and phenotypic diversity [10]. Bacteria can be characterised by their distinctive morphologies including rods, cocci, spiral or lancet (pointed) shapes, and are often found in pairs or groups such as pairs or chains [11]. Bacterial DNA is found as a single circular

chromosome in a central nuclear body called the nucleoid, as prokaryotes lack descrete membrane-bound cytoplasmic organelles [11]. As a result of this, many of the functions carried out by organelles in eukaryotic organsisms are instead performed by the plasma membrane in bacteria [11], making this a key structure for maintaining the viability of a bacterial cell. Some bacteria also contain separate small circular DNA molecules called plasmids, which they are capable of acquiring or exchanging. Other common surface structures include flagella and fimbriae, responsible for motility and surface adhesion, respectively [11].

The most common categorisation of bacterial species is by their cell surface structure, as identified by the Gram staining procedure [12]. The surface of bacterial cells is the first point of contact for antimicrobial molecules when they contact bacteria, and can be either a barrier that must be traversed in order to reach an intracellular target site, or may even be the target site itself. As a result, understanding the different categories of bacterial cell surface structure is of critical importance to understanding the activity of antimicrobials. The two categories of bacterial cell surface structure are Gram positive and Gram negative, as discussed below.

1.1.1.1. Gram-positive bacteria

S. aureus and bacteria of the enterococci genus are examples of Gram-positive bacteria. These cells consist of a single cytoplasmic membrane and a thick cell wall consisting primarily of peptidoglycan and negatively-charged lipoteichoic acid (LTA) that protrudes from the outer leaflet of the cytoplasmic membrane (see Figure 1b) [13], [14]. The cell wall also consists of teichoic acid within its structure (Figure 1b) [13], [14]. These teichoic acids provide a net negative charge at the outside surface of Gram-positive cells. The periplasm of Gram-positive bacteria has a smaller volume than that of Gram-negative bacteria.

1.1.1.2. Gram-negative bacteria

Gram-negative bacteria consist of a thin peptidoglycan layer located between two membrane layers, the plasma membrane and the outer membrane. The cell wall does not contain anionic teichoic acids, however the outer membrane does contain anionic LPS in the outer leaflet (see Figure 1a) [13], which provides a net negative charge to the outer leaflet of the outer membrane Gram-negative bacteria. The presence of LPS on the outer leaflet of the outer membrane of Gram-negative bacteria act as a barrier that prevent hydrophobic molecules accessing the membrane, which they would otherwise be able to cross to the cell interior [15].

While hydrophobic molecules can pass through membranes, the outer membrane acts as a permeability barrier to hydrophilic molecules. This gives Gram-negative bacteria an additional

degree of control over what molecules diffuse in and out of the periplasm, and in turn the cytoplasm of the cell. Porins are proteins formed of beta-barrels that perforate the outer membrane and are able to selectively allow certain low molecular weight molecules (usually 600 Daltons (Da) or less) into the periplasm (see Figure 1a) [16]. As a result they regulate outer membrane permeability, and can prevent or limit the ability for disinfectants to reach the inner layers of the cell [15].

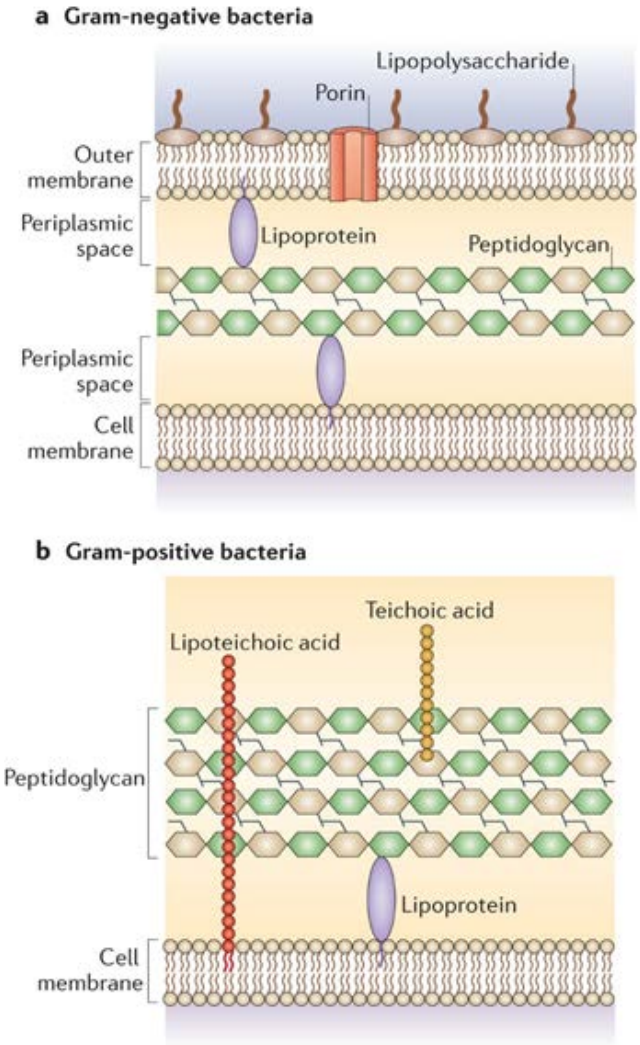

Figure 1. Schematic diagrams of the envelope structures of Gram-negative and Gram-positive bacteria. a) The cell surface structure of Gram-negative bacteria. The blue region at the top of the diagram is extracellular space. The yellow region between the two membranes is the periplasm. The region below the cell membrane is the cytoplasm of the cell. Characteristic structures are labelled accordingly. b) The cell surface structure of Gram-positive bacteria. The yellow region is extracellular space. The blue region below the cell membrane is the cytoplasm of the cell. Characteristic structures are labelled accordingly. Adapted with permission from Brown, L., Wolf, J., Prados-Rosales, R. *et al.* Through the wall: extracellular vesicles in Gram-positive bacteria, mycobacteria and fungi. Nat Rev Microbiol 13, 620–630 (2015). https://doi.org/10.1038/nrmicro3480 [17].

1.2. Overview of infection control measures

With such widespread prevalence of HAIs, it is important to understand the infection control measures and practices that are currently employed, with the view that any improvements would aid in mitigating the impact of HAIs. As of 2018, Schreiber *et al.* published a meta-analysis of HAI mitigation studies that estimated that 35%-55% of all HAIs are preventable with the application of evidence-based infection control strategies, irrespective of the economic development of the country [18]. With this in mind it is clear that improvements to infection control methods can save lives.

However, the identification of novel improvements to infection control strategies first requires an understanding of the current measures. In this section the various common infection control measures are overviewed, and key limitations are highlighted.

1.2.1. Behavioural controls

The most obvious, simple, cheap, and effective infection control measure is behavioural controls, which include hand washing, using personal protective equipment (for example gloves and face masks), aseptic technique and conforming to disinfection practices [19]–[21]. When implemented appropriately, proper behavioural controls have repeatedly been shown to reduce the prevalence of HAIs by up to 84% in studies conducted across the world [22]–[25].

However, the crucial issue with behavioural controls is the willingness of medical professionals and hospital visitors to comply with guidance. A systematic review of 96 studies that investigated hand hygiene compliancy rates in hospitals located in economically developed countries concluded that the overall median compliancy rate for healthcare professionals was as low as 40% [26]. This statistic was 32% and 48% for physicians and nurses respectively, and there was a lower hand washing compliancy rate before coming into contact with a patient (21%) rather than after (47%) [26]. This highlights that even in countries with more established healthcare systems and higher levels of education the compliancy rates of healthcare professionals is still alarmingly low.

1.2.2. Disinfectants

Disinfectants are chemical or physical agents that kill or otherwise inactivate microorganisms, and are routinely used alongside behavioural controls in order to control the spread of infection. There are multiple terms that are often used synonymously when describing disinfectants and other types of antimicrobials. For clarity, the terms to be used within this thesis are defined and distinguished below.

Under the EU Biocide Regulations, a biocide is defined as a substance or mixture that contains or generates active substances that destroy, deter, prevent the action of, or exert a controlling effect on any harmful organism [27]. Antimicrobials are a broad subset of biocides that kill or inhibit the growth of microorganisms, while antibacterials are antimicrobials with activity against bacteria specifically [28]. Disinfectants are a sub-type of antimicrobials that exclude cleaning products that do not have an intentional biocidal effect, such as washing up liquids [27]. Finally, an antibiotic is a substance (or a chemical derivative) that is produced by a microorganism that selectively inhibits or kills other microorganisms [28].

In healthcare environments disinfectants are most commonly used in hand sanitisers, surface sprays and wipes [29]. They are a critical infection control measure that are depended on globally both within and outside of healthcare environments. However, there are limitations associated with their use, including lack of compliance to infection control guidance (as discussed in Chapter 1.2.1), phenotypic or behavioural adaptation and genetically-acquired tolerance. As this thesis focuses on the topic of disinfectants as a disinfection control measure, the various types of disinfectants, mechanisms of action and limitations are comprehensively overviewed separately in Chapters 1.3, 1.4 and 1.5.

1.2.3. Antimicrobial surfaces

Bacteria are found ubiquitously in our environment, with inanimate surfaces providing a reservoir capable of harbouring bacteria. Despite our best efforts contaminated surfaces present a cross-contamination risk in hospitals and healthcare environments [30]–[33]. HAI-associated pathogenic species including *S. aureus* [30]–[32], *Klebsiella pneumoniae* [31], [32], *Acinetobacter baumannii* [31], [32] and *Pseudomonas aeruginosa* [32] have been isolated from a variety of hospital surfaces including floors [32], door handles [31], [32], bed rails [30], [31] and mobile phones [33].

If bacteria deposited on surfaces are rendered non-viable, then they will be unable to be transmitted further and cause HAIs. Chemical disinfectants are used upon inanimate surfaces in an attempt to achieve bacterial deactivation, however this is limited to cleaning routines as constant cleaning of all surfaces is not practical. However, if a given surface was intrinsically antimicrobial a constant bacterial deactivation could be achieved.

Certain raw materials, such as copper [34] or silver [35], are known to demonstrate antimicrobial properties, so it has been proposed that such materials could be utilised and installed in healthcare facilities [36] and health care products [37] in order to reduce the cross-contamination risk. Other antimicrobial surfaces are being investigated that rely upon a variety of mechanisms

such as “contact-killing”, the release of antimicrobial agents or simply through preventing bacterial adhesion to the surface [38].

However, currently there are a variety of challenges in the field of antimicrobial surfaces. In brief, these include the stability and longevity of the surfaces and their antimicrobial properties, controlling the release of the active agent by surfaces that rely on antimicrobial release mechanism and a lack of mechanistic multi-functionality leading to limitations in efficacy [39].

As a result of these factors, the potential of antimicrobial surfaces as an additional infection control measure is yet to be fully realised or implemented. Nonetheless, their future use in healthcare settings will no doubt demonstrate a beneficial impact on mitigating the prevalence of HAIs.

1.3. The use of disinfectants as an infection control measure

1.3.1. Classification of antimicrobials by application

Before discussing disinfectants specifically, it is important to first distinguish between disinfectants and other types of antimicrobials, such as preservatives or sterilising agents. Due to the varying properties of antimicrobial agents, some provide advantages over others when applied to certain functions. Thus, antimicrobials are often classified by the function that they are applied to. For the purpose of this thesis the various applications of antimicrobials are defined as follows.

Antibiotics are substances that are produced by a microorganism to selectively inactivate or destroy other microorganisms [28], [40]. Due to antibiotics generally being selective toxic towards bacteria and not eukaryotic cells, antibiotics are widely used in the treatment of internal bacterial infections and diseases in medicine and agriculture.

Antiseptics are substances that inactivate or destroy microorganisms on living tissue [40], [41], and are see widespread use in health care. Examples include hand rubs and sanitisers.

S**terilisers** are substances that completely destroy all microorganisms, including spores [40], [41]. In medical settings, sterilisers and sterilisation methods are commonly used on critical items such as surgical equipment and medical implants [42].

Disinfectants directly or indirectly generate active substances that destroy, deter, prevent the action of, or exert a controlling effect on any harmful organism [27]. Cleaning products that are not intentionally biocidal are not included under this definition [27]. In addition, disinfectants are not necessarily sporicidal [40], [41]. Disinfectants are used on various items medical equipment and environmental surfaces in medical settings [42]. Both disinfectants (e.g. phenol-derivatives, aldehydes) and sterilisers (e.g. ethylene oxide, ozone) are often toxic, so are not typically used on living tissue. Instead, they are commonly used for the disinfection of inanimate objects [41].

Preservatives (e.g. benzoates, sorbates) prevent the replication of microorganisms and are used in the food and medical industries to prevent microbial contamination of consumables and medicines [41].

For clarity, it should be noted that many of these terms can also be applied to procedures in addition to agents and substances. For example, autoclaving and canning are examples of

sterilisation and preservation, respectively. However, this work focuses on chemical agents, so these physical procedures are not discussed further.

In addition, it is important to note that the majority of antimicrobial compounds have multiple applications, often depending on concentration. For example, ethanol can be used as an antiseptic, sanitiser, disinfectant or preservative, but not as a steriliser [41]. However, all of the antimicrobial agents discussed from hereon have the common functionality of being utilised as disinfectants (Table 1). Therefore, to simplify discussion and prevent unnecessary confusion, this work will hereby refer to these antimicrobial agents as "disinfectants", unless they are not utilised as such. Despite this, it is important to remember that the various disinfectants can be applied to other functions, as overviewed in Table 1.

1.3.2. Classification of disinfectants by mechanism of action

The mechanism of action (MOA) of disinfectants typically enables them to be effective against multiple types of microorganisms. However, as bacterial infections account for the overwhelming majority of HAIs [5], [6] this thesis focuses on the antibacterial action of disinfectants. Depending on the MOA, antibacterial disinfectants can prevent the growth of bacteria (bacteriostatic) or can completely kill bacteria (bactericidal). The MOA of many antimicrobial agents can be either bacteriostatic or bactericidal depending on the exposure concentration [43].

Typically, the MOAs of disinfectants affect a broad range of target sites within bacterial cells. This is in contrast to antibiotics for example, which typically have very specific target sites. As a result, the broad MOAs of disinfectants can have off-target affects, often causing irritability or toxicity. The varying mechanisms that underpin disinfectants leads to large variations in their efficacy both relative to each other and relative to different target organisms. As a result of this it is important to understand the mechanisms that underpin the antimicrobial activity of disinfectants to ensure they are utilised safely and appropriately. The following section describes our current understanding of the MOAs of many of the most commonly available classes of disinfectants and discusses their applications in health care. A summary of the properties of the disinfectants discussed is displayed in Table 1.

1.3.2.1. Alcohols

Alcohols are widely used as antiseptics, disinfectants and preservatives due to their broad-spectrum activity against bacteria, mycobacteria, fungi and viruses [41]. The mechanism of action is thought to be primarily due to the perturbation of membrane function [44]–[46], and also

through the denaturation of proteins and subsequent disruption of cellular functions [41], [47], [48]. The hydroxyl group present in alcohols is able to form hydrogen bonds, which allows them to interfere and substitute with the hydrogen bonds that maintain the structural integrity of proteins. As a result, the proteins lose their conformational shape and denature; inhibiting their functionality [47]. Alcohols are able to prevent sporulation [49]. However, as this has been shown to be reversible [50] they are primarily used for disinfecting surfaces and as antiseptics, and not used for sterilisation of critical medical equipment [29].

The effectiveness of alcohol as an antimicrobial is heavily dependent on its concentration. For example the effectivity of ethanol is significantly lower at concentrations below 50%, with an optimal antimicrobial range between 60% and 90% [51].

An issue with the use of alcohols as an antimicrobial is the readiness by which they vaporise, making extended exposure times challenging [29], [52]. Furthermore, alcohol can damage various surfaces if routinely used, such as rubber or plastic [53], and it is also a skin and eye irritant [29]. Some of these shortcomings can be overcome by the addition of other agents to formulations, for example hand sanitisers often contain emollients and skin conditioning agents.

1.3.2.2. Aldehydes

Disinfectants of the aldehyde class contain the aldehyde functional group, characterised by a carbon atom covalently bound to a hydrogen and an oxygen atom, the latter via a double bond. Aldehyde functional groups readily react with the primary and secondary amine functional groups, leading to their alkylation. Amine functional groups are abundant in protein structures [54] and the nitrogenous bases in deoxyribonucleic acid (DNA) [55]. As the structures of proteins and DNA are directly associated with their function, alkylation has a negative impact on functionality, and results in preventing cells from undertaking essential functions [41]. The two most prevalent aldehydes used for disinfection are glutaraldehyde and formaldehyde.

Glutaraldehyde consists of two aldehyde groups connected by three carbons. Glutaraldehyde has been shown to inhibit the functionality of dehydrogenases [56], transport machinery [41] protein synthesis and both DNA and ribonucleic acid (RNA) synthesis [57]. The flexible carbon chain between the two functional groups reflects a similar spacing between reactive groups in biological structures, allowing the glutaraldehyde to cross-link two groups and impede functionality [54]. However, the ability of glutaraldehyde to penetrate bacterial spores is limited [58], so high concentrations are required to exert a sporicidal effect on the outer spore layers [41]. Glutaraldehyde is used as a disinfectant and, at higher concentrations, a sterilising agent [41].

Formaldehyde simply consists of a single aldehyde functional group. The principles behind the MOA remain the same however, relying on impeding functionality of macromolecular structures as a result of the alkylation of thiol groups [54], [59]–[61]. The smaller size of formaldehyde allows for quicker cellular penetration, allowing it to more readily penetrate and kill bacterial spores, and allowing it to be used as both a disinfectant and sterilising agent [29]. Both glutaraldehyde and formaldehyde are used as fixative agents in electron microscopy.

Aldehydes are not selectively toxic towards bacteria, and will readily react with functional groups in macromolecules in eukaryotic and prokaryotic cells alike [54], [55], [59], [60]. Therefore aldehydes are known to be irritant, harmful and carcinogenic due to their ability to cross-link DNA [29], [55]. As a result, they are not used as antiseptics.

1.3.2.3. Biguanides

Many antimicrobials, such as chlorhexidine and polyhexamethylene biguanide (PHMB), contain the biguanide functional group. The nitrogen-rich biguanide functional groups are cationic, causing the disinfectant to have a high affinity to the negatively charged outer surface of bacteria, with maximum chlorhexidine uptake into *E. coli* and *P. aeruginosa* occurring in as little as 20 seconds [62]. Once localised to this region, the disinfectant is attracted to anionic sites in the cell wall and outer leaflet of the cell membrane, particularly anionic lipids phosphatidylglycerol (PG) and di-PG [63], [64]. This leads to the displacement of divalent cations, leading to disruption of lipid organisation which results in a reduction in membrane integrity, and an increase in membrane permeability [43], [64], [65]. This in turn leads to a loss of membrane potential and proton motive force, loss of adenosine 5'-triphosphate (ATP) production and a bacteriostatic effect [66]–[68]. At higher concentrations biguanides are capable of completely disrupting the structural integrity and functionality of membranes, leading to the precipitation and eventual loss of intracellular components [68]. A diagram depicting the MOA of chlorhexidine on bacterial membranes can be seen in Figure 2.

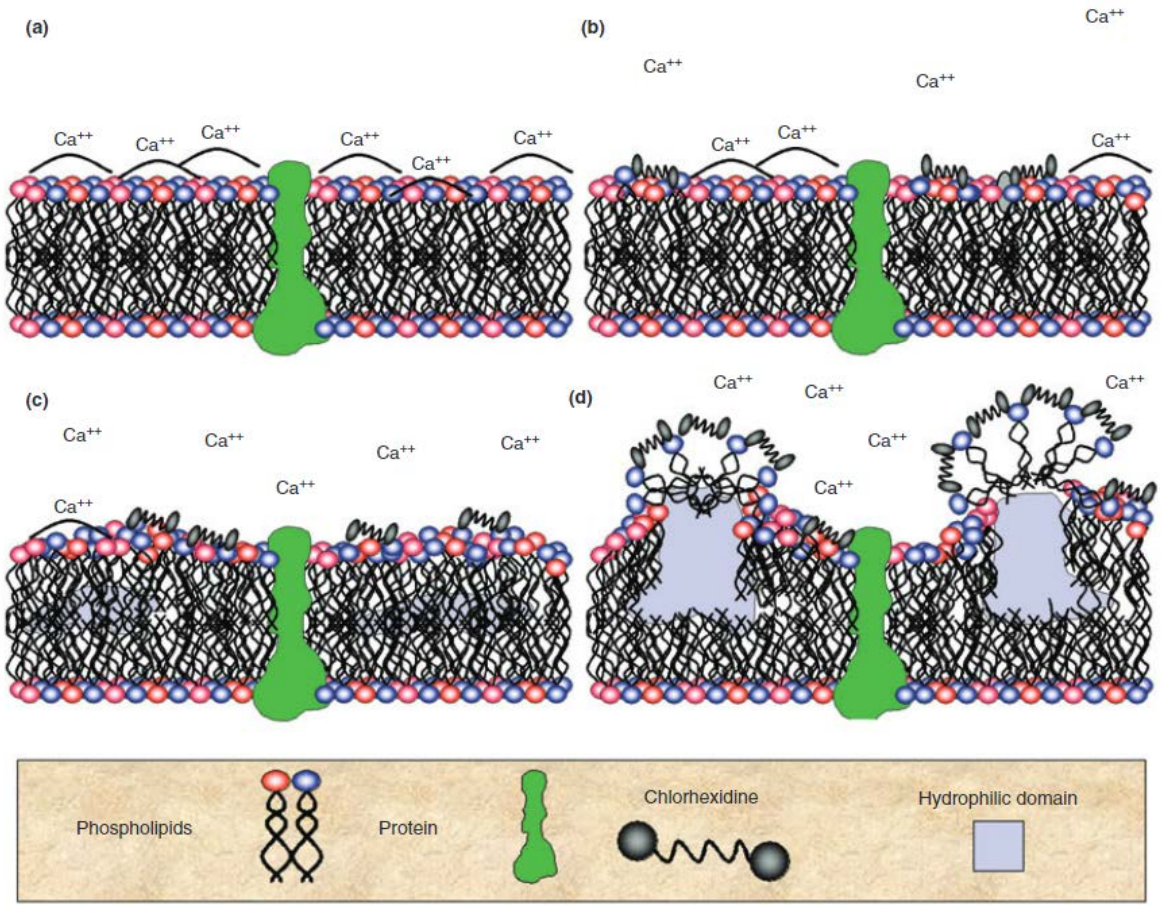

Figure 2. Diagram depicting the mechanism of action of chlorhexidine on bacterial membranes. a) The outer membrane of a bacterial cell, formed from two layers of phospholipids containing membrane proteins. The other leaflet typically has a net negative charge, which is stabilised by cationic calcium ions. b) Cationic chlorhexidine has a high affinity to the negatively charged outer leaflet of the bacterial cell, causing the displacement of associated calcium cations. c) The displacement of cations leads to the disruption of outer leaflet organisation and the formation of internal hydrophilic domains. d) The reduction in membrane integrity leads to an increase in membrane permeability and loss of proton motive force, causing a bacteriostatic effect. Adapted with permission from: P. Gilbert and L. E. Moore, "Cationic antiseptics: diversity of action under a common epithet," J. Appl. Microbiol., vol. 99, pp. 703–715, 2005. [64]

Biguanides can also exist in a polymer form, known as polyhexamethylene biguanide (PHMB) or polyhexanide. PHMB has been shown to act in a manner similar to chlorhexidine and other biguanides, whereby the molecule rapidly associates to anionic lipids of bacterial membranes as a result of electrostatic attraction [63], [69], [70], and also to lipopolysaccharides (LPS) and peptidoglycan cell wall components [64]. Initial interactions of PHMB have been hypothesised to concentrate around integral membrane proteins due to increased charge density and stronger electrostatic interaction, leading to changes in the lipid environment and consequent loss of function of these proteins [64]. In addition, the chain-like polymer sequence of guanide functional groups leads to the sequestering of anionic lipids into discrete domains, causing breaches in the permeability barrier [63], [71], [72] and eventual phase separation [64]. A diagram depicting the membrane-active MOA of PHMB on bacterial membranes can be seen in Figure 3.

However, research conducted by Chindera *et al.* (2016) observed fluorescein isothiocyanate-tagged PHMB entering into the cytoplasm of bacterial cells rather than accumulating at the surface [73]. Furthermore, the DNA of bacteria was observed to condense, leading the authors to hypothesise that the MOA of PHMB is not reliant on membrane disruption, and instead enters bacterial cells and condenses DNA, arresting cell division [73]. Recent molecular dynamics simulations have suggested that PHMB is able to translocate the membrane through bonding to anionic lipids, and forms extensive interactions with DNA [74].

The authors of these studies suggest that the MOA of PHMB is unlikely to operate via membrane disruption, despite the prior evidence to the contrary [69], [71], [72]. Given the evidence of both mechanisms occurring, it is therefore more probable that both mechanisms occur simultaneously. Membrane perturbation facilitates further PHMB uptake, leading to the condensing of DNA and arresting cell growth and division. However, the exact mechanism remains to be fully elucidated.

Biguanides are not sporicidal, potentially due to an inability to penetrate spores [75], [76]. However they do offer a comparatively low level of irritation on human skin, and can remain active long after administration, unlike more volatile alcohol-based antiseptics [41]. As a result, biguanides are widely used as antiseptics and disinfectants.

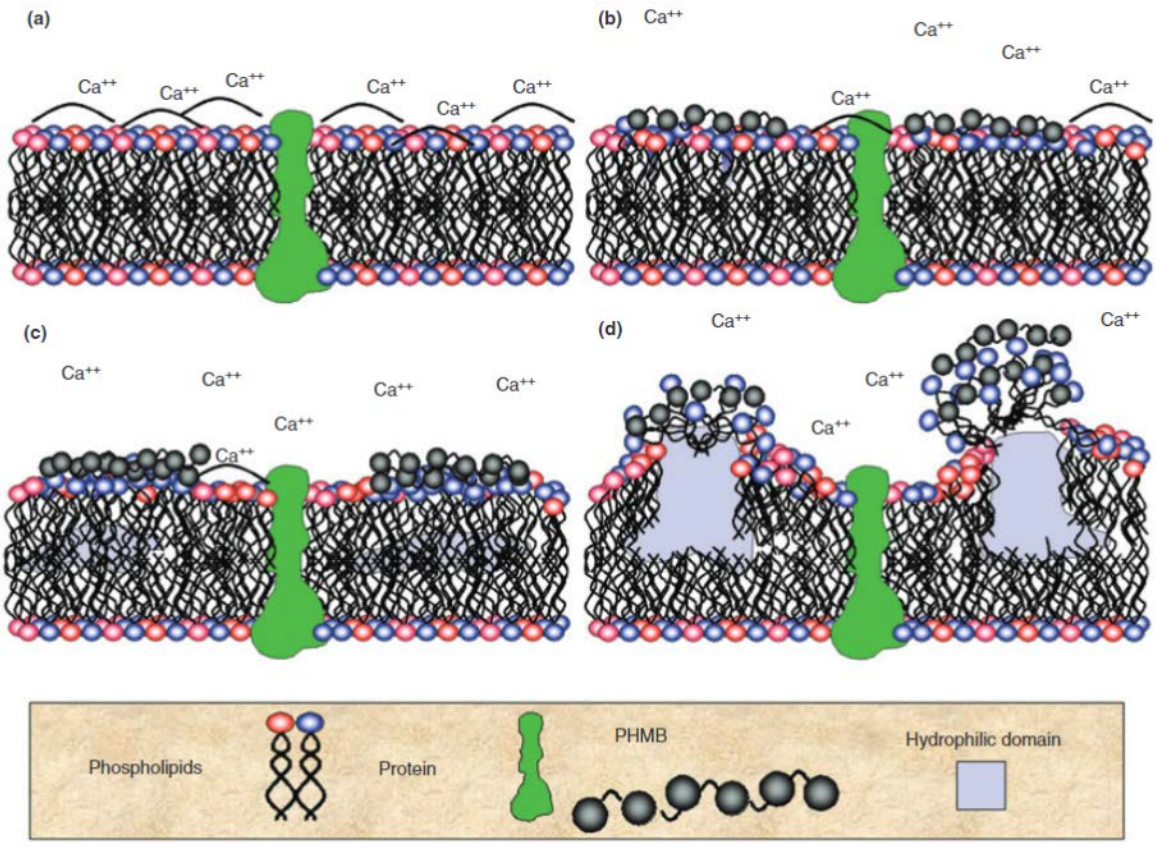

Figure 3. Diagram depicting the membrane-active mechanism of action of polyhexamethylene biguanide (PHMB) on bacterial membranes. a) The outer membrane of a bacterial cell, formed from two layers of phospholipids containing membrane proteins. The other leaflet typically has a net negative charge, which is stabilised by cationic calcium ions. b) The cationic moieties along the chain of PHMB have a high affinity to the negatively charged outer leaflet of the bacterial cell, causing the displacement of associated calcium cations. c) The displacement of cations and sequestering of anionic lipids leads to the disruption of outer leaflet organisation and the formation of internal hydrophilic domains. d) The formation of anionic lipid domains triggers the formation of protrusions from the membrane known as "blebs". The reduction in membrane integrity leads to an increase in membrane permeability and eventual phase separation. Adapted with permission from: P. Gilbert and L. E. Moore, "Cationic antiseptics: diversity of action under a common epithet," J. Appl. Microbiol., vol. 99, pp. 703–715, 2005. [64]

1.3.2.4. Halogen-releasing agents

Some antimicrobial agents operate via the release of halogens, for example chlorine or iodine. When chlorine is exposed to water it reacts to form hypochlorous acid, which can in turn form hypochlorite ions, depending on the pH [41]. Hypochlorous acid is a strong oxidising agent that is able to react with and disrupt macromolecular structures, which leads to impeded functionality. It has been demonstrated to have a major influence on DNA synthesis [77], protein synthesis [77], membrane stability [77], membrane transport functionality [78] and oxidative phosphorylation [79]. Chlorine-releasing agents are considered sporicidal at higher concentrations [80] depending on the pH [64], so are therefore used as surface disinfectants [29]. In hospital settings chlorine is often used to disinfect blood and body fluid spills, and is more broadly used for water treatment [29].

Iodine, although less reactive than chlorine, is a very quick and effective antimicrobial, even at low concentrations. The mechanism of action remains relatively unclear, however it is likely that iodine penetrates bacteria and reacts with functional groups in the various cellular structures, such as the thiol-containing amino acids methionine and cysteine [29], [41]. The latter amino acid plays a key role in the integrity of protein structure as it forms disulphide bonds, which are key for the secondary, tertiary and quaternary structural stability of proteins. Thus, impacts on disulphide bonds cause major conformational changes and will therefore heavily impede protein function. Iodine-releasing agents, much like chlorine-releasing agents, are used as disinfectants [41]. Historically, iodine has also long been used as an antiseptic, however it is an irritant and stains tissue [29]. This has led to a gradual shift towards other less irritant antiseptics.

1.3.2.5. Peroxygens

Hydrogen peroxide (H_2O_2) produces hydroxyl free radicals (·OH) which readily react with macromolecular structures within the cell including proteins, DNA and lipids [41], [81]. The free radicals also target amino acids containing thiol groups [82], which form intramolecular disulphide bonds that are key for maintaining the structural integrity of proteins. This oxidative stress leads to the functionality of macromolecular structures being impeded, and loss of bacterial viability. Peracetic acid is another example of a peroxygen disinfectant that decomposes into hydrogen peroxide and acetic acid. As a result, the MOA is considered similar to that of hydrogen peroxide [81].

Peroxygens are effective even at low concentrations against bacteria, mycobacteria and bacterial spores [83], [84], although higher concentrations and contact times are required for the latter [41]. Additionally, as both hydrogen and peracetic acid naturally degrades into water and oxygen, they are viewed as environmentally friendly. Their ability to deactivate spores results in their use as a sterilising agent, alongside as disinfectants and occasionally as antiseptics [29].

1.3.2.6. Phenolic compounds and derivatives

Phenol-based agents have been demonstrated to be active against microbial membranes, causing disruption to the permeability barrier and leakage of low molecular weight intracellular components [43]. Experiments conducted by Joseph Judis observed the leakage of carbon^{14}-labelled intracellular material when *E.coli* cells were exposed to various phenol derivatives, indicating membrane damage [85], [86]. This was later confirmed via the investigation of the uptake of carbon^{14}-labelled phenol derivatives, revealing localisation to bacterial lipids [87]. Later experiments linked the phenol MOA to the disruption of substrate uptake [88], [89] and

metabolism [90], indicating protein damage. Phenol derivatives are also able to directly interact with proteins [91], suggesting a potential direct mechanism of protein inhibition.

The resulting membrane disruption and protein function inhibition leads to loss of proton motive force and uncoupling of oxidative phosphorylation [92]–[94]. Examples of phenol-based compounds include fenticlor, chlorocresol and hexachlorophene [41]. Phenols are used for a variety of applications, depending on the agent. These include antiseptics, disinfectants and preservatives [41]. It is important to note that phenols are not charged so are relatively hydrophobic, unlike other membrane-active antimicrobials on this list.

1.3.2.7. Quaternary ammonium compounds

The quaternary ammonium compound (QAC) class of antimicrobial are used extensively in a variety of commercially available biocidal products including, but not limited to, common surface cleaners such as "Dettol®" and "Mr Muscle®", and clinical wipes such as "Clinell® Universal Wipes" and "TECcare® CONTROL".

QACs are cationic surfactants that contain a central quaternary nitrogen moiety and four surrounding carbon chains. The positively charged hydrophilic quaternary nitrogen moiety interacts with the anionic lipids located within the outer leaflet of bacterial membranes via electrostatic interactions, while the hydrophobic carbon chains protrude into the phospholipid bilayer, causing disruption of the organisation of phospholipids [64]. The lack of anionic lipids or peptidoglycan on the surface of mammalian cells enables QACs and other cationic surfactants to display a slight degree of selective toxicity towards bacteria.

The positive charge of the cationic nitrogen moiety in QACs causes these disinfectants to have a high affinity to the negatively charged outer surfaces of bacterial cells, with the presence of anionic lipids and either teichoic acids or LPS [64]. Once localised to this region, the hydrophobic tails of QACs are able to insert into the outer leaflet of bacterial membranes, leading to the negatively charged anionic lipids clustering around the positively charged quaternary nitrogen [64], as supported by a recent computational modelling study conducted by Alkhalifa *et al.* [95]. The presence of QACs results in an increased surface pressure within the outer leaflet, decreasing membrane fluidity and impacting the functionality of membrane proteins [64]. This can cause the loss of osmoregulation and other key physiological functions, resulting in the uncoupling of proton motive force and the impediment of the production of ATP [96], ultimately leading to a bacteriostatic effect.

At high enough concentrations the rearrangement of lipids leads to defects within the surface of the membrane causing subsequent breaches in the permeability barrier, loss of membrane integrity and leakage of bacterial cell components. Thus at high enough concentrations, QACs act via a bactericidal mechanism [41], [96], [97]. A schematic diagram of the MOA of QACs against bacterial membranes can be seen in Figure 4.

QACs are not used as sterilizing agents as they are ineffective against bacterial endospores [29], [41]. However, their use in health care as disinfectants and antiseptics is widespread [29], and they can also be used as preservatives [41].

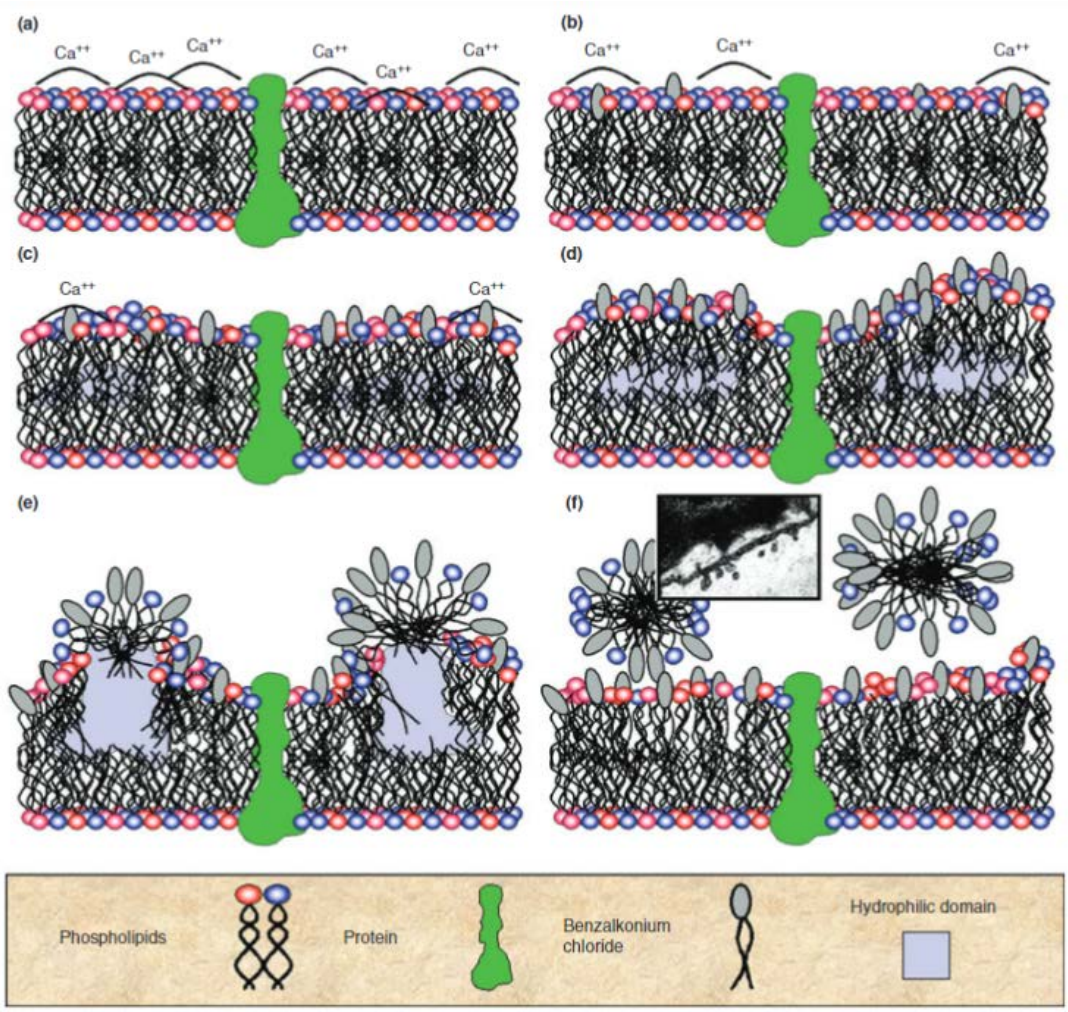

Figure 4. Diagram depicting the mechanism of action of quaternary ammonium compounds (QACs) on bacterial membranes. a) The outer membrane of a bacterial cell, formed from two layers of phospholipids containing membrane proteins. The other leaflet typically has a net negative charge, which is stabilised by cationic calcium ions. b and c) The cationic quarternary nitrogen moiety in QACs has a high affinity to the negatively charged outer leaflet of the bacterial cell, causing the displacement of associated calcium cations. The hydrophobic tails of QACs insert into the membrane, causing anionic phospholipids to cluster around them. d and e) The displacement of cations and sequestering of anionic lipids leads to the disruption of outer leaflet organisation and the formation of internal hydrophilic domains. This triggers the formation of protrusions from the membrane known as "blebs". f) The blebs pinch off to form micelles, causing a complete loss of membrane integrity. Inset micrograph shows vesicle formation from outer membrane caused by QAC treatment. Adapted with permission from: P. Gilbert and L. E. Moore, "Cationic antiseptics: diversity of action under a common epithet," J. Appl. Microbiol., vol. 99, pp. 703–715, 2005. [64]

1.3.2.8. Bronopol

Of interest to this study is the aliphatic halogen-nitro compound 2-bromo-2-nitropropan-1,3-diol (bronopol). This compound was originally noted by Crowshaw and colleagues as having a high activity against Gram-negative bacteria, especially *P. aeruginosa* [98].

This compound was demonstrated to impede protein function through the oxidation of thiol-group containing amino acids, forming disulphide bonds and impeding protein functionality [99]. Shepherd *et al.* (1988) later expanded on the known mechanism via nuclear magnetic resonance (NMR) experiments, discovering that bronopol acts in two stages. Firstly, bronopol oxidises the thiol groups within cysteine and glutathione residues, causing the formation of disulphide bonds and eventual bacteriostasis [100]. Secondly, this reaction leads to the formation of reactive oxygen species (ROS) which inflict non-specific damage on cellular components, thus having a secondary bactericidal MOA [100]. This is supported by experiments conducted in the presence of superoxide dismutase and catalase. These proteins function to protect cells from ROS including superoxide and peroxide, and caused the mitigation of the bactericidal effect of bronopol [100].

Bronopol is actively utilized in this reaction, so the ability for a bacteriostatic or bactericidal MOA is dependent on exposure concentration and time [100]. Bronopol is utilised as a disinfectant and preservative in household cleaning products, toiletries and cosmetics [101].

Table 1. Summary of the properties of the disinfectant classes discussed, categorised by mechanism of action.

Antimicrobial Class	Function	Target	Antimicrobial mechanism
Alcohols	Antiseptics, disinfectants, preservatives	Proteins	Compromising of membrane function [44]–[46]. Interfere and disrupt with hydrogen bonds that maintain structural integrity of proteins, leading to denaturation and loss of functionality [41], [47], [48].
Aldehydes	Disinfectants, sterilising agents, fixative agents	Proteins, Nucleic acids	Aldehyde functional groups react with amine and thiol functional groups present in proteins and DNA, leading to the formation of cross-links and a loss of structural integrity [54]. This impedes the functionality of proteins [41], [54], [56], [57], [59]–[61].
Biguanides	Antiseptics, disinfectants	Membranes	Biguanide group interacts with anionic lipids [63], [64], [69], [70], disrupting bilayer organisation [43], [64], [65]. This leads to permeability of membrane and intracellular leakage [63], [66]–[68], [71], [72].
Halogen-releasing agents	Antiseptics, disinfectants	Macromolecular structures	Chlorine forms hypochlorous acid, a powerful oxidising agent that reacts with and disrupts macromolecular structures. [77]–[79]. Iodine reacts with thiol groups in proteins [29], [41]. Alteration of macromolecular structures leads to loss of functionality [29], [41], [77].
Peroxygens	Sterilising agents, Disinfectants, Antiseptics	Macromolecular structures	Peroxygens form hydrogen peroxide, which produces hydroxyl free radicals. These powerful oxidising agents are able to react with various functional groups present in macromolecular structures. Specifically shown to interact with proteins, DNA and lipids [41], [81]. Loss of macromolecular structure leads to loss of functionality [41], [82].
Phenols	Antiseptics, disinfectants, preservatives	Membranes	Interacts with membrane structures, leading to disruption and permeability [85], [86]. This results in leakage of low molecular weight intracellular components, loss of proton motive force and uncoupling of oxidative phosphorylation [92]–[94]. High concentrations can completely impede membrane integrity and result in lysis [41], [43], [102].
Quaternary Ammonium Compounds	Antiseptics, disinfectants, preservatives	Membranes	Positively charged quaternary nitrogen interacts with anionic lipids, causing disruption of organisation and breaches in the permeability barrier [95]. Leads to leakage of low molecular weight material, loss of proton motive force [96] and uncoupling of oxidative phosphorylation [41], [103].
Bronopol	Antiseptics, disinfectants	Thiol functional groups. Secondary reaction targets macromolecular structures	Initial reaction causes the oxidation of thiol containing amino acids, resulting in the formation of disulphide bonds and impeding protein function [99]. Reaction forms reactive oxygen species which cause non-specific damage to macromolecular structures [100].

1.4. The known limitations of the use of disinfectants as an infection control measure

Disinfectants are relied upon globally for infection control in a variety of settings, including in industrial household and medical environments. However, they are often used with a blind acceptance of their efficacy, without consideration of the potential limitations that may mitigate their effectiveness.

This section overviews established limitations that impact the efficacy of the use of disinfectants as an infection control measure.

1.4.1. Compliance

Disinfectants, antiseptics and sanitisers have to actively be used in order to be effective. As a result, antimicrobials are limited by the compliance of individuals to infection control guidance. For example, Pittet and colleagues demonstrated the effectiveness of the use of alcohol-based hand rubs, demonstrating a decrease in nosocomial infection rate from 16.9% to 9.9% over 4 years [25]. This was attributed to an increase in compliance to hand hygiene guidance from 48% to 66%, with a 4-fold increased consumption of alcohol hand sanitizers observed [25]. This demonstrates that the effectiveness of hand sanitisers is highly dependent on the willingness of hospital staff and visitors using the dispensers that are available.

Education and awareness of the importance of hand hygiene guidance has been repeatedly been shown to reduce the prevalence of HAIs by up to 84% in studies conducted across the world [22]–[25]. Improvements to compliance have also been demonstrated through psychological methods such as "nudging"; the use of cognitive biases and environment cues to promote specific infection-prevention behaviours such as hand washing [104].

The issue of compliance also applies to how the disinfectants are used, as antimicrobial efficacy is dependent on external factors such as the presence of organic load [105], [106], dilution factor [107] and exposure time [107]. West *et al.* (2018) documented how exposing *S. aureus* and *P. aeruginosa* to QAC, sodium hydroxide and sodium hypochlorite-based disinfectants at concentrations and exposure times below the manufacturer's recommendations resulted in significantly reduced efficacy [107].

In hospitals of the United Kingdom, Clinell® Universal Wipes are routinely used for surface disinfection, which require a contact time of 10-60 seconds to inactivate bacteria and 30 seconds to inactivate severe acute respiratory syndrome coronavirus 2 (SARS-CoV-2) [108]. In high

pressure medical environments it is unlikely that a full 60 second contact time is routinely adhered to, especially in light of a recent study that reported that only 44% of healthcare workers had received training on cleaning and disinfection procedures [109]. Similarly, household disinfection products require varying wet contact times of up to 5 minutes to be effective [110].

Another study conducted by West *et al.* (2018) demonstrated how using ready to use wipes on surface areas above 2-square feet results in a significant reduction in efficacy [111]. This was associated with a reduction in the amount of liquid released onto the surfaces per square foot, and thus the overall reduction in efficacy was attributed to a lack of active compounds being released [111].

For these reasons the full efficacy of the use of disinfectants as an infection control measure is reliant on users being aware of and conforming to appropriate disinfection procedures. However, this project focuses on the bacteriological aspects of disinfectant usage as an infection control measure. Therefore, identifying and addressing limitations in compliance and behaviour is outside the scope of this project. However, the studies overviewed here demonstrate the relevance of investigating the impact of low concentrations of disinfectant on HAI-related pathogenic bacteria, as further discussed in Chapter 1.4.2.4.

1.4.2. Disinfectant tolerance

Bacteria are incredibly genetically diverse, both within populations and between them. They have been demonstrated to be able to adapt and survive in seemingly incredibly hostile conditions such as deep sea vents [112], thermal springs [113], arctic snow [114] and in the near-vacuum of space [115]. As a result, it is unsurprising that bacteria are also able to adapt and survive exposure to various disinfectants.

For the purpose of this thesis, tolerance is defined as an increased ability for a given bacterial population or sample to survive a given disinfectant. In the case of antimicrobials generally, this it usually measured via a change in minimum inhibitory concentration (MIC).

Variations in the efficacy of disinfectants can result from the broad range of characteristics displayed by different bacterial species, providing varying degrees of intrinsic tolerance. In addition, certain bacterial species are able to induce specific behaviours and changes in gene expression in response to disinfectant exposure, mitigating the efficacy of disinfectants. Finally, a growing body of evidence suggests that bacteria are able to acquire tolerance to disinfectants through genetic adaptations accumulated over time as a result of repeated exposure to low

concentrations of disinfectant. The following section discusses the various established mechanisms of disinfectant tolerance demonstrated by clinically-relevant bacterial species.

1.4.2.1. Intrinsic tolerance

Due to the large genetic diversity seen between the various species of bacteria that we are aware of, it is unsurprising that the efficacy of all disinfectants varies depending on the species it is applied to. In general, antimicrobial agents need to penetrate bacteria in order to reach their target site, therefore the outer composition of the various types of bacteria contributes heavily towards the natural intrinsic level of disinfectant tolerance [41]. In this section the properties that influence disinfectant tolerance in various types of bacteria are overviewed, in order of ascending intrinsic disinfectant tolerance.

1.4.2.1.1. Gram-positive bacteria

Gram-positive bacteria consist of a single cytoplasmic membrane and a thick cell wall [13] as described in Chapter 1.1.1.1 and Figure 1b. The cell wall provides little physical protection from the penetration of disinfectant agents as it does not act as a permeability barrier [116]. It is therefore unsurprising that Gram-positive bacteria are, in general, relatively susceptible to the MOA of disinfectants [41].

The negatively-charged LTA that protrudes from the outer leaflet of the cytoplasmic membrane provides a net negative charge at the outside surface of Gram-positive cells, causing cationic disinfectants such as QACs and biguanides to have a very high affinity to the cell surface [64]. Malonavic *et al.* (2016) suggested that the presence of LTA may attract positively charged antimicrobial peptides away from the membrane target site and thus provide a degree of intrinsic protection [117]. However, this potential interaction does not provide any discernible real-world benefit in the ability of Gram-positive bacteria to tolerate cationic disinfectants.

As a result of the permeability of the cell wall and the net negative charge of the outer surface of cells, Gram-positive bacteria such as *S. aureus* display a relatively low level of intrinsic tolerance to disinfectants in comparison to other types of microorganisms.

1.4.2.1.2. Gram-negative bacteria

Gram-negative bacteria consist of a thin peptidoglycan layer located between the plasma membrane and the outer membrane, as described in Chapter 1.1.1.2 and Figure 1a. The outer membrane contains anionic LPS in the outer leaflet (Figure 1a) [13] which acts as a barrier that prevents hydrophobic molecules accessing the membrane, and in turn the cell interior [15]. Combined with the regulation of porin proteins, the outer membrane provides an additional

level of control over what molecules are able to diffuse into the periplasm and the cell interior, and are thus able to prevent or limit the ability for disinfectants to reach the inner layers of the cell [15].

However, it should be noted that LPS is negatively charged, so provides a net negative charge to the outer leaflet of the outer membrane of Gram-negative bacteria. This results in cationic disinfectants displaying a high affinity to the outer surface of Gram-negative cells, increasing their susceptibility to these disinfectants.

As a result of these factors, Gram-negative bacteria such as *K. penumoniae* have more barriers to limit disinfectant entry than Gram-positive bacteria, so therefore exhibit a higher intrinsic resistance to disinfectants. However, the presence of anionic LPS on the outer leaflet causes these bacteria to be susceptible to cationic disinfectants.

1.4.2.2. Behavioural adaptations to disinfectants

1.4.2.2.1. Biofilms

Bacteria are capable of attaching to surfaces and forming complex communities contained within a gel-like extracellular polymeric substance (EPS), known as a biofilm [118]. One key characteristic of biofilms is their intrinsic resistance to external stressors, including disinfectants. There are many in-depth reviews available that cover the topic at length [119]–[122], from which some the relevant mechanisms of disinfectant tolerance are summarised here.

Firstly, in order to induce antimicrobial activity a disinfectant must penetrate the biofilm to reach the target site. The rate of which a disinfectant agent is able to penetrate into a biofilm varies depending on the chemical properties of the disinfectant, whether it interacts with constituents of the EPS and the species of bacteria present within the biofilm [122]. If a disinfectant is unable to penetrate a biofilm effectively, it is unable to have a disinfectant effect. For example, Stewart *et al.* (2001) investigated the penetration of halogen-releasing agents hypochlorite and chlorosulphamate into *P. aeruginosa* and *K. pneumoniae* biofilms [123]. The disinfectants displayed varying abilities to penetrate the biofilm, presumed to be due to hypochlorite reacting more readily with EPS components [123]. In addition, cationic antimicrobial penetration into *Streptococcus mutans* biofilms has been shown to be limited by interactions with anionic components of the EPS [124].

Secondly, bacteria within a biofilm are exposed to various conditions and micro-environments as a result of nutrient availability, oxygen availability and temperature [125]. Bacteria in different microcosms within the biofilm will exhibit physiological heterogeneity, resulting in variations in

gene expression, metabolic pathways and stress responses [122], [125]. This ultimately results in variation in the levels of disinfectant susceptibility within the biofilm.

Additionally, specific bacterial cells within biofilms have been demonstrated to enter a dormant physiological state whereby they are not growing, and are able to survive disinfectant treatments that other non-dormant bacteria could not [122]. These cells are referred to as "persister cells", and are naturally present in biofilms. Their ability to survive antimicrobial treatments is believed to at least partially contribute to antimicrobial treatment failure and recurrent infections [119], [122]. Persister cells are discussed in further detail in chapter 1.4.2.2.3.

Biofilms have been shown to develop on surfaces exposed to liquids and gases, referred to as wet surface and dry surface biofilms respectively. Of particular interest to this work is the prevalence of dry surface biofilms in hospital environmental surfaces [126], [127], which are capable of being transferred via contact [128]. Dry surface biofilms have been shown to commonly contain *S. aureus* [127], [128], a common HAI-associated pathogen, so thus these biofilms present a significant HAI risk. In addition, research conducted by Almatroudi *et al.* (2016) demonstrated sodium hypochlorite does not completely clear *S. aureus* dry surface biofilms [129], demonstrating the increased disinfectant tolerance that is characteristic of biofilms irrespective of whether they form in liquid or gaseous environments.

1.4.2.2.2. Viable but nonculturable bacteria

In 1982, a study published by Rita Colwell's group reported the presence of bacterial cells that were unable to be cultured on routine bacteriological media but were viable and metabolically active [130]. Bacteria in this state have since been shown to be able to take up nutrients [131], maintain membrane integrity [132], maintain active metabolism [133] and control gene transcription [134] but are otherwise in a dormant-like state where they are unable to reproduce [135], [136]. Bacteria in this state are referred to as viable but nonculturable, or VBNC.

Behavioural and phenotypical changes observed in bacteria that have entered the VBNC state include dwarfing [137], a reduction in macromolecular synthesis [138], and production of proteins associated with starvation and cold-shock [139]. Modifications to the fatty acid composition of the cytoplasmic membrane have been demonstrated, which are likely to be in order to maintain membrane fluidity and viability [140]. Changes in cell wall composition such as increased peptidoglycan cross-linking account for an increased structural stability of VBNC cells [141], [142]. Ultimately, VBNC cells show an elevated survivability in comparison to cultural bacteria, allowing them to potentially outlast the stressor that induced the VBNC state in the first place [143]. As a result, the VBNC state is believed to be a bacterial stress response.

As of 2021, at least 101 bacterial species have been documented as able to enter the VBNC state [144], of which at least 68 are known to be pathogenic [145]. Bacteria have been demonstrated to enter the VBNC state as a result of stressful environmental conditions such as starvation [146], desiccation [147], low or high temperatures [146], [148], low oxygen availability [149], reactive oxygen species [150], [151], cold plasma [152] and variations in pH [153].

As the principle of disinfectants is to disrupt bacterial functionality to the point of inducing a bacteriostatic or bactericidal effect, it is unsurprising that disinfectants have been demonstrated to induce the VBNC response. Recent research has implicated that various disinfectants are able to induce the VBNC state in varying pathogenic bacterial species including *Listeria monocytogenes* [151], [154]–[156], *Salmonella enterica* [151], [155], and HAI-associated pathogens *S. aureus* [155], *K. pneumoniae* [157], *A. baumannii* [158] and *E. coli* [155], [157], [159]. Disinfectants shown to induce the VBNC state include benzalkonium chloride (BAC) [154], non-ionic surfactants [155], peracetic acid [156], sodium hypochlorite [151], [156], [159] and hydrogen peroxide [157], alongside disinfectant formulations containing didecyldimethylammonium chloride (DDAC) and PHMB [158]. Furthermore, research conducted by Robben *et al.* (2019) demonstrated the ability for *E. coli, Bacillus cereus, P. aeruginosa,* and *L. monocytogenes* VBNC cells to maintain ATP production when exposed to concentrations of antimicrobials above their MIC [160]. This indicates that VBNC cells are able to tolerate higher concentrations of a range of disinfectants, preservatives and antibiotics, including QACs and bronopol [160]. The methodologies used to detect and quantify VBNCs used in these studies are discussed in chapter 1.4.2.2.2.3.

1.4.2.2.2.1. Molecular underpinnings of the viable but nonculturable state

The exact molecular mechanisms involved in VBNC induction are not fully understood, however there have been a number of genes that are implicated to be involved. The *rpoS* gene is known to be a stress regulatory gene that enables bacteria to be able to tolerate various stressful environmental conditions [136], [145]. The action of the *rpoS* gene therefore hinders the formation of the VBNC state in bacteria, demonstrated by Boaretti *et al.* (2003) whereby the deletion of the *rpoS* gene in *E. coli* caused the VBNC state to be more readily induced [161]. However, the RpoS knockout VBNCs lost viability rapidly, and were limited in their ability to resuscitate [161]. This implies that the *rpoS* gene must be closely regulated during stages of VBNC induction and maintenance, with negative regulation required during VBNC induction while the gene still being necessary for the maintenance of cell viability [161]. These findings were later supported by a similar study conducted on *S. enterica rpoS* mutants [162].

VBNC cell induction is also believed to be related to the stringent response. The increased regulation of *relA*, has been reported in VBNC cells [163], which is responsible for the production of guanosine pentaphosphate ((p)ppGpp) in response to amino acid starvation [164]. This results in the inhibition of resource-intensive cellular processes (such as cell division) and the increased transcription of genes associated with biosynthetic processes [165]. As a result, *relA* is believed to be necessary for VBNC induction.

Polyphosphate kinases are key proteins for protein regulation in bacteria, so it is unsurprising that the deletion of polyphosphate kinase 1 (PPK1) in *Campylobacter jejuni* resulted in a reduced ability for the bacteria to enter the VBNC state [166]. This suggests that PPK1 and other kinases are also likely to be heavily involved in VBNC induction and regulation.

Currently, it is unknown if the mechanisms of VBNC induction vary depending on the VBNC induction-stressor, and if different induction factors result in differences in terms of VBNC phenotype. Most studies to date have investigated the VBNC response in specific species and only as a result of starvation and low temperature, so more studies are needed in order to investigate potential variations between different species and VBNC induction factors [145]. The specific molecular mechanisms that underpin VBNC induction via disinfectants have not been thoroughly investigated.

1.4.2.2.2.2. Resuscitation of viable but nonculturable bacteria

Upon removal of the environmental stressor, bacteria in the VBNC state are able to resuscitate and become viable once more, and in the case of pathogens, become pathogenic once more [151], [167], [168]. This is likely an underlying reason behind recurrent infections and antimicrobial treatment failure. Resuscitation has been demonstrated in foodborne pathogens *L. monocytogenes* and *S. enterica* induced into the VBNC state via chlorine stress [151]. The ability for these pathogens to enter the VBNC state, avoid detection by culture-based methods (which are exclusively used to test contaminated environments in food-processing plants [169], [170]) and resuscitate back to a pathogenic state are likely contributing to outbreaks of food pathogens. *Legionella pneumophila* has been demonstrated to be able to survive chlorine-based water disinfection treatments and avoid culture-based detection in hospital water systems via entering the VBNC state [171]–[173], presenting an additional HAI risk.

The mechanisms that underlie VBNC resuscitation remain even more elusive than the mechanisms involved in VBNC induction [145]. One of the reasons for this is the challenge of proving that the return to culturability observed is true VBNC resuscitation and not simply the revival or regrowth of culturable cells. This is especially challenging when most studies are

conducted on cultures that contain bacteria in varying states, for example at any given time any single bacteria in a culture could be culturable, VBNC, resuscitated from VBNC or dead [145], [174]. Selectively identifying bacteria in each state is challenging enough, let alone attempting to quantify or isolate them for further study. Despite this, fully understanding the factors that induce and facilitate VBNC resuscitation would provide an invaluable insight into the conditions in which pathogenic bacteria in the VBNC state are able to regain virulence and cause disinfectant treatment failure and recurrent infections. This would provide opportunities to improve infection prevention measures and bacterial infection treatments.

1.4.2.2.2.3. Viable but nonculturable identification and quantification methods

As VBNC cells do not proliferate, standard culture-based methods cannot be used to identify or quantify them. Instead, all current methods rely upon enumerating the total number of viable bacterial cells within a sample, and the number of culturable bacterial cells via plate counts. The difference between these two populations provides an estimate of the number of VBNCs within the sample. The varying methods of total viable bacterial cell count enumeration are summarised here, alongside the associated disadvantages.

Membrane integrity is often used as an indicator of bacterial cell viability, with the assumption that if the membrane integrity of a cell is compromised, the cell must be dead. The fluorescent stains SYTO9 and propidium iodide (PI) are commonly used for this purpose, often bought together in the LIVE/DEAD BacLight™ staining kit. Both stains bind to nucleic acids, however PI cannot penetrate bacterial membranes, so selectively stains cells that are assumed to be dead, leaving cells with intact membranes (assumed to be viable) stained with SYTO9 [175]. The total number of live (SYTO9-stained) cells can then be enumerated via epifluorescence microscopy or flow cytometry.

Ethidium monoazide (EMA) and propidium monoazide (PMA) dyes are also used on the basis of being excluded by intact membranes [176]. These dyes intercalate DNA and are capable of inducing crosslinking, which prevents the DNA from being amplified during quantitative polymerase chain reaction (qPCR) [176]. As a result, the only DNA in a sample that is able to be analysed via qPCR is DNA from bacterial cells with an intact membrane, assumed to be alive. This can then be used to estimate the number of viable cells and, in turn, the number of VBNCs [177].

Both of these methodologies rely on the assumption that bacterial cells that have an intact membrane are viable, and those that have compromised membranes are not. However, it is very likely that this is not always the case, with non-viable cells maintaining membrane integrity or

cells with somewhat compromised membranes remaining viable [178]. This will result in inaccurate quantification of VBNCs.

In 1979, Kogure *et al.* published a methodology of directly enumerating viable bacteria present in seawater samples, termed the direct viable count (DVC) method [179]. The samples are incubated while exposed to an antibiotic that prevents DNA replication, such as nalidixic acid or pipemidic acid, and minimal nutrients [175]. Viable cells begin the process of growth, but are unable to undergo division, so elongate [179]. Non-viable cells do not elongate. On this basis, viable and non-viable cells can be differentiated via microscopy, and the total number of viable cells can be enumerated [179], which can then be used for VBNC estimation.

This methodology provides the benefit of not counting non-viable cells with intact membranes. However, distinguishing between cells that have elongated and those that have not is subjective, leading to potential operator error [175]. In addition, by definition VBNC cells do not proliferate or grow, and have been demonstrated to actively reduce in size compared to viable cells [137]. This raises the question of why VBNCs are expected to elongate during the DVC methodology, which in turn questions the validity of the method as a whole.

A more direct measure of viability is to measure the metabolic activity of bacterial cells. 5-cyano-2,3-ditolyl tetrazolium chloride (CTC) is a fluorescent stain that is reduced at the surface of aerobically respiring bacterial cells, forming a fluorescent dye that selectively stains metabolically active cells [180]. A similar stain, BacLight™ RedoxSensor™ Green, has been shown to penetrate cells where it is reduced to a fluorescent dye by active enzymes in the electron transport chain [181]. The use of these stains can differentiate between cells that are actively respiring and those that are not through fluorescence microscopy or flow cytometric analysis, providing a relatively direct method of quantifying viable bacterial cells.

Viability can also be inferred through enzymatic activity. Carboxyfluorescein diacetate (CFDA) is a chemical containing an ester group that can readily enter bacterial cells, whereby it is cleaved by esterases in an ATP-dependant reaction [182]. The product is carboxyfluorescein (CF), which is fluorescent [182]. This fluorescence is measurable via epifluorescence microscopy or flow cytometry, allowing for the measurement of cells with active esterase enzymes [175], [182]. This method assumes that only viable cells are able to trigger fluorescence through ATP-induced esterase activity.

All of these methods provide indirect estimations of the number of VBNCs. To date, no method has been demonstrated as able to directly enumerate VBNC populations.

1.4.2.2.3. Persister cells

Persister cells are bacteria that demonstrate an antimicrobial-tolerant phenotype as a result of stochastic or environmentally-induced physiological changes [183]. These cell populations also have a higher tolerance towards disinfectant exposure, including BAC [184]. Originally observed by Hobby *et al.* in 1942 when a small subpopulation of cells were observed to survive penicillin treatment [185], persister cells were later named by Joseph Bigger in 1944 during experiments on the effects of penicillin against *S. aureus* [186]. The ability for a small population of cells to survive the treatment was attributed to lack of growth at the time of exposure rather than resistance through genetic variation [186], a hypothesis that was later confirmed during live imaging experiments [187]. However, enhanced efflux activity has been shown to also contribute to their enhanced antibiotic and disinfectant tolerance [188], [189], demonstrating that environmentally-induced changes in gene expression are involved in the persister phenotype.

Persisters arise both stochastically within bacterial communities and as a result of environmental stressors such as starvation [190], oxidative stress [191] and antimicrobial exposure [192]. The presence of various micro-environments within biofilms inevitably causes some bacterial populations to experience varying degrees of stress, so thus biofilms facilitate persister cell populations, as described in chapter 1.4.2.2.1.

The molecular mechanisms of persister cell formation are aligned with those that underpin VBNC induction, specifically the stringent response-mediated pathways. This is evidenced by multiple knockout studies that have identified RelA as necessary for the formation of persister cells [193]–[195]. RelA is a key mediator of the stringent response, resulting in downstream inhibition of resource-intensive cellular processes and increased transcription of genes associated with biosynthetic processes. The role of RelA in bacterial dormancy is further discussed in chapter 1.4.2.2.2.1. This highlights the similarities in the molecular underpinnings of persister cells and VBNCs.

A noteworthy recent study by Pu *et al.* (2019) investigated the relationship between bacterial persisters and protein aggregation [196]. They demonstrated that antibiotic treatment resulted in variation in the level of intracellular aggregated protein, which was correlated with the time it took for cells to be able to regain culturability [196]. Further examination identified cells with lower levels of aggregation and lower dormancy depth were persister cells, while bacteria that displayed higher levels of protein aggregation had a deeper dormancy depth and were identified as VBNC cells [196], further highlighting the similarities between persister cells and VBNCs.

Persister cells are able to rescusitate and regain culturability upon removal of the induction stress, while VBNCs require a longer rescusitation time and specific conditions. This collectively suggests that bacterial cells are able to induce varying "depths of dormancy", from which it takes longer for bacteria to regain culturability [183]. It has therefore been suggested that the persister cell and VBNC phenotypes are not completely discrete states, but instead both exist along a dormancy continuum. This is known as the "dormancy continuum hypothesis" [164].

It is assumed that all bacterial species are able to form persister cells [197], including HAI-associated pathogens. As a result, persister cells are known to at least partially contribute to antibiotic treatment failure and recurrent infections [119], [122]. Their association with biofilms cause cells in this state to be of particular note when considering the limitations of disinfectant use in healthcare environments.

1.4.2.2.4. Endospores

In addition to structural differences between the various types of bacteria, some bacteria are able to undergo phenotypical changes that alter their susceptibility to disinfectants. Some bacteria, including the Gram-positive *Clostridium* and *Bacillus* genera, are capable of forming endospores [41]. This phenomenon occurs as a result of stress and not in order to reproduce. Bacteria in the endospore form are able to remain viable for thousands of years, and once the correct conditions are met, are able to resuscitate [198]. Whilst in the endospore form, cells are not pathogenic, do not require nutrients and are resistant to temperature changes, desiccation and disinfectants [41], [199].

The central "core" of a spore is the bacterial cell itself, surrounded by the inner membrane and peptidoglycan cell wall as is typical of Gram-positive bacteria [200]. The core is partially dehydrated, with the water being replaced with dipicolinic acid which has been suggested to be the primary mechanism behind the heat tolerance of endospores [199]. The core also contains small acid-soluble spore proteins (SASPs) [199]. SASPs have been indicated to have a role in coating and protecting the DNA in the core of endospores, protecting them from reactive oxygen species and chemical attack [199]. Surrounding the core is the cortex; a thick layer of peptidoglycan that is less cross-linked than the peptidoglycan present in a typical peptidoglycan cell wall [200]. Surrounding the cortex is the outer membrane followed by a proteinaceous coat which consists of at least 70 individual proteins [200]. Finally, some species form an outer coat known as the exosporium, which is known to primarily contain protein, but also lipids and carbohydrates [201].

Some of these layers provide a permeability barrier to many disinfectants, rendering alcohol, QACs, biguanides and even phenolics to be unable to induce a sporicidal effect [41]. The proteinaceous coat has demonstrated to provide a physical barrier against large molecules and react with hydrogen peroxide and other highly-reactive biocides, preventing their penetration into the deeper layers of the spore [202], [203]. There is evidence suggesting that the outer membrane provides a permeability barrier [204], however it appears that this membrane does not prevent penetration of methylamine, a small lipophilic molecule [205] so it is likely that small lipophilic disinfectants are also able to penetrate this layer. The inner membrane acts as a strong permeability barrier [206], although the mechanisms behind this are not fully understood [199]. There is little evidence to suggest that the exosporium and cortex provide protection from the action of disinfectants [199].

As a result of these mechanisms, bacteria that have adopted the endospore behavioural state are considered the most resistant form of bacteria to disinfectants. Whether a disinfectant treatment is sporicidal or not is a key factor in determining whether a disinfectant can be used as a sterilising agent or a disinfectant [29], [41].

1.4.2.3. Bacterial adaptations to disinfectants

Bacteria are able to adapt to environmental changes through adaptive evolution by natural selection, as proposed by Darwin in 1882 [207]. This occurs as a result of the natural genetic variation within a population allowing individuals to have a competitive advantage over others upon exposure to a selection pressure. Examples of unfavourable environmental conditions that may act as a selection pressure on bacteria include starvation, osmolarity, dessication and antimicrobials. Bacteria within a population that could not survive these unfavourable environmental conditions do not pass on their genetic material, while the competitive individuals that were able to survive the selection pressure reproduce and pass on their genetic information vertically from parent to offspring. Over generations the genetic adaptations accumulate and give rise to subpopulations of bacteria that have adapted to survive the selection pressure. This is one method of adaptive evolution used by bacterial populations to adapt to stressful environments, including the presence of disinfectants.

Adaptations can also arise through the duplication of key genes, allowing for increased expression and the potential for genomic variability and further adaptation [208]. Examples of this include the increased copy number of efflux genes and hydrolytic enezmes facilitating an increased resistance to various antibiotics [209].

Bacteria are also able to transfer genetic information horizontally between bacteria of the same generation, even between bacteria of different species. This can allow bacteria to develop new metabolic capabilities [210], and facilitate adaptive evolution [208]. Genetic material can also be transferred horizontally via plasmids or phages, for example various *qac* efflux genes are known to be plasmid-encoded and promote resistance to QACs [211], as discussed further in chapter 1.4.2.3.1.

As a result of adaptive evolution, the widespread overuse of antimicrobials is selecting for genes that confer antimicrobial resistance through natural selection. This is a well-established and widespread problem that has led to many bacterial strains becoming completely resistant to multiple antibiotics, for example Methicillin-resistant *Staphylococcus aureus* (MRSA) [212] or New Delhi metallo-β-lactamases (NDM)-producing strains of *K. pneumoniae* [213]. Antimicrobial resistance is a particularly problematic issue in hospitals, as antibiotic treatments are widely used; there is a high density of ill patients; and they all have frequent interactions with medical staff who provide a vehicle for cross infection [214]. Antimicrobial resistance therefore poses a significant problem in terms of infection control and mitigating the impact of HAIs.

However, the MOA of disinfectants typically impacts a range of macromolecular structures in bacterial cells, so thus have "broad" MOAs as overviewed previously in Chapter 1.3.2. Typically, the mechanisms that underpin tolerance to antimicrobials fall into 3 categories; preventing the agent from accessing the target site; alteration of the target site or inactivating the disinfectant.

The broad MOAs of disinfectants provide a great evolutionary challenge to bacteria attempting to develop tolerance. For example, preventing access to the target site is challenging when the target site is the entirety of the outer surface of bacterial cells, in the case of QACs, biguanides and phenol-derivatives. The modification of disinfectant target sites is challenging when the agents act non-specifically against exposed thiol groups in all proteins, in the case of aldehydes, halogen-releasing agents or peroxygens.

Despite these difficulties, there is a growing body of evidence to suggest that bacteria are able to develop tolerance to disinfectants. Concerns have grown to the point that there have recently been calls to introduce stewardship of disinfectants as a result of demonstrated adaptive response and cross-tolerance to other antimicrobials [215], [216]. Furthermore, triclosan was banned from soaps in the US in 2016 alongside 18 other antimicrobials [217]. This was in part due to the contribution of these disinfectants to antimicrobial resistance [217]. Currently, six active ingredients of health care antiseptic products are under review (including BAC) due to

concerns regarding antiseptic resistance and cross-tolerance to other antiseptics and antibiotics [218].

Bacteria have also been shown to be able to manipulate gene expression in order to adapt to disinfectant exposure. The following sections overview the current understanding of the molecular mechanisms that underpin induced and acquired molecular adaptations of bacteria to disinfectants.

1.4.2.3.1. Preventing disinfectant access to the target site

In order for a disinfectant to inflict antimicrobial activity it must first reach the required target site, a process which can be prevented. One such method that is demonstrated to contribute to disinfectant tolerance is the removal of antimicrobials from cells via broad-spectrum efflux pumps [219]. Various studies have identified a broad range of efflux pumps that are capable of ejecting disinfectants from cells, for example the *qacA* gene was originally identified by Gillespie *et al.* in 1986 [220], and has since been demonstrated to provide tolerance to BAC, biguanides and diamidines [221]. Other efflux genes include *qacBCDEFGH*, *mdfA*, *acrAB* and *ydgEF* [219].

More recently, Abdelaziz *et al.* demonstrated an increase in efflux pump activity after clinical isolates of *K. pneumoniae* were adapted to BAC [222]. Efflux genes *acrB*, *mdfA*, *norE* and *yihV* were found to have been up-regulated in tolerant samples, indicating disinfectant efflux as a mechanism of tolerance to BAC. Wand *et al.* (2022) recently published results demonstrating that impeding AcrAB-TolC functionality results in increased susceptibility to chlorhexidine, BAC and didecyldimethylammonium bromide (DDAB) in *K. pneumoniae* cells [223]. In addition, an up-regulation of AcrAB-TolC was demonstrated in samples that had adapted to chlorhexidine [223]. Other studies have established a link between the presence of the *qacΔE* gene and tolerance to BAC and DDAC in *K. pneumoniae*, *E.coli* and *S. enterica* [224]. This is also reflected in other bacterial species, for example variations in *E.coli* susceptibility to chloroxylenol have been associated with AcrAB activity [225], and *S. enterica* susceptibility to phenol correlated with efflux pump activity [226].

This collectively suggests that the expression of broad-spectrum efflux pumps influences tolerance to QACs, biguanides and phenol-derived disinfectants in a range of pathogenic bacterial species associated with HAIs.

However, it should be noted that a study using the efflux pump inhibitor carbonyl cyanide 3-chlorophenylhydrazone demonstrated that loss of efflux pump function in *K. pneumoniae* isolates caused an increased susceptibility to chlorhexidine, but not BAC and a PHMB-containing

disinfectant [227]. This indicates that efflux pumps are likely to not be the only mechanism of disinfectant tolerance.

Preventing access of antimicrobials to the target site is thought to be a contributing factor that underpins biofilm tolerance, as overviewed in Chapter 1.4.2.2.1. It is therefore unsurprising that BAC-exposed *K. pneumoniae* isolates have been shown to up-regulate the expression of biofilm regulatory gene *bssS*, suggesting increased biofilm formation may provide a mechanism of BAC adaptation [228].

1.4.2.3.2. Alteration of antimicrobial target site

Antimicrobial adaptation can also arise through the manipulation of the antimicrobial target site, reducing the affinity of the disinfectant and therefore facilitating an increased tolerance. While this is significantly more challenging for disinfectants than antibiotics as a result of the broad range of target sites affected, research has shown that it is still possible.

The MOA of many disinfectants is via the disruption of membranes, so therefore various bacterial species have been shown to adapt and modify their lipid content and outer surface organisation in response to these classes of antimicrobial.

Guérin-Méchin *et al.* (1999) noted the increased presence of hydroxylated fatty acids in *P. aeruginosa* samples exposed to QACs, which were suggested to be due to modifications to lipid A [229]. The modification of lipid A has been identified as a mechanism of *E. coli* and *Salmonella enterica* serovar Typhimurium resistance to cationic peptides and polymyxin, whereby lipid A is modified with 4-amino-4-deoxy-L- arabinose (L-Ara4N) in order to neutralise the negative charge of lipid A [230]–[232]. This reduces the net negative charge of the outer leaflet of Gram-negative bacteria and thus cationic peptides have a reduced affinity to the outer surface of cells. The observation by Guérin-Méchin and colleagues suggests that this mechanism may also contribute to Gram-negative bacterial adaptation to cationic surfactants such as QACs and biguanides.

This mechanism has been demonstrated to have influenced BAC tolerance in *P. aeruginosa* samples by Kim *et al.* (2018) [233]. Mutations in the *pmrB* polymyxin resistance gene were observed, which result in constitutive activation of the *pmrA* regulon and downstream expression of lipid A modification proteins *arnABCDTEF* [233]. The down-regulation of porins were also noted in adapted samples, indicating that modifications to the permeability barrier of the outer membrane may also contribute to BAC tolerance in *P. aeruginosa* [233].

Bisbiroulas *et al.* quantified the lipid content of *L. monocytogenes* samples exposed to BAC via thin-layer chromatography, finding a decrease in branched-chain fatty acids, and an increase in anionic phospholipids [234]. These adaptations were suggested to decrease membrane fluidity in response to BAC, potentially reducing the ability for it to penetrate into the membrane. However, it is unclear exactly how these mechanisms may contribute to BAC tolerance.

1.4.2.3.3. Disinfectant inactivation

Bacteria are also able to demonstrate an increased tolerance to disinfectants through the inactivation of disinfectant agents. Gao and Liu (2014) demonstrated the increased activity of superoxide dismutase and catalase in chlorine-adapted *L. monocytogenes* [235]. These proteins inactivate the ROS generated by chlorine, preventing damage to intracellular macromolecular structures.

Similarly, early studies on the MOA of bronopol against *E. coli* noted that the presence of catalase or superoxide dismutase mitigated the bactericidal activity of bronopol via the removal of ROS [100]. Therefore, the expression and activity of these proteins may facilitate or be associated with bacterial tolerance to halogen-releasing disinfectants and bronopol.

Tandukar *et al.* (2013) showed the ability for *Pseudomonas* spp. to develop tolerance to BAC through the use of enzymatic degradation [236]. In addition, bacterial pathogens are able to degrade formaldehyde into formate or pyruvate through three distinct pathways [237]. In both of these examples, the disinfectants were utilised by the bacteria as a carbon source, and therefore may provide a mechanism of tolerance through the manipulation of expression of associated enzymes.

1.4.2.4. The relevance of disinfectant tolerance

The various behavioural and adaptive disinfectant tolerance mechanisms overviewed are only possible if bacteria are able to survive long enough to mount a response. As the "at use" concentration of disinfectants is typically many orders of magnitude above the MIC, one may question the relevance of investigating the exposure of HAIs to sub-MIC concentrations of disinfectant.

However, the use of chemical disinfectants relies upon them being used correctly, as overviewed in Chapter 1.4.1. Variations in wipe usage including drying time, force applied, and surface area all impact the amount of disinfectant that bacteria are exposed to. This can have a demonstrable influence on the efficacy of the disinfection procedure [111]. In the case of West *et al.* (2018), wiped surface areas above 2 square feet resulted in a decrease in the $\log_{10}$ reduction in *S. aureus*

and *P. aeruginosa* colony-forming units (CFUs) present on the surface [111]. It is safe to assume that any bacteria that were present after the wiping procedure were exposed to disinfectant, but not enough to impact viability. Thus, the bacteria were exposed to a non-lethal concentration of disinfectant, even though the respective products contained disinfectants at concentrations orders of magnitude above the MIC.

In addition, recent research investigating the residual activity of a novel "persistent disinfectant" 24 hours after application only showed a 3-5 $\log_{10}$ reduction of *S. aureus* and *E. coli* CFUs, and a 1-2 $\log_{10}$ reduction of *K. pneumoniae* CFUs [238]. The disinfectant in question consists of a combination of quaternary ammonium compounds and ethanol, and claims to demonstrate activity up to 24 hours after application [238]. While a reduction in CFUs can be viewed as a promising demonstration of prolonged activity, it could equally be argued that the **lack** of reduction of CFUs is somewhat concerning, as any bacteria that survived the residual activity of the disinfectant were only able to do so because they were exposed to a non-lethal concentration.

Another study conducted on the same product documented variation in the residual activities of various disinfectant treatments by measuring the detectable accumulation of bacteria on surfaces after treatment [239]. The variability in efficacy observed between the disinfectant procedures demonstrates that bacteria are being impacted by the residual disinfectant treatments but are still being detected so are not all being killed. Once again, this provides evidence of prolonged exposure to concentrations of disinfectant below the MIC in a medical setting.

As a result of these factors, it is clear that although disinfectants are intended to be used at concentrations significantly higher than the MICs of HAIs, this is often not the case when used in practice. As a result, bacteria are unintentionally being exposed to non-lethal concentrations of disinfectants, and as such are being given opportunity to survive, respond and develop tolerance mechanisms.

1.5. The use of disinfectant formulations

Disinfectants to be sold or distributed in the USA must be registered with either the Environmental Protection Agency (EPA) or Food and Drug Administration (FDA) to ensure the product meets minimum efficacy and safety standards. Equivalent legislation can be found globally, for example the European Union enforces the Biocidal Products Regulations (BPR) [27]. Inadvertently, the implementation of pesticide regulations have effectively stopped most research into novel antimicrobial compounds due to the unfavourable cost of development and registration [240]. It remains more financially viable for companies to develop formulations containing currently approved active compounds than to risk the cost of developing and attempting to authorise novel antimicrobials. In the EU this remains the case even after the BPR revision in 2012 which aimed, among other things, to simplify the process of product authorisation [27].

As a result, many of the most widely available antimicrobial disinfectant and sanitizer products consist of varying combinations of the limited number of individual compounds that are currently registered under local regulations. These formulations are routinely used as disinfectants and antiseptics in healthcare settings, industrial environments and in day-to-day life in the form of surface sprays, wipes and hand sanitizers. The central axiom that synergistic interactions can occur between antimicrobials with different mechanisms of action and target sites has resulted in the liberal use of claims of "synergy" when describing and marketing multi-component disinfectants products.

However, correctly classifying the type of interaction between antimicrobial agents is a challenging process. For example, inconsistencies regarding the classification of an antimicrobial interaction can arise depending on the method employed [241]–[244]. Common techniques used to investigate antimicrobial interactions include the E test, time kill and checkerboard methods.

Of these methods, the most widely used is the checkerboard assay; a variation of the broth microdilution technique to determine MIC. In brief, each compound is serially diluted along either the X or the Y axis of a multi-well plate containing growth medium. The wells are then inoculated with the test species and incubated. The output of the test is the fractional inhibitory concentration index (FICI). The lower the FICI value, the higher the level of interaction between the two tested compounds.

The checkerboard method provides a high-throughput technique that can yield a large amount of information about how pairs of antimicrobials interact in a relatively short period of time.

Despite this the checkerboard method does raise significant challenges when it comes to interpreting results and thus classifying antimicrobial interactions. Firstly, the outcome of a checkerboard assay varies depending on the method of interpretation [245], which is especially significant when many published articles do not explicitly state the method of interpretation used. In addition, the FICI thresholds that can be set to define the verdict of an interaction often vary between publications, creating issues around standardisation and comparability of results.

Further complications arise when comparing data between species or strains, with publications reporting significant variations in the classification of combined activities of mixtures of both disinfectants [246], [247] and antibiotics [248], [249]. This has resulted in the same combinations being reported as synergistic, additive or indifferent depending on the species or even strain it was tested upon. While certain academic journals have implemented FICI standards when reporting checkerboard data [250]–[252], these are not universally adhered to between journals which further contributes to inconsistencies between publications.

A lack of universal consensus on the definitions of antimicrobial interactions provides additional issues. For the purposes of this thesis, the definitions used are in accordance with those set out by the European Committee on Antimicrobial Susceptibility Testing (EUCAST). According to EUCAST, an indifferent interaction is one whereby the activity of both components combined is equal to the activity of the most active component [253]. An additive interaction has a combined activity of no greater than the sum of the activities of each component, while the sum of the individual activities has to be exceeded by the combined activity in order for the interaction to be classed as synergistic [253]. Antagonism is the inverse, whereby the activity of both components combined is lower than the most active component [253].

These definitions are not universally accepted or adhered to, for example multiple leading journals in the field do not accept 'additive' checkerboard interpretations due to the definition being commonly misunderstood and the intrinsic variability of the method [250], [252]. In the guidance to authors it is even suggested that alternative terms are used such as "nonsynergistic" [251], thus encouraging researchers to disregard intermediate levels of activity and focus exclusively on interactions that demonstrate synergy [250], [251]. This does not mean that these journals completely disregard the existence of additive interactions, instead that additivity is too difficult to pinpoint and identify reliably using the checkerboard methodology.

The confusion between additivity and synergism and the methods employed to distinguish between them has led to the two terms often being used interchangeably and potentially erroneously. The confusion is especially significant as synergism in an antimicrobial formulation

is considered "surprising" and thus is patentable [240]. This, alongside the increased marketability the "synergy" buzzword brings, provides a commercial incentive to classify such formulations as synergistic, even if the evidence is circumstantial and the definitions are misunderstood. In addition, results that support patentable ideas often remain unpublished in order to prevent potential loss of intellectual property. This means that the evidence required to support a patent is not often subjected to the same scrutiny as peer-reviewed publications.

These factors combined lead to academic and commercial-related research being "all or nothing"; exclusively focusing on synergistic antimicrobial interactions and completely disregarding additive interactions. Furthermore, this lack of clarity raises questions regarding the validity of our current understanding of disinfectant interactions.

However, it is possible that the use of multiple disinfectants simultaneously may overcome various limitations of disinfectant use. Firstly, certain disinfectants require the surface to be clean and unsoiled in order to maintain efficacy, while others do not. By combining multiple disinfectants, it is possible to avoid inappropriate use of disinfectants on unclean surfaces due to human error.

In addition, the presence of multiple disinfectants with varying MOAs and cellular targets may mitigate the development of tolerance, under the assumption that bacterial cells would need to develop tolerance to multiple mechanisms simultaneously. *In vitro* experiments have demonstrated this benefit when applied to antibiotic combinations [248], [254]–[256], however it is unknown if this benefit applies to disinfectant formulations.

Finally, it is unknown how the combined effect of multiple antimicrobials influence the induction and survivability of cell in the VBNC state. It is possible that multiple disinfectants with varying MOAs may overwhelm VBNC cells, overcoming their increased tolerance to disinfectants and mitigating VBNC induction that would otherwise occur via exposure to individual disinfectants. On the other hand, the increased stress of being exposed to multiple disinfectants with multiple MOAs may instead enhance the formation of VBNC cells and be insufficient to overcome their increased tolerance. This remains to be elucidated.

1.6. Project aims

The prior literature review overviews our current understanding of disinfectants, and their limitations when utilised as an infection control measure. It is clear that there are major gaps in our current understanding, which are overviewed here alongside the research aims of this thesis. The chapter-specific aims are discussed further in each corresponding chapter.

Firstly, disinfectant formulations containing multiple active compounds are commonly used in a variety of settings including healthcare environments. The interactions between disinfectants and the resulting effect on the overall antimicrobial efficacy of disinfectant formulations is not well understood. This study aims to classify the nature of the interactions between common disinfectants and elucidate the influence these interactions have on the overall efficacy of disinfectant formulations. This is discussed further in Chapter 3. Synergism vs Additivity - Defining the Interactions between Common Disinfectants.

Secondly, the ability for pathogenic bacterial species to develop tolerance to various disinfectants has been demonstrated. However, the literature that is currently available is limited to specific bacterial species and disinfectants, and it is not known if disinfectant combinations are able to mitigate the development of tolerance. Therefore, this study aims to investigate whether HAI-associated pathogens *K. pneumoniae* and *S. aureus* are able to develop tolerance to disinfectant commonly used in healthcare environments. This is discussed further in Chapter 4. The Development of Tolerance to Common Disinfectants used Individually and in Combination.

Our understanding of the underpinning mechanisms of disinfectant tolerance in *K. pneumoniae* are limited to specific disinfectants. It is therefore aimed to expand on this knowledge by investigating the underlying molecular mechanisms of tolerance displayed by *K. pneumoniae* samples adapted to tolerate disinfectants commonly used in healthcare environments, as discussed in Chapter 5. Mechanisms of *K. pneumoniae* Tolerance to Common Disinfectants.

The ability for disinfectants to induce the VBNC state in *K. pneumoniae* has been established. However, it is not known if the disinfectants investigated herein induce the VBNC state in *K. pneumoniae*. This is investigated further in Chapter 6. The Induction of the Viable but Nonculturable State via Exposure to Common Disinfectants.

Finally, a novel methodology of VBNC quantification has been hypothesised that aims to directly enumerate VBNC populations. This methodology may be able to be applied to fluorescence-activated cell sorting to isolate VBNC cells from mixed cultures, which is not

possible using current methods. Initial proof-of-concept experiments aim to validate this methodology as a potential method of VBNC quantification, as presented in Chapter 6.

2. Characterising the Antibacterial Activities of Common Disinfectants

2.1. Introduction

The overall aim of this thesis is to elucidate limitations of common disinfectants used for infection control. Before being able to characterise combined antimicrobial interactions, the development of antimicrobial tolerance and the induction of the VBNC state, it is pertinent to first establish the base characteristics of the disinfectants to be examined, namely the mechanism of action and antimicrobial efficacy. Our current understanding of the mechanism of action of each disinfectant used in this study has previously been discussed in Chapter 1.3.2, and is summarised in Table 2 and Table 3. The elucidation and understanding of disinfectant efficacy, however, raises significant challenges that need to be overcome.

Antimicrobial efficacy varies between disinfectants [41], [82], [107] as a result of the wide variety of potential target sites, mechanisms and chemical properties. Environmental factors can also affect efficacy such as pH [257], [258], temperature [259] and the presence of interfering organic matter [259]. Additionally, antimicrobial activity is influenced by the target organism and strain the disinfectant is tested against [107], [260]–[262], as species and strains vary in terms of morphology, surface structure, membrane composition and protein expression. All of these factors can contribute to a bacterial cell's intrinsic tolerance to disinfectants, as summarised in Chapter 1.4.2.1.

Variation in disinfectant efficacy can also be introduced depending on the experiment methodology. Variations between methods have been observed when testing sodium hypochlorite [263], ethanol [264], peracetic acid [264] and QACs [224], [264], with up to a 500-fold difference in efficacy depending on the methodology used [263]. Furthermore, it has long been established that minor experimental alterations within methodologies can also lead to significant variation in the efficacy of the disinfectants tested [265]. This includes variations in aerobic conditions, neutralisation method, post-exposure plating method and incubation temperature [265].

Existing reports investigating the efficacy of the disinfectants to be tested are available in the literature [266]–[270], however these data do not cover all of the disinfectants to be examined and have been generated using varying methodologies and strains. Additionally, a number of these studies tested efficacy when disinfectants were used in combination with other active

compounds [269], [270]. As all of these factors introduce variation between reports, it was considered necessary to directly establish the efficacies of the disinfectants to be tested against the specific strains to be used to ensure data completeness and comparability.

2.2. Chapter aims

The aim of the work in this chapter was to establish the efficacies of 5 common disinfectants and 1 disinfectant formulation (BAC, DDAC, PHMB, bronopol, chlorocresol and "SQ53", respectively) when challenged with HAI-associated pathogenic bacterial species *A. baumannii* NCTC 12156, *E. faecalis* NCTC 13379, *K. pneumoniae* NCTC 13443 and *S. aureus* NCTC 13143.

Establishing the core characteristics of the disinfectants to be examined affords us greater insights when moving forward to examine antimicrobial interactions, resistance development and VBNC induction in later chapters.

2.3. Materials and methods

2.3.1. Bacterial strains and growth media

The following bacterial strains were used throughout this study: *Acinetobacter baumannii* NCTC 12156, *Enterococcus faecalis* NCTC 13379, *Klebsiella pneumoniae* NCTC 13443 and *Staphylococcus aureus* NCTC 13143. The strains were selected due to their clinical relevance and association with HAIs [7], [8], [238], [271]. Clinically-relevant strains that display a degree of antibiotic resistance were selected in order to provide a stringent test.

All bacterial strains were cultured on Mueller Hinton Agar (MHA) (Thermo Scientific) and cultured overnight at 37°C. To generate stock cultures, single colonies were used to inoculate 10 ml of Mueller Hinton Broth (MHB) (Thermo Scientific), which was then incubated overnight at 37°C. MHB and MHA were used as recommended for antimicrobial susceptibility testing by the Clinical Laboratory Standards Institute (CLSI) [272].

2.3.2. Stock solutions of disinfectants

Disinfectants were selected based on their prevalence in healthcare environments and commercial disinfectant formulations. Benzalkonium chloride (BAC) and didecyldimethylammonium chloride (DDAC) are both quaternary ammonium compounds commonly found as components in disinfectant formulations. Polyhexamethylene biguanide (PHMB) and phenol-derivatives such as chlorocresol are also common components seen in a variety of settings, including in healthcare environments. Bronopol was selected as it acts via a different mechanism in comparison to the other selected compounds. The characteristics of these antimicrobial compounds are summarised in Table 2.

"SQ53" is a novel disinfectant formulation that was selected due to our thorough understanding of its composition as a result of a longstanding industrial collaboration with JVS Products Ltd. From here on the product is referred to as SQ53. Insights into the composition of SQ53 afforded us a unique level of comprehension that for other products is typically hidden behind intellectual property barriers. SQ53 contains all of the other disinfectants to be examined. The full composition of the formulation is presented in Table 3. SQ53 was selected due to our in-depth knowledge regarding its formulation and components.

Benzalkonium chloride (Thor Specialities Limited), didecyldimethylammonium chloride (Thor Specialities Limited), polyhexamethylene biguanide (Thor Specialities Limited), bronopol (Thor Specialities Limited) and SQ53 (JVS Products Limited) were made up to a stock concentration of

10,000 μg/ml in dH_2O immediately before testing. Chlorocresol (Lanxess Limited) was made up to a stock concentration of 10,000 μg/ml in undiluted dimethyl sulphoxide (DMSO) (Corning) immediately before testing.

Table 2. Summary of the properties of the disinfectants used throughout this work.

Disinfectant	Application	Disinfectant classification	Bacterial cell target site	Mechanism of action
Benzalkonium chloride	Antiseptics disinfectants preservatives	Quaternary ammonium compound (Chapter 1.3.2.7)	Membrane	Positively charged quaternary nitrogen interacts with anionic lipids, causing disruption of organisation and breaches in the permeability barrier [95]. Leads to leakage of low molecular weight material, loss of proton motive force [96] and uncoupling of oxidative phosphorylation [41], [103]
Didecyldimethyl-ammonium chloride	Antiseptics disinfectants preservatives	Quaternary ammonium compound (Chapter 1.3.2.7)	Membrane	Positively charged quaternary nitrogen interacts with anionic lipids, causing disruption of organisation and breaches in the permeability barrier [95]. Leads to leakage of low molecular weight material, loss of proton motive force [96] and uncoupling of oxidative phosphorylation [41], [103]
Polyhexamethylene biguanide	Antiseptics disinfectants	Polymeric biguanide (1.3.2.3)	Membrane and/or DNA	Biguanide group interacts with anionic lipids [63], [64], [69], [70], disrupting bilayer organisation [43], [64], [65]. This leads to permeability of membrane and intracellular leakage [63], [66]–[68], [71], [72]. Recent findings dispute this, suggesting that the mechanism relies condensing DNA, preventing growth and arresting cell division [73].
Bronopol	Antiseptics disinfectants	Aliphatic halogenonitro compound (Chapter 1.3.2.8)	Thiol functional groups. Secondary reaction targets macromolecular structures	Initial reaction causes the oxidation of thiol containing amino acids, resulting in the formation of disulphide bonds and impeding protein function [99]. Reaction forms reactive oxygen species which cause non-specific damage to macromolecular structures [100].
Chlorocresol	Antiseptics disinfectants preservatives	Phenol derivative (Chapter 1.3.2.6)	Membrane	Interacts with membrane structures, leading to disruption and permeability [85], [86]. This results in leakage of low molecular weight intracellular components, loss of proton motive force and uncoupling of oxidative phosphorylation [92]–[94]. High concentrations can completely impede membrane integrity and result in lysis [41], [43], [102].

Table 3. Summary of the chemical components of the disinfectant formulation "SQ53".

Component	Percentage (% v/v)	Function within the formulation
Benzalkonium chloride	3.00	Active antimicrobial component
Didecyldimethyl-ammonium chloride	3.00	Active antimicrobial component
Polyhexamethylene biguanide	3.30	Active antimicrobial component
Bronopol	0.90	Active antimicrobial component
Chlorocresol	0.04	Active antimicrobial component
Ethanol	4.90	Solvent
Ethylene glycol	1.00	Solvent
Water	83.86	Solvent

2.3.3. Minimum inhibitory concentration quantification via broth microdilution

The MICs of the disinfectants when used against *A. baumannii* NCTC 12156, *E. faecalis* NCTC 13379, *K. pneumoniae* NCTC 13443 and *S. aureus* NCTC 13143 were elucidated using the broth microdilution technique. This was conducted as described by CLSI [272] with minor variations as described here. Due to disinfectant compounds demonstrating a wide range of potential activities, serial dilutions began from 10,000 μg/ml instead of 128 μg/ml as recommended for antibiotics. Experimentation was performed using 96-well plates in triplicate, with disinfectants being two-fold serially diluted in 150 μl MHB, to which 20 μl of bacterial stock was added to each well so that the final concentration is equal to 5 x 10^5 CFU/ml. After preparation, 96-well plates were incubated at 37°C overnight. The MIC was defined as the lowest concentration of active compound that completely inhibited bacterial growth in the microdilution wells as detected by the unaided eye. A positive control well was included for each dilution series which contained sterile dH_2O instead of disinfectant in order to confirm bacterial culturability. A sterility control well was included for each dilution series which contained only MHB. If growth was detected in any of the sterility control wells the 96-well plate was assumed to be contaminated, so was discarded. In addition, the MIC of DMSO was calculated for all tested species to ensure validity of chlorocresol MICs.

2.3.4. Scanning electron microscopy

2.3.4.1. Individual disinfectants

High resolution images of *K. pneumoniae* NCTC 13443 and *S. aureus* NCTC 13143 samples were captured via SEM imaging in order to visualise the impact of varying disinfectant treatments on bacteria. Samples were incubated overnight at 37°C in MHB containing the respective MIC of either BAC, DDAC, PHMB, bronopol or chlorocresol, as identified previously. Untreated control samples were also prepared in the absence of disinfectant treatment.

Samples were pelleted via centrifugation at 5400 G for 10 minutes and re-suspended in fixative (3% glutaraldehyde, 0.15% Alcian blue in 0.1 M cacodylate buffer, pH 7.2). After a 1-hour incubation at 4°C the suspensions were pipetted onto poly-L-lysine treated round glass coverslips such that the coverslips were completely covered but the surface tension was not broken. Samples were incubated on the coverslips at room temperature for 30 minutes in order for cells to adhere to the treated glass.

The samples were then gently rinsed twice via suspension in 0.1 M cacodylate buffer, pH 7.2, before the coverslips were immersed in 1% w/v osmium tetroxide in 0.1 M cacodylate buffer at pH 7.2 for 1 hour at room temperature. The coverslips were again washed twice with 0.1 M cacodylate buffer, pH 7.2 before sequential immersion in 30% v/v, 50% v/v, 75% v/v and 95% v/v ethanol with each immersion step lasting 10 minutes at room temperature. Finally, the samples were immersed in absolute ethanol twice, each time for 20 minutes at room temperature before critical point drying (Balzers CPD 030 critical point dryer). Coverslips were then mounted on specimen stubs and sputter-coated with platinum using a Quorum Q150T ES coater before being imaged on a FEI Quanta 250 SEM. Observations were made as the samples were viewed via SEM. At least 6 fields of view (FOV) were captured of each sample, selected randomly.

2.3.4.2. Disinfectant formulation SQ53

In addition, *K. pneumoniae* NCTC 13443 and *S. aureus* NCTC 13143 samples were incubated overnight at 37°C in MHB containing a concentration of SQ53 equal to 0.5 x, 1 x, 1.5 x or 2 x the respective MIC, as identified previously. Untreated control samples were also prepared in the absence of SQ53. Sample preparation and imaging steps were performed as described in Chapter 2.3.4.1.

2.3.5. Transmission electron microscopy

Transmission electron microscopy (TEM) was utilised to visualise the intracellular impact of SQ53 on bacteria. *K. pneumoniae* NCTC 13443 and *S. aureus* NCTC 13143 samples were incubated

overnight at 37°C in MHB containing a concentration of SQ53 equal to their respective MICs (200 μg/ml and 60 μg/ml SQ53, respectively). Untreated control samples were also prepared in the absence of SQ53.

Treated bacterial samples were pelleted via centrifugation at 5400 G for 10 minutes and re-suspended in fixative (3% (v/v) glutaraldehyde, 4% (w/v) formaldehyde in 0.1 M piperazine-N,N'-bis(2-ethanesulfonic acid) (PIPES) buffer, pH 7.2). After a 1-hour incubation at 4°C the fixed bacterial samples were centrifuged at 1250 G for 5 minutes. 2 drops of 5% (w/v) sodium alginate solution were added directly to the pellet and gently mixed with the micropipette tip. 10 μl of alginate-pellet mixture was then ejected into fixative with 0.1 M calcium chloride and allowed to set at room temperature for 15 minutes.

The alginate-embedded cells were rinsed in 0.1 M PIPES buffer, pH 7.2 twice via immersion, before being immersed in 1% w/v osmium tetroxide in 0.1 M phosphate buffer at pH 7.2 for 1 hour at room temperature. The samples were then rinsed twice in 0.1 M PIPES buffer, pH 7.2 before immersion in 2% v/v uranyl acetate for 10 minutes. The samples were dehydrated via sequential immersion in 30% v/v, 50% v/v, 75% v/v and 95% v/v ethanol, with each immersion step lasting 10 minutes. Samples were then immersed in absolute ethanol twice for 20 minutes at each step, and then acetonitrile for 10 minutes before the addition of epoxy resin diluted 50:50 with acetonitrile, which was incubated overnight at room temperature. Diluted resin was replaced with pure epoxy resin and samples were incubated for 6 hours at room temperature, before samples were added to an embedding capsule and polymerised at 60°C for 24 hours, hardening the resin.

Thin sections were cut from the sample stubs using glass knives produced using an LKB 7800 knife maker on a Leica Reichert Ultracut E ultamicrotome and picked up via a copper grid. Grids were stained with 2% (w/v) uranyl acetate in 50% v/v ethanol and Reynolds' lead stain (2.66% (w/v) lead nitrate, 3.56% (w/v) tri-sodium citrate in 0.16 M sodium hydroxide) for 15 and 5 minutes respectively. Samples were then rinsed gently in sterile water and blotted dry, before images were captured on a Hitachi HT7700 Transmission Electron Microscope. Observations were made as the samples were viewed via TEM. At least 6 fields of view (FOV) were captured of each sample, selected randomly.

2.4. Results and discussion

2.4.1. Disinfectant efficacy quantification via the calculation of minimum inhibitory concentrations

The MIC values of common disinfectants when tested on clinically relevant bacterial species are displayed in Table 4. Of the species tested, *A. baumannii* and *K. pneumoniae* displayed the highest MIC values to BAC and DDAC, indicating a high intrinsic tolerance (Table 4). This is consistent with previous reports that QACs demonstrate a lower efficacy against Gram-negative bacterial species rather than Gram-positive species, by account of the outer membrane providing an additional barrier to disinfectant penetration and action [273]–[276]. This characteristic is especially evident in the case of BAC, whereby the Gram-positive species demonstrated a significantly lower MIC than the Gram-negative species (Table 4).

Conversely, both bronopol and chlorocresol demonstrated low MIC values against Gram-negative *A. baumannii* and *K. pneumoniae* in comparison to the Gram-positive *E. faecalis* and *S. aureus* (Table 4). This indicates a higher antimicrobial efficacy against these species. This observation has been previously reported for bronopol [98], [277], and is reflected in results published by Stretton *et al.* (1973) [99] who noted *P. aeruginosa* as being particularly sensitive. However, a mechanism behind this observation has never been proposed. In addition, other publications did not show a significant difference in efficacy between Gram-positive and Gram-negative species both for bronopol [101], [278] and other nitrogen based disinfectants [279]. To our knowledge this observation has not been previously reported for chlorocresol or similar phenol derivatives. Due to the small number of species tested we are unable to conclusively say whether our observations are a result of differences between Gram-positive and Gram-negative species or a product of intra-species variation generally. Repeating this experiment on a broader range of species would be needed to establish this.

PHMB MIC values were not consistent based on Gram staining classification. *A. baumannii* achieved the highest MIC of 16 μg/ml, while *K. pneumoniae* and *S. aureus* both demonstrated an MIC of 6 μg/ml when challenged against PHMB (Table 4). This illustrates that although cell surface structure has a major influence on the activity of a given disinfectant, there are many other influential characteristics that can limit or enhance efficacy. Examples include lipid composition [63], [229], [280], the levels of expression of broad-spectrum efflux pumps [219], [281] and the presence of disinfectant-inactivating enzymes [219]. All of these factors influence the quantity of disinfectant that is able to reach the required target site and thus affect

antimicrobial efficacy. These preliminary results open the possibility of more detailed future work.

Across all species, chlorocresol required a concentration at least one order of magnitude higher to inhibit growth in comparison to the other disinfectants tested (Table 4). This indicates that chlorocresol has a lower efficacy than the other disinfectants, most notably BAC, DDAC and PHMB which also act via membrane disruption. This large variation in efficacy can be partially attributed to the high affinity cationic antimicrobials have to their anionic target sites [64], as reflected by their L/H isotherm patterns [282], [283]. In comparison chlorocresol is uncharged and relies upon hydrophobic interactions with the lipid bilayer, thus having a relatively weaker affinity to the target site as reflected by its S isotherm pattern [284], therefore requiring higher concentrations of active compound to achieve a comparable level of antimicrobial efficacy.

Table 4. Minimum inhibitory concentration (MIC) values of common disinfectants against clinically relevant bacterial species. BAC: benzalkonium chloride. DDAC: didecyldimethylammonium chloride. PHMB: polyhexamethylene biguanide. n=3.

Bacterial species	**MIC (µg/ml)**				
	BAC	**DDAC**	**PHMB**	**Bronopol**	**Chlorocresol**
Acinetobacter baumannii NCTC 12156	31	8	16	4	125
Enterococcus faecalis NCTC 13379	8	4	8	16	500
Klebsiella pneumoniae NCTC 13443	20	6	6	8	200
Staphylococcus aureus NCTC 13143	4	2	6	20	600

2.4.2. Efficacy quantification of disinfectant formulation SQ53 via the calculation of minimum inhibitory concentrations

The MIC values of disinfectant formulation SQ53 when challenged against *A. baumannii, E. faecalis, K. pneumoniae* and *S. aureus* are shown in Table 5. At first glance the efficacy of disinfectant formulation SQ53 appears to be low in comparison to the individual disinfectants tested, by account of the high MIC values required to inhibit growth (Table 5). However, upon examining the concentrations of the individual components that make up the SQ53 formulation it is clear that the active compounds are at lower concentrations than what would be required for the compounds to achieve the same inhibitory effect when used individually against *A. baumannii*, *E. faecalis* and *S. aureus* (Table 5 compared to Table 4).

Combined antimicrobial interactions are classified according to whether the combined is greater or less than the efficacy of the most active individual component, as discussed in Chapter 1.5. As a lower concentration of each antimicrobial is required to inhibit growth for these species, these data suggest that there are beneficial antimicrobial interactions between the compounds present in the SQ53 formulation. However, it is not clear which specific disinfectant components are contributing to these beneficial interactions from these data, and it is also not possible to deduce if these interactions are additive or synergistic. This is further investigated during Chapter 3.

In contrast, 6.6 μg/ml PHMB is required to inhibit growth of *K. pneumoniae* when used in combination in SQ53 (Table 5), compared to 6 μg/ml when used individually (Table 4). This provisionally indicates an antagonistic interaction, as the efficacy of PHMB is impeded when used in combination against *K. pneumoniae*. In addition, it is not possible to deduce the active compounds that contribute to this antagonistic interaction with PHMB from these data. This is investigated further during Chapter 3.

It is well established that the efficacy of disinfectants varies between species and strains [107], [260]–[262]. These data suggest that this variation also extends to the nature of antimicrobial interactions between disinfectant compounds too.

Hereby, these data suggest that SQ53 contains disinfectant combinations that enhance the efficacy of the overall formulation. However, these interactions vary depending on the species tested upon, with evidence of antagonistic interactions impacting the efficacy of PHMB when tested against *K. pneumoniae*. The identification of specific beneficial and antagonistic interactions of disinfectants will allow for a greater efficacy in disinfectant formulations used for infection control.

Table 5. Minimum inhibitory concentration (MIC) values of disinfectant formulation "SQ53" (SQ53) and the constituent active compounds against clinically relevant bacterial species. BAC: benzalkonium chloride. DDAC: didecyldimethylammonium chloride. PHMB: polyhexamethylene biguanide. n=3.

Bacterial species	SQ53 MIC (µg/ml)	Concentration of each active compound at the respective SQ53 MIC (µg/ml)					Concentration of total active compound at the respective SQ53 MIC (µg/ml)
		BAC	DDAC	PHMB	Bronopol	Chloro-cresol	
Acinetobacter baumannii NCTC 12156	240	7.2	7.2	7.9	2.2	0.1	24.58
Enterococcus faecalis NCTC 13379	60	1.8	1.8	2.0	0.5	<0.1	6.14
Klebsiella pneumoniae NCTC 13443	200	6.0	6.0	6.6	1.8	0.1	20.48
Staphylococcus aureus NCTC 13143	60	1.8	1.8	2.0	0.5	<0.1	6.14

2.4.3. Visualisation of the mechanism of action of individual disinfectants via scanning electron microscopy

2.4.3.1. Visualisation of the mechanism of action of individual disinfectants against *K. pneumoniae*

SEM images of *K. pneumoniae* NCTC 13443 shown in Figure 5 are representative of all FOVs captured for each sample. Figure 5a and b show untreated *K. pneumoniae* cells, with their rod morphology and textured outer surface. A filament-like substance can be seen projecting from a small number of cells which is likely to be pili in accordance with SEM images previously reported on *K. pneumoniae* [285]. The textured surface is a result of the dehydration and critical point drying steps during sample preparation causing a loss of sample volume [286], thus causing a slight folding of the outer cell surface [287]. This observation is consistent with SEM images captured in previous reports [285], [288], [289].

After 24-hour exposure to 20 µg/ml BAC (Figure 5c, d) *K. pneumoniae* demonstrate a 'deflated' appearance with a smooth surface that varies from the control samples. These cells remain relatively intact but show a loss of intracellular volume as a result of BAC-induced permeabilization of bacterial membranes and leakage of intracellular material. In severe cases BAC reduces membrane organisation to the point of total loss of membrane integrity, which causes the cell to rupture entirely [41], [64], [273]. This leaves behind aggregated cellular debris as shown in Figure 5c.

A 24-hour exposure to 6 μg/ml DDAC (Figure 5e, f) has an effect on *K. pneumoniae* samples comparable to that of BAC (Figure 5c, d). Intact cells have a 'deflated' morphology as a result of the loss of intracellular material (Figure 5e), while other cells have completely ruptured, leaving only aggregated rod-shaped cellular debris as shown in Figure 5f. DDAC and BAC are both QACs and thus share a similar mechanism of action [41], [64]. As a result, the intact deflated cells and ruptured cells can be attributed to partial and complete loss of lipid organisation and membrane integrity respectively. These observations are consistent with a prior study examining morphological changes in *E. coli* after DDAC exposure [290].

An exposure of 6 μg/ml PHMB resulted in *K. pneumoniae* cells exhibiting a generally smoother texture, with the exception of projections of varied sizes scattered across their surface (red arrows, Figure 5g, h) known as blebs. These blebs are a result of the sequestering of anionic lipids by the positively charged nitrogen moieties along the PHMB molecule, which causes phase separation of the lipids and disruption of membrane structural integrity [64]. There is no evidence of cellular debris in images captured of samples exposed to PHMB, indicating that *K. pneumoniae* cells did not completely rupture despite the action of PHMB [70]. This provides support for the case presented by Chindera *et al.* (2016), whereby it was suggested that PHMB passes through bacterial membranes and condenses DNA, arresting cell growth [73]. However, this alternative mechanism was suggested to occur instead of the previously-established membrane disruption MOA, which seems unlikely in this case given the presence of blebbing. These images suggest that both mechanisms may occur concurrently with PHMB causing membrane perturbation, facilitating its own uptake and binding to DNA.

The images captured of *K. pneumoniae* cells after 24-hour exposure to 8 μg/ml bronopol show extracellular material that has a mesh-like appearance and is visibly different from the aggregated cellular debris seen in *K. pneumoniae* samples exposed to DDAC (Figure 5f). This material is therefore likely to be EPS (Figure 5i, j). The presence of EPS was not unique to the bronopol sample but was randomly distributed across the samples as a result of the random attachment to the APES-treated slides during sample preparation. The *K. pneumoniae* cells themselves do not show significant visible differences compared to the control samples (Figure 5i, j). This is due to bronopol not having a direct action on the integrity of the membrane or surface of bacteria [99], [100] (Table 2), so it is unsurprising that any influence is not visible via SEM.

Figure 5k and l shows *K. pneumoniae* cells after 24-hour exposure to 200 μg/ml chlorocresol. These cells exhibited a loss of cellular content without the formation of blebs as seen previously by the cationic disinfectant PHMB (red arrows, Figure 5g, h). This is a result of the accumulation

and intercalation of chlorocresol in the lipid bilayers causing disruption of membrane function leading to and leakage of cellular material [82], [85]–[90], [291], as opposed to PHMB sequestering of anionic lipids leading to bleb formation and eventual disruption of the lipid bilayer (Figure 5g, h) [43], [64]. The perturbation of bacterial membranes by chlorocresol leads to the rupturing of cells as shown by the blue arrow in Figure 5k. The mechanism of action of chlorocresol may also rely upon associating with and disrupting protein function [90], [91], but the influence of this mechanism is not directly visible via SEM.

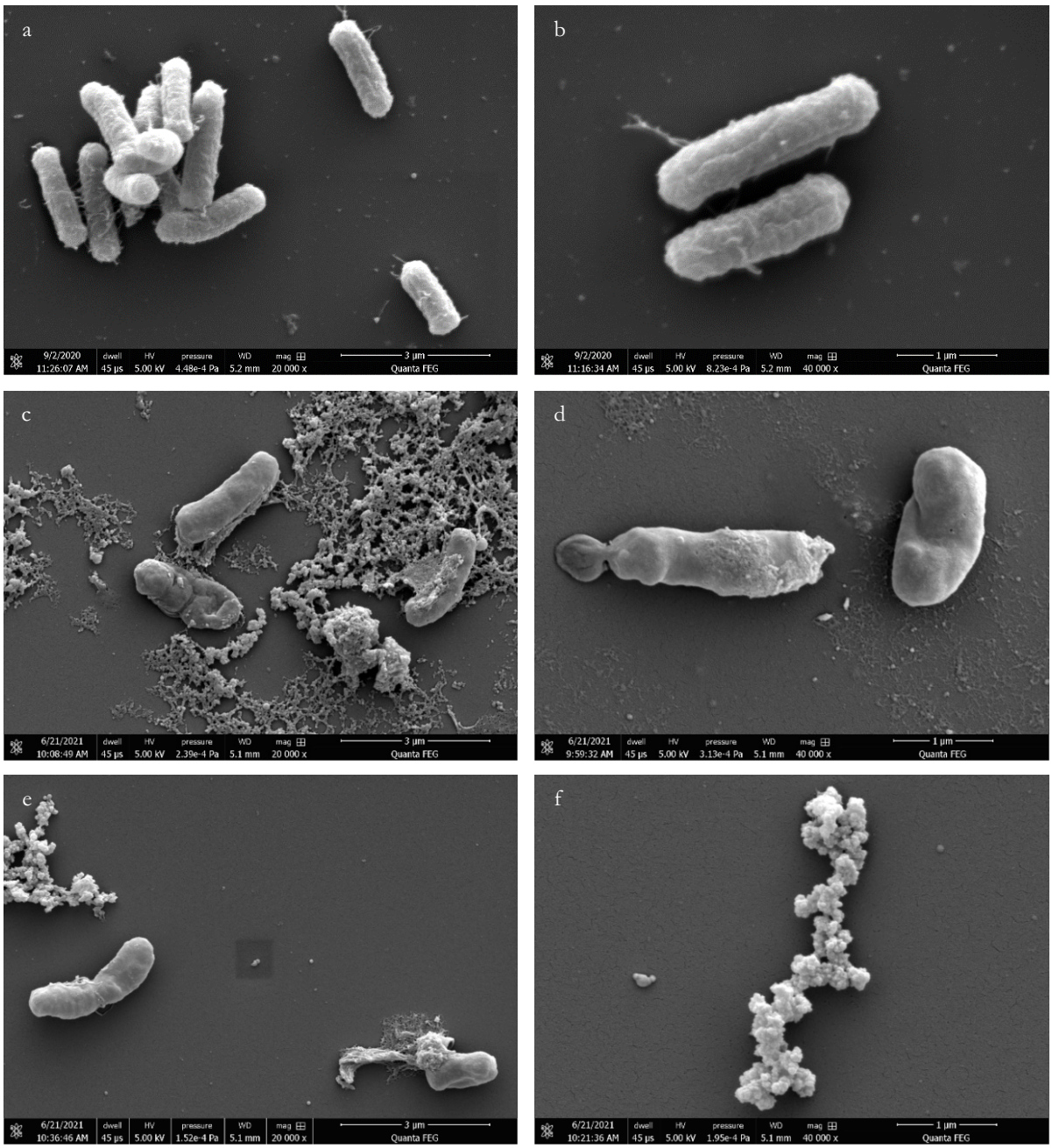

Figure 5. Scanning electron microscopy images of *Klebsiella pneumoniae* NCTC 13443 after 24-hour exposure to common disinfectants at their respective minimum inhibitory concentrations. a and b) untreated control. c and d) 20 µg/ml benzalkonium chloride. e and f) 6 µg/ml didecyldimethylammonium chloride. Images a, c and 3 are at 20,000 x magnification. Images b, d, and f are at 40,000 x magnification. Scale bars are shown at the bottom right of each image, measured in µm. Figure continued on the next page.

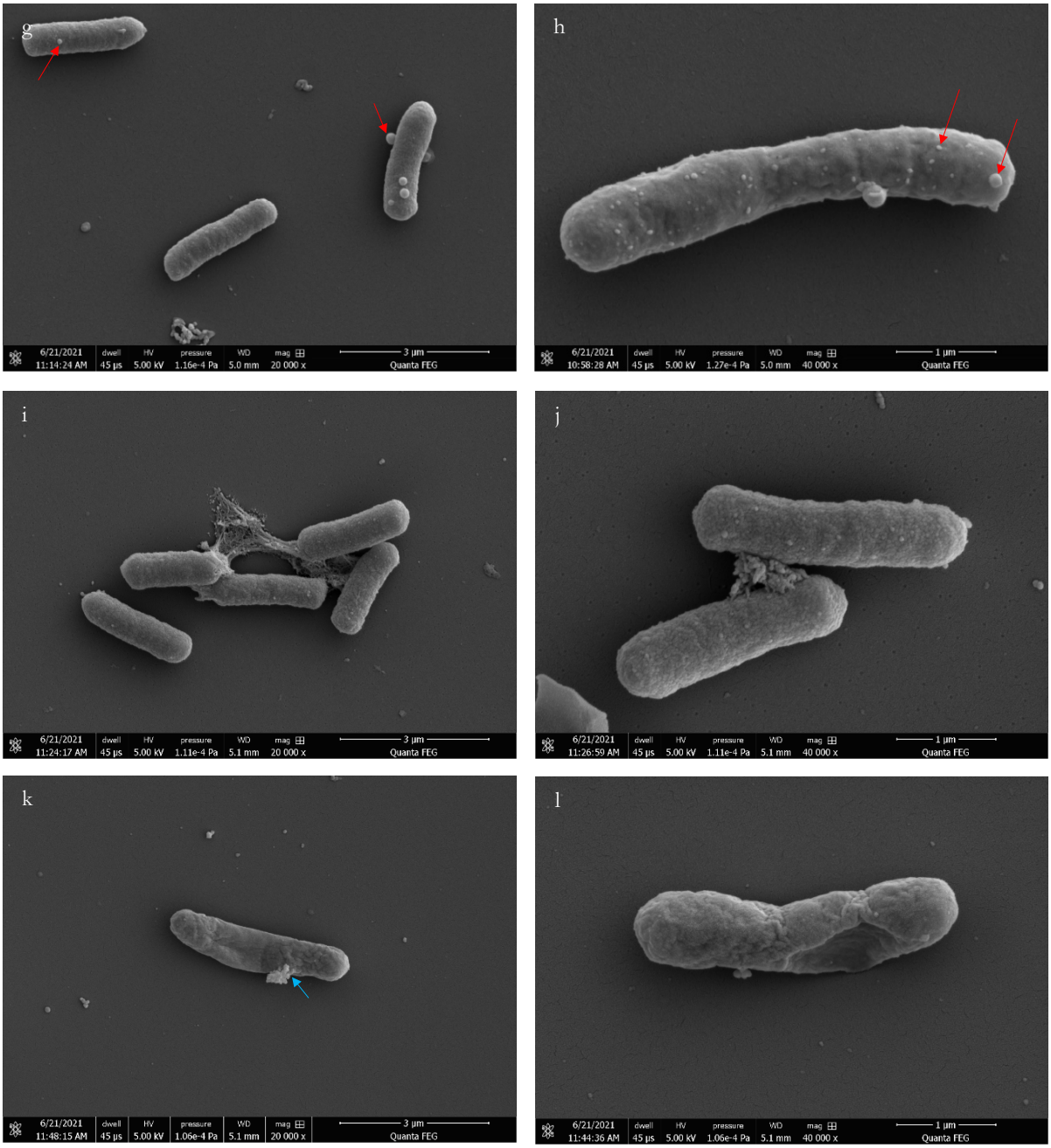

Figure 5 (continued). g and h) 6 µg/ml polyhexamethylene biguanide. Red arrows show the formation of blebs. i and j) 8 µg/ml bronopol. k and l) 200 µg/ml chlorocresol. Blue arrow highlights the rupturing of the cell surface. Images g, I and k are at 20,000 x magnification. Images h, j and l are at 40,000 x magnification. Scale bars are shown at the bottom right of each image, measured in µm.

2.4.3.2. Visualisation of the mechanism of action of individual disinfectants against *S. aureus*

SEM images of *S. aureus* NCTC 13143 shown in Figure 6 are representative of all FOVs captured of each sample. SEM images of untreated *S. aureus* cells are shown in Figure 6a and b. They have a distinct regular coccoid morphology, and form clusters of cells. Some individual cells can be seen to be in varying stages of the cell division cycle with a visible division septum, shown more

clearly in Figure 6b. Also of note are the presence of small quantities of extracellular material of various sizes around individual *S. aureus* cells, likely EPS in accordance with *S. aureus* images in previous publications [292]–[294].

After exposure to 4 μg/ml BAC or 2 μg/ml DDAC there is visible aggregated *S. aureus* cell debris (Figure 6c, d, e), similar to that observed with the *K. pneumoniae* samples (Figure 5c, e, f). Other cells remained intact but appear less smooth with surface imperfections and blebbing visible (Figure 6e, f). Some individual cells exhibit visible lesions in their surfaces, as highlighted by red arrows. These observations are indicative of varying severities of integrity loss at the cell surface, consistent with the known mechanism of BAC and DDAC (Table 2) [64], [273].

S. aureus cells exposed to 6 μg/ml PHMB display a significant increase in the irregularity of their surfaces with many bleb-like projections on their surfaces (Figure 6g, h), consistent with the known membrane-disruptive mechanism of action of PHMB [63], [64], [70], [71], as previously described (Table 2). The images also contain a large amount of aggregated cellular debris as a result of cells losing their membrane integrity entirely, suggesting that the MOA of PHMB on *S. aureus* is likely to involve a loss of membrane integrity, rather than solely be a result of DNA condensation and arresting of the cell cycle as suggested by Chindera *et al.* [73]. Initial PHMB uptake experiments reported by Chindera *et al.* were conducted on *S. aureus*, however all subsequent experiments were conducted on other bacterial species [73]. As the observed MOA of PHMB varies between *S. aureus* (Figure 6g, h) and *K. pneumoniae* (Figure 5g, h), this collectively suggests that both membrane and DNA-active MOAs occur, but to varying degrees depending on the bacterial species PHMB is acting upon. The greater influence of a membrane-active MOA in *S. aureus* is a result of the cells being Gram-positive. The lack of outer membrane acting as an additional permeability barrier leaves Gram-positive bacterial cells more susceptible to membrane-active disinfectants, as discussed previously in Chapter 1.4.2.1.1.

After 24 hour exposure to 20 μg/ml bronopol, *S. aureus* cells demonstrated minimal surface variation when compared to untreated cells (Figure 6i, j) due to bronopol not having direct action on surface structures of bacterial cells [99], [100], consistent with images captured of *K. pneumoniae* after bronopol exposure (Figure 5i, j). There are fewer cells visibly undergoing stages of cell division as a result of bronopol-induced bacteriostasis [100].

Chlorocresol exposure caused *S. aureus* cells to demonstrate a less spherical, more irregular morphology (blue arrows, Figure 6k, l). Individual cells can be seen in both images that have completely ruptured, leaving behind an empty husk-like shell (yellow arrow, Figure 6 l). This is a result of the membrane-active component of the chlorocresol mechanism of action compromising the structural integrity of the bacterial cell membrane and causing the cells to rupture [85]–[91], [291]. Chlorocresol is has also been suggested to have a role in the disruption of protein structure and function, but this is not visible via SEM.

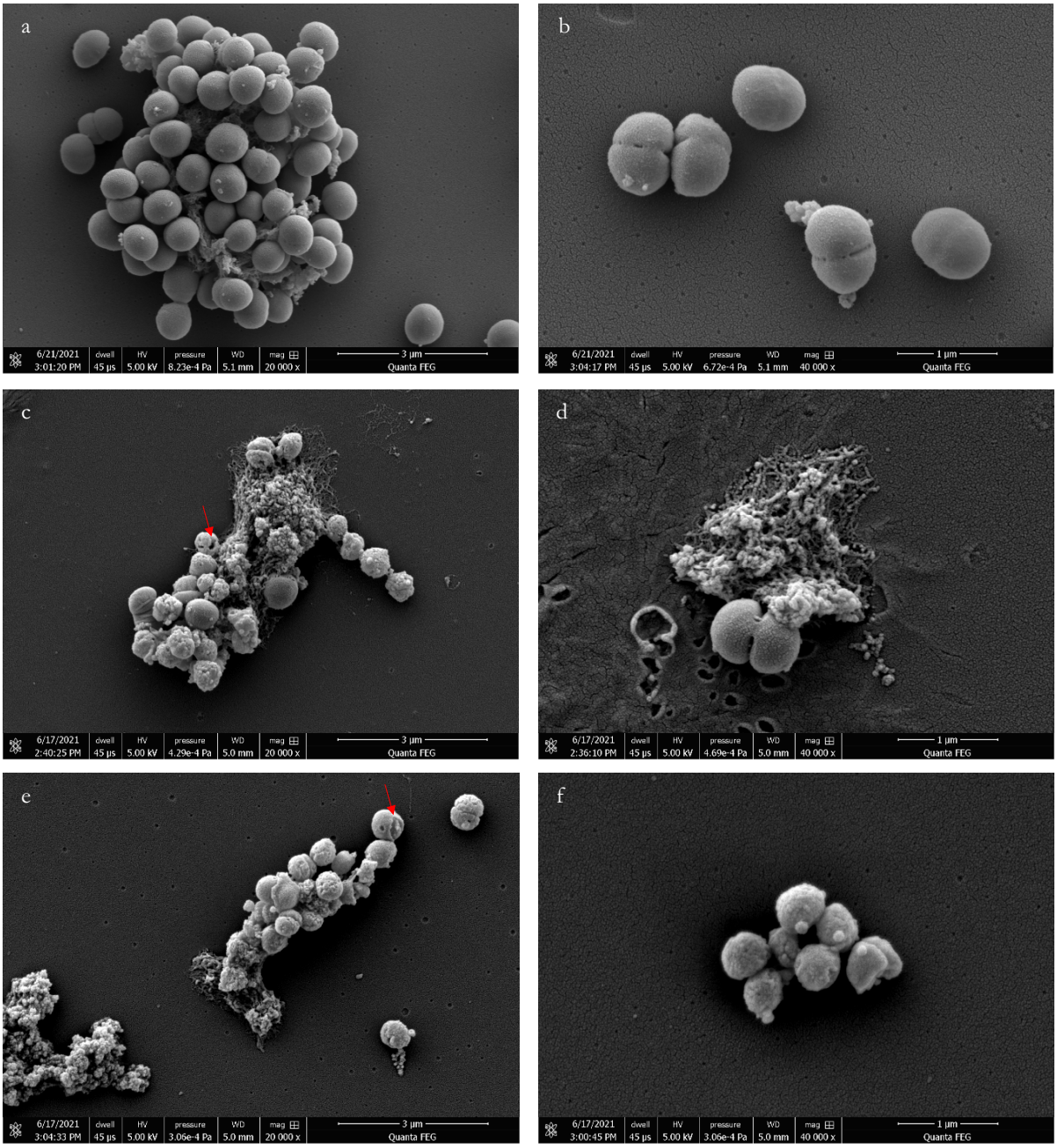

Figure 6. Scanning electron microscopy images of *Staphylococcus aureus* NCTC 13143 after 24-hour exposure to common disinfectants at their respective minimum inhibitory concentrations. a and b) untreated control. c and d) 4 µg/ml benzalkonium chloride. e and f) 2 µg/ml didecyldimethylammonium chloride. Red arrows indicate visible lesions in the cell surface. Images a, c and e are at 20,000 x magnification. Images b, d, and f are at 40,000 x magnification. Scale bars are shown at the bottom right of each image, measured in µm. Figure continued on the next page.

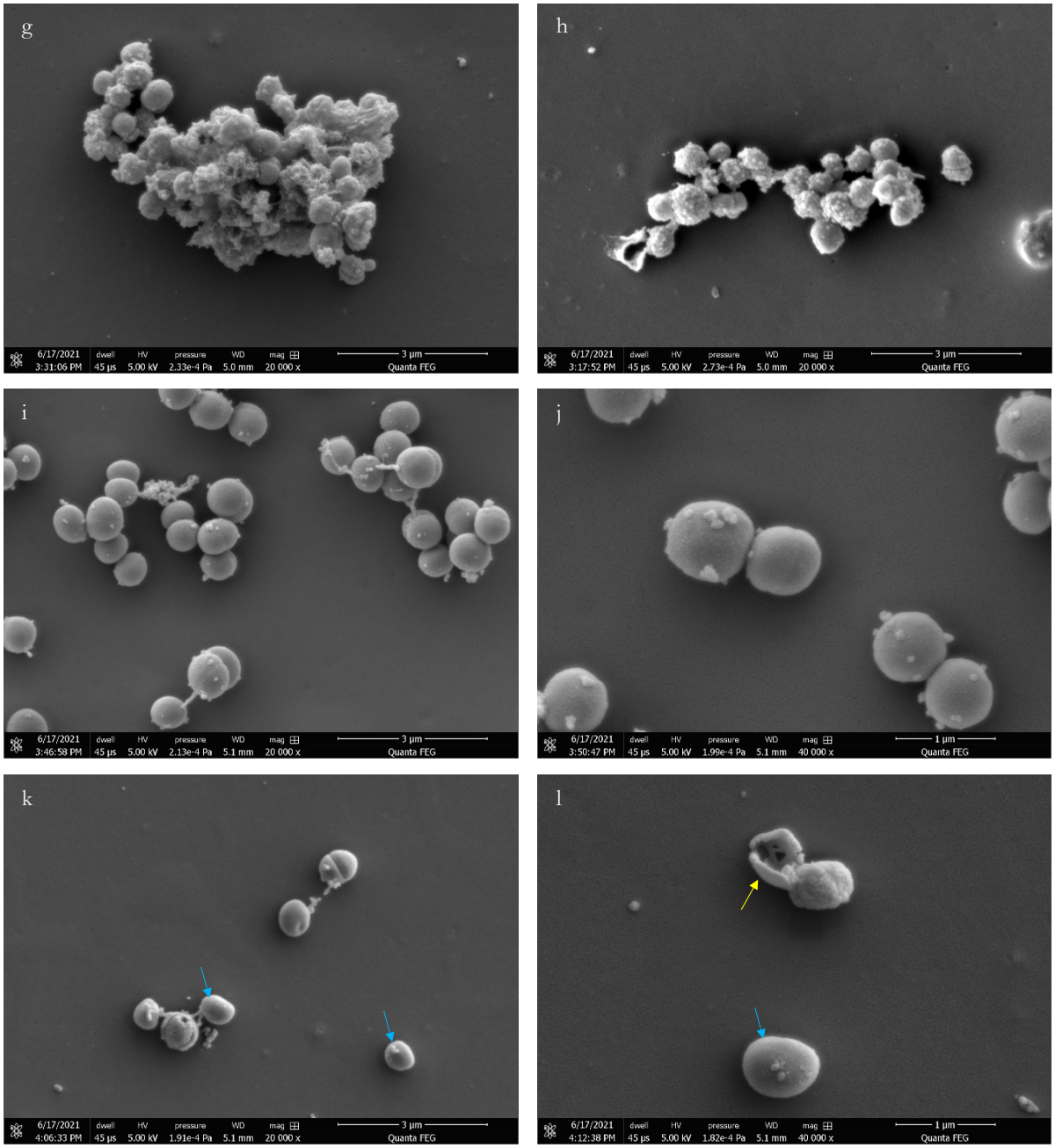

Figure 6 (continued). g and h) 6 µg/ml polyhexamethylene biguanide. i and j) 20 µg/ml bronopol. k and l) 600 µg/ml chlorocresol. Blue arrows indicate cells with an irregular, non-spherical morphology.The yellow arrow indicates cellular debris. Images g, h, i and are at 20,000 x magnification. Images h, j and l are at 40,000 x magnification. Scale bars are shown at the bottom right of each image, measured in µm.

2.4.4. Visualisation of the mechanism of action of disinfectant formulation SQ53 via scanning electron microscopy

Untreated *K. pneumoniae* cells imaged via SEM display a rod morphology, with a textured and uneven surface, as shown in Figure 7a and b. Cells exposed to 100 μg/ml SQ53 demonstrated no obvious variation when observed via SEM (Figure 7c), which is consistent with the MIC data as this concentration of SQ53 is not high enough to inhibit growth. At SQ53 concentrations 200 μg/ml and greater, cells exhibited varying degrees of visible damage, with some individual cells having lost intracellular content and demonstrating a 'deflated' or 'withered' appearance, while others display no visible differences in comparison to the untreated samples (Figure 7d, e).

Similar observations are seen upon exposure of SQ53 to *S. aureus* (Figure 8). Untreated *S. aureus* cells display a coccoid morphology of consistent size and shape (Figure 8a, b). Individual cells can be seen to be undergoing stages of cell division, with division septa visible (red arrows, Figure 8a, b). However, upon exposure to 30 μg/ml SQ53 or greater *S. aureus* cells display a range of severities of visible damage, with some cells appearing unaffected, while others have a rough surface texture as a result of cell surface damage (blue arrows, Figure 8d, e). When exposed to concentrations of SQ53 equal to 60 μg/ml and above individual cells can be seen to have completely ruptured, with aggregated cellular debris visible (yellow arrows, Figure 8d, e, f).

This variation in visible impact shows that it is not necessary for the disinfectants tested to completely disrupt cell surface structural integrity in order to achieve growth inhibition. In addition, the varying disinfectant compounds within the formulation have a wide range of targets both intracellularly and at the bacterial surface (Table 3), so it is not surprising that the possible visible impacts of the formulation on each individual cell can vary.

'Deflated' *K. pneumoniae* cells and ruptured *S. aureus* cells have lost cell surface structural integrity, as a result of the membrane active components BAC, DDAC, PHMB and chlorocresol (Table 3) [41], [63], [64], [71], [82], [295]–[297]. The growth inhibition achieved in cells with no obvious visible damage may be attributed to the intracellular action of bronopol [100] or non-visible breaches in the permeability barrier of bacterial membranes leading to leakage of low molecular weight material and uncoupling of oxidative phosphorylation [41], [82]. Examination via TEM is required to further investigate the intracellular impact of SQ53 on bacterial cells.

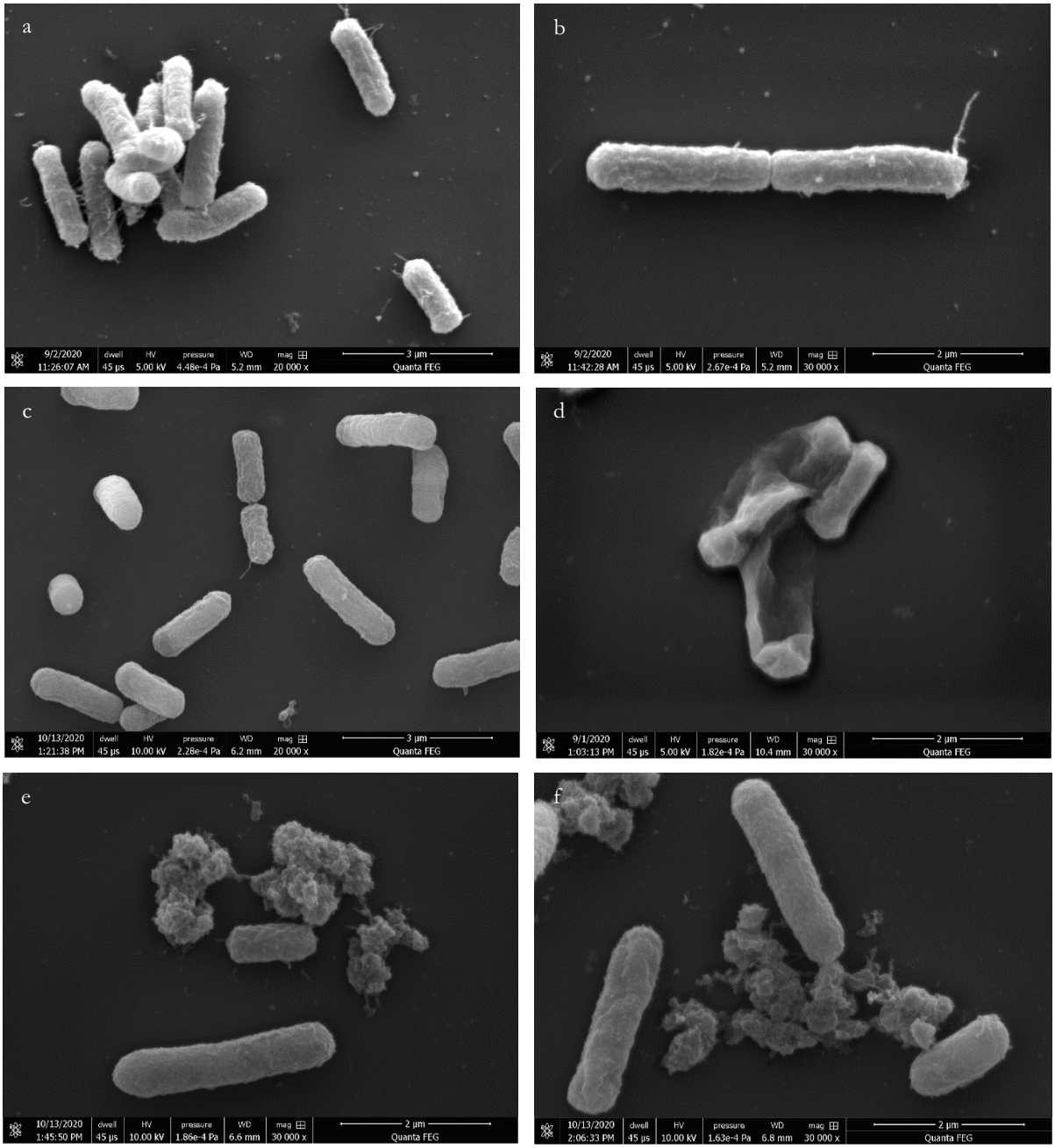

Figure 7. Scanning electron microscopy images of *Klebsiella pneumoniae* NCTC 13443 after 24-hour exposure to varying concentrations of disinfectant formulation "SQ53" (SQ53). a and b) untreated control. c) 100 µg/ml SQ53, 0.5 x MIC. d) 200 µg/ml SQ53, 1 x MIC. e) 300 µg/ml SQ53, 1.5 x MIC. f) 400 µg/ml SQ53, 2 x MIC. Images a, b and c are at 20,000 x magnification. Images d, e and f are at 30,000 x magnification. Scale bars are shown at the bottom right of each image, measured in µm.

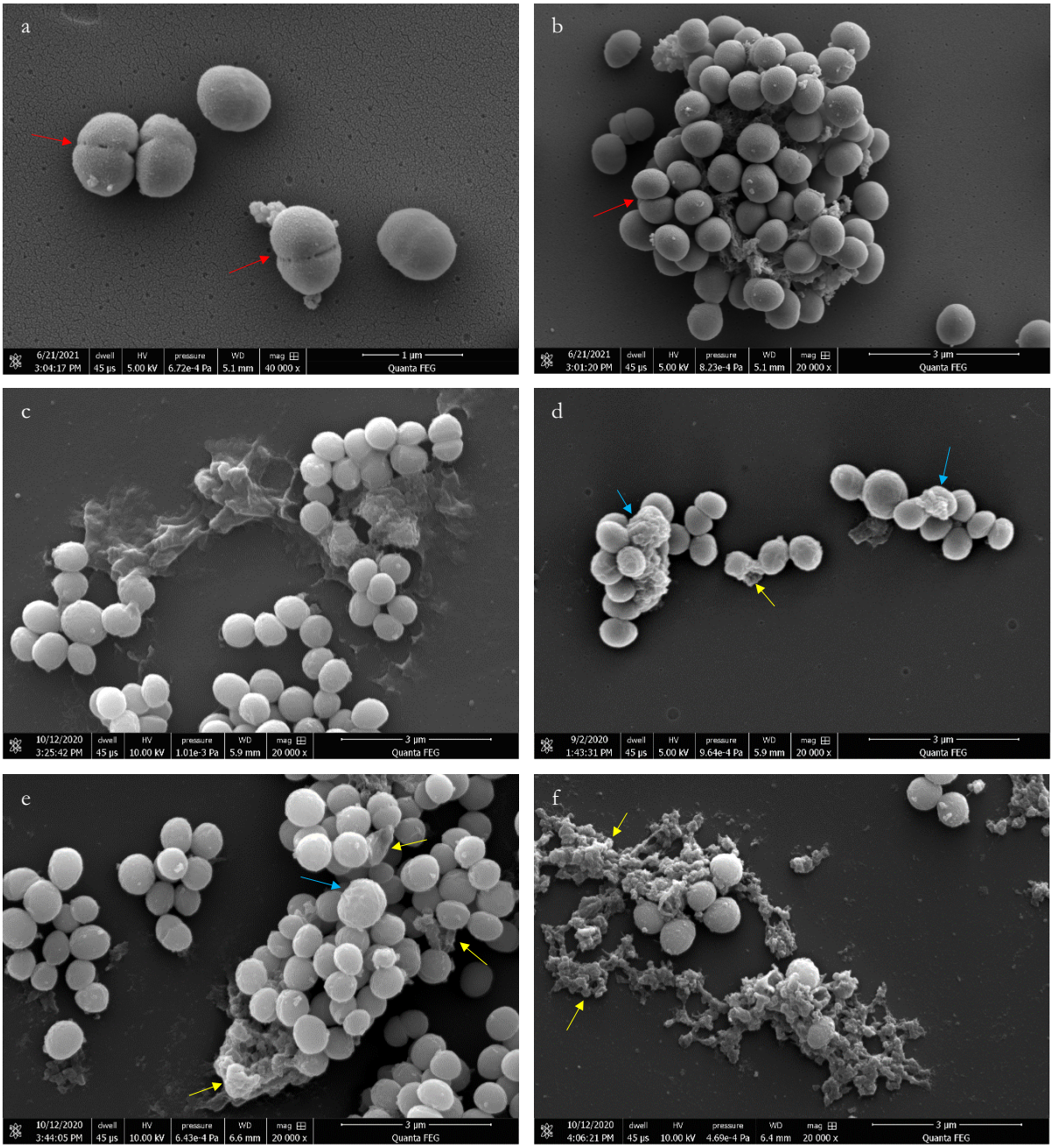

Figure 8. Scanning electron microscopy images of *Staphylococcus aureus* NCTC 13143 after 24-hour exposure to varying concentrations of disinfectant formulation "SQ53" (SQ53). a and b) untreated control. Red arrows indicate division septa. c) 30 µg/ml SQ53, 0.5 x MIC. d) 60 µg/ml SQ53, 1 x MIC. e) 90 µg/ml SQ53, 1.5 x MIC. f) 120 µg/ml SQ53, 2 x MIC. Blue arrows inidicate cells with a rough surface texture caused by damage inflicted by SQ53. Yellow arrows indicate cells that have completel ruptured as a result of SQ53 exposure. Image a is at 40,000 x magnification. Images b, c, d, e and f are at 20,000 x magnification. Scale bars are shown at the bottom right of each image, measured in µm. Coloured arrows indicate points of interest.

2.4.5. Visualisation of the mechanism of action of disinfectant formulation SQ53 via transmission electron microscopy

S. aureus cells have a spherical morphology with a high level of rotational symmetry, so the coccoid morphology of *S. aureus* is always visible irrespective of the orientation of the cells in relation to the plane of the thin section (Figure 9d). In contrast, *K. pneumoniae* cells have a rod morphology so are polarised and have limited rotational symmetry. As a result of this the orientation of the bacterial cells in relation to the plane of the cross-section heavily influences the shape of the cell in the image. This is why the distinct rod-shaped morphology of *K. pneumoniae* cells is not always visible when imaging via TEM (Figure 9a). In addition, both *K. pneumoniae* and *S. aureus* cells appear to vary in size as a result of cells differing in proximity to the plane of the thin section (Figure 9a, d).

TEM images of untreated *K. pneumoniae* and *S. aureus* show that the intracellular content of cells is uniformly electron-dense (Figure 9a, d). Membranes are visible due to osmium staining, which adds electron density and thus contrast in the final images [298]. The peptidoglycan cell wall is visible in both species, although it has a greater thickness in Gram-positive *S. aureus* as expected (Figure 9a, d).

In Figure 9a, one *K. pneumoniae* cell's plasma membrane can be seen to be withdrawing away from the peptidoglycan cell wall and outer membrane. This slight loss of volume and folding of the *K. pneumoniae* surface is the same as that seen in *K. pneumoniae* samples imaged via SEM (Figure 5), and is attributed to fixation artefacts and the dehydration steps during sample preparation [299], as described previously (Chapter 2.4.3.1).

In accordance with the SEM images, both *K. pneumoniae* and *S. aureus* cells display widely varying effects as a result of SQ53 exposure, with individual cells exhibiting minimal changes compared to untreated samples (red arrows, Figure 9b, e, f), while others display widespread cell surface disruption and a reduction in electron-dense intracellular content (blue arrows, Figure 9b, c, e, f). This variation in observable impact is attributed to the range of mechanisms utilised by the different active compounds in the SQ53 formulation (Table 3) resulting in circumstantial variation in the visible impacts of SQ53 on bacterial cells.

In *K. pneumoniae* cells where the impact is clearly visible, the plasma membrane can be seen to have ruptured as a result of the presence of membrane active disinfectants BAC, DDAC and PHMB (orange arrows, Figure 9b, c). Chlorocresol is also likely to have had a minor influence,

but its concentration is significantly lower in SQ53 than its MIC when used individually (Table 5).

The impact on *S. aureus* plasma membrane is difficult to distinguish due to its proximity to the cell wall. However, as cells have visibly ruptured and are losing intracellular content in both Figure 9e and f (orange arrows), it can be assumed that SQ53 is causing widespread disruption akin to that visible in *K. pneumoniae* cells (Figure 9b, c).

The intracellular content of *K. pneumoniae* cells that have ruptured are less consistent in electron density in comparison to untreated cells, consisting of small regions of electron-dense aggregates and large regions of empty space (Figure 9b, c). In addition, the *K. pneumoniae* peptidoglycan cell wall remains whole and intact even after SQ53 treatment, resulting in cellular debris remaining contained. This reflects the previous observations made of SEM images captured of *K. pneumoniae* exposed to BAC, DDAC, chlorocresol and SQ53, with the surface of the cellular structure intact but a loss of intracellular content causing the cells to appear deflated (Figure 5c, d e, f, k, l and Figure 7). As a result, this is attributed to the complete breakdown of the plasma membrane permeability barrier causing the condensing and aggregation of intracellular content, explaining the 'deflated' appearance of *K. pneumoniae* cells. The consistency of these images between cells exposed to BAC, DDAC and SQ53 indicate that the mechanism of action of BAC and DDAC are critical to the overall activity of the SQ53 formulation.

This condensing of intracellular content is visible in TEM images of SQ53-treated *S. aureus* cells too, although some cells can also be seen to be in the process of rupturing, with intracellular content spilling out from cells but not having yet aggregated (Figure 9e, f). Interestingly, incomplete sections of *S. aureus* peptidoglycan cell wall can be seen with no intracellular debris within (Figure 9e), indicating that SQ53 directly or indirectly causes *S. aureus* cell wall breakdown, in contrast to the structurally intact cell walls of *K. pneumoniae* as seen in Figure 9b and c. Furthermore, electron-dense aggregates consistent with the intracellular debris observed in *K. pneumoniae* cells after SQ53 exposure can be seen extracellularly in images of SQ53-exposed *S. aureus* samples (green arrows, Figure 9e, f). As the cell wall of *S. aureus* cells is broken down at the location of cell rupturing it seems likely that this is an indirect influence of SQ53, caused by the release of intracellular autolytic enzymes upon membrane rupturing. This has previously been suggested as a routine stage of surface-active disinfectant action once membrane integrity has been impeded [300]. However, it is unclear why this effect is limited to *S. aureus* and not observed in *K. pneumoniae*.

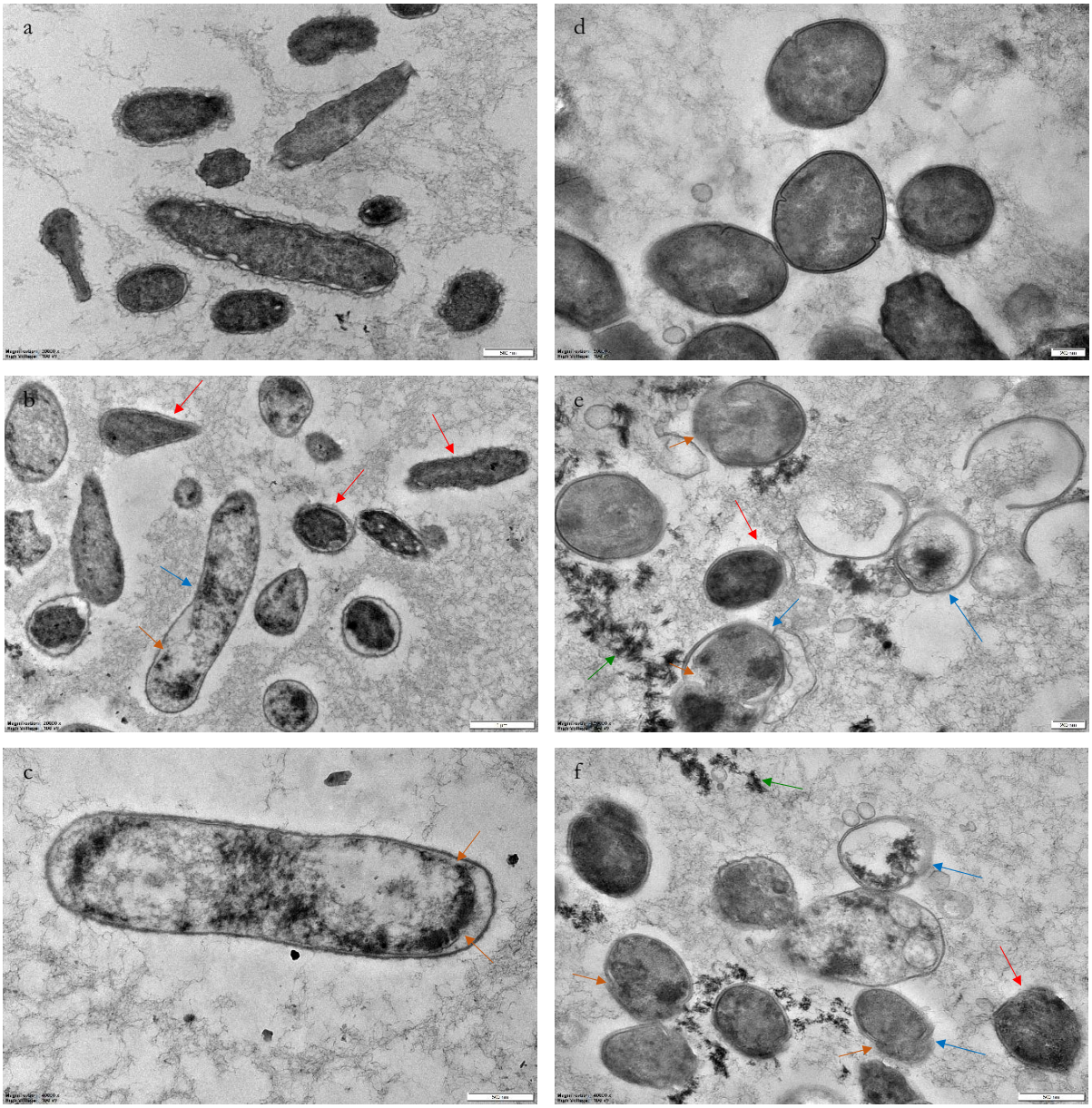

Figure 9. Transmission electron microscopy images of *Klebsiella pneumoniae* NCTC 13443 and *Staphylococcus aureus* NCTC 13143 after 24-hour exposure to the disinfectant formulation "SQ53" (SQ53) at their respective MICs. a) *Klebsiella pneumoniae* untreated control. b and c) *Klebsiella pneumoniae* exposed to 200 µg/ml SQ53. d) *Staphylococcus aureus* untreated control. e and f) *Staphylococcus aureus* exposed to 60 µg/ml SQ53. Red arrows indicate individual cells that demonstrate minimal changes in comparison to untreated control samples. Blue arrows indicate cells that demonstrate surface disruption and a reduction in electron-dense intracellular content. Orange arrows indicate the rupturing of the plasma membrane. Green arrows indicate electron-dense aggregated intracellular debris. Image a is at 30,000 x magnification. Image b is at 20,000 x magnification. Images c and f are at 40,000 x magnification. Images d and e are at 50,000 x magnification.

2.5. Conclusions

The antimicrobial activities of disinfectants varies depending on the mechanism of action of the disinfectant [41], [82], [107], the species and strain tested upon [107], [260]–[262] and the methodology used [224], [263]–[265]. The efficacies of the disinfectants to be investigated had not been fully characterised against the specific strains and species to be tested. As a result, it is pertinent to establish the initial antimicrobial activities of the full range of disinfectants and bacterial strains to be used. Additionally, relying on in-house data ensured that the results are reproducible and consistent across all tested strains, rather than results reported in the literature that may only be accurate to other strains or methodologies.

BAC, DDAC, PHMB and bronopol demonstrated a higher level of efficacy than chlorocresol across all species tested, likely by account of chlorocresol having a weaker affinity to the target site [284]. QACs displayed a higher level of activity against Gram-positive bacteria compared to Gram-negative bacteria, in accordance with the literature [273]–[276]. This is due to the outer membrane of Gram-negative bacteria providing an additional permeability barrier to prevent the action of QACs, mitigating their efficacy. Conversely, bronopol and chlorocresol demonstrated an increased efficacy against the Gram-negative bacterial species tested in comparison to the Gram-positive species tested. This observation has been reported in the literature previously with regards to bronopol [98], [99], [277], but remains unexplained and is contested by results from other publications [101], [278], [279]. As a result of the lack of consensus in the literature and the small number of species tested in this study, we are unable to conclusively confirm if this observation is a result of random variation or not.

The MIC values achieved by disinfectants used in combination were lower than when used individually when tested against *A. baumannii*, *E. faecalis* and *S. aureus*. This suggests that these disinfectants have a beneficial interaction when combined together, although the nature of these interactions remain to be elucidated. Interestingly the concentration of PHMB in SQ53 at its MIC against *K. pneumoniae* was higher than its MIC when acting independently, potentially indicating an antagonistic interaction. However, as the difference was less than 1 μg/ml this cannot be stated with certainty from this experiment alone. This work is expanded upon in Chapter 3, whereby the types of combined antimicrobial activities displayed by these disinfectants are defined.

Disinfectants that operate via the disruption of bacterial membranes (BAC, DDAC, PHMB and chlorocresol) demonstrated a visible impact on *K. pneumoniae* and *S. aureus* cells when imaged via SEM. In general, the outer surfaces of imaged bacteria displayed evidence of perturbation and

breaches in structural integrity, in accordance with the literature [64], [103], [290]. Individual cells were also observed to have lost intracellular volume and, in extreme cases, only aggregated cellular debris remained. In contrast, bronopol acts via the formation of disulphides in protein structures [99] and the generation of ROS as a secondary mechanism [100], neither of which have an observable effect on *K. pneumoniae* and *S. aureus* cells when imaged via SEM.

The disinfectant formulation SQ53 showed a wide range of visible effects on both *K. pneumoniae* and *S. aureus* cells, with some displaying no visible effect while other cells ruptured. This demonstrates that disinfectants do not necessarily need to completely impede the structural integrity of cells in order to inhibit growth, and illustrates the broad range of activities that disinfectants employ to achieve inhibition. TEM revealed the condensing and aggregation of intracellular content of bacterial cells that experienced membrane breakdown. Interestingly, we observed that the peptidoglycan cell wall of *K. pneumoniae* did not undergo autolysis after cells ruptured, unlike *S. aureus*.

The data compiled and presented in this chapter provides the core understanding of the mechanisms of action of these disinfectants when targeting the selected species. This basis was critical to establish before moving forward to further experiments detailed in later chapters.

3. Synergism vs Additivity - Defining the Interactions between Common Disinfectants

Note: Data in this chapter has undergone peer review and has been published. As such, some passages have been quoted verbatim from the following source:

Noel DJ, Keevil CW, Wilks SA. 2021. Synergism versus Additivity: Defining the Interactions between Common Disinfectants. mBio. Vol. 12, Issue 5. DOI: https://doi.org/10.1128/mBio.02281-21 [301]

In addition, this chapter is formatted in accordance with mBio formatting guidelines. As a result, the format of this chapter varies from the others within this thesis, as described here. This chapter contains separate Abstract (Chapter 3.1), Importance (Chapter 3.2) and Chapter discussion (Chapter 3.5.3) sections, and the aims of the chapter are integrated into the end of the chapter Introduction (Chapter 3.3).

3.1. Abstract

Many of the most common disinfectant and sanitizer products are formulations of multiple antimicrobial compounds. Products claiming to contain synergistic formulations are common, although there is often little supporting evidence. The antimicrobial interactions of all pairwise combinations of common disinfectants (benzalkonium chloride (BAC), didecyldimethylammonium chloride (DDAC), polyhexamethylene biguanide (PHMB), chlorocresol and bronopol) were classified via checkerboard and validated by time-kill analyses. The underlying mechanism of synergistic combinations were further investigated via scanning electron microscopy (SEM). Combinations were tested against *Acinetobacter baumannii* NCTC 12156, *Enterococcus faecalis* NCTC 13379, *Klebsiella pneumoniae* NCTC 13443 and *Staphylococcus aureus* NCTC 13143. Synergistic interactions were only identified between chlorocresol with BAC, and chlorocresol with PHMB. Synergism was not ubiquitously demonstrated against all species tested and was on the borderline of the synergism threshold. When observed via SEM, synergism between BAC and chlorocresol displayed no unique observable influence on bacterial cells, whereas synergism between chlorocresol and PHMB caused the formation of elongated chains of *Enterococcus faecalis* displaying aberrant septation. Overall, these data demonstrate that synergism between disinfectants is uncommon and circumstantial. Most of the antimicrobial interactions tested were characterised as additive. We suggest that this is due to the broad, non-specific mechanisms associated with disinfectants not providing opportunity for the combined activities of these compounds to exceed the sum of their parts.

3.2. Importance

The scarcity of observed synergistic interactions suggests that many disinfectant-based products may be misinterpreting combined mechanisms of interaction. We emphasise the need to correctly differentiate between additivity and synergism in antimicrobial formulations, as inappropriate classification may lead to unnecessary issues in the event of regulatory changes. Furthermore, we question the need to focus on synergism and disregard additivity when considering combinations of disinfectants, as the benefits that synergistic interactions provide are not necessarily relevant to the application of the final product.

3.3. Introduction

The properties and MOA of common disinfectants have been examined on pathogenic bacteria associated with HAIs. However, many commercially available disinfectant products used in healthcare, households and industry are formulations consisting of multiple disinfectants. The reasons behind the prevalence of disinfectant formulations were discussed comprehensively in Chapter 1.5. In brief, disinfectant regulations have inadvertently made it financially unfavourable to develop and register novel disinfectants [240]. In order to establish intellectual property a company requires a patent, which requires a disinfectant formulation to be novel [302]. As a result, disinfectant formulations typically contain a "novel" formulation of currently approved disinfectants. Furthermore, a successful patent application requires the demonstration of an "inventive step", which can be achieved through an "unexpected property" [302]. In this case of disinfectant formulations, synergy between two or more disinfectants in the formulation is deemed unexpected, so provides grounds for a patentable product [240]. A further benefit is provided by the increased marketability the "synergy" buzzword brings. Collectively this provides a commercial incentive to classify such formulations as synergistic.

It is commonly assumed that synergistic interactions occur between antimicrobials with different mechanisms of action and target sites, however the definitive classification of antimicrobial interactions presents many challenges. Inconsistencies in classification can be introduced through a variety of means.

Firstly, definitions of antimicrobial interactions are not universally adhered to. For the purposes of this thesis the definitions used conform to the definitions laid out by EUCAST [253], as described in Chapter 1.3.1 and presented in the List of definitions. Briefly, if the activity of both components combined is equal to the activity of the most active component, it is indifferent [253]. If both antimicrobials combined have an activity of no greater than the sum of their parts, they are additive [253]. Synergism is achieved if the combined activity is greater than the sum of the individual activities, and antagonism is achieved if combined activity is lower than the most active component [253].

However, many leading journals do not accept these definitions [250], [252], even suggesting the use of alternative terms such as "nonsynergistic" [251]. This collectively leads to both industrial and academic research focusing exclusively on synergistic interactions and disregarding all other interactions as unimportant.

Additional inconsistencies in the classification of antimicrobial interactions can be introduced depending on the methodology employed [241]–[244]. The most common methodology used is the checkerboard method; a two-dimensional version of the broth microdilution method that examines varying combinations of two antimicrobials diluted along perpendicular axes of a 96-well plate. However, the outcome of the checkerboard method varies depending on the method of interpretation and FICI thresholds used [245], which are often inconsistent and occasionally not even reported in publications. Specific academic journals have implemented FICI threshold standards for checkerboard data [250]–[252], however these are not universally adhered to between journals. Further variation in classification arises depending on the species or strain tested upon when examining combinations of antibiotics [248], [249] and disinfectants [246], [247].

Collectively, these factors have led to inconsistencies and confusion when attempting to distinguish between additive and synergistic interactions. It is unsurprising that the two terms are often used interchangeably and erroneously.

With these issues in mind, this study classifies the nature of the interactions between antimicrobials that are commonly used in disinfectant and sanitizer formulations. The MOA of compounds examined in this study are overviewed in Table 2 alongside their applications. Previous research has indicated variability between species and strains [246]–[249], therefore clinically-relevant bacterial species that display a degree of antibiotic resistance were selected in order to provide a stringent test. In addition, strict activity classification thresholds were used to provide clarity and to maintain consistency with the standards set by leading journals in the field [250]–[252]. Additivity was included as a classification due to the context of the test.

Synergistic combinations identified via the checkerboard methodology were validated via time-kill assay. SEM imaging was conducted in order to visualise and elucidate the underlying synergistic interaction. A comprehensive explanation of the methods used can be found in Chapter 3.4.

3.4. Materials and methods

Acinetobacter baumannii NCTC 12156, *Enterococcus faecalis* NCTC 13379, *Klebsiella pneumoniae* NCTC 13443 and *Staphylococcus aureus* NCTC 13143 were cultured as described in Chapter 2.3.1. The justification for the use of these strains is also described in Chapter 2.3.1. Details on the disinfectants utilised and the justification for their use are overviewed in Chapter 2.3.2.

3.4.1. Checkerboard assay

The checkerboard assay was used to determine the combined activities of antimicrobial compounds in combination. Each well of a 96-well plate contained a final volume of 200 µl. Arrangements of antimicrobial compounds were made whereby one compound was serially-diluted twofold on the horizontal axis and another on the vertical axis, with final concentrations ranging from 4 x to 1/128 x MIC, as identified previously in Chapter 2.4.1 (Table 4). Once prepared, each checkerboard plate had 4 sterility controls, 5 growth controls, 10 different concentrations of antimicrobial A alone, 7 different concentrations of antimicrobial B alone, and 70 different combinations of both antimicrobials A and B combined. Checkerboard were plates performed in biologically-independent triplicates and were incubated overnight at 37°C. The OD584 values of each well were measured using a BMG Labtech FLUOstar Optima microplate reader.

3.4.2. Checkerboard analysis

After normalisation, wells that demonstrated an OD584 increase of ≥ 0.1 were considered positive for bacterial growth. Classification of the interaction of any two antimicrobials is based on the fractional inhibitory concentration (FIC):

$$\frac{A}{MIC_A} = FIC_A$$

Where A is equal to the MIC of compound A when in combination and MIC_A is equal to the MIC of compound A when alone.

FIC Index (FICI) values were calculated as the FIC_A + FIC_B from the same well. FICI values were deduced for all non-turbid wells along the turbidity/non-turbidity interface, as described by Bonapace *et al.* (2002) [245]. The lowest FICI value was used to characterise the interaction between the two antimicrobial compounds. FICI values were averaged and the 95% confidence interval (CI) values were calculated. Average FICI values were used to interpret combined antimicrobial activity, counting as synergistic if FICI ≤ 0.5, additive if 0.5 < FICI ≤ 1.0,

indifferent if 1.0 < FICI ≤ 4 and antagonistic if FICI > 4.0. These commonly-used thresholds were selected to maintain comparability with other academic publications [250]. Thresholds for additivity were included as non-selective, broad-activity disinfectants were being tested. 95% CI values were used to demonstrate the certainty of the combined antimicrobial activities that were inferred from these data.

3.4.3. Time-kill assay

For further validation, disinfectant combinations that were identified as synergistic via the checkerboard method were tested for synergy via time-kill assays as described by CLSI [303]. MHB cultures containing 5 x 10^5 CFU/ml bacteria were exposed to either both antimicrobial compounds, one of the compounds alone or neither as a growth control. Antimicrobial concentrations were equal to those present in the well containing the lowest FICI value in the checkerboards previously conducted. Cultures had a final volume of 20 ml, with MHB used as the culture medium. Aliquots were taken at 0-, 1-, 3-, 6-, 12- and 24-hour time-points and the number of CFUs were quantified via culture analysis. All test conditions were conducted in triplicate.

A synergistic interaction was characterised as demonstrating a ≥2 $\log_{10}$ reduction in CFU/ml between the combination and its most active constituent alone after 24 hours. In addition, the number of CFU/ml must demonstrate a decrease of ≥ 2 $\log_{10}$ CFU/ml below the starting inoculum when exposed to the antimicrobial combination.

3.4.4. Scanning electron microscopy

SEM imaging was utilised to visualise the impact of synergistic combinations of disinfectants as identified previously. *E. faecalis* NCTC 13379 samples were incubated overnight at 37°C in MHB while exposed to varying disinfectant conditions. Samples were exposed to either 2 μg/ml BAC, 2 μg/ml PHMB, 125 μg/ml chlorocresol, both 2 μg/ml BAC and 125 μg/ml chlorocresol or both 2 μg/ml PHMB and 125 μg/ml chlorocresol. *S. aureus* NCTC 13143 samples were incubated overnight at 37°C in MHB while exposed to either 1 μg/ml BAC, 100 μg/ml chlorocresol or both 1 μg/ml BAC and 100 μg/ml chlorocresol. Untreated control samples were also prepared in the absence of disinfectant treatment. Sample preparation and imaging steps were performed as described in Chapter 2.3.4.1.

3.5. Results and discussion

3.5.1. Elucidating the antimicrobial interactions between pairs of disinfectants

Many antimicrobial products used in medical, industrial and domestic environments consist of formulations of multiple individual disinfectants. Claims are often made regarding the synergistic mechanism of such formulations based on the various compounds present in the solution demonstrating varying mechanisms of action.

Despite these claims there is limited evidence to support the synergistic interactions between many of the most common disinfectants. In addition, previous reports indicate that the various methods employed to investigate these interactions can produce inconsistent results [241]–[244], and varying thresholds are often implemented to distinguish between synergistic, additive or indifferent mechanisms which can ultimately lead to variation between publications [304]–[306].

For example Soudeiha *et al.* reports an 'additive' interaction between colistin and meropenem when tested against *A. baumannii* clinical isolates *in vitro*, with 'additive' FICI values ranging from 0.61 to 1.83 [304]. In contrast, when the same antimicrobial combination was tested against *A. baumannii* clinical isolates by Oliva *et al.*, many of the interactions were reported as 'indifferent', despite the FICI values often being lower than those reported by Soudeiha *et al.* [304], [305]. These discrepancies in the classification of antimicrobial interactions are simply due to different thresholds being used.

In addition, neither of the studies explicitly define the terms used (synergy, additive or indifference) to classify the antimicrobial interaction between colistin and meropenem [304], [305]. Another similar study on the same antimicrobials conducted by Kheshti *et al.* reported FICI values of between 0.5 and 1 as "partial synergism" [306]. The lack of clarification introduces additional ambiguity and hinders the ability to draw an overall conclusion between the published reports [304]–[306]. While these examples investigate antibiotics specifically, the underlying issues extend to all antimicrobial interactions that are examined via the checkerboard methodology.

Collectively, these factors could lead to the incorrect classification of a combined antimicrobial activity. This is significant as it may result in consumers placing too much faith in a product, leading to potential inappropriate and ineffective usage. The goal of this study was to investigate the type of interactions between common disinfectants present in formulations.

The nature of the interactions between 5 common disinfectants when used in pairwise combinations were classified via the widely used checkerboard method. The characteristics of the antimicrobial compounds used in this study are established in Chapter 2.4. A synergistic interaction between BAC and chlorocresol was observed against *E. faecalis* and *S. aureus*, and between PHMB and chlorocresol against *E. faecalis* (Table 6 and Figure 10). The synergism demonstrated in all cases is considered borderline as the FICI value was 0.5, equal to the threshold of synergism. Additionally, these combinations did not demonstrate synergism against *A. baumannii* or *K. pneumoniae*, indicating that this synergistic mechanism is species-specific.

These synergistic combinations were tested further via the time-kill methodology. The antimicrobials combined resulted in a ≥5 log reduction in CFU/ml after 24 hours compared to when they were used individually, confirming synergistic interactions (Figure 11).

By observing the range of FICI values covered by the 95% CIs, it is possible that other interactions are potentially synergistic, as shown in Table 6 and Figure 10. However, the likelihood of these combinations being truly synergistic is low when considering the lack of any variability observed in the confirmed synergistic interactions (Table 6 and Figure 10). This uncertainty further highlights the variability of the checkerboard method whe attempting to classify antimicrobial interactions. To overcome this, further biological replicates should be conducted to improve data accuracy.

Indifferent mean average FICI values were observed in various combinations that contained bronopol, although it is important to note that these indifferent interactions were not consistent across the species tested (Table 6 and Figure 10). It has previously been reported that BAC and bronopol synergistically inhibit sulphide production in sulphate-reducing bacteria [307]. As antimicrobial activity was measured via sulphide production it is difficult to draw comparisons between the results. This variation between reports further demonstrates that disinfectant interactions are not ubiquitous and vary in nature depending on the test species and methodologies used.

When considering the 95% CIs, it is possible that a further 5 combinations of disinfectants may have indifferent interactions rather than additive interactions (Table 6 and Figure 10). Once again, this highlights the variability of the checkerboard methodology, and could be overcome by conducting additional biological replicates.

Interestingly, it was observed that every combination of cationic membrane-active antimicrobial (BAC, DDAC, PHMB) interacted additively across all species tested, with mean average FICI

values ranging consistently between 0.54 and 1.00. This suggests that disinfectants with similar mechanisms and cellular targets (Table 2) consistently benefit from being in combination, although not to the point of synergism. We propose that this is due to similar-acting compounds having a limited but consistent scope to complement each other's activities when used in combination. At the sub-lethal concentrations tested, the cationic membrane-active compounds all disrupt membrane stability and cause intracellular leakage [41], [82], [103], and thus will each mechanistically benefit from the presence of the other. With broadly overlapping mechanisms the combined activity never has the opportunity to be greater than the sum of its parts, therefore the interaction is limited to additivity.

Of the 40 test conditions tested, 30 demonstrated an additive interaction against the respective target species (Table 6). In addition, all disinfectant combinations demonstrated at least one additive interaction against the various species. We believe that the abundance of additive antimicrobial interactions is due to the broad, non-selective mechanisms demonstrated by disinfectants. The wide range of cellular targets and high level of activity leaves little room for other additional disinfectant compounds to provide a suitably varying mechanism that would enable a synergistic interaction. As a result, any combined activities would simply be accumulative and would rarely ever be greater than the sum of its parts. Thus, the majority of the interactions observed are additive. We therefore postulate that finding synergistic combinations of antimicrobials is more challenging when investigating compounds that have non-specific, broad mechanisms (for example disinfectants) than those that have more specific mechanisms of action (antibiotics).

Table 6. Combined antimicrobial activities of pairwise combinations of five common disinfectants. FICI: fractional inhibitory concentration index. CI: 95% confidence interval. BAC: benzalkonium chloride. DDAC: didecyldimethylammonium chloride. PHMB: polyhexamethylene biguanide hydrochloride. A: additive (0.5 < FICI ≤ 1.0). I: indifferent (1.0 < FICI ≤ 4.0). S: synergistic (FICI ≤ 0.5). * denotes uncertainty due to CIs crossing combined antimicrobial activity FICI thresholds. n=3.

Disinfectant A	**Disinfectant B**	***Acinetobacter baumannii* NCTC 12156**			***Enterococcus faecalis* NCTC 13379**			***Klebsiella pneumoniae* NCTC 13443**			***Staphylococcus aureus* NCTC 13143**		
		FICI	**CI**	**Activity**	**FICI**	**CI**	**Activity**	**FICI**	**CI**	**Activity**	**FICI**	**CI**	**Activity**
BAC	DDAC	0.75	0.00	A	0.75	0.00	A	0.54	0.04	A*	0.54	0.04	A*
	PHMB	0.71	0.18	A	0.71	0.18	A	0.83	0.36	A*	1.00	0.00	A
	Bronopol	2.00	0.00	I	0.75	0.00	A	2.00	0.00	I	2.00	0.00	I
	Chlorocresol	0.64	0.27	A*	0.50	0.00	S	0.71	0.18	A	0.50	0.00	S
DDAC	PHMB	0.65	0.24	A*	1.00	0.00	A	0.71	0.18	A	0.94	0.41	A*
	Bronopol	2.00	0.00	I	1.00	0.00	A	1.00	0.00	A	1.00	0.00	A
	Chlorocresol	1.00	0.00	A	0.57	0.15	A*	0.83	0.36	A*	1.00	0.00	A
PHMB	Bronopol	2.00	0.00	I	1.00	0.00	A	0.58	0.18	A*	0.83	0.36	A*
	Chlorocresol	0.63	0.00	A	0.50	0.00	S	0.63	0.29	A*	0.75	0.00	A
Bronopol	Chlorocresol	1.00	0.00	A	0.92	0.36	A*	2.00	0.00	I	3.00	0.00	I

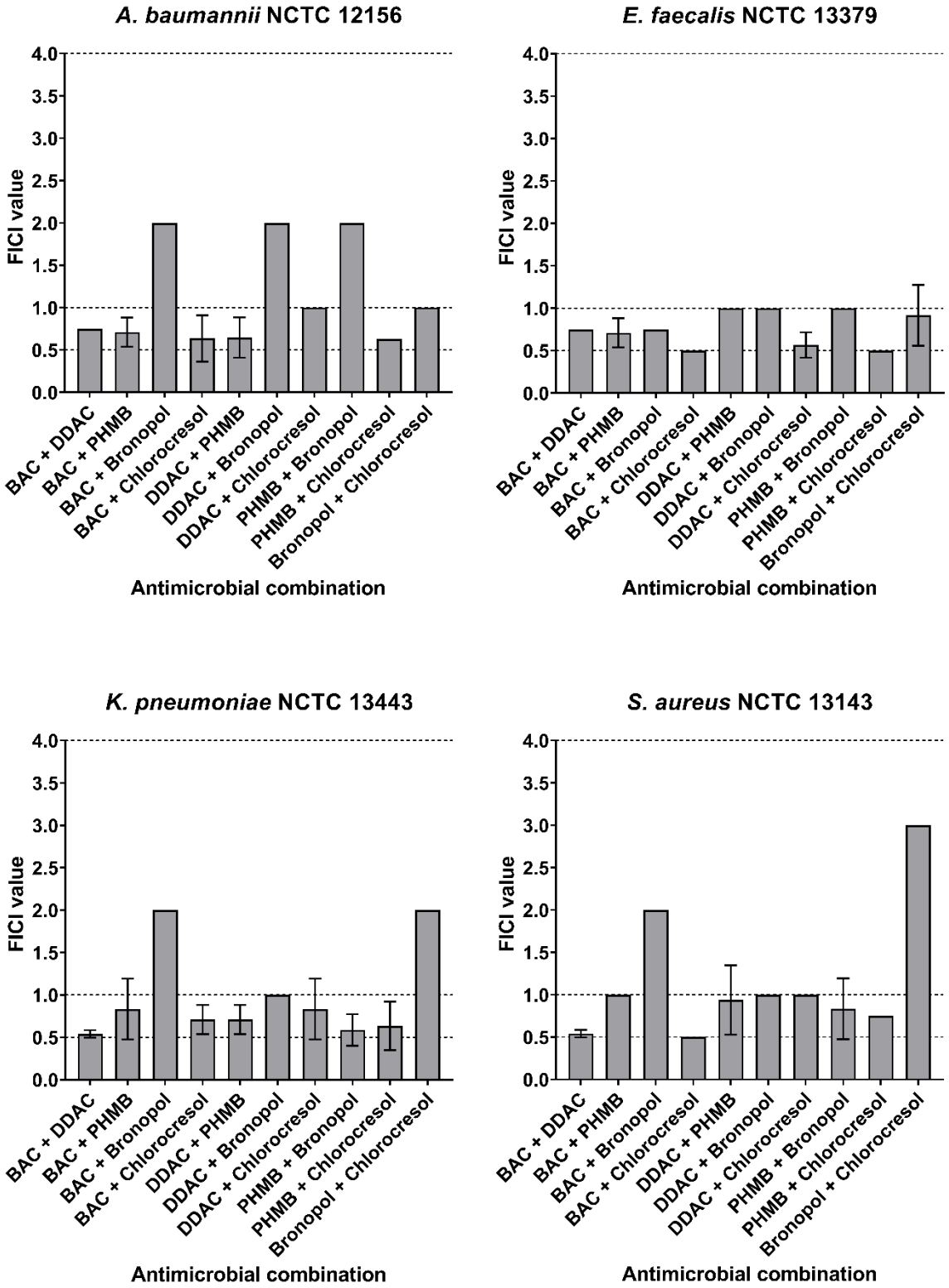

Figure 10. Fractional inhibitory concentration Indices (FICIs) of combinations of five common antimicrobial disinfectants. Error bars show 95% confidence intervals. BAC: benzalkonium chloride. DDAC: didecyldimethylammonium chloride. PHMB: polyhexamethylene biguanide hydrochloride. Dotted lines depict the thresholds between synergism (FICI ≤ 0.5), additivity (0.5 < FICI ≤ 1.0) and indifference (1.0 < FICI ≤ 4.0). n=3.

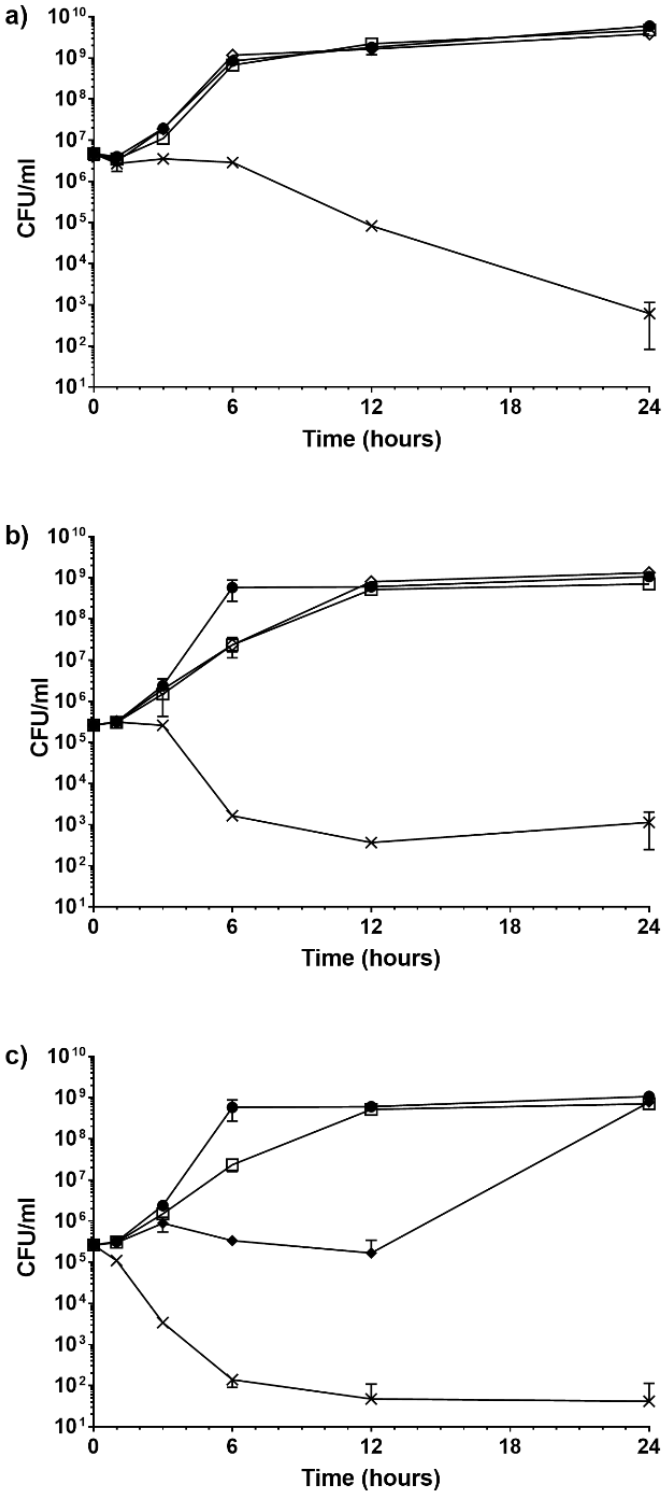

Figure 11. Time-kill curves of synergistic combinations of common disinfectants. a) *Staphylococcus aureus* NCTC 13143 exposed to a combination of benzalkonium chloride (BAC) and chlorocresol. •, growth control; ◇, 0.0001% v/v BAC; □, 0.01% v/v chlorocresol; X, 0.0001% v/v BAC and 0.01% v/v chlorocresol in combination. b) *Enterococcus faecalis* NCTC 13379 exposed to a combination of BAC and chlorocresol. •, growth control; ◇, 0.0002% v/v BAC; □, 0.0125% v/v chlorocresol; X, 0.0002% v/v BAC and 0.0125% v/v chlorocresol in combination. c) *Enterococcus faecalis* NCTC 13379 exposed to a combination of polyhexamethylene biguanide (PHMB) and chlorocresol. •, growth control; ◆, 0.0002% v/v PHMB; □, 0.0125% v/v chlorocresol; X, 0.0002% v/v PHMB and 0.0125% v/v chlorocresol in combination. Error bars show standard deviation. n=3.

3.5.2. Visualisation of synergistic combinations of disinfectants via scanning electron microscopy

E. faecalis cells are characterised by their lancet shape and are often found in pairs, as shown when viewed via SEM (Figure 12a). Other than the stage of cell division, *E. faecalis* cells are consistent in shape and size.

When exposed to 2 μg/ml BAC (Figure 12b) and 125 μg/ml chlorocresol (Figure 12c), *E. faecalis* cells demonstrated little variation from cells imaged in the untreated control sample (Figure 12a), with a consistent size and shape. This is expected as the concentrations are below the respective MICs (Table 4), so most bacterial cells will remain viable. Some individual *E. faecalis* cells appear to have completely lysed, with only aggregated cell debris or membrane husks remaining (red arrows, Figure 12b, c). This cellular debris is visually similar to the debris seen when *S. aureus* cells were exposed to MICs of BAC (Figure 6c, d) and chlorocresol (Figure 6k, l) respectively. This indicates that although the concentrations of BAC and chlorocresol are not high enough to inhibit the growth of all *E. faecalis* cells in the culture, some individual cells still succumb to the biocidal impacts of the disinfectants. The similarity of the debris between species demonstrates the consistency of the mechanism of antimicrobial action.

In comparison, *E. faecalis* exposed to both 2 μg/ml BAC and 125 μg/ml chlorocresol were consistent in size and shape with the other conditions, but appear more textured (Figure 12d). Previously, increased surface texture has been attributed to a loss or condensing of intracellular content, likely as a result of a loss of membrane integrity. TEM would be required to visualise intracellular variation between the different treatments but is outside the scope of the present work. Spaces can be seen between bacteria as a result of cells shrinking during the critical point drying step (Figure 12d) [286].

E. faecalis exposed to 2 μg/ml PHMB also displays no significant morphological changes when compared to the untreated control sample (Figure 13b). 2 μg/ml PHMB is below the MIC in this treatment, so no visible impact on the cells is expected.

When treated with both 2 μg/ml PHMB and 125 μg/ml chlorocresol, *E. faecalis* exhibits a more rounded or domed morphology, and forms elongated chains of cells with aberrant septation (Figure 13d). Previous studies have suggested that the manipulation of membrane content can result in the incorrect localisation of cell replication machinery [308], [309], leading to asymmetric and irregular chains of bacteria [310]. Furthermore, Patel *et al.* (2006) observed that *Bacillus subtilis* cells that have experienced irregular septation have had their DNA condensed,

which has been suggested by Chindera *et al.* as a secondary mechanism of PHMB activity [73]. Collectively the implication is that this observed aberrant septation morphology is a result of a combination of factors; the perturbation of membrane integrity by both PHMB and chlorocresol and the condensing of microbial DNA via PHMB. It is therefore suggested that the decreased membrane integrity caused by the presence of chlorocresol may facilitate a greater uptake of PHMB, giving rise to the observed synergistic effect.

S. aureus cells, as previously described, have a regular coccoid shape. Once again, the division septum can be seen on individual cells undergoing the cell cycle (red arrows, Figure 14a). Some cells exhibit occasional small bud-like projections of varying size (blue arrows, Figure 14a).

S. aureus cells exposed to 1 μg/ml BAC demonstrate a higher frequency of bud-like projections on their surface as a result of blebbing caused by BAC (blue arrows, Figure 14b). Otherwise, the cells display little variation in consistency of size and morphology compared to the untreated control sample.

When exposed to 100 μg/ml chlorocresol there were a lower frequency of *S. aureus* cells undergoing division with the few division septa present being barely visible (Figure 14c). Studies conducted by Srivastava and Thompson report the potential for phenols to act specifically on dividing cells at the point of separation [311], [312], potentially explaining the lack of cells visibly undergoing later stages of division. In a series of studies published by Joseph Judis on the mechanism of action of phenol it is suggested that cell membrane disruption prevents energy production and thus arrests cell division [87]–[89]. This was later supported in studies that demonstrated that fentichlor causes an increase in proton permeability and thus resulting in loss of proton motive force and the uncoupling of oxidative phosphorylation in *S. aureus* cells [92], [93]. Chlorocresol is known to act similarly to fentichlor [94], so collectively these studies suggest that the lack of cell division visible in the SEM images are a result of chlorocresol action, even at concentrations below the MIC.

S. aureus exposed to both 1μg/ml BAC and 100 μg/ml chlorocresol have an inconsistent size and shape in comparison to untreated *S. aureus* cells (Figure 14d). There is also a low frequency of cells that have undergone cell division, with those that have being arrested in the early stages of division septa formation (Figure 14d). This is due to the bacteriostatic action of chlorocresol as discussed previously. The surfaces of the cells display a high number of bud-like projections (blue arrows, Figure 14d), similar to those seen in Figure 14b. This is a result of the membrane-active action of BAC, likely enhanced by the membrane perturbation achieved by chlorocresol.

These observations are characteristic of *S. aureus* cells impacted by each of the disinfectants individually, but in the case of BAC with a higher severity. This indicates that the synergistic activity of BAC and chlorocresol combined are not a result of a unique combined activity, but instead an enhancement of their individual mechanisms.

Synergy is broadly defined as the combined activity being greater than the sum of its parts [253]. These SEM images of synergistic pairs of disinfectants reveal that only 1 of the observed combinations (PHMB and chlorocresol) demonstrated a distinct mechanism that was unique to the disinfectant combination. The synergistic activity between BAC and chlorocresol was either a result of enhancement of the individual disinfectant's efficacies or simply not visible via SEM. Characterisation of the intracellular content of bacteria effected by synergistic interactions would be required for further insight, however this is outside of the scope of the current work.

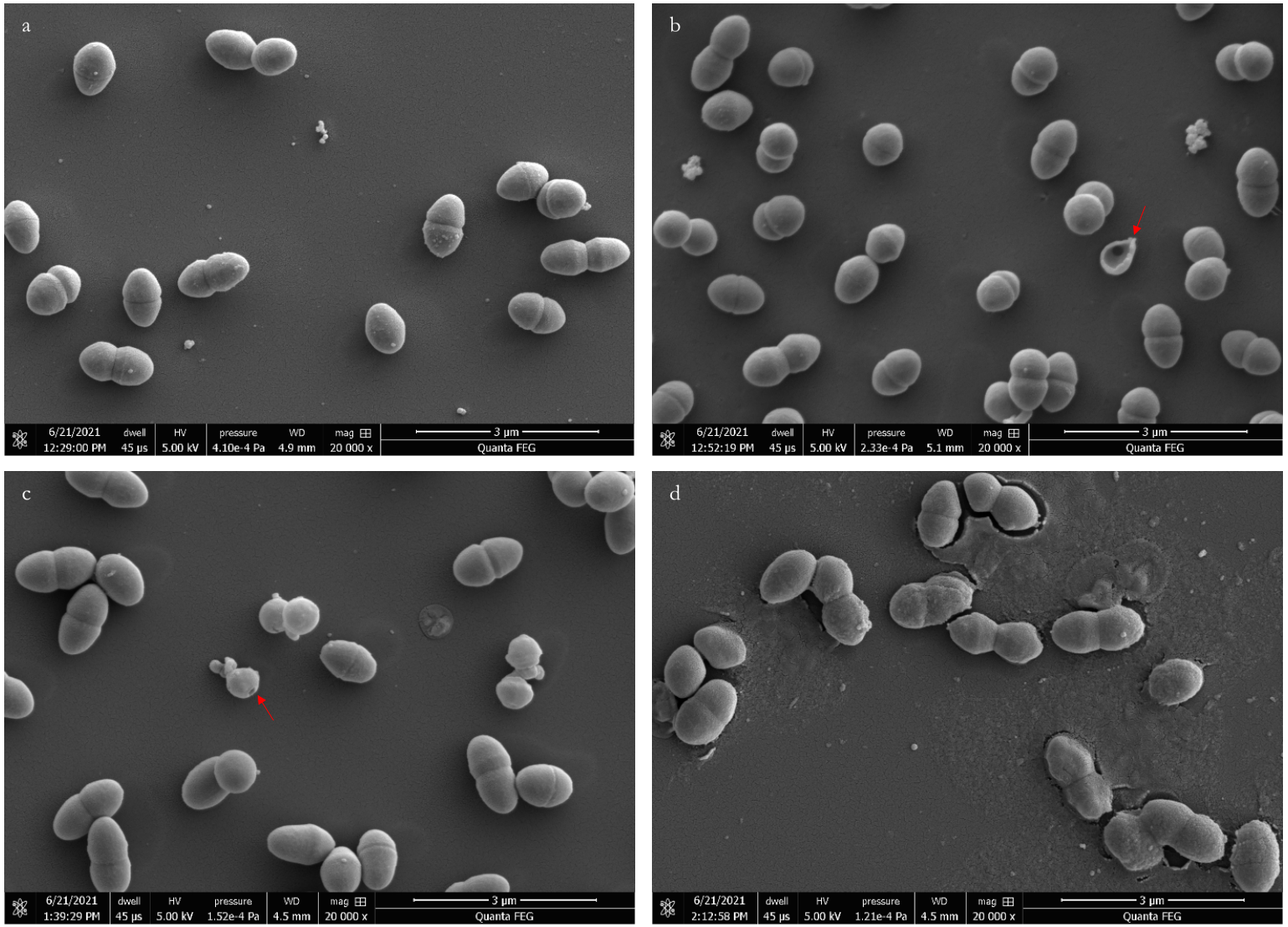

Figure 12. Scanning electron microscopy images of *Enterococcus faecalis* NCTC 13379 after 24-hour exposure to varying combinations of sub-inhibitory concentrations of benzalkonium chloride (BAC) and chlorocresol. a) Untreated control. b) 2 µg/ml BAC. c) 125 µg/ml chlorocresol. d) Both 2 µg/ml BAC and 125 µg/ml chlorocresol. Red arrows indicate cellular debris left behind from lysed cells.

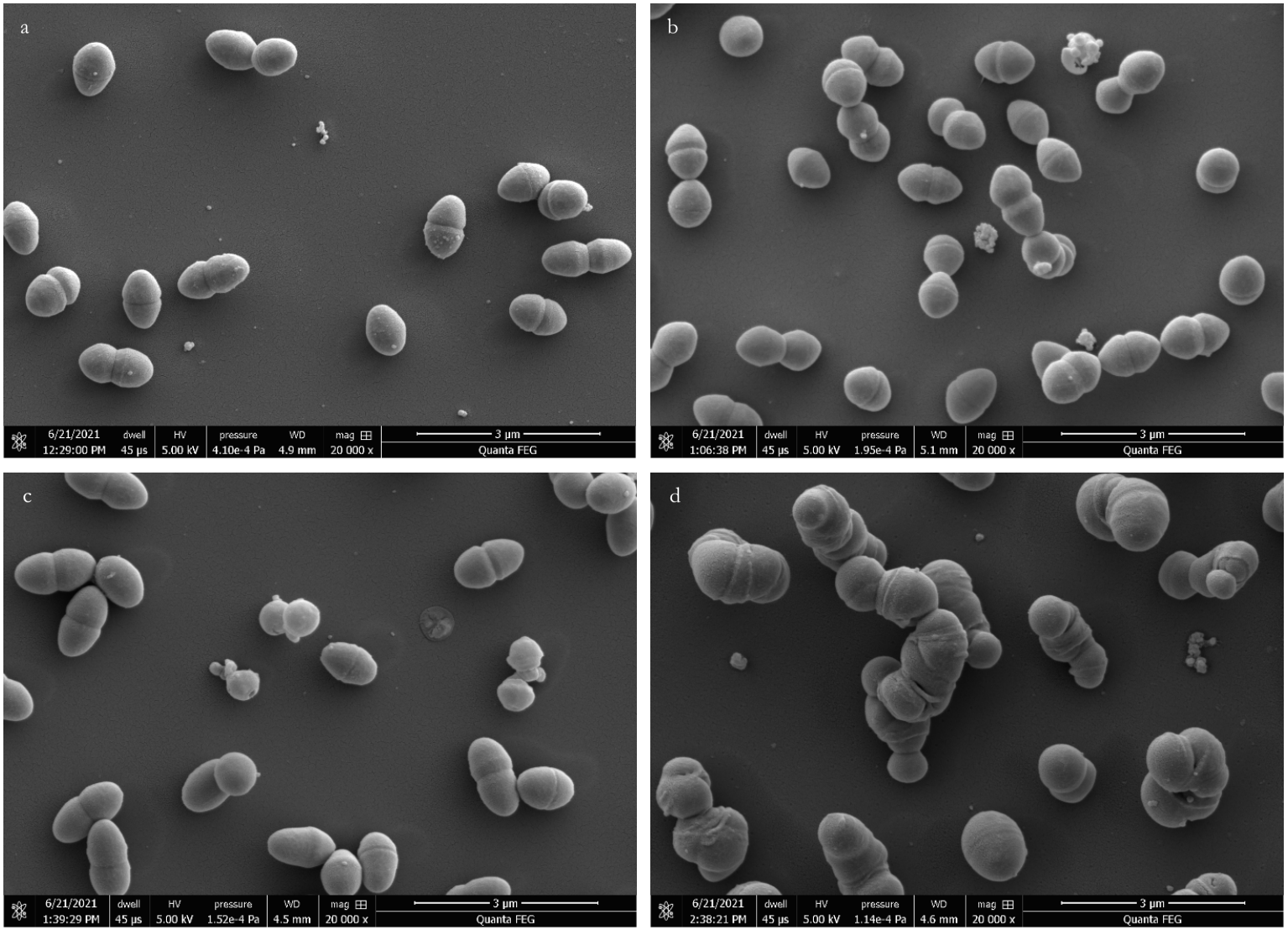

Figure 13. Scanning electron microscopy images of *Enterococcus faecalis* NCTC 13379 after 24-hour exposure to varying combinations of sub-inhibitory concentrations of polyhexamethylene biguanide (PHMB) and chlorocresol. a) Untreated control. b) 2 µg/ml PHMB. c) 125 µg/ml chlorocresol. d) Both 2 µg/ml PHMB and 125 µg/ml chlorocresol.

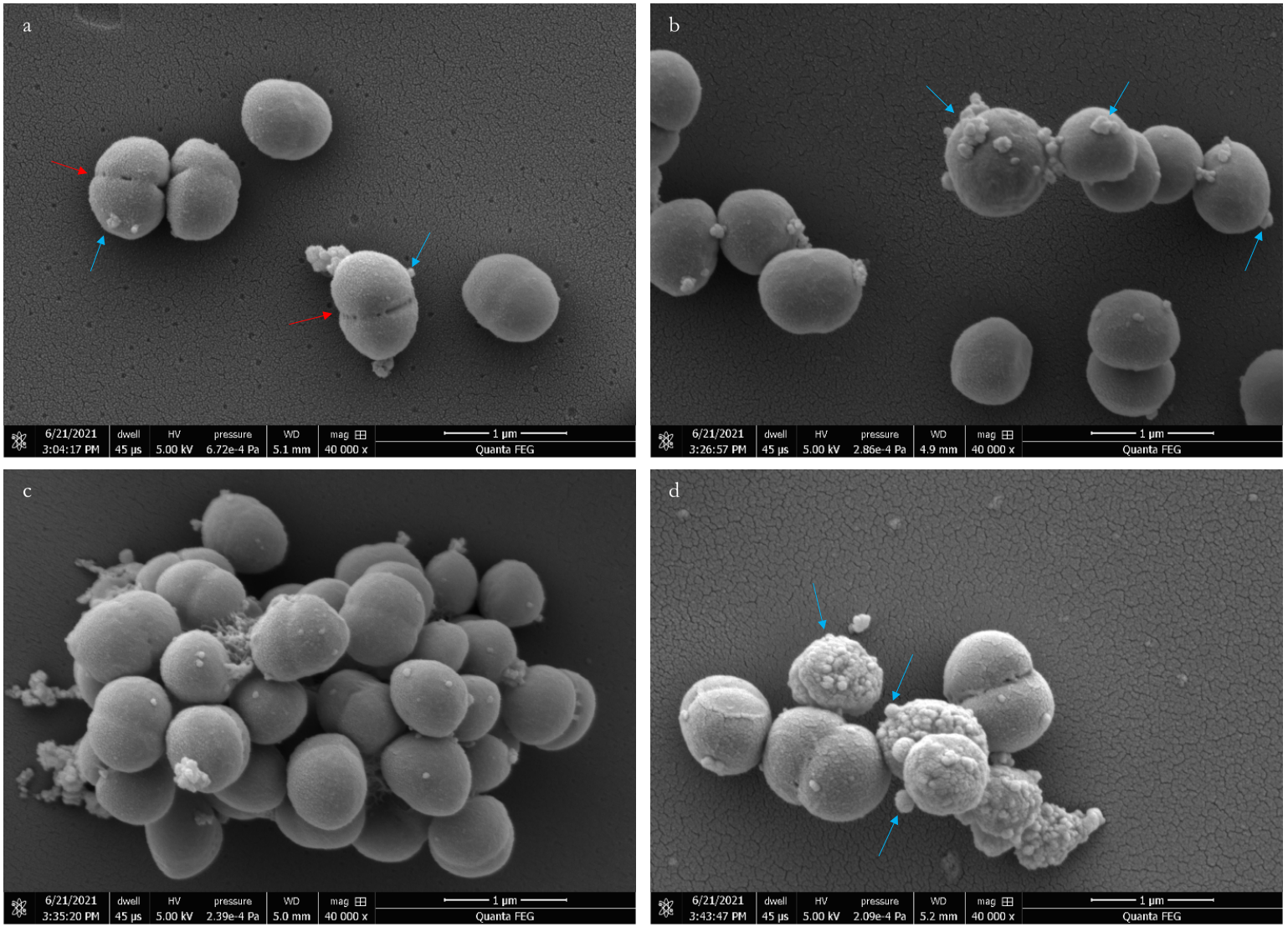

Figure 14. Scanning electron microscopy images of *Staphylococcus aureus* NCTC 13143 after 24-hour exposure to varying combinations of sub-inhibitory concentrations of benzalkonium chloride (BAC) and chlorocresol. a) Untreated control. b) 1 µg/ml BAC. c) 100 µg/ml chlorocresol. d) Both 1 µg/ml BAC and 100 µg/ml chlorocresol. Red arrows indicate division septa. Blue arrows indicate bud-like projections. A higher frequencing of these projections can be seen on cells exposed to BAC as a result of bleb formation.

3.5.3. Chapter discussion

Despite these data indicating a scarcity in synergistic interactions between disinfectant products, claims of synergy are common when commercialising disinfectant products. It is possible that products may be being inappropriately classified as synergistic due to the commercial incentives surrounding a "synergistic" claim combined with non-peer-reviewed supporting data and a lack of understanding of the terminology. Clarifying and identifying the differences between any additive and synergistic mechanisms within a disinfectant formulation is of vital importance and should not be dismissed. Synergistic combinations may provide unique and powerful activities that influence not only the effectiveness of the formulation, but impact how it can be effectively used. Overstating the effectiveness of such formulations by erroneously identifying interactions as 'synergistic' can lead to consumers placing too much faith in a product, which could lead to inappropriate use.

Furthermore, disinfectants are often under scrutiny by regulatory bodies and can be tightly controlled or withdrawn from use. Regulations vary between countries and regions, and are often reviewed and changed, for example in 2016 and 2017 the FDA banned a total of 24 active ingredients including triclosan for use in soaps [217], [313]. Two of these listed active ingredients applied to specific antimicrobial combinations [313]. Other active compounds, including benzalkonium chloride, have had their FDA rulings deferred on a year-by-year basis since 2016 at the request of manufacturers [314]–[319]. This is in order to complete ongoing research into the safety and effectiveness, and as of time of writing the most recent deferral expired on October 31st 2021 [318].

The uncertainty surrounding biocide regulations creates a need for international products to be able to adapt and change their formulations to conform to local regulations. Making a substitution in a formulation is incredibly challenging if the component relies upon a synergistic interaction, as our data suggests that such interactions are very specific and uncommon (Table 6). In contrast, substituting an antimicrobial that provided an additive interaction to a mixture can be achieved relatively easily via a functional analogue, as such interactions are relatively common (Table 6). A formulation that has been inappropriately characterised as synergistic could lead to unnecessary challenge and expense if legislations change and a key component needs substituting. For these reasons fully understanding the nature of antimicrobial interactions is of paramount importance both to the commercial sector and to consumers.

The observed scarcity of synergistic interactions between broad-spectrum disinfectants also raises the question of whether the benefits of synergistic interactions outweigh the challenges

required to identify them. In short, is it worth it? The obvious answer is yes, as there are significant benefits of synergistic interactions. Perhaps most obviously is enhanced antimicrobial activity leading to a higher efficacy, meaning a more effective and reliable product. However, broad-spectrum antimicrobial formulations contain concentrations of active compounds that are typically multiple orders of magnitude greater than the MIC of any likely target organism, and therefore efficacy is not usually a limitation that needs addressing. For example, most supermarket-branded antibacterial sprays and wipes contain between 1,000-20,000 μg/ml BAC, while the MICs against clinically relevant bacterial species lie multiple orders of magnitude lower in the ranges of 4-31 μg/ml (Table 4). Additionally, there are many widely used disinfectants available that only contain one active component, therefore demonstrating that combined antimicrobial interactions are not **necessary** for a product to be effective and successful.

A second advantage of synergistic interactions is the ability to minimise resistance development, as targets would have to become resistant to multiple distinct mechanisms simultaneously [248], [320], [321]. However, this benefit is not unique to synergistic interactions – it also applies to additive and even indifferent interactions too. Furthermore, resistance to disinfectants at optimal concentrations is not a widespread issue that regularly impacts the efficacy of products; thus, it could be argued that this advantage is (currently) a moot point.

An additional advantage of a unique synergistic interaction is that it could enable compounds to be effective against entirely new targets that they otherwise could not. However, to our knowledge there is little evidence to demonstrate this occurring when considering disinfectant combinations specifically.

With multiple academic journals not accepting additive interactions [250] the current bar is set at distinguishing between synergistic interactions and everything else. However, synergistic interactions do not necessarily provide any discernible advantages over additive interactions when considering the quality and functionality of a disinfectant product. We therefore question whether these standards are necessary and suggest that the focus instead be shifted to distinguishing between additive and indifferent interactions when assessing the combined activity of broad-spectrum disinfectants.

It is important to note that disinfectant products routinely contain more than two 'active' components, alongside 'inactive' additives such as solvents, surfactants, emulsion stabilisers and fragrance enhancers. Such formulations therefore contain a network of complex interactions between multiple 'active' and 'inactive' compounds which will inevitably influence the overall product efficacy. To our knowledge the interactions between common 'inactive' components

and ‘active’ disinfectants within a formulation have not been explored in the literature. Furthermore, the characterisation of complex interaction networks between combinations of more than two disinfectants has not been investigated. This study comprehensively and systematically classifies the interactions between common disinfectants, representing an important initial step toward fully elucidating the interaction networks that underpin the efficacy of disinfectant formulations used ubiquitously across the world.

3.6. Conclusion

Disinfectant formulations are globally depended upon in healthcare environments, industrial settings and in day-to-day life. Their use as an infection control measure is critical, especially as the world looks for sustainable routes out of the coronavirus disease 2019 (COVID-19) pandemic. Many common formulations claim to be or are advertised as synergistic. However, the definitions surrounding synergism, additivity and indifference between antimicrobial compounds are often poorly understood and regularly misused. Understanding and not overstating the nature of these interactions is critical because it influences the correct usage of antimicrobial formulations, and also dictates the viability of substituting antimicrobials for functional analogues in the event of regulatory changes.

These data demonstrate that synergism between common disinfectants is a rare occurrence, and any synergistic mechanisms are not necessarily ubiquitous across bacterial species. The majority of the interactions were characterised as additive, which we suggest is likely due to the broad range of cellular targets providing little opportunity for any given antimicrobial combination to be greater than the sum of its parts.

We therefore question whether the current emphasis on synergistic interactions in academia and product development is necessary in the context of broad-spectrum disinfectants. Synergistic interactions are not likely to provide any discernible or impactful benefit over additive interactions in terms of the quality of the final product.

Further examination of the synergistic interactions via high resolution SEM imaging revealed that the synergistic interaction between BAC and chlorocresol is not a result of a unique combined MOA. In contrast, *E. faecalis* cells exposed to the synergistic combination PHMB and chlorocresol demonstrated elongated chains of cells with aberrant cell septation, suggesting a unique combined MOA. It is proposed that this unique interaction is caused by enhanced membrane perturbation as a result of chlorocresol, facilitating an increased uptake of PHMB which condenses intracellular DNA, leading to the observed aberrant morphology.

4. The Development of Tolerance to Common Disinfectants used Individually and in Combination

4.1. Introduction

One of the key potential limitations of all antimicrobials is the mitigation of efficacy by the development of resistance in the target organism. While the topic of antimicrobial resistance (AMR) is usually associated with antibiotics, research has repeatedly found bacteria to be able to develop strategies to resist the action of disinfectants too. A comprehensive overview of established disinfectant tolerance mechanisms can be found in Chapter 1.4.2.3.

While there is limited evidence of widespread disinfectant resistance in the environment, the continually growing evidence from lab-based studies is still a cause for concern. In 2016, 19 antimicrobials were banned from soaps in the US as a result of evidence that these antimicrobials were contributing to AMR [217]. BAC, and 5 other active ingredients of health care antiseptic products are under review due to concerns regarding antiseptic resistance and cross-tolerance [218]. Recently there have been calls to introduce stewardship of antimicrobials as a result of demonstrated adaptive response and cross-tolerance to other antimicrobials [215], [216]. It is clear that although there is no established immediate danger of widespread disinfectant resistance, the area of research is of serious concern.

Tolerance is defined as an increased ability for a given bacterial population or sample to survive a given disinfectant, and has been demonstrated in a range of clinically-relevant bacterial species including *K. pneumoniae* [223], [224], [322], *S. aureus* [266], [323]–[326], *E. coli* [224], [232], *S. enterica* [224], *L. monocytogenes* [234], [235] and *P. aeruginosa* [229], [236]. This topic is further discussed in Chapter 1.4.2.3.

This work specifically focuses on *K. pneumoniae* and *S. aureus* due to their widespread prevalence and association with HAIs [7], [8], [238], [271]. The ability for *K. pneumoniae* to develop tolerance to disinfectants has been studied via the investigation of variation in susceptibilities in clinical and environmental isolates, with decreased susceptibilities reported to chlorhexidine [327]–[330], iodophor [327], [329] and BAC [222], [331]. *In vitro* experiments have demonstrated the ability for *K. pneumoniae* to develop tolerance to chlorhexidine [332] and BAC [222], [333], while López-rojas *et al.* (2017) demonstrated that *K. pneumoniae* was unable to develop tolerance to PHMB in

combination with betaine [326]. However, the ability for *K. pneumoniae* to develop tolerance to DDAC, bronopol, chlorocresol and PHMB in isolation has not previously been evaluated.

In vitro tolerance development experiments have demonstrated that *S. aureus* is able to develop tolerance to triclosan [266], [323]–[325], [334], BAC [266], DDAC [266] and PHMB [266], [326]. Although prior experimentation on BAC, DDAC and PHMB has been conducted by Cowley *et al.* (2015), the experiments were conducted on solid medium for only 14 passages [266]. Therefore, *S. aureus* tolerance to bronopol and chlorocresol has not been investigated previously. In addition, long-term serial passage experiments investigating *S. aureus* tolerance to BAC, DDAC and PHMB have not been conducted.

Finally, it is established that utilising combinations of antibiotics can mitigate the development antibiotic resistance [335], so it is possible that this benefit applies to disinfectants too. To our knowledge there have been no studies elucidating the benefits of using multiple disinfectants within a formulation to mitigate disinfectant tolerance development.

4.2. Chapter aims

The aim of the work presented in this chapter was to investigate the potential for *K. pneumoniae* NCTC 13443 and *S. aureus* NCTC 13143 to develop tolerance to 5 common disinfectants (BAC, DDAC, PHMB, bronopol and chlorocresol). In addition, tolerance to the disinfectant formulation SQ53 was quantified in order to establish if utilising multiple disinfectants within a single combination mitigates tolerance development. After initial disinfectant adaptation, the adapted samples were tested for variations in susceptibility to the other disinfectants in order to elucidate the potential of disinfectant cross-tolerance as a limitation of disinfectant use.

Elucidating the ability for *K. pneumoniae* NCTC 13443 and *S. aureus* NCTC 13143 to develop tolerance to common disinfectants and quantifying the cross-tolerance to other disinfectants will afford us novel insights into the limitations of disinfectants as an infection control measure. Additionally, any tolerant samples developed will be taken forward for molecular characterisation via whole genome sequencing and proteomic analysis in Chapter 5.

4.3. Materials and methods

Klebsiella pneumoniae NCTC 13443 and *Staphylococcus aureus* NCTC 13143 were cultured as described in Chapter 2.3.1. The justification for the use of these strains is also described in Chapter 2.3.1. Details on the disinfectants utilised and the justification for their use are overviewed in Chapter 2.3.2.

4.3.1. The development of disinfectant tolerance via serial passage

K. pneumoniae NCTC 13443 and *S. aureus* NCTC 13143 samples were serially passaged at increasing concentrations of the respective disinfectant treatments in 200 µl volumes in 96-well plates. Each well consisted of 160 µl MHB, 20 µl disinfectant and 20 µl bacterial stock. As the MICs of the disinfectants range across multiple orders of magnitude, the initial concentration and step increments varied depending on the disinfectant treatment and bacterial species, as summarised in Table 7. The concentrations listed were the final concentrations of disinfectant in the 200 µl volumes.

Samples were incubated for 24 hours at 37°C before visual inspection for growth. If growth was observed by the unaided eye, 20 µl of growth-positive culture was used to inoculate the next disinfectant concentration, in ascending order, before incubation again. Used 96-well plates were stored at 4°C for 10 days before being disposed of, in order to provide a backup in the event of contamination.

The daily passages at increasing disinfectant concentrations continued until growth inhibition occurred, upon which the stability of the disinfectant tolerance was validated by maintaining the adapted sample at the respective disinfectant concentration for 15 passage cycles. If samples were unable to tolerate concentrations of disinfectant above the respective MIC (Table 4, Table 5), the experiment was terminated after no less than 45 passage cycles. Adaptation to each respective disinfectant treatment was conducted on cultures sourced from the same 10 biologically independent replicates. After adaptation all samples were frozen at -20°C in the presence of 30% v/v glycerol until required.

Contamination checks were performed at least once per week throughout the adaptation experiment. After growth-positive cultures were used to inoculate the next passage cycle, a sterile loop was used to streak growth-positive culture onto MHA agar plates and Urinary Tract Infection (UTI) ChromoSelect Agar, modified (MilliporeSigma). Plates were then incubated overnight at 37°C before visual inspection for contamination. UTI ChromoSelect Agar medium allowed for allowed for quick and reliable identification of contamination, as *K. pneumoniae* forms

distinct green-blue colonies, while *S. aureus* forms golden opaque colonies. If contamination was detected further contamination checks were performed on backup plates stored at 4°C. The most recent non-contaminated 96-well plate was used to continue the passages without contamination.

4.3.2. Disinfectant cross-tolerance of disinfectant-tolerant samples via the calculation of minimum inhibitory concentrations

To establish disinfectant cross-tolerance profiles of disinfectant-tolerant *K. pneumoniae* samples, the MIC values of BAC, DDAC, PHMB, bronopol, chlorocresol and disinfectant formulation SQ53 were elucidated against 3 biological replicates of disinfectant-adapted *K. pneumoniae* samples. The 3 biological replicates were from the same 3 parent samples, regardless of disinfectant treatment. A schematic overview of the experiment workflow can be found in Figure 15. The MIC values were determined using the broth microdilution method as previously described in Chapter 2.3.3.

Percentage increase in MIC for each sample was calculated compared to the MIC demonstrated by the respective parent sample. The percentage increase values were arranged into a heatmap via GraphPad Prism 9.4.1.

4.3.3. Replicate selection for further examination

Once disinfectant-tolerant samples had been generated, 3 biological replicates were selected for further examination and molecular characterisation. These samples were given shorthand names, firstly after the disinfectant they have adapted to (Bz = BAC, Dd = DDAC, Ph = PHMB, Br = bronopol, Cc = chlorocresol, SQ= SQ53), then the number corresponding to the biological replicate they originated from. The original untreated cultures are referred to as Parent Samples (PS). A schematic overview illustrating the experiment workflow and sample names can be found in Figure 15.

During contamination checks conducted during the cross-tolerance experiment, it was noted that 2 of the BAC-exposed *K. pneumoniae* biological replicates formed colonies with 2 distinct colourations on UTI ChromoSelect Agar. Some colonies appeared consistent with the other samples, demonstrating a green-blue colouration, while others demonstrated a dark blue colouration. It is hypothesised that the selection pressure may have caused the samples to develop into two distinct populations with varying mechanisms of tolerance to BAC. To examine this possibility, the "green" and "dark" colony phenotypes were isolated for further molecular characterisation. These samples were given the additional denotation "G" for the

"green" phenotype, and "D" for the "dark" phenotype. Thus, the additional samples are termed Bz1G, Bz1D, Bz2G and Bz2D, isolated from Bz1 and Bz2 accordingly. Bz3 did not demonstrate varying phenotypes. As a result of this, 5 BAC-tolerant samples were analysed in all future experiments. For a schematic overview of the experiment workflow, see Figure 15.

Table 7. Initial disinfectant concentrations and disinfectant concentration increments used during bacterial adaptation experiment.

Disinfectant	***Klebsiella pneumoniae* NCTC 13443**		***Staphylococcus aureus* NCTC 13143**	
	Initial concentration (µg/ml)	**Concentration increment (µg/ml)**	**Initial concentration (µg/ml)**	**Concentration increment (µg/ml)**
Benzalkonium chloride	1	1	1	0.25
Didecyldimethylammonium chloride	1	1	1	0.25
Polyhexamethylene biguanide	1	1	1	0.25
Bronopol	1	1	1	1
Chlorocresol	20	20	20	20
SQ53	20	20	20	20

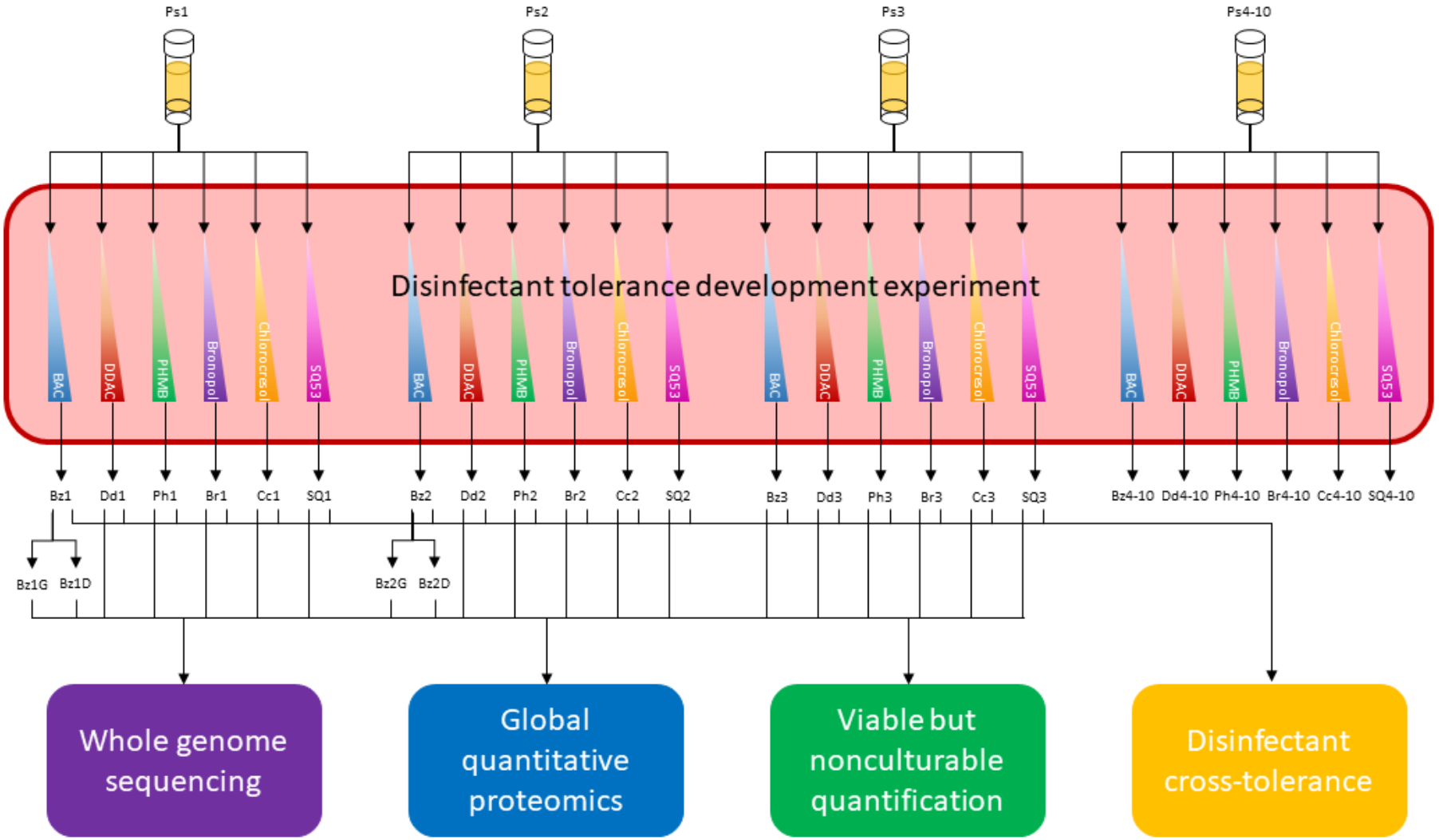

Figure 15. Schematic representation of the experimental workflow conducted on *Klebsiella pneumoniae* NCTC 13443 samples during and after the disinfectant tolerance development experiment. Arrows indicate how the samples were used during the experimental workflow. BAC: benzalkonium chloride. DDAC: didecyldimethylammonium chloride. PHMB: polyhexamethylene biguanide. Ps: Parent sample. Bz: BAC-tolerant sample. Dd: DDAC-tolerant sample. Ph: PHMB-tolerant sample. Br: BR-tolerant sample. Cc: CC-tolerant sample. SQ: Sample that is tolerant to disinfectant formulation "SQ53".

4.4. Results and discussion

4.4.1. The development of disinfectant tolerance via serial passage

K. pneumoniae and *S. aureus* cultures were exposed to a sub-MIC concentration of each of the disinfectants as outlined previously (Table 7, Chapter 4.3.1). Samples were then serially passaged daily into media containing sequential incrementally increasing concentrations of disinfectant. Graphs displaying the level of disinfectant tolerance over time during the serial passage experiment can be seen in Figure 16 and Figure 17, and a summary of the pre and post-acclimatisation MIC values is shown in Table 8.

4.4.1.1. The development of disinfectant tolerance by *K. pneumoniae*

K. pneumoniae samples steadily developed tolerance when exposed to BAC, demonstrating growth at concentrations greater than the parent sample *K. pneumoniae* MIC of 20 µg/ml on day 23 (Figure 16a). The tolerance of individual biological replicates began to collapse at 50 µg/ml, however each time this occurred the cultures recovered, with all 10 replicates continuing on to hit the limit of tolerance development at 55 µg/ml, with a final MIC of 56 µg/ml (Figure 16a). The MIC of BAC after tolerance development of *K. pneumoniae* is 180% higher than the non-tolerant parent strain (Table 8).

The ability for bacterial species to develop tolerance to QACs is well documented, with multiple potential mechanisms established. Known adaptations include the modification of membrane composition [233], [336]–[339], up-regulation of broad-spectrum efflux pumps [222], [233], [340], [341] and down-regulation of porins [233] as described previously in Chapter 1.4.2.3. Abdelaziz *et al.* (2018) observed an increase in the number of BAC-adapted *K. pneumoniae* hospital isolates after serial passage, which was attributed to an increase in membrane depolarization and efflux pump activity [222]. In addition, Gadea *et al.* (2017) previously reported the adaptation of a *Klebsiella sp.* sample to BAC via a similar methodology, with a final adapted MIC of 90 µg/ml [333]. However, the adaptation was not stable once the BAC stress was removed, indicating that the adaptation was a result of a phenotypical response rather than genetic mutations [333]. As a result, the sample was not subject to further molecular characterisation, so the underlying mechanisms remain unknown.

As the data presented here consists of 10 biological replicates that all generated consistent tolerance development, the tolerance observed is considered reliable (Table 8, Figure 16). Therefore, the variation between the adaptability of *Klebsiella* spp. reported by Gadea *et al.* and the *K. pneumoniae* observed in this experiment (Table 8, Figure 16a) is likely a result of species and

strain variation, especially as the specific *Klebsiella* species of the sample tested in Gadea *et al.* (2017) was not identified in the study or prior work [333], [342], [343].

K. pneumoniae tolerance to DDAC, PHMB and bronopol developed rapidly, with the parent sample MIC being exceeded on days 9, 9 and 11 respectively (Figure 16b, c, d). However, for each of these disinfectants the tolerance began to collapse at 15 μg/ml, 9 μg/ml and 51 μg/ml respectively (Figure 16b, c, d), indicating the limit of sustainable tolerance had been reached. Interestingly, the samples were always able to recover, but could not maintain tolerance on consecutive days (Figure 16b, c, d). Upon lowering the concentrations of DDAC, PHMB and bronopol, all biological replicates were able to sustain their tolerance at 13 μg/ml, 8 μg/ml and 40 μg/ml respectively (Figure 16b, c, d), showing an MIC increase of 133%, 40% and 413% respectively (Table 8).

DDAC is a QAC that operates via a similar MOA as BAC, so the predicted mechanisms of tolerance are the same as those described previously. However, the final limit of sustainable tolerance to DDAC was 13 μg/ml, only a 133% increase on the parent strain MIC in comparison to a 180% MIC increase demonstrated by *K. pneumoniae* when adapted to BAC (Table 8). This indicates that the limits of *K. pneumoniae* disinfectant adaptation vary depending on the disinfectant in question, even if they operate via a similar MOA. This could be a result of variations in affinity of the disinfectant to the target site, for example. This difference in adaptation may also be indicative of variations in the underpinning mechanisms of tolerance, although this is not possible to deduce from these data. This is investigated further in Chapter 5. To our knowledge, there are no previous reports investigating *K. pneumoniae* tolerance to DDAC.

The mechanism of action of PHMB relies upon sequestering anionic lipids within biological membranes [64], as previously described (Chapter 1.3.2.3.), but *K pneumoniae* was only able to sustainably achieve a 50% increase in MIC after a total of 92 days of PHMB acclimatisation (Table 8). Samples were able to tolerate as much as 14 μg/ml PHMB, a 133% increase in MIC, however this tolerance was not able to be sustained in repeated passages, often with tolerance completely collapsing and growth visible only in the 0 μg/ml viability control wells (Figure 16c). This indicates that *K. pneumoniae* cells were able to tolerate and proliferate when exposed to between 8-14 μg/ml PHMB for short periods of up to 48 hours, but sustained exposure at these concentrations resulted in loss of culturability. The ability for cultures to subsequently recover after being cultured in the absence of disinfectant suggests that the tolerance mechanisms are able to recover after being overwhelmed.

Small scale changes in PHMB tolerance have only reported by Broxton *et al.* (1984) when testing on *E. coli*. These changes were explained as due to alterations in lipid composition of the outer leaflet, specifically a reduction in the anionic phospholipids [63]. Our data is in consensus with these previous findings, although it is not possible to conclude on the underlying mechanism from these data. Interestingly, López-rojas *et al.* (2017) demonstrated that 2 *K. pneumoniae* strains (ATCC 25922 and ST-512) were unable to develop tolerance to PHMB in combination with betaine [326]. The variation between the datasets is likely a result of the addition of betaine influencing the ability for *K. pneumoniae* to develop tolerance. In addition, disparities may arise from methodological and strain variations.

Regarding bronopol, previous experiments by Croshaw *et al.* (1964) and Bryce *et al.* (1978) demonstrated no tolerance development when bacteria were cultured in the presence of bronopol for 12 and 20 passages respectively [98], [101]. However, our data shows that *K. pneumoniae* samples exposed to bronopol were able to develop tolerance, with a MIC 413% higher after adaptation (Table 8). The full experimental procedures were not expanded upon in the reports by Croshaw *et al.* (1964) and Bryce *et al.* (1978), likely as the results reported were negative [98], [101]. Therefore, we are unable to say whether our results conflict with their findings, as the variation may be accounted for by discrepancies in methodology and test organisms.

Regardless, the ability for *K. pneumoniae* to adapt to bronopol so readily was unexpected, as bronopol is known to operate via two distinct mechanisms, as previously described (Chapter 1.3.2.8). In brief, the primary mechanism of bronopol is via the crosslinking of primary amines in protein structures, impeding protein functionality [99]. This reaction generates ROS, which have broad-spectrum antimicrobial activity and form a secondary antimicrobial mechanism of action [100]. In order for *K. pneumoniae* samples to have developed tolerance, the bacteria must therefore have developed mechanisms to deal with both aspects of the antimicrobial activity.

As the primary target of bronopol is the thiol group in the amino acid cysteine [99], it is unlikely that tolerance has been acquired through modification of the disinfectant's target site. Therefore, it seems likely that observed tolerance is a result of reducing the concentration of disinfectant able to reach the target site, either through enzymatic breakdown or via the up-regulation of broad-spectrum efflux pumps.

As the secondary mechanism of bronopol is via the by-product of the initial reaction with thiol groups, a reduction in the concentration of bronopol may also account for tolerance to the secondary mechanism. In addition, the presence of superoxide dismutase and catalase has

previously been shown to reduce the bactericidal effect of bronopol [100], so up-regulation of these proteins may lead to enhanced enzymatic neutralisation of the disinfectant bi-products and thus limiting the antimicrobial activity. Tolerance may also develop through *K. pneumoniae* being able to mitigate intracellular damage via the up-regulation of thiol repair and DNA repair mechanisms such as thioredoxins and the SOS response respectively. It is not possible to confirm more detail without further genomic sequencing and proteomic analysis, which are presented in Chapter 5.

K. pneumoniae developed tolerance to chlorocresol, with a 30% increase in MIC after 69 days of chlorocresol acclimatisation (Table 8). This is the lowest percentage increase in MIC of the disinfectants tested, indicating that it is challenging for *K. pneumoniae* to develop tolerance to chlorocresol. The mechanism of action of chlorocresol is via disruption of the permeability barrier and induced leakage of low molecular weight material [82], [85]–[90], [291].

Bacterial tolerance to phenolic disinfectants has been reported *in vitro*, but the underlying mechanisms have not been extensively elucidated. Hugo and Franklin (1968) studied the potential tolerance mechanisms of *S. aureus* to multiple phenolic disinfectants and reported an increase in survivability in cells with a higher lipid content when exposed to phenols with a longer hydrocarbon chain. This was proposed to be due to an inability to penetrate the cell surface due to the higher lipid content [344]. However, this finding is contrasted by Hamilton (1968) who was unable to establish a link between cellular lipid content of *S. aureus* and phenol tolerance [345].

Gilbert and Brown (1977) observed a correlation between the LPS content of *P. aeruginosa* and tolerance to phenol-derivatives, which was suggested to be a result of the LPS forming a barrier that prevents disinfectants from being able to sufficiently penetrate cells [346]. However, a lack of qualitative difference in LPS content was observed by sodium dodecyl sulphate (SDS) polyacrylamide gel electrophoresis when *P. aeruginosa* samples were adapted to 2,2'-methylenebis(4-chlorophenol) [347]. The observed adaptation was instead attributed to an observed decrease in phosphate uptake protein OprP, which was suggested to be a point of entry for the phenolic disinfectant [347].

Finally, Moken *et al.* (1997) linked the deletion of the *acrAB* efflux system to a 10-fold increase in susceptibility of *E. coli* strains to chloroxylenol, indicating a link between broad-spectrum efflux pumps and phenolic disinfectant tolerance [225]. The correlation between efflux pump activity and phenol disinfectant susceptibility was further demonstrated in *S. enterica* by Randall *et al.* (2007) [226].

Overall, various species have been shown to be able to develop tolerance to phenolic disinfectants, with the only well-established mechanism of tolerance being efflux pump activity. As such, the literature suggests that the potential mechanism underlying the observed chlorocresol tolerance in *K. pneumoniae* (Table 8) may involve the AcrAB-TolC efflux system [225], [226], but further investigation via genomics and proteomics-based methods will be required to validate this, as presented in Chapter 5.

K. pneumoniae samples exposed to the SQ53 disinfectant formulation demonstrated a 30% increased MIC in comparison to the parent *K. pneumoniae* samples, the same percentage increase in MIC as chlorocresol (Table 8). As SQ53 contains chlorocresol within its formulation (Table 3) it therefore likely that *K. pneumoniae* is unable to develop tolerance to the combined formulation beyond what it can develop against chlorocresol individually. Even though *K. pneumoniae* is able to develop a higher level of tolerance to each of the other disinfectants in isolation, it is unable to reach these levels of tolerance when the disinfectants are used in combination with chlorocresol (Table 8). The implication is that disinfectant formulations may be able to mitigate bacterial tolerance development, opening up an interesting line of enquiry for further study.

4.4.1.2. The development of disinfectant tolerance by *S. aureus*

In contrast to *K. pneumoniae*, *S. aureus* samples exposed to each of the disinfectants were unable to develop tolerance to any of the disinfectants and maintain it for 15 days (Figure 17). Of the samples, *S. aureus* was only able to meet or exceed the MICs of BAC, DDAC and bronopol (Figure 17a, b, d). *S. aureus* was able to tolerate the MIC of 4 μg/ml BAC after 6 days, however the tolerance was unsustainable, with tolerance levels consistently collapsing when BAC exposure was greater or equal to 3 μg/ml (Figure 17a). Similarly, the bronopol MIC of 20 μg/ml was able to be tolerated after 12 days, but concentrations greater or equal to the MIC caused the tolerance to collapse repeatedly throughout the experiment, so the tolerance was unsustainable (Figure 17d). The MIC of DDAC is 2 μg/ml, which was met by individual biological replicates between days 6 and 16, but was once again unsustainable (Figure 17b).

Upon exposure to PHMB, chlorocresol and SQ53, *S. aureus* was able to tolerate the same concentrations they could in the previous MIC experiments (4 μg/ml, 200 μg/ml and 60 μg/ml respectively) (Figure 17c, e, f) (Table 4, Table 5), but were unable to develop tolerance to the MICs of 6 μg/ml, 400 μg/ml and 80 μg/ml respectively (Figure 17c, e, f). The tolerance began collapsing at concentrations equal to or exceeding 3 μg/ml PHMB, 250 μg/ml chlorocresol and 35 μg/ml SQ53, so the tolerance was unsustainable (Figure 17c, e, f). All of the *S. aureus* experiments were continued for at least 45 days, as described in Chapter 4.3.1. As no sample was

able to develop stable tolerance to the respective disinfectant, *S. aureus* was deemed to be unable to develop stable tolerance to any of the disinfectant treatments via this methodology.

These data suggest that *S. aureus* is unable to develop tolerance to the tested disinfectants, in contrast to the literature. Previous *in vitro* studies have demonstrated that *S. aureus* is able to develop tolerance against BAC [266], DDAC [266] and PHMB [266], [326], alongside triclosan [266], [323]–[325], [334]. In addition, variations in susceptibility between *S. aureus* strains isolated from the environment has been established for BAC [348]–[351] and DDAC [352], demonstrating that *S. aureus* is able to develop tolerance to at least these two disinfectants given the correct environment conditions and timescales. The lack of reported variations in *S. aureus* susceptibility to PHMB, bronopol, chlorocresol or SQ53 in the literature aligns with our data, suggesting that *S. aureus* is unable to develop tolerance to these disinfectants.

The lack of tolerance development observed in this experiment is likely a result of strain and methodological variations between the datasets. However, as *S. aureus* was unable to develop tolerance to any of the tested treatments it is not possible to conclusively determine if the negative results are due to an inability for *S. aureus* to develop tolerance, or a result of unforeseen limitations with the methodology.

Table 8. Minimum inhibitory concentration (MIC) values of common disinfectants against *Klebsiella pneumoniae* NCTC 13343 before and after disinfectant tolerance development. n=10.

Disinfectant	**MIC (µg/ml)**		**MIC increase (%)**
	Parent samples	**Tolerant samples**	
Benzalkonium chloride	20	56	180
Didecyldimethylammonium chloride	6	14	133
Polyhexamethylene biguanide	6	9	50
Bronopol	8	41	413
Chlorocresol	200	260	30
Disinfectant formulation "SQ53"	200	260	30

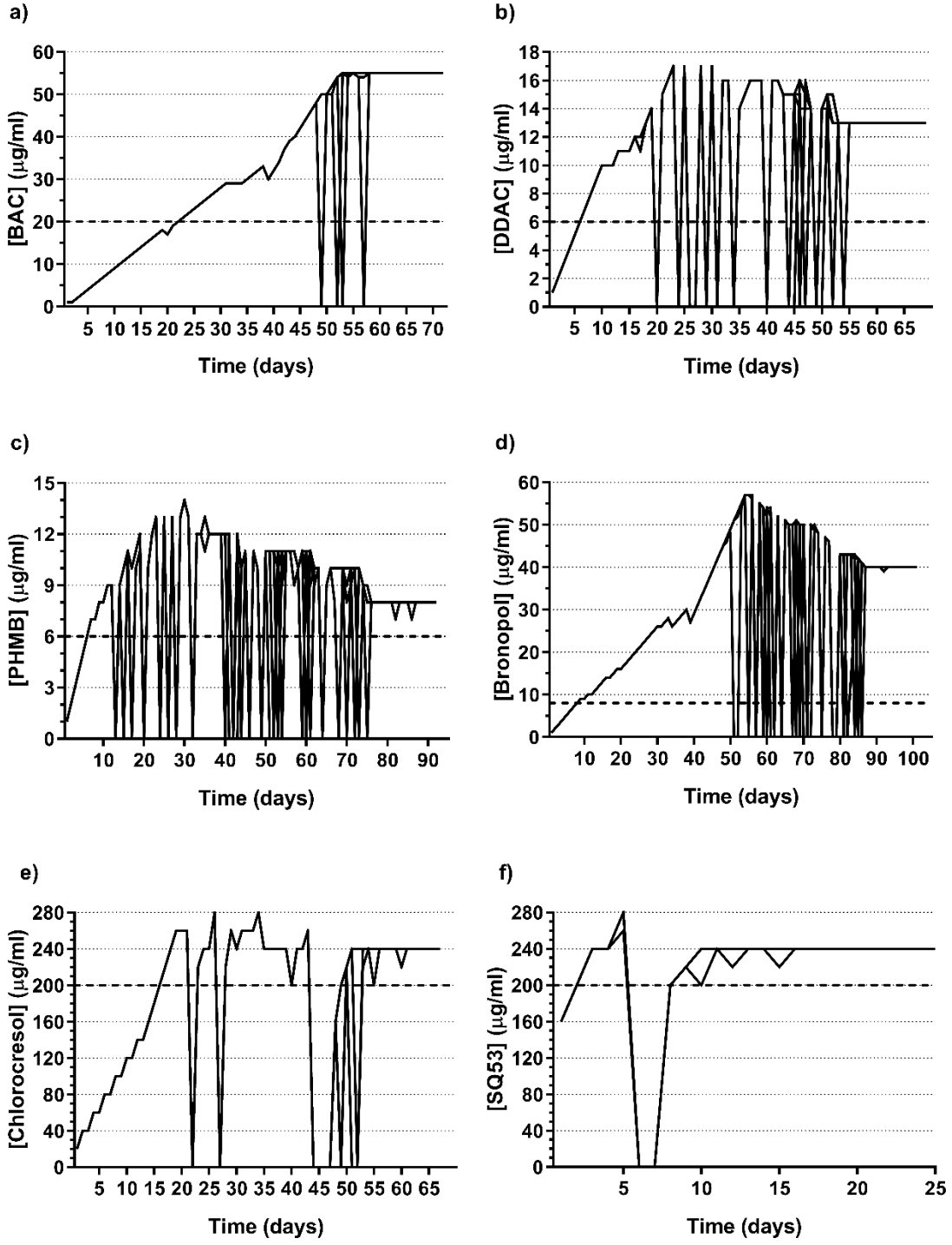

Figure 16. Tolerance of *Klebsiella pneumoniae* NCTC 13443 to common disinfectants over time. Solid lines indicate the highest concentration of disinfectant that demonstrated growth on any given day. n=10. All 10 biological replicates are overlayed on each graph. Dashed lines indicate the original minimum inhibitory concentration of the untreated parent samples to each respective disinfectant. a) Benzalkonium chloride (BAC). b) Didecyldimethylammonium chloride (DDAC). c) Polyhexamethylene biguanide (PHMB). d) Bronopol. e) Chlorocresol. f) Disinfectant formulation "SQ53" (SQ53).

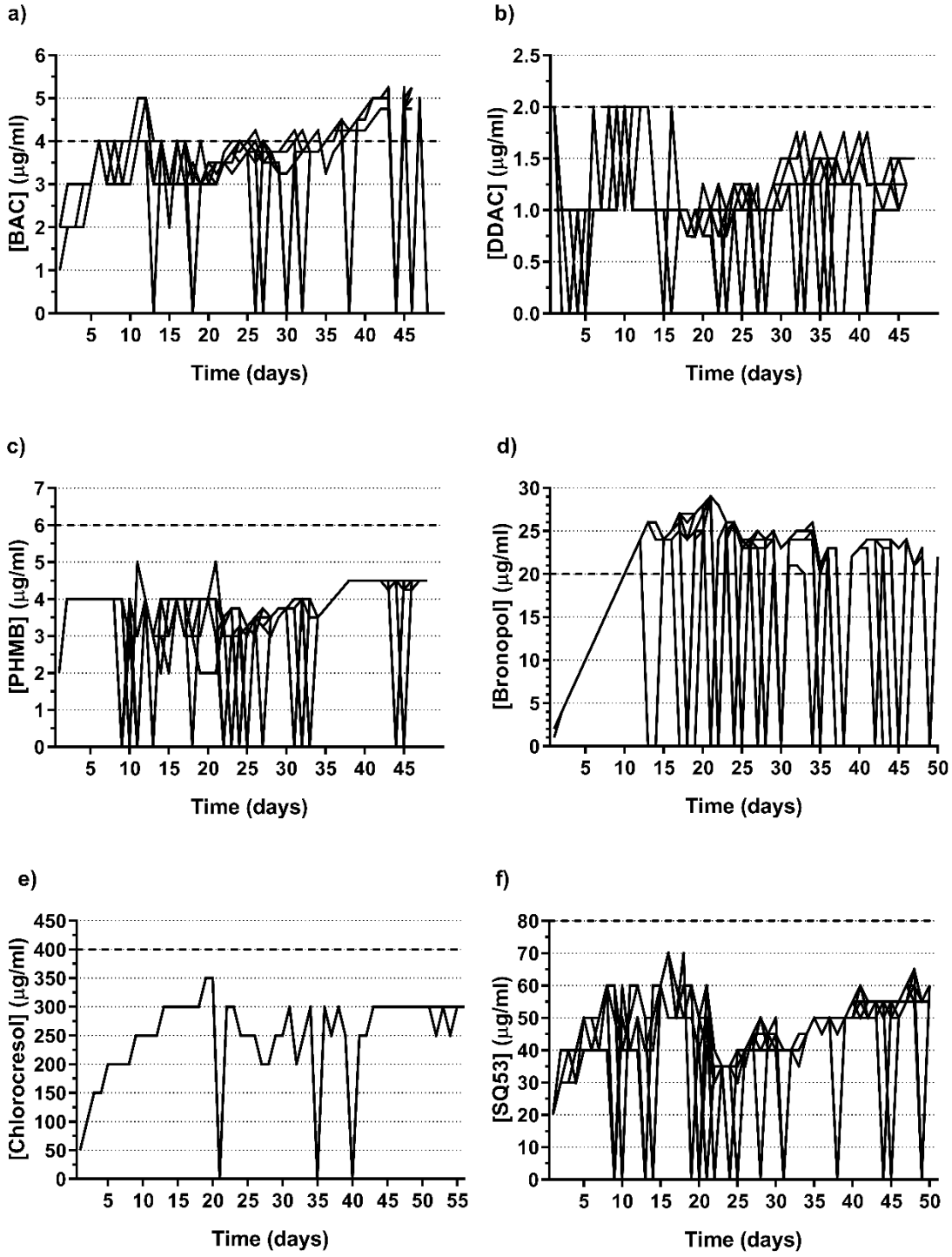

Figure 17. Tolerance of *Staphylococcus aureus* NCTC 13143 to common disinfectants over time. Solid lines indicate the highest concentration of disinfectant that demonstrated growth on any given day. n=10. All 10 biological replicates are overlayed on each graph. Dashed lines indicate the original minimum inhibitory concentration of the untreated parent samples to each respective disinfectant. a) Benzalkonium chloride (BAC). b) Didecyldimethylammonium chloride (DDAC). c) Polyhexamethylene biguanide (PHMB). d) Bronopol. e) Chlorocresol. f) Disinfectant formulation "SQ53" (SQ53).

4.4.2. Disinfectant cross-tolerance

To investigate the possibility of cross-tolerance between disinfectants, the new MICs of each disinfectant were elucidated on the tolerant *K. pneumoniae* samples. The raw MIC values are displayed in Table 9, and the percentage change in MIC between parent samples (before tolerance development) and the tolerant samples (after tolerance development) are displayed as a heatmap in Figure 18.

The ability of disinfectant-tolerant samples to tolerate other disinfectants varied, with MIC percentage change values ranging from -91.7% to 233.3% (Figure 18). Of the 90 possible cross-tolerance combinations, 48 demonstrated a negative percentage change in MIC after tolerance development, indicating an increase in susceptibility (Figure 18). This is likely a result of any adaptations the samples have developed as a result of prolonged exposure to the original disinfectant leaving them vulnerable to the mechanism of action of the second disinfectant. For example, alterations in membrane composition to a membrane-active disinfectant may allow another disinfectant to penetrate the membrane more readily to reach the required target site, causing an increase in susceptibility. Alternatively, adaptation to one disinfectant may cause a reduction in expression of proteins responsible for enzymatic degradation of a second disinfectant, again resulting in an increased susceptibility to the latter.

Thirty-one combinations displayed a positive percentage change in MIC after tolerance development, indicating that the samples are less susceptible after adaptation (Figure 18). This indicates that the mechanisms of tolerance developed through long-term exposure to the original disinfectant confer cross-tolerance to the second disinfectant.

Finally, 11 combinations displayed no change in MIC after tolerance development, indicating that any acquired adaptations offer no benefit or vulnerability to the second disinfectant.

The directionality of BAC, DDAC, chlorocresol and SQ53 cross-tolerance was consistent across all biological replicates tested, with only minor variations in the level of relative susceptibility (Figure 18). In contrast, samples Ph3 and Br3 displayed contrasting cross-tolerance susceptibilities to the other biological replicates (Figure 18). This is a provisional indicator that the developed mechanisms of tolerance are consistent across BAC, DDAC, chlorocresol and SQ53-tolerant biological replicates, whereas the mechanisms that underpin PHMB and bronopol tolerance may vary between biological replicates. It is not possible to conclude more from these data without further molecular analysis into the underpinning tolerance mechanisms.

The highest level of cross-tolerance observed was between BAC-tolerant samples exposed to DDAC, which displayed a 150%-233.3% increase in DDAC MIC from 6 μg/ml to 15-20 μg/ml as a result of BAC adaptation (Table 9, Figure 18). Both BAC and DDAC are QACs that act via membrane disruption as discussed previously (Chapter 1.3.2.7) so it is unsurprising that the mechanisms that enable BAC-tolerant *K. pneumoniae* to survive would also be advantageous when cells are exposed to DDAC. Potential mechanisms include the up-regulation of efflux pumps [222], [233], [340], [341], changes to membrane surface charge [233], [336]–[339] and down-regulation of porins [233].

Interestingly, this relationship was not reciprocated when DDAC-tolerant samples were exposed to BAC, with no change in BAC MIC observed as a result of DDAC tolerance development (Figure 18). This indicates that cross-tolerance relationships between disinfectants are not automatically reciprocated, even if the respective MOAs are similar. This may be due to subtle variations in the physiochemical properties of the disinfectants themselves causing one to be better suited at overcoming a commonly developed mechanism of tolerance, for example variations in affinity to the outer surface of bacterial cells. Alternatively, *K. pneumoniae* may develop different mechanisms of tolerance to BAC in comparison to DDAC. More detailed molecular analysis is required to investigate this further, which is presented in Chapter 5.

PHMB is also a cationic surfactant that acts via membrane disruption [64], as explained previously (Chapter 1.3.2.3), so the MOA is similar to BAC and DDAC. However, despite this, BAC and DDAC-tolerant bacteria were respectively ~33.3% and ~91.7% more susceptible to PHMB (Figure 18). Similarly, PHMB tolerance led to a ~25% increase in susceptibility to BAC and DDAC in 2 out of the 3 biological replicates tested (Figure 18). This implies that the mechanism(s) that underpin BAC and DDAC tolerance cause *K. pneumoniae* to be vulnerable to PHMB, and vice versa. This result is unexpected, as there is overlap in the documented tolerance mechanisms to QACs and PHMB. For example, Broxton *et al.* 1984) documented a reduction in phosphatidylethanolamine and phosphatidylglycerol in *E. coli* in response to PHMB exposure [63], and Bisbiroulas *et al.* (2010) reported the same adaptation mechanism in *L. monocytogenes* in response to BAC exposure [234].

However, while there are similarities in tolerance mechanisms between PHMB and QACs, there are also notable differences. Efflux pump up-regulation [222], [233], [340], [341] and porin down-regulation [233] are characteristic of QAC tolerance, but are not reported for PHMB tolerance. As a result, QAC-adapted *K. pneumoniae* samples may be investing excessive resources

into adaptation strategies that provide no advantage against PHMB MOA, so thus are unable to respond quickly enough to the new threat (PHMB), leaving them more susceptible.

PHMB has also been suggested to act via the binding and condensing of microbial nucleic acids [73], [74], unlike QACs. As a result, PHMB-adapted *K. pneumoniae* may be overinvesting in tolerance strategies related to DNA repair and intracellular aggregation, and thus be unable to respond quickly enough to tolerate BAC or DDAC upon exposure, once again leaving the cells more susceptible. This would explain the cross-tolerance profiles of PHMB-tolerant biological replicates 1 and 2. Biological replicate 3 displayed a 75% and 16.7% reduced susceptibility to BAC and DDAC respectively (Figure 18), possibly due to the underlying tolerance mechanism being related to shared membrane adaptations as previously observed in the literature [63], [234]. The different underpinning mechanisms of PHMB tolerance displayed across the biological replicates also correlates with variations in cross-tolerance to bronopol and SQ53. Once again, these explanations cannot be substantiated based on these data alone, and require further molecular analysis.

The MOA of bronopol relies upon the crosslinking of proteins, a reaction which causes the formation of ROS as a secondary antimicrobial mechanism [99], [100]. The theoretical potential mechanisms to resist the activity of such an antimicrobial are very broad, varying from up-regulation of efflux pumps, thiol repair mechanisms and DNA repair machinery. Additionally, the presence of catalase or superoxide dismutase has been shown to reduce the bactericidal activity of bronopol, presumably as a result of the removal of ROS [100]. These adaptations would vary in their effectiveness against the other disinfectants tested. For example, up-regulation of efflux pumps may provide cross-tolerance to the QACs, while thiol repair enzyme up-regulation is not likely to have a discernible benefit. The potential for variations in tolerance mechanisms may explain the disparity in cross-tolerance results between the different bronopol-tolerant biological replicates when exposed to DDAC, PHMB and SQ53.

Interestingly, all BAC-tolerant *K. pneumoniae* replicates displayed a 12.5%-50.0% higher susceptibility to bronopol, whereas DDAC-tolerant replicates displayed a 50%-100% lower susceptibility to bronopol (Figure 18). This further supports the previous observation that although BAC and DDAC act via near-identical mechanisms, the underpinning tolerance mechanisms vary significantly between them, such that the samples display opposite cross-tolerance profiles to bronopol.

Chlorocresol-tolerant *K. pneumoniae* displayed a 50%, ~15% and ~25% increased susceptibility to QAC, DDAC and SQ53 respectively (Figure 18). In addition, *K. pneumoniae* samples that have

developed tolerance to BAC, DDAC, PHMB and SQ53 all demonstrated an increase in susceptibility to chlorocresol of between 20%-80% (Figure 18).

Once again, these increases in susceptibility can be attributed to variations in MOAs of the disinfectants. Chlorocresol is a membrane-active antimicrobial that disrupts the permeability barrier and causes the leakage of low molecular weight material [85]–[91], [291] (Chapter 1.3.2.6). Unlike the cationic surfactants (BAC, DDAC, PHMB), chlorocresol is not charged so relies upon hydrophobic interactions with the lipid bilayer, demonstrating a lower level of affinity to the target site as described previously [284] (Chapter 2.4.1). As a result, it is not surprising that the mechanisms *K. pneumoniae* developed for tolerating chlorocresol may not necessarily confer cross-tolerance to BAC, DDAC or SQ53, and vice versa. Surprisingly, the samples demonstrated a 0%-13.3% decrease in susceptibility to PHMB however (Figure 18), which is also a cationic surfactant (Chapter 1.3.2.3). It is not possible to explain this discrepancy in the underlying mechanisms without further molecular characterisation of the samples.

The MOAs of chlorocresol and bronopol have little overlap, so it is unsurprising that bronopol-tolerant samples displayed a ~25% increase in susceptibility to chlorocresol (Figure 18). However, chlorocresol-tolerant samples demonstrated a wide range of lower susceptibilities to bronopol, ranging from 25% to 200% (Figure 18). As there is little overlap in the MOAs, the mechanism of tolerance to chlorocresol providing cross-tolerance to bronopol implies that the mechanism of tolerance is broad and non-selective. Potential examples of this include efflux pump up-regulation or the induction stress response pathways.

SQ53-tolerant *K. pneumoniae* samples displayed relatively minor changes to BAC tolerance, with a drop in susceptibility of between 0% and 50% (Figure 18). The tolerance mechanisms developed by the samples to mitigate the activity of SQ53 therefore have no negative impact in BAC tolerance, indicating a potential overlap or indifference in tolerance mechanisms. The same can be observed for bronopol cross-tolerance, with no change in MICs observed after SQ53 adaptation (Table 9, Figure 18). However, the samples displayed a drop in susceptibility to DDAC of ~190% (Figure 18). This suggests that the tolerance mechanisms of SQ53 are closely related to the mechanisms of tolerance to DDAC.

In contrast, the SQ53-adapted samples displayed a 33.3% and ~70% increase in PHMB and chlorocresol susceptibility (Figure 18), despite the overlap in MOA against bacterial membranes. As previously suggested, this may be due to PHMB's activity against bacterial nucleic acids [73], [74], and chlorocresol not being cationic and thus being unaffected by modifications to cell surface charge.

As SQ53 is a formulation that contains each of the other disinfectants as individual components, the cross-tolerance profile provides an indication of which components *K. pneumoniae* had to adapt to in order to tolerate SQ53, and which components it could afford to become more susceptible to. In turn, this indicates which individual components are contributing to the overall activity of the formulation against *K. pneumoniae*, with DDAC seeming to be the component with the highest level of activity, and chlorocresol and PHMB providing the lowest. DDAC being a critical component is supported by data shown in Chapter 2.4.1, whereby the MIC of DDAC against *K. pneumoniae* is shown to be 6 μg/ml (Table 4), which correlates exactly with the concentration of DDAC within SQ53 at the MIC of SQ53 (Table 5). Additionally, when imaged via SEM and TEM, *K. pneumoniae* cells exposed to SQ53 were consistent with cells exposed to BAC and DDAC (Figure 5, Figure 7 and Figure 9).

Interestingly, the MIC of PHMB against *K. pneumoniae* is 6 μg/ml (Table 4), and the concentration in the SQ53 formulation at SQ53's MIC is 6.6 μg/ml (Table 5). This indicates that a greater concentration of PHMB is required to achieve the same activity when it is used within the SQ53 formulation compared to when it is used individually. Furthermore, the cross-tolerance profiles for SQ53 and DDAC-adapted *K. pneumoniae* demonstrate a comparable trend (Figure 18), further suggesting MOA similarities.

Collectively, these data imply that DDAC contributes heavily to the overall activity and efficacy of the SQ53 formulation and PHMB contributes less, despite PHMB having a higher concentration in the formulation (Table 5).

BAC and DDAC-adapted samples have a ~20% and ~35% decrease in susceptibility to SQ53 (Figure 18), further indicating an overlap in the underpinning mechanisms of tolerance. Chlorocresol-adapted samples demonstrate a ~25% increased susceptibility to SQ53 (Figure 18) due to a lack of overlap in underlying tolerance mechanisms leaving the adapted samples vulnerable to other disinfectants. Finally, PHMB and bronopol-adapted samples display an inconsistent level of cross-tolerance to SQ53 between the biological replicates, likely due to the multiple MOAs of these disinfectants giving rise to multiple potential tolerance mechanisms, as discussed previously.

Table 9. Cross-tolerance minimum inhibitory concentration values of common disinfectants tested against disinfectant-tolerant *Klebsiella pneumoniae* NCTC 13343 samples. MIC: minimum inhibitory concentration. BAC: benzalkonium chloride. DDAC: didecyldimethylammonium chloride. PHMB: polyhexamethylene biguanide. SQ53: disinfectant formulation "SQ53". Bz: BAC-tolerant sample. Dd: DDAC-tolerant sample. Ph: PHMB-tolerant sample. Br: bronopol-tolerant sample. Cc: chlorocresol-tolerant sample. SQ: SQ53-tolerant sample. n=3.

Tolerant Sample	MIC (µg/ml)					
	BAC	**DDAC**	**PHMB**	**Bronopol**	**Chlorocresol**	**SQ53**
Bz1	-	20	0.5	4	60	220
Bz2	-	17	0.5	4	80	240
Bz3	-	15	2	7	100	280
Dd1	20	-	4	12	80	260
Dd2	20	-	5	16	80	280
Dd3	20	-	4	12	100	260
Ph1	15	5	-	8	120	140
Ph2	15	3	-	8	100	120
Ph3	35	7	-	24	160	300
Br1	15	13	18	-	140	320
Br2	15	8	14	-	160	280
Br3	10	3	2	-	160	140
Cc1	10	5	6	10	-	160
Cc2	10	4	6	16	-	140
Cc3	10	5	7	24	-	160
SQ3	25	17	4	8	40	-
SQ4	20	17	4	8	60	-
SQ5	30	18	4	8	80	-

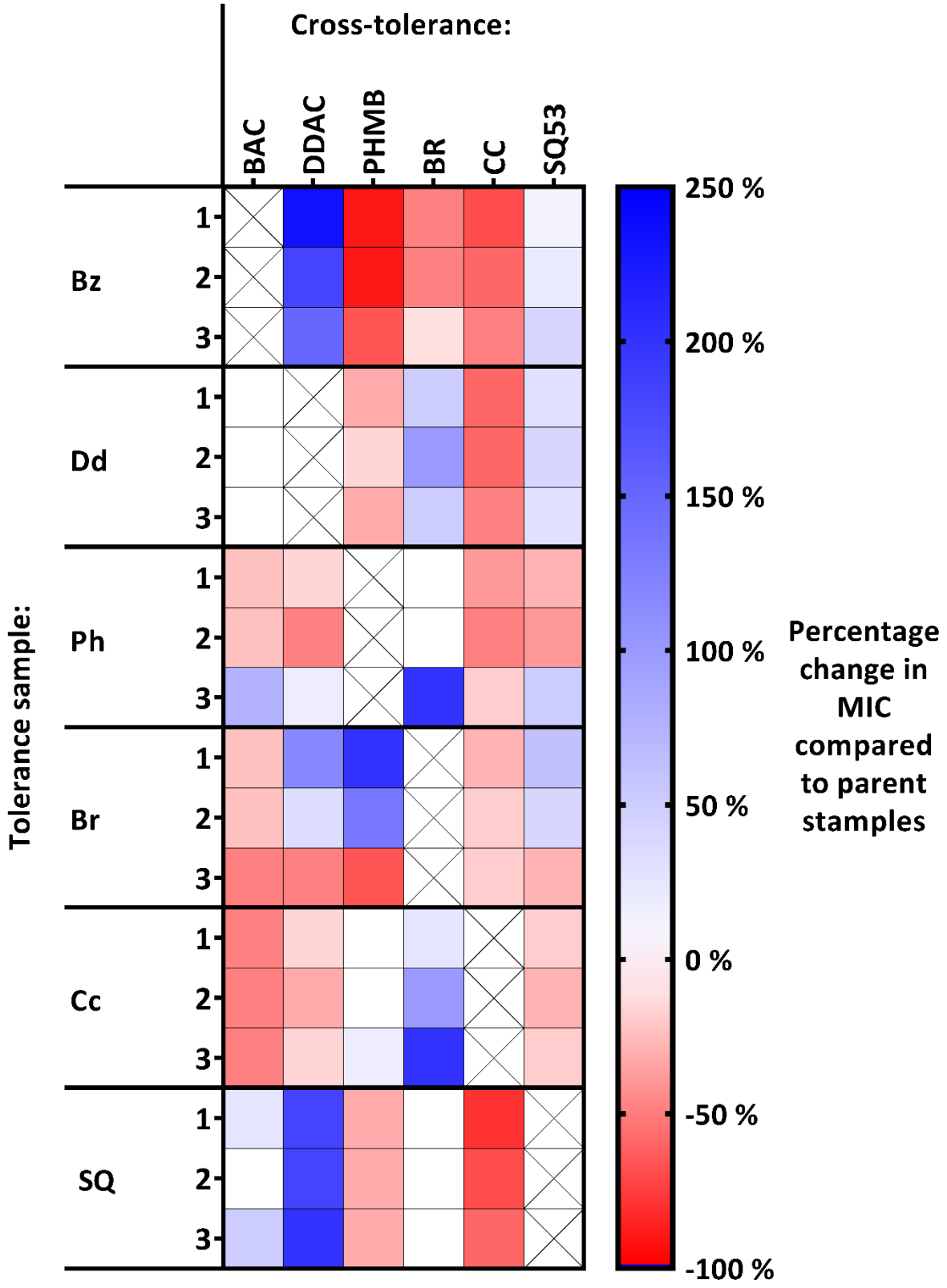

Figure 18. Cross-tolerance of disinfectant-tolerant samples of *Klebsiella pneumoniae* NCTC 13443 to other common disinfectants. Colour gradient represents the percentage change in minimum inhibitory concentration of the tolerant samples compared to the untreated parent samples, with blue and red indicating an increase or decrease in minimum inhibitory concentration, respectively. BAC: benzalkonium chloride. DDAC: didecyldimethylammonium chloride. PHMB: polyhexamethylene biguanide. BR: bronopol. CC: chlorocresol. SQ53: disinfectant formulation "SQ53". Bz: BAC-tolerant sample. Dd: DDAC-tolerant sample. Ph: PHMB-tolerant sample. Br: BR-tolerant sample. Cc: CC-tolerant sample. SQ: SQ53-tolerant sample.

4.5. Conclusions

The ability of *K. pneumoniae* and *S. aureus* to develop tolerance to the common disinfectants BAC, DDAC, PHMB, bronopol and chlorocresol, and the disinfectant formulation SQ53 was elucidated. *K. pneumoniae* was found to readily be able to develop tolerance to all of the tested disinfectants and also to disinfectant formulation SQ53. The degrees of tolerance varied between a 30% to 413% increase in MIC (Table 8), indicating that different disinfectants have varying susceptibilities to tolerance development. This is likely a result of the various MOA of the disinfectants and the ability for *K. pneumoniae* to overcome them. The development of tolerance to the SQ53 formulation indicates that combining disinfectants does not necessarily mitigate tolerance development.

However, it should be noted that the ability for *K. pneumoniae* to develop tolerance to SQ53 was limited to a 30% increase, the same as the lowest individual disinfectant MIC increase (Table 8). This implies that the ability for *K. pneumoniae* to develop tolerance to the formulation as a whole was limited by the ability for *K. pneumoniae* to develop tolerance to each of the individual components individually. Further study on other bacterial species and combinations of disinfectants should be conducted to further investigate this hypothesis.

S. aureus was unable to develop tolerance to any of the tested disinfectants within the parameters of the experiment (Figure 17). *S. aureus* tolerance against bronopol, chlorocresol or the SQ53 disinfectant formulation has not been demonstrated previously, indicating that it is not possible for *S. aureus* to develop tolerance to these disinfectants. However, previous studies have demonstrated the ability for *S. aureus* to develop tolerance to BAC, DDAC, PHMB, chlorhexidine and triclosan *in vitro* [266], [323]–[325], [334]. This demonstrates that the ability to develop tolerance may vary between strains or experimental procedures.

Disinfectant cross-tolerance between each of the *K. pneumoniae* tolerant samples and the other disinfectants was established by comparing the MICs of the disinfectants before and after the tolerance development experiment (Figure 18). The samples displayed a wide range of cross-tolerance, ranging from -91.7% to 233.3% difference in MIC after treatment (Figure 18). Of the 90 combinations and biological replicates examined, 11 displayed no change in susceptibility to the second disinfectant treatment (Figure 18). This is likely a result of differences in the MOA of the two disinfectants, leading to adaptations to the first treatment not providing any advantages upon exposure to the second.

Thirty-one combinations demonstrated a reduced susceptibility to the second disinfectant treatment after tolerance development (Figure 18). This is a result of overlaps in the MOA of the two disinfectants meaning that adaptations to one confers a survival advantage when adapted bacteria are exposed to the other.

Interestingly, 48 out of the 90 combinations demonstrated an increase in susceptibility to the second disinfectant (Figure 18). This indicates that the accumulated adaptations to the first treatment provided a disadvantage when the samples were exposed to the second (Figure 18). We hypothesise that over-adaptation to the first disinfectant leaves the samples limited in their available resources and ability to respond to the second disinfectant, especially if the disinfectants have a different MOA.

The degree of cross-tolerance was also dependant on the order of exposure, so tolerance is not automatically mutual. For example, initial tolerance to BAC granted a 150%-233% decreased susceptibility to DDAC, but a tolerance to DDAC did not grant any change in susceptibility to BAC (Figure 18). This is likely a result of the different disinfectants promoting different tolerance mechanisms, or variation in physiochemical properties between the disinfectants causing variation in the ability for the disinfectants to overcome a single common tolerance mechanism.

Disinfectants that operated via a single MOA generated consistent cross-tolerance profiles across the biological replicates (Figure 18). In contrast, PHMB and bronopol generated cross-tolerance profiles that varied between replicates (Figure 18), which we hypothesise is a result of the multiple mechanisms these disinfectants utilise. As a result, the *K. pneumoniae* cells have multiple possible mechanisms to adapt to, leading to variation in their ability to tolerate other disinfectants.

Finally, SQ53 provided cross-tolerance to DDAC, indicating that the mechanisms are similar (Figure 18). As SQ53 contains each of the other disinfectants, this heavily implies that DDAC is the main active component of the formulation. The samples were more susceptible to PHMB and chlorocresol, indicating that the samples were able to become vulnerable to these components and still resist a higher overall concentration of SQ53, despite these two components being present within the formulation. This indicates that these two components do not provide a high level of activity to the formulation as a whole, supporting conclusions made previously in Chapters 2.4.2 and 2.4.5.

To our knowledge, cross-tolerance profiles of disinfectant-tolerant samples developed in this manner have not been reported in the literature before. These data therefore provide novel insights into the plasticity of disinfectant tolerance mechanisms in *K. pneumoniae* when challenged with other disinfectants.

5. Mechanisms of *K. pneumoniae* Tolerance to Common Disinfectants

5.1. Introduction

Previously, *K. pneumoniae* NCTC 13443 samples have been shown to be able to develop tolerance to a range of common disinfectants (Chapter 4.4.1). While it is possible to use cross-tolerance experiments to identify potential similarities and differences between the underlying resistance mechanisms, full characterisation of the samples requires in-depth molecular analysis. A multiomics approach will afford detailed insights into the underlying mechanisms of disinfectant tolerance that would otherwise not be possible.

Previous studies have elucidated various mechanisms that underpin bacterial tolerance to a range of disinfectants, as discussed in Chapter 1.4.2.3. However, when examining *K. pneumoniae* tolerance to the disinfectants investigated in this study, the existing literature is limited.

BAC tolerance has been attributed to an increase in membrane depolarisation and efflux pump activity in clinical *K. pneumoniae* [222]. Membrane depolarisation is associated with a reduction in susceptibility to specific antibiotics [353], although it is not clear how this may contribute to BAC tolerance specifically. An increased activity of efflux pumps leads to the removal of the antimicrobial from the outer membrane and thus affords the cell a degree of tolerance to the antimicrobial mechanism of action. More recently it has been demonstrated that the loss of function of the AcrAB-TolC efflux pump complex in *K. pneumoniae* is associated with an increased susceptibility to both BAC and DDAB [223]. Other studies have established a link between the presence of the *qacΔE* gene and tolerance to BAC and DDAC in *K. pneumoniae* [224]. This collectively suggests that efflux pump activity influences the efficacy of QACs.

However, efflux pump activity is unlikely to be the sole contributor to QAC tolerance in *K. pneumoniae*. For instance, efflux pump inhibition via carbonyl cyanide 3-chlorophenylhydrazone was shown to not reduce susceptibility of *K. pneumoniae* isolates containing the *cepA*, *qacΔE* and *qacE* efflux pumps to BAC and a PHMB-containing disinfectant [227].

Another study of *K. pneumoniae* isolates exposed to BAC demonstrated an increased cell hydrophobicity and up-regulation of expression of biofilm regulatory gene *bssS*, suggesting increased biofilm formation as a method of BAC tolerance [228]. In other species, the down-

regulation of porins and the alteration of membrane charge via lipid A modification has been shown to potentially contribute to BAC tolerance [233].

Collectively, the literature suggests that broad-spectrum efflux pumps may contribute to BAC, DDAC and PHMB tolerance. However, there are likely to be other contributing mechanisms too, such as biofilm regulation, porin down-regulation and lipid A modification.

Bacterial tolerance to bronopol has not been widely investigated. An early study on the MOA of bronopol against *E. coli* noted that the presence of catalase or superoxide dismutase mitigated the bactericidal activity of bronopol via the removal of ROS [100]. Therefore, bronopol tolerance may be associated with expression changes in these proteins.

Chlorocresol tolerance has not been identified before, so any potential underlying tolerance mechanisms are unknown. However, investigations on bacterial tolerance to other phenol-derivatives have been conducted on other bacterial species. Variations in *E.coli* susceptibility to chloroxylenol have been associated with AcrAB activity [225], and *S. enterica* susceptibility to phenol correlated with efflux pump activity [226]. This suggests a potential link between the expression of broad-spectrum efflux pumps and tolerance to chlorocresol.

Finally, to our knowledge there is no previous research investigating the mechanisms of bacterial tolerance to complex disinfectant formulations. As a result, it is unclear how the presence of multiple disinfectants with varying MOAs will influence the mechanisms of tolerance development.

5.2. Chapter aims

There is a scarcity of existing literature regarding underlying mechanisms of *K. pneumoniae* tolerance to the disinfectants examined. To afford detailed insights into the wide range of potential underlying tolerance mechanisms, a broad multiomics approach was employed.

The first objective was to establish if the observed tolerance was induced through phenotypic adaptation, or mutations acquired through selection pressure. This would be achieved through whole genome sequencing of the tolerant samples and untreated parent samples. Variations between each tolerant sample and their respective parent sample were identified to elucidate potential genetic adaptations that underpin the disinfectant tolerance observed.

The genetic variations identified were used to infer the phylogenetic relationships between each of the samples to elucidate potential common tolerance mechanisms. In addition, the genomes were screened for mutations that were conserved between biological replicates, allowing the identification of mutations that are consistently advantageous for survival against the respective disinfectant treatment. Finally, the genomes were screened using the Antimicrobial Resistance Finder plus (AMRF) tool to identify mutations in genes known to be associated with mechanisms of tolerance [354].

The second objective was to elucidate the underpinning molecular mechanisms of the disinfectant tolerance observed in the samples. To investigate this, label-free quantitative proteomic analysis of each sample was performed. The relative changes in protein content were quantified between each disinfectant-tolerant sample and their respective parent strain. This allows for the identification of specific proteins, biological processes and pathways that are over or under-represented in the samples, which in turn gives an indication of the underlying mechanisms that allow the sample to tolerate the disinfectant treatment.

5.3. Materials and methods

The specific disinfectant-tolerant *K. pneumoniae* NCTC 13443 samples to be examined were generated during disinfectant adaptation experiments conducted in Chapter 4. For details on the biological replicates selected and a schematic diagram of the experimental workflow see Chapter 4.3.3 and Figure 15, respectively.

5.3.1. Whole genome sequencing

5.3.1.1. DNA extraction and sample quality control

DNA extractions were performed on disinfectant-tolerant *K. pneumoniae* NCTC 13443 samples developed in Chapter 4. Three biological replicates from each disinfectant treatment were selected for further analysis, as described in Chapter 4.3.3 and displayed in Figure 15. Unique phenotypes were observed in 2 of the biological replicates of the BAC-tolerant samples ("green" and "dark", as described in Chapter 4.4.1), which were each isolated and subject to molecular characterisation. As a result, 5 BAC-tolerant samples were analysed from 3 BAC-tolerant biological replicates. Extractions were also performed on the original parent biological replicate samples from before the disinfectant tolerance experiment.

Samples were incubated overnight at 37°C in MHB. Disinfectant-tolerant samples were incubated in the presence of the adapted MIC of respective disinfectant treatment, as displayed in Table 8. 1 ml aliquots were taken from each sample and spun down at 5400 G for 10 minutes before being re-suspended in sterile phosphate-buffered saline (PBS). This wash step was repeated a further 2 times, before DNA extractions were performed using the DNeasy PowerSoil Pro Kit (Qiagen, Venlo, Netherlands) following the manufacturer's instructions. The resulting lysates were frozen at -20°C until required.

Extracted DNA samples were analysed via a NanoDrop™ 2000/2000c Spectrophotometer (Thermo Scientific™) to assess the concentration and purity of DNA samples. All samples demonstrated an optical density (OD) 260/280 of between 1.8 and 2.0, and contained a concentration of DNA ≥ 10 ng/µl. Results are shown in Chapter 8. Appendix, Table 19. As a result, the samples met the requirements for further analysis and were sent to Novogene (UK) Company Limited, Cambridge, UK.

5.3.1.2. Library preparation and sequencing

Novogene conducted additional quality control steps to assess the DNA quality of the samples via agarose gel electrophoresis and fluorescence-based Quibit™ quantitation assays using a

Quibit® 2.0 Fluorometer. Library preparation was performed via DNA fragmentation, end repair and A-tailing, adapter ligation, PCR amplification and sample purification. Library quantification was performed using a Quibit™ quantitation assay followed by qPCR to validate the presence of illumina anchor sequences. Finally, the sizing and quality assessment of the library was performed using an Agilent 2100 Bioanalyser. Samples were sequenced using an Illumina® NovaSeq™ 6000.

5.3.1.3. Data analysis

Data analysis steps performed by Novogene are as follows. Original image data were transformed into raw reads by Consensus Assessment of Sequence And Variation (CASAVA) base calling. Quality control was conducted by discarding read pairs if either one read contains adapter contamination, a number of uncertain nucleotides greater than 10%, or if over 50% of the nucleotides were of low quality. Clean paired-end reads were mapped to the reference genome by Burrows-Wheeler Aligner (BWA). The reference genome was located and downloaded from National Centre for Biotechnology Information website under entry number 32868_D02, GenBank assembly accession GCA_900451585.1 [355].

The statistics of the sequencing data and mapping statistics for each sample can be found in Table 10. Variant-calling was performed using the genome analysis toolkit (GATK), generating variant call format (VCF) files containing a list of all single nucleotide polymorphisms (SNPs) or insertions or deletions of ≤ 50 base pairs (bp) in length (InDels). The bcftools 'isec' command was used to compare the VCF file from each disinfectant-tolerant sample to the VCF file of the untreated parent sample. Three separate VCF files were generated, containing either variants that are unique to the disinfectant-tolerant sample (variants gained during disinfectant exposure), parent sample (variants "lost" during disinfectant exposure), or variants common to both disinfectant-tolerant and parent samples (variants that existed before disinfectant exposure and were maintained).

The remaining analysis steps were conducted manually as follows. Variants identified as unique to either the disinfectant-tolerant samples or parent samples were annotated using the Annotate Variation (ANNOVAR) software tool, providing information regarding the type of mutation, the impacted gene (if any) and the influence on the encoded protein (if any).

The resulting annotated VCF file was converted to a spreadsheet format and analysed using Microsoft® Excel®. The SNPs and InDels identified across different samples were collated into a central database containing all identified mutations, which could then be filtered and sorted according to various properties including mutation type, mutation effect, gene name or ID,

protein name or samples that contained the mutation. This allowed for manual analysis of SNPs and InDels. The statistics regarding the SNPs and InDels lost and gained by disinfectant-tolerant samples were compiled into bar graphs using GraphPad Prism 9.4.1.

5.3.1.3.1. Phylogeny

Phylogenetic trees were generated using the CSI Phylogeny 1.4 online tool [356]. The programme requires sequences to be uploaded in the fasta file type. These were generated by applying the original list of variants called by GATK to the reference genome. The SNP and InDel VCF files for each sample were combined into a single VCF file using the Picard tools 'MergeVCFs' command, which was then applied to the reference genome using the GATK command 'FastaAlternateReferenceMaker'. This generated fasta sequences of the genomes for every sample, from which phylogeny could be inferred using the CSI Phylogeny 1.4 online tool [356].

The tool was used with default parameters (10x minimum depth at SNP positions, 10% minimum relative depth at SNP positions, 10 bp pruning, minimum SNP quality of 30, minimum read mapping quality of 25 and minimum Z-score of 1.96). The *K. pneumoniae* NCTC 13443 reference genome [355] was used as the reference sequence when relative phylogeny was inferred across all samples. Each respective parent strain was used as the reference sequence to infer the relative phylogenies of individual biological replicates. FigTree.v1.4.4 [357] was used to generate the phylogenetic tree figures from the newick file generated by CSI Phylogeny 1.4.

5.3.1.3.2. Manual analysis of mutations

For manual analysis the list of mutations were refined to exclude SNPs that did not result in a change in the amino acid sequence (synonymous SNPs), mutations in non-coding regions and mutations that are not conserved across all biological replicates. The remaining mutations represent the mutations that are likely to impact the function of the protein, and are conserved across all biologically-independent tolerant samples.

The refined gene lists were used to assemble a network diagram based on their associated Gene Ontology (GO) biological function terms using the ClueGO v2.5.9 plugin [358] within the Cytoscape v3.9.1 programme [359]. *K. pneumoniae* strain 342 was used as the reference genome, as this was the closest relative with an annotated genome available in the software. If there were insufficient genes in the lists to form a network, the gene lists are presented as a table instead. Analysis of gene and protein function was conducted via the UniProt database [360]. If functional information was not available for the gene or protein in *K. pneumoniae* NCTC 13443, the search was broadened to include all *K. pneumoniae* strains and then to *E.coli* K12, as noted in

each case. The functionality of these genes and associated proteins was assumed to be synonymous across the bacterial species and strains.

5.3.1.3.3. Analysis of mutations in antimicrobial resistance genes

The second methodology of data refinement utilised the Antimicrobial Resistance Finder Plus (AMRF) tool [354]. The genomes of all disinfectant-tolerant samples generated previously during phylogenetic analysis (Chapter 5.3.1.3.1) were screened for any genes known to be associated with AMR using the AMRF software [354]. The resulting lists of AMR-associated genes were cross-referenced with the lists of mutations conserved across biological replicates to identify conserved mutations in AMR-related genes. The resulting genes were manually examined using the UniProt database [360] as previously described in Chapter 5.3.1.3.2.

5.3.2. Global quantitative proteomics

5.3.2.1. Protein extraction

Proteomic analysis was performed on disinfectant-tolerant *K. pneumoniae* NCTC 13443 samples developed in Chapter 4. Three biological replicates from each disinfectant treatment were selected for further analysis, as described in Chapter 4.3.3 and displayed in Figure 15. Unique phenotypes were observed in 2 of the biological replicates of the BAC-tolerant samples ("green" and "dark", as described in Chapter 4.4.1), which were each isolated and subject to molecular characterisation. As a result, 5 BAC-tolerant samples were analysed from 3 BAC-tolerant biological replicates. Protein extractions were also performed on the original parent biological replicate samples from before the disinfectant tolerance experiment.

Samples were incubated overnight at 37°C in MHB. Disinfectant-tolerant samples were incubated in the presence of the respective disinfectant treatment. Samples were washed in PBS three times before resuspension in lysis buffer (50 mM tris(hydroxymethyl)aminomethane (tris), 150 mM NaCl, 0.1% w/v SDS, ethylenediaminetetraacetic acid-free protease inhibitor cocktail (Roche)). Samples were sonicated on ice (Fisherbrand™ 505 Sonicator with Fisherbrand™ FB4418 3.1mm Microtip Probe) for 120 s at 12% amplitude with 10 s pulses, before cellular debris was removed via centrifugation at 12,000 G for 20 minutes at 4°C. The supernatant was isolated, and the protein concentration was quantified using the Pierce™ Bicinchoninic Acid Protein Assay Kit (Thermo Scientific™) following the manufacturer's instructions. The resulting lysates were frozen at -20°C until required.

5.3.2.2. Protein digest

Lysates were thawed and centrifuged at 14,000 G for 10 minutes. Volumes of lysate containing 100 µg of protein were added to 600 µl methanol and 150 µl chloroform and vortexed thoroughly. 450 µl dH_2O was added before vortexing thoroughly and subsequent centrifugation at 14,000 G for 10 minutes. The upper aqueous layer was carefully removed, and 450 µl methanol was added before subsequent vortexing and centrifugation to pellet the proteins. The supernatant was then removed, and the pellet allowed to air dry. The protein pellet was subsequently re-suspended in 100 µl of 6 M urea/50mM tris-HCl at pH 8.0, before the addition of 5 mM dithiothreitol and a 30-minute incubation at 37°C. 15 mM iodoacetamide was added and samples were incubated for 30 minutes at room temperature. Finally, 4 µg trypsin/Lys-C mix (Promega Corporation, UK) was added to each sample before a 4-hour incubation at 37°C. 750 µl 50 mM tris-HCl at pH 8.0 was then added and the samples were incubated overnight at 37°C. The digestion was terminated via the addition of 4 µl trifluoroacetic acid, before centrifugation at 14,000 G for 10 minutes. The peptide mixture was purified using an Oasis PRiME HLB 96-well µElution plate (Waters™) by elution in 70% acetonitrile according to the manufacturers' instructions. The samples were spin-dried in an evaporator centrifuge under vacuum and stored at 4°C until use.

For analysis samples were re-suspended in 50 µl 0.1% v/v formic acid before being analysed via mass spectrometry (separation via UltiMate 3000 RSLC nano system (Thermo Scientific™) coupled on-line to an Orbitrap Fusion™ Tribrid™ Mass Spectrometer (Thermo Fisher Scientific, UK)).

5.3.2.3. Data analysis

Peptide/protein identification and area under the curve protein quantification was conducted using PEAKS Studio Xpro (Bioinformatics Solutions Inc.). The resulting list of proteins were filtered to only include proteins identified across all parent and disinfectant-tolerant biological replicates. The false discovery rate (FDR) was set to 1%, and results were filtered to include only include proteins with a minimum fold change of +/-2. The resulting list contained all of the differentially expressed proteins, with fold-changes set in comparison to the parent sample.

Overall proteome statistics were compiled from PEAKS Studio Xpro. Lists of differentially expressed proteins were inputted into a web-based Venn diagram tool (Bioinformatics and Evolutionary Genomics, Venn Diagram Tool) [361], generating a list of proteins that were unique for every combination of samples. These lists were then compiled into figures via

GraphPad Prism 9.4.1. The top 10 proteins that demonstrated an increased expression change were compiled into a table for manual analysis.

GO term enrichment analysis of differentially expressed proteins was performed via the Database for Annotation, Visualization and Integrated Discovery (DAVID) online tool [362], [363] with *K. pneumoniae* MGH 78578 used as the background list. All enriched biological process and cellular component GO terms with a p-value ≤ 0.05 were compiled into a heatmap via GraphPad Prism 9.4.1.

Network maps of differentially expressed proteins were generated using the ClueGO v2.5.9 plugin [358] within the Cytoscape v3.9.1 programme [359]. The genes that encode the differentially expressed proteins were arranged according to their Kyoto Encyclopedia of Genes and Genomes (KEGG) database annotations [364], [365], showing the biological pathways that the genes are associated with. *K. pneumoniae* strain 342 was used as the reference gene list, as this was the closest relative to *K. pneumoniae* NCTC 13443 available in the software.

5.4. Results and discussion

5.4.1. Whole genome sequencing

5.4.1.1. Sequencing statistics and mutation distribution

The full methodology for both the sample preparation and data analysis steps can be found in Chapter 5.3.1. The sequencing reads for each sample were mapped to the *Klebsiella pneumoniae* NCTC 13443 reference genome [355], before variations between the mapped genome and the reference genome were identified. The SNPs and InDels were compiled into a list of mutations for each sample. The mutation lists of each disinfectant-tolerant sample were compared to their respective parent samples to identify mutations that were unique to either the disinfectant-tolerant sample or the parent sample. The mutations that were unique to the tolerant sample or parent sample represented the mutations that had been gained or lost (respectively) as a result of long-term disinfectant exposure.

The sequencing statistics for each of the samples can be found in Table 10. The total number of reads after quality control ranged from 8-24 million (Table 10). The variation in the number of reads generated by each sample did not correlate with any particular treatment, so this was assumed to be a result of experimental variation between the samples. From the total reads, between 99.07% and 99.78% reads were mapped to the reference genome, with the exception of Ph2 which achieved a mapping rate of 81.41% (Table 10). The possible reasons for this include contamination, a poorly assembled reference genome or a distant genetic relationship between the sample and the reference genome. As all other samples achieved a high mapping rate it was deemed unlikely that the issue is a result of the reference genome or distant genetic relationship. It is possible that the sample contained contamination, however the sample was not excluded from further analysis as the mapping rate remained within typical mapping ranges of 70%-90% [366].

Between 96.01% and 99.88% of each assembled genome had a read depth of ≥4, with the average read depths of all samples ranging from 170.17-365.60 (Table 10). As a read depth of at least 50 is required to accurately detect SNPs [367], the data was deemed acceptable for further analysis.

The mutation types discussed are defined as follows. A single nucleotide polymorphism (SNP) is a mutation characterised by the substitution of a single nucleotide for another. SNPs can be either non-synonymous or synonymous, whereby the substituted nucleotide does or does not lead to a change in the amino acid sequence, respectively. Sequence insertions or deletions of ≤

50 bp in length are referred to as InDel mutations. InDels can be either frameshift or non-frameshift, depending on whether the mutation leads to a shift in the open reading frame or not, respectively. Stop gain or Stop loss mutations refer to changes in the nucleotide sequence that lead to the introduction or deletion of stop codon, respectively. These definitions can be also found in the List of definitions.

The compiled statistics of the annotated mutations are presented in Figure 19. The raw data are available in Chapter 8. Appendix, Table 20, Table 21, Table 22 and Table 23. Tolerant samples gained a varying number of SNPs during the tolerance experiment, with Bz1G and D acquiring 500 and 506 SNPs respectively, while Ph1 only acquired 9 (Figure 19a). Interestingly, all *K. pneumoniae* samples exposed to the two QACs (BAC and DDAC) acquired a high number of SNPs, from 365-506 (Figure 19a). In contrast bronopol and chlorocresol-exposed *K. pneumoniae* samples only gained between 9 and 20 SNPs (Figure 19a). This is also reflected for the InDel mutations statistics, with QAC-tolerant samples developing 84-142 mutations, compared to just 5-10 mutations in samples exposed to bronopol or chlorocresol (Figure 19c). This indicates that the QACs may induce a stronger selection pressure on *K. pneumoniae* than bronopol or chlorocresol, with more genetic adaptation being required for tolerance to develop.

The highest number of mutations in any individual sample was observed in Bz1G and D, with a total of 500 and 506 SNPs respectively, and 139 and 142 InDels respectively (Figure 19a, c). This indicates variability in the mechanisms of tolerance between biological replicates, despite the same selection pressure. This variation can also be seen between SQ53-tolerant samples (Figure 19a, c) and in the number of SNPs gained by PHMB-tolerant samples (Figure 19a).

The parent strains contained between 1 and 7 unique SNPs when compared to each of the tolerant samples, indicating that their sequences reverted back to conform to the reference sequence (Figure 19b). There does not seem to be any trend between the SNPs lost and the different disinfectant treatments, so this is all assumed to be a result of the stochastic nature of mutations. In contrast, the samples all lost between 121 and 155 InDels, with the sequences reverting back to conform to the consensus sequence (Figure 19d). This is consistent across all samples except Dd3, SQ2 and SQ3, which lost 226, 11 and 13 InDels respectively (Figure 19d). The high number of InDels seeming to conform to the reference sequence is unexpected, but may be a result of random chance. Alternatively, this may be a result of the experimental conditions themselves. In order to account for this, the parent strains would need to be repeatedly passaged in the absence of disinfectant and analysis repeated. Unfortunately, this is outside of the scope of the project. However, even this does not account for the inconsistency in

the number of InDels lost between biological replicates exposed to SQ53 and DDAC. This remains unexplained.

The proportions of each type of SNP gained were consistent across *K. pneumoniae* samples that were tolerant to BAC, DDAC and SQ53, with 50%-55% of SNPs being non-synonymous, then 25%-35% being synonymous, followed by the remaining SNP types (Figure 19a). This consistency can also be observed for the various InDel mutation types gained (Figure 19c). These similar distributions are likely a result of similarities in the MOAs of these disinfectants and thus the associated mechanisms of resistance. However, as the remaining disinfectant treatments displayed a relatively low number of SNPs and InDels gained, it is not possible to detect variations in the distributions of mutation types when comparing across all of the samples (Figure 19a, c). As a result, the similar distribution of mutation types may simply be due to the stochastic nature of mutations.

Similar observations can be made when considering InDels lost, with a similar distribution of mutation types across all samples except SQ2 and SQ3 (Figure 19d). This even distribution indicates that the mutations lost are likely a result of the random stochastic nature of mutations, or alternatively due to common experimental factors rather than any specific treatment difference. Due to the low number of SNPs lost it is not possible to draw any conclusions regarding the distribution of SNP mutation types lost across the samples (Figure 19b).

Table 10. Sequencing data and mapping statistics of disinfectant-tolerant *Klebsiella pneumoniae* NCTC 13443 samples sequenced via whole genome sequencing. Effective data (%): The ratio of clean data to raw data. Error (%): Overall error rate. GC content (%): Percentage of G and C in the total bases. Total reads: total no. of effective, clean reads after quality control. Mapped reads: No. of clean reads mapped to the reference sequence. Mapping rate: Ratio of mapped reads to total clean reads. Average read depth: The average depth of mapped reads at each site. Total no. of bases in mapped reads divided by the no. of bases in the assembled genome. Coverage >1X/≥4X (%): Percentage of assembled genome with more than 1 or ≥ 4 mapped reads at each site, respectively.

Sample name	No. of raw reads (n)	Effective data (%)	Error rate (%)	GC content (%)	Total reads (n)	Mapped reads (n)	Mapping rate (%)	Average read depth (X)	Coverage >1X (%)	Coverage ≥4X (%)
Ps1	11,728,348	99.91	0.03	56.00	11,720,044	11,645,661	99.37	237.37	99.92	99.88
Ps2	8,043,258	99.91	0.03	55.95	8,036,996	7,989,743	99.41	170.17	99.90	99.87
Ps3	11,474,396	99.90	0.03	56.11	11,464,361	11,393,694	99.38	231.06	99.91	99.88
Bz1G	14,957,694	99.88	0.03	55.22	15,002,227	14,906,849	99.36	242.13	97.25	97.21
Bz1D	18,420,048	99.87	0.03	55.46	18,455,205	18,356,610	99.47	289.99	97.27	97.22
Bz2G	20,030,292	99.88	0.03	55.58	20,037,140	19,928,311	99.46	308.54	97.26	97.22
Bz2D	11,188,512	99.86	0.03	55.23	11,215,344	11,190,950	99.78	229.09	97.25	97.21
Bz3	12,431,370	99.85	0.03	55.33	12,464,387	12,374,720	99.28	250.87	96.76	96.01
Dd1	17,323,274	99.86	0.03	55.74	17,340,439	17,206,646	99.23	278.62	97.28	97.22
Dd2	21,396,106	99.85	0.03	55.66	21,411,590	21,243,706	99.22	325.60	97.26	97.22
Dd3	12,690,616	99.91	0.03	56.16	12,682,254	12,606,893	99.41	255.28	96.25	96.21
Ph1	20,792,940	99.89	0.03	55.91	20,788,551	20,601,220	99.10	317.96	97.34	97.31
Ph2	11,880,734	99.91	0.03	57.04	11,872,091	9,665,371	81.41	199.04	96.70	96.64
Ph3	17,707,914	99.88	0.03	56.12	17,699,304	17,545,090	99.13	279.90	97.35	97.31
Br1	17,695,082	99.90	0.03	56.34	17,684,075	17,603,418	99.54	272.92	97.16	97.11
Br2	9,860,580	99.91	0.03	56.44	9,855,542	9,804,349	99.48	202.90	97.15	97.09
Br3	24,081,048	99.91	0.03	56.39	24,069,437	23,925,789	99.40	365.60	97.17	97.13
Cc1	19,361,616	99.88	0.03	56.17	19,371,087	19,191,343	99.07	311.47	97.13	97.07
Cc2	11,397,156	99.88	0.03	55.64	11,418,956	11,315,682	99.10	236.79	96.96	96.07
Cc3	23,621,270	99.89	0.03	55.78	23,659,204	23,472,534	99.21	352.68	97.11	97.02
SQ1	18,032,126	99.89	0.03	55.77	18,130,215	17,985,528	99.20	284.29	97.34	97.30
SQ2	11,436,624	99.89	0.03	55.42	11,465,872	11,435,637	99.74	230.94	99.92	99.88
SQ3	10,547,968	99.87	0.03	55.50	10,566,034	10,475,855	99.15	213.79	99.91	99.88

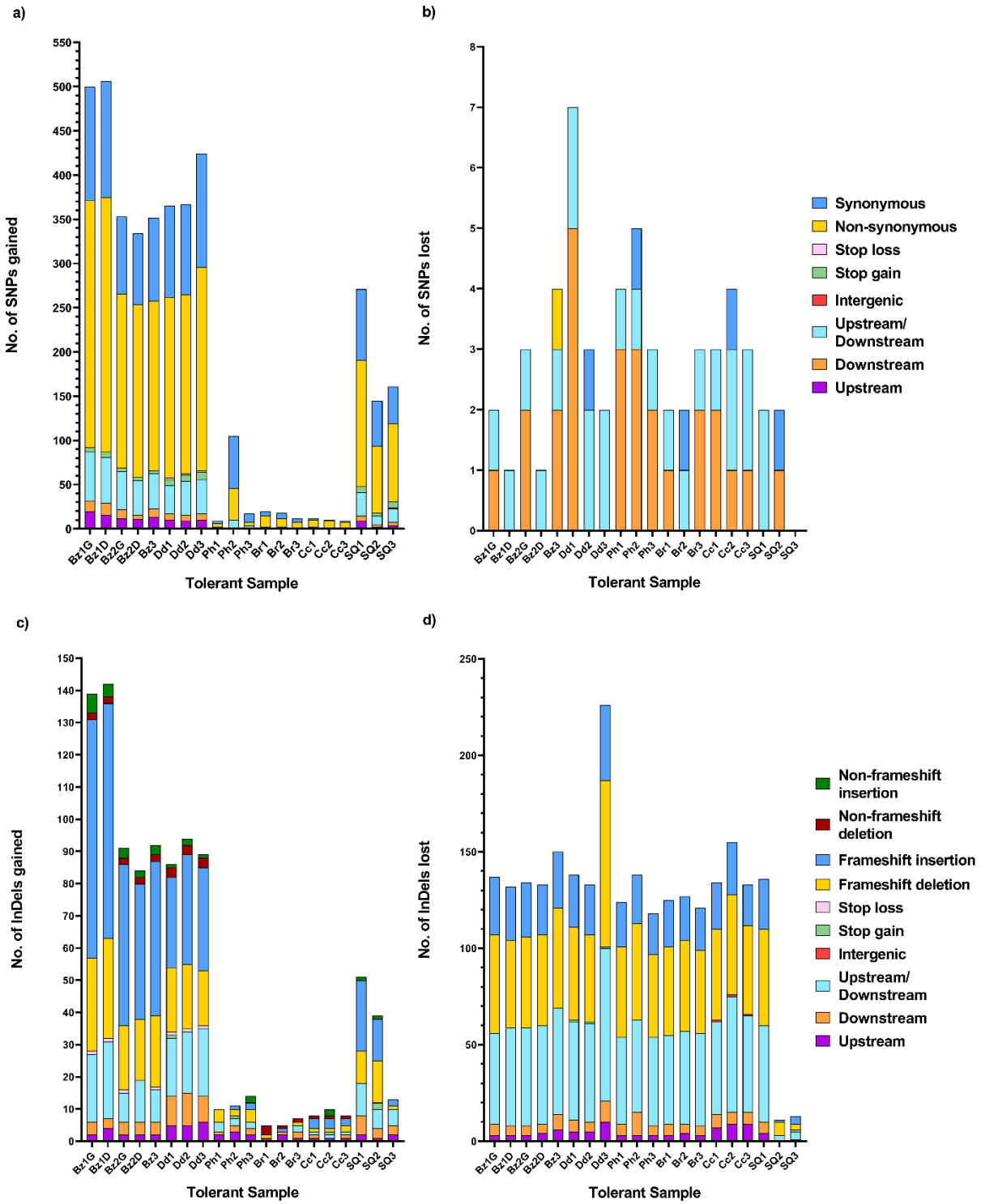

Figure 19. Mutations acquired or lost by *Klebsiella pneumoniae* NCTC 13443 disinfectant-tolerant mutants compared to untreated parent samples. a) Single nucleotide polymorphisms (SNPs) gained by disinfectant-tolerant samples. b) SNPs lost by disinfectant-tolerant samples. c) Insertions or deletions that are ≤ 50 base pairs in length (InDels) gained by disinfectant-tolerant samples. d) InDels lost by disinfectant-tolerant samples. Mutation types are as follows. Upstream: Mutations located within 1 kb upstream of a gene start site. Downstream: Mutation located within 1 kb downstream of a gene region. Upstream/Downstream: Mutation located between 2 genes that are ≤ 2kb apart. Intergenic: Mutation located in the > 2 kb intergenic region. Stop gain/loss: Mutation leads to the introduction or deletion of stop codon. Non-synonymous: SNP leads to a change in the amino acid sequence. Synonymous: SNP does not lead to a change in the amino acid sequence. Frameshift: Insertion/deletion changes the open reading frame. Non-frameshift: Insertion/deletion does not change the open reading frame.

5.4.1.2. Phylogeny

The phylogenetic relationships between the *K. pneumoniae* mutant samples were inferred using the CSI Phylogeny 1.4 online tool. A comprehensive overview of the methodology can be found in Chapter 5.3.1.3.1. In brief, CSI Phylogeny aligns the sequences and calls SNPs, from which variation in the SNPs is used to infer phylogenetic distance and relationships. The phylogenetic trees are then generated using FastTree [368], [369]. A phylogenetic tree depicting the overall phylogenetic relationships of all mutant samples is shown in Figure 20. The inferred phylogenetic relationships of each biological replicate individually when using each respective parent strain as a reference are shown in Figure 21, Figure 22 and Figure 23.

The tips of the phylogenetic tree depicting all tolerant samples (Figure 20) can be seen to be grouped into clades by disinfectant treatment, with separate biological replicates exposed to the same disinfectant treatment being closely related. This indicates that the selection pressure of each disinfectant gives rise to mutations that are conserved across biological replicates.

Interestingly, the phylogenetic trees depicting each biological replicate separately (Figure 21, Figure 22 and Figure 23) are inconsistent in their overall arrangement, despite being clustered into clades by treatment in Figure 20. Although overall there are significant numbers of mutations conserved across biological replicates treated with the same disinfectant treatment, there is still variability within individual biological replicates. This indicates a variability in the mutations that can lead to tolerance to the same disinfectant (Figure 21, Figure 22 and Figure 23). From these data it remains unclear if the underlying mechanisms of tolerance are the same or different between biological replicates.

The exception to the observed clustering of biological replicates in Figure 20 is the SQ53-tolerant samples, 2 of which are clustered together and are closest related to the parent strains (Figure 20). However, sample SQ1 has more mutations in common with sample Ph3 than any of the parent strains (Figure 20), with a bootstrap confidence value of 99.9% (Figure 20b). In addition, despite being clustered together with a bootstrap confidence value of 100% (Figure 20b), the SQ2 and SQ3 display a relatively distant genetic relationship with each other (Figure 20a). This inconsistency is reflected by the inconsistencies between the intra-biological replicate phylogenetic trees (Figure 21, Figure 22 and Figure 23). The lack of genetic homogeneity between biological replicates is unexpected. It has been assumed that multiple antimicrobials in combination will limit the potential mechanisms by which tolerance is able develop, as bacteria have to develop resistance to multiple MOAs simultaneously [370], [371]. The implication from these data is that the selection pressure applied on *K. pneumoniae* by SQ53 allows for multiple

possible tolerance mechanisms to occur, possibly as a result of it containing multiple disinfectants with varying MOAs.

Although the association between Ph3 and SQ1 may imply a potential similarity in the selection pressures between the two treatments, it should be noted that the SQ53-tolerant samples are genetically distant from all other tolerant samples, with only the DDAC and BAC-tolerant samples displaying a greater genetic distance (Figure 20a). Previously, the MIC data (Table 4 and Table 5), electron microscopy imaging (Chapters 2.4.3 and 2.4.4) and cross-tolerance profiles (Chapter 4.4.2) have collectively suggested a potential association between the MOA of DDAC and SQ53 as a whole. However, the data displayed in Figure 20a indicates little genetic homogeneity between the SQ53 and DDAC-tolerant samples. This is a result of the presence of the other disinfectants within the SQ53 formulation.

This demonstrates that although the mechanisms that underpin SQ53-tolerance confer cross-tolerance to DDAC (Chapter 4.4.2), this does not necessarily result from the same underlying mutations or even adaptations. The implication is that although the formulation contains the other disinfectants that each contribute varying degrees of activity, the formulation collectively applies a different selection pressure upon *K. pneumoniae* than any one of its individual components.

Furthermore, the genetic distance between the disinfectant-tolerant clusters do not align with similarities in the MOAs of the disinfectants. The two clusters that are most distant across all phylogenetic trees are BAC and DDAC (Figure 20a, Figure 21a, Figure 22a and Figure 23a), the two QACs that both operate via a similar MOA (Table 2). These disinfectants caused the largest number of both SNPs and InDels of all of the treatments, implying a strong selection pressure (Figure 19a, c), and the genetic distance between the clusters in Figure 20a indicate that the tolerant-samples have few mutations in common. The resulting accumulated mutations may be different but have previously been shown to confer cross-resistance (Chapter 4.4.2). It is possible that the mutations themselves vary, but the resulting mechanism of tolerance is the same.

Ph2 accumulated a large number of different mutations in comparison to Ph1 and Ph3, despite being exposed to the same selection pressure (Figure 20a, Figure 22a). PHMB-tolerant samples have previously demonstrated varying cross-tolerance characteristics, which has been attributed to variation in mechanisms by which PHMB is believed to act upon bacteria [64], [73], [74]. This variation in MOA may allow for varying mechanisms of tolerance, giving rise to different mutations and thus the lack of homogeneity between the biological replicates, in accordance with

the genetic distances observed between the SQ53-tolerant samples. The closest genetic relatives of Ph2 remain to be Ph1 and Ph3, despite the variation in the number of SNPs (Figure 20a).

Chlorocresol and bronopol-tolerant samples, alongside samples Ph1 and Ph3 all display a low genetic distance to the parent strains (Figure 20a) and each other (Figure 20a, Figure 21a, Figure 22a and Figure 23a). This indicates that few mutations were required for tolerance to develop in these samples, and is reflected by the number of mutations gained by these samples as shown in Figure 19a and c.

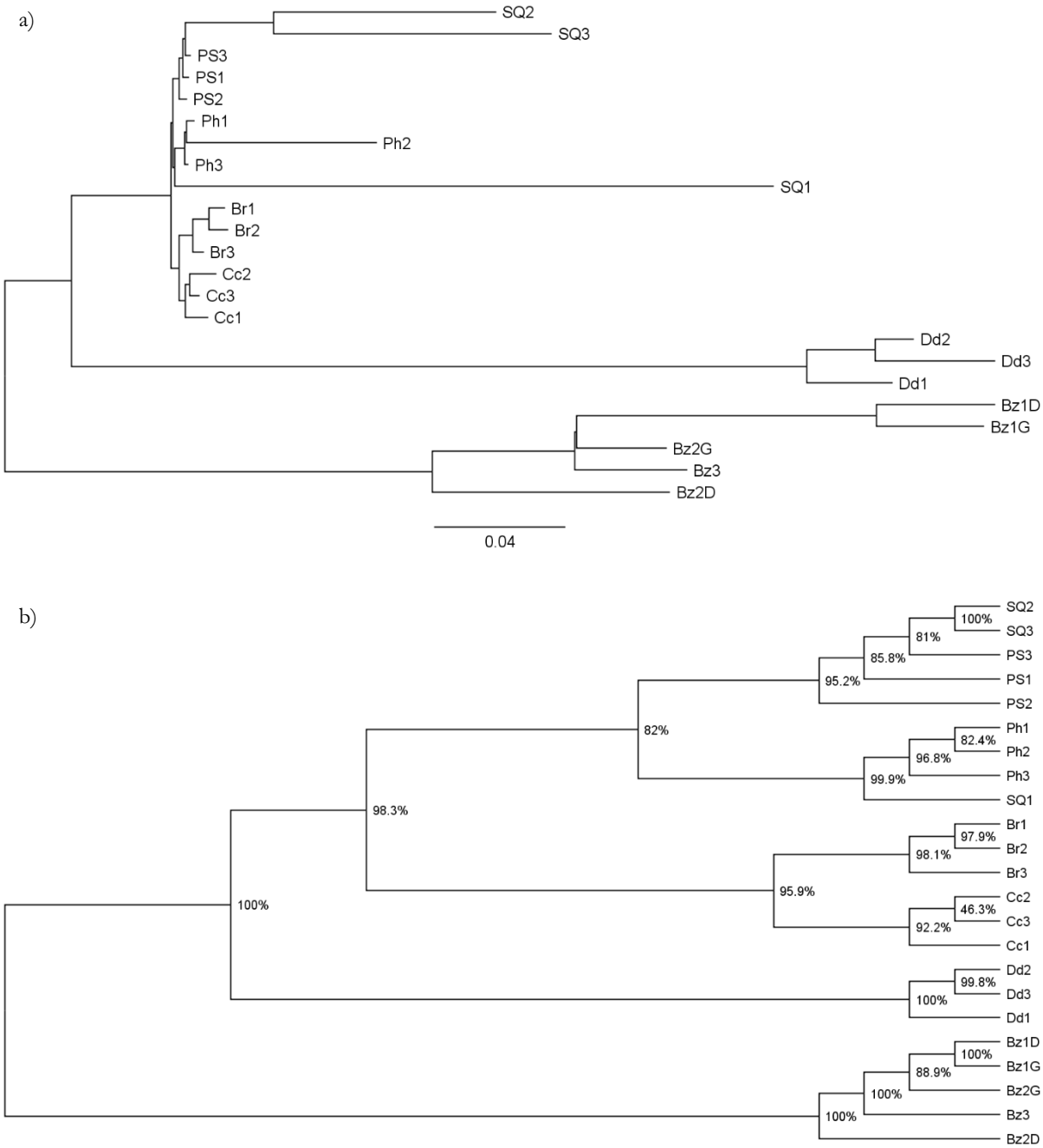

Figure 20. Unrooted phylogenetic trees of *Klebsiella pneumoniae* NCTC 13443 disinfectant-tolerant mutants. a) Scaled phylogenetic tree. Distance scale indicates the number of nucleotide substitutions per site at variable sites. b) Unscaled phylogenetic tree. Node values indicate bootstrap values as a percentage. SQ: disinfectant formulation "SQ53"-tolerant samples. PS: parent samples. Ph: polyhexamethylene biguanide-tolerant samples. Br: bronopol-tolerant samples. Cc: chlorocresol-tolerant samples. Dd: didecyldimethylammonium chloride-tolerant samples. Bz: benzalkonium chloride-tolerant samples.

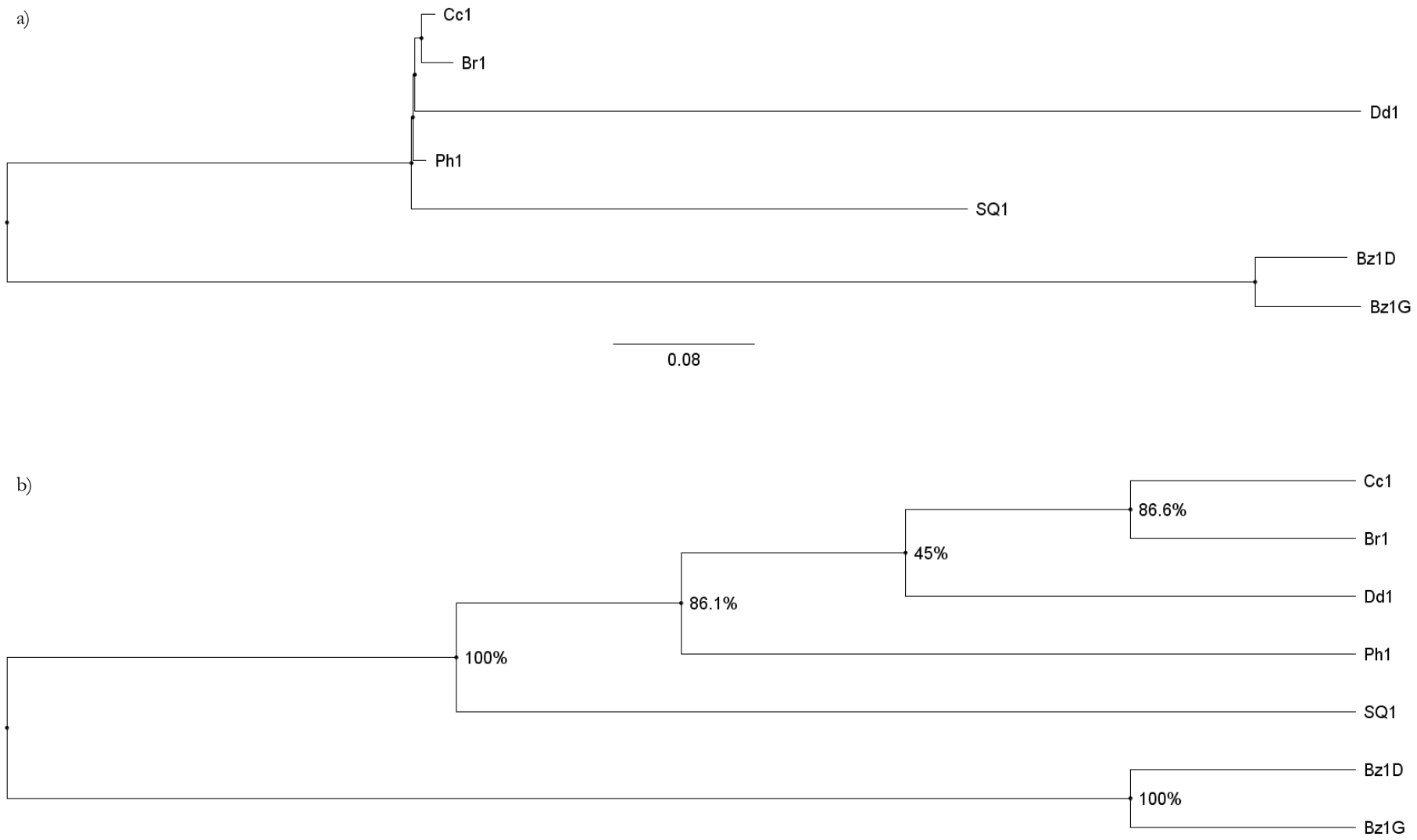

Figure 21. Unrooted phylogenetic trees of *Klebsiella pneumoniae* NCTC 13443 disinfectant-tolerant mutants from parent sample 1. a) Scaled phylogenetic tree. Distance scale indicates the number of nucleotide substitutions per site at variable sites. b) Unscaled phylogenetic tree. Node values indicate bootstrap values as a percentage. Cc: chlorocresol-tolerant sample. Br: bronopol-tolerant sample. Dd: didecyldimethylammonium chloride-tolerant sample. Ph: polyhexamethylene biguanide-tolerant sample. SQ: disinfectant formulation SQ53-tolerant sample. Bz: benzalkonium chloride-tolerant sample.

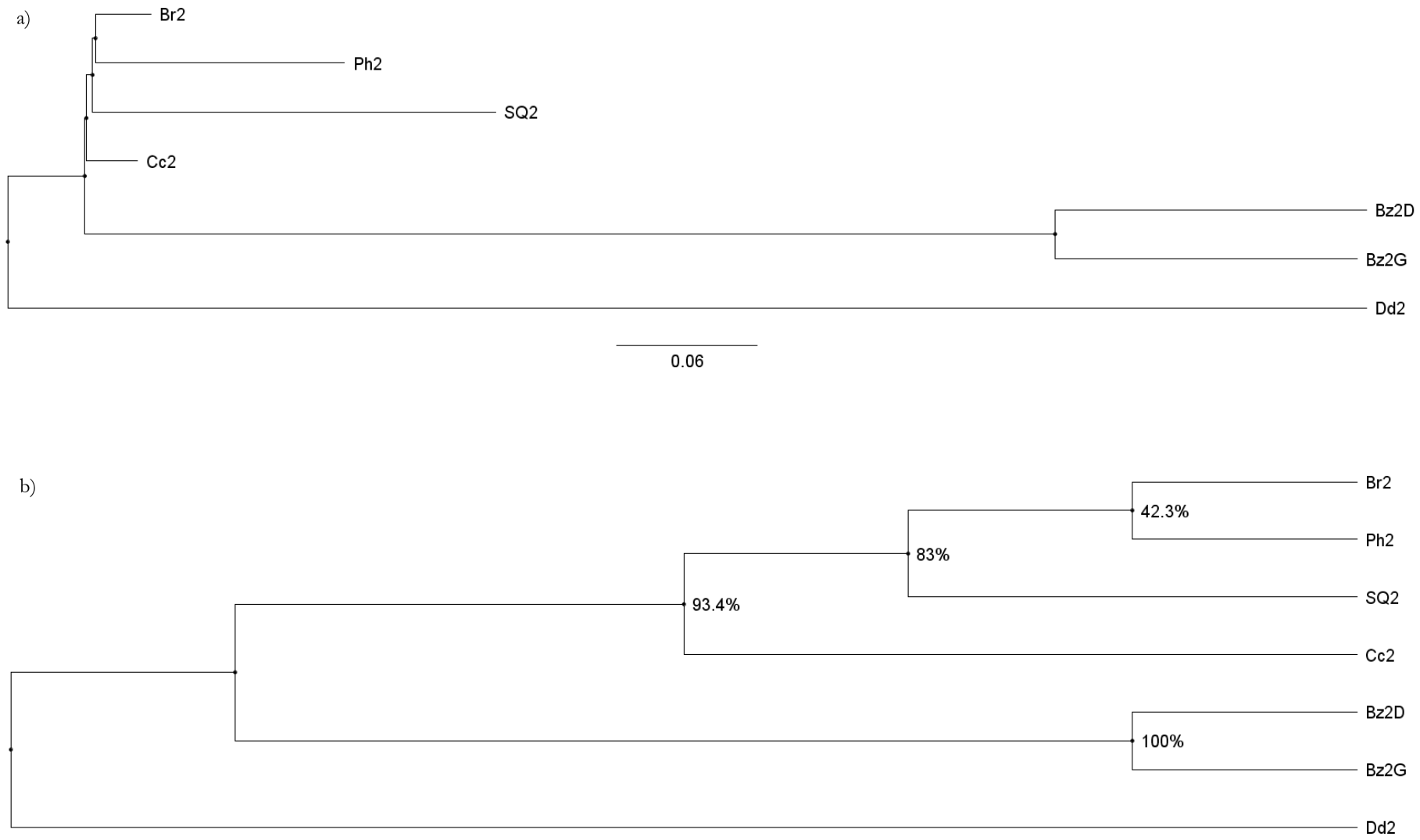

Figure 22. Unrooted phylogenetic trees of *Klebsiella pneumoniae* NCTC 13443 disinfectant-tolerant mutants from parent sample 2. a) Scaled phylogenetic tree. Distance scale indicates the number of nucleotide substitutions per site at variable sites. b) Unscaled phylogenetic tree. Node values indicate bootstrap values as a percentage. Br: bronopol-tolerant sample. Ph: polyhexamethylene biguanide-tolerant sample. SQ: disinfectant formulation SQ53-tolerant sample. Cc: chlorocresol-tolerant sample. Bz: benzalkonium chloride-tolerant sample. Dd: didecyldimethylammonium chloride-tolerant sample.

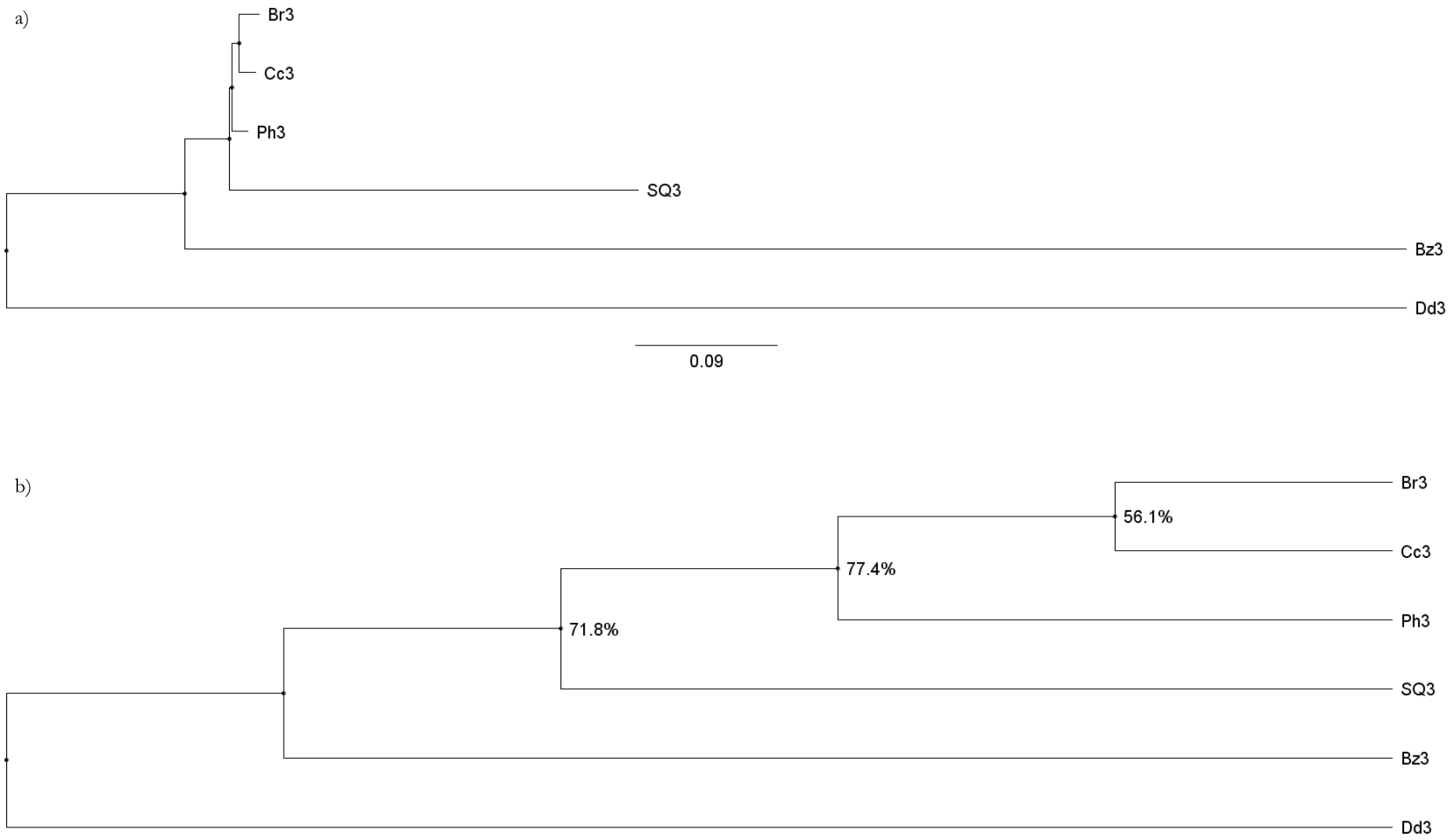

Figure 23. Unrooted phylogenetic trees of *Klebsiella pneumoniae* NCTC 13443 disinfectant-tolerant mutants from parent sample 3. a) Scaled phylogenetic tree Distance scale indicates the number of nucleotide substitutions per site at variable sites. b) Unscaled phylogenetic tree. Node values indicate bootstrap values as a percentage. Br: bronopol-tolerant sample. Cc: chlorocresol-tolerant sample. Ph: polyhexamethylene biguanide-tolerant sample. SQ: disinfectant formulation SQ53-tolerant sample. Bz: benzalkonium chloride-tolerant sample. Dd: didecyldimethylammonium chloride-tolerant sample.

5.4.1.3. Analysis of mutation sites

In order to elucidate potential underlying mechanisms of tolerance, the SNP and InDel mutations identified were annotated using the ANNOVAR software tool. A more detailed overview of this process is outlined in Chapter 5.3.1.3. Comprehensive analysis of these data is ongoing. Unfortunately, due to strict time constraints, a full and detailed analysis of all mutations identified is outside of the scope of this PhD thesis. The preliminary analysis presented here focused on genes of immediate interest based on previous literature and experimental work. A more comprehensive analysis of these data is required in future, as discussed in Chapter 7.2. In order to conduct an initial analysis, two methods were devised to refine the dataset for further analysis, as detailed below.

In addition, all mutations that were found to be unique to the parent strains were not analysed further. While these mutations may represent adaptations in the parent strains that were important to "lose" to develop disinfectant tolerance, they were likely to be less important than the adaptations acquired by the tolerant samples, so in the interest of time were not included. These mutations will be analysed at a later date, as discussed in Chapter 7.2.

5.4.1.3.1. Manual analysis

The first methodology of refinement relied upon cutting down the list to focus on a more manageable number of mutation sites. The first filter cut out all mutations that were in non-coding regions. Secondly, synonymous SNPs were filtered out, as they do not have an impact on the functionality of the protein. Lastly, only mutations that were consistent across all of the biological replicates were analysed, as these represent the mutations that are conserved across all biologically-independent tolerant samples.

The refined list of mutations were broadly assumed to have impacted the functionality of the respective proteins. The potential impacts of specific mutations were examined manually for key proteins of interest. In addition, as the mutations were present in all biological replicates, they were assumed to be relevant to the selection pressure applied by disinfectant exposure.

The refined gene lists were assembled into a network diagram based on their GO biological function terms. *Klebsiella pneumoniae* strain 342 was used as the reference genome, as this was the closest relative with an annotated genome to *K. pneumoniae* NCTC 13443 available in the software. The resulting BAC and DDAC networks can be found in Figure 24 and Figure 25, respectively. The remaining samples did not contain enough genes in the lists to form a network, so instead are listed in Table 11. Tables containing the refined mutation lists for BAC and DDAC are presented in Chapter 8. Appendix, Table 24, Table 25.

Analysis of gene and protein function was conducted via the UniProt database [360]. If functional information was not available for the gene or protein in *K. pneumoniae* NCTC 13443, the search was broadened to include other *K. pneumoniae* strains and then to *E.coli* K12, as noted in each case. The functionality of these genes and associated proteins was assumed to be synonymous across the bacterial species and strains. Mutations of interest are discussed below.

5.4.1.3.1.1. Benzalkonium chloride-tolerant samples

BAC-tolerant samples developed 174 mutations that were conserved across all biological replicates. This includes 12 frameshift deletions, 28 frameshift insertions, 2 non-frameshift deletions, 129 non-synonymous SNPs and 3 stop gain mutations (Table 25). Of these, 80 were functionally annotated and placed into a network map using the ClueGO v2.5.9 plugin [358] within the Cytoscape v3.9.1 programme [359], as shown in Figure 24.

Mutated genes can be seen to be associated with various cellular processes, of note including lipid metabolic and biosynthetic processes. The *arnT* gene has been demonstrated to be involved in *E. coli* and *S. enterica* resistance to polymyxin [372]. This is achieved through ArnT modifying lipid A via the addition of 4-amino-4-deoxy-L-arabinose (L-Ara4N), neutralising the negative charge of lipid A and thus decreasing the net negative charge of the outer leaflet [230], [322], [373], [374]. This decreases the affinity of cationic antimicrobials to the outer surface of the bacterial cell and thus confers a degree of tolerance [374]. It is unexpected that this gene contains a non-synonymous SNP across all BAC-tolerant samples (Figure 24). The mutation causes a substitution of asparagine to serine in position 457. Both amino acids are polar and uncharged, so the mutation may have little impact on the functionality of ArnT. Alternatively, the mutation may enhance ArnT activity, leading to tolerance.

Mutations can also be found in genes associated with membrane transport, including sulphur and nitrogen compound transport. Mutations can be seen in genes associated with amino acid transport such as *livJ*, *lysP* and *tyrP*, alongside genes associated with vitamin B1, sulphate and nickel transport in *K. pneumoniae* [360]. All of these genes regulate uptake of various substances, although any benefit conferred via these conserved mutations remains unknown.

Genes involved in macromolecular modification that acquired conserved mutations include genes encoding histidine kinases *envZ* and *basS* and two membrane-associated sensory proteins *pho*R and *narX* [360]. The latter 2 proteins are kinases that sense phosphate and nitrate availability respectively and regulate downstream protein expression accordingly.

BasS is synonymously referred to as PmrB, which is a kinase that causes the downstream positive-regulation of lipid A modifications in *K. pneumoniae* [375]. Of the genes regulated, the *arnABCDEFT* genes are responsible for the synthesis of L-Ara4N and its attachment to lipid A [376]. This causes the net negative charge of the outer leaflet of the outer membrane to decrease, decreasing the affinity of cationic peptides to the membrane in *E. coli* and *S*. Typhimurium and causing tolerance [231], [374].

The conserved mutation in both the BAC and DDAC-tolerant samples causes a substitution of an alanine to a valine in position 68. These amino acids have hydrophobic side chains and are structurally similar, so it is likely that the protein retains functionality. The known non-synonymous SNPs that lead to polymyxin resistance have been comprehensively reviewed by Huang *et al.* (2020). Interestingly, no mutations at this site have been identified previously, indicating that this mutation is novel, or does not confer tolerance to polymyxin [377]. The mutation is within the transmembrane region of the protein, responsible for the detection of physiological signals and subsequent conformational changes which leads to downstream up-regulation of the *arnABCDEFT* genes [377]. Mutations in this region have been shown to constitutively activate PmrB and cause increased expression of *arnT* [378]. This indicates that this mutation may contribute to the increased modification of lipid A, leading to a net decrease of negative charge on the outer leaflet of the outer membrane, causing a reduction in the affinity of cationic surfactants BAC and DDAC, and thus an increased tolerance to these disinfectants.

Mutations can also be seen in genes associated with stress responses. *cstA* is associated with starvation, *treF* with osmotic stress and *lon* with protein misfolding [360]. Additionally *ada*, *mutY* and *sbcB* are associated with DNA repair [360]. A loss of function of DNA repair mechanisms has been shown to contribute to hypermutable phenotypes [379], potentially allowing for more opportunities for the stochastic development of beneficial mutations. Loss of function mutations in DNA repair mechanisms are likely to be the underlying cause of the large number of mutations (Figure 19) and long genetic distance seen in BAC-tolerant samples (Figure 20).

Finally *cue*R, malt and *rhaS* are all helix-turn-helix transcriptional regulators [360]. In *E. coli, cue*R activates the transcription of *copA* and *cueO* (copper efflux and copper oxidase, respectively) in response to increased cytoplasmic copper concentrations [380]. These genes are involved in bacterial response to oxidative stress, so it is possible that these proteins demonstrate pleiotropic effects and that the mutations observed confer BAC tolerance. *malT* and *rhaS* regulate transcription of the maltose and rhamnose operons respectively, in response to either maltose or

rhamnose [360]. Loss of function mutations within these positive transcriptional regulators may result in a lower level of transcription of the downstream operons.

Collectively, the conserved genetic adaptations demonstrated by BAC-tolerant samples are associated with promoting the modification of lipid A with L-Ara4N, causing a reduction in the net negative charge of the outer leaflet of the outer membrane. This causes cationic disinfectant BAC to have a lower affinity to the bacterial surface, so a higher concentration of BAC is required to perturb bacterial membranes and thus the mutations confer BAC tolerance. Other conserved mutations are associated with DNA repair mechanisms, potentially giving rise to hypermutable *K. pneumoniae* phenotypes.

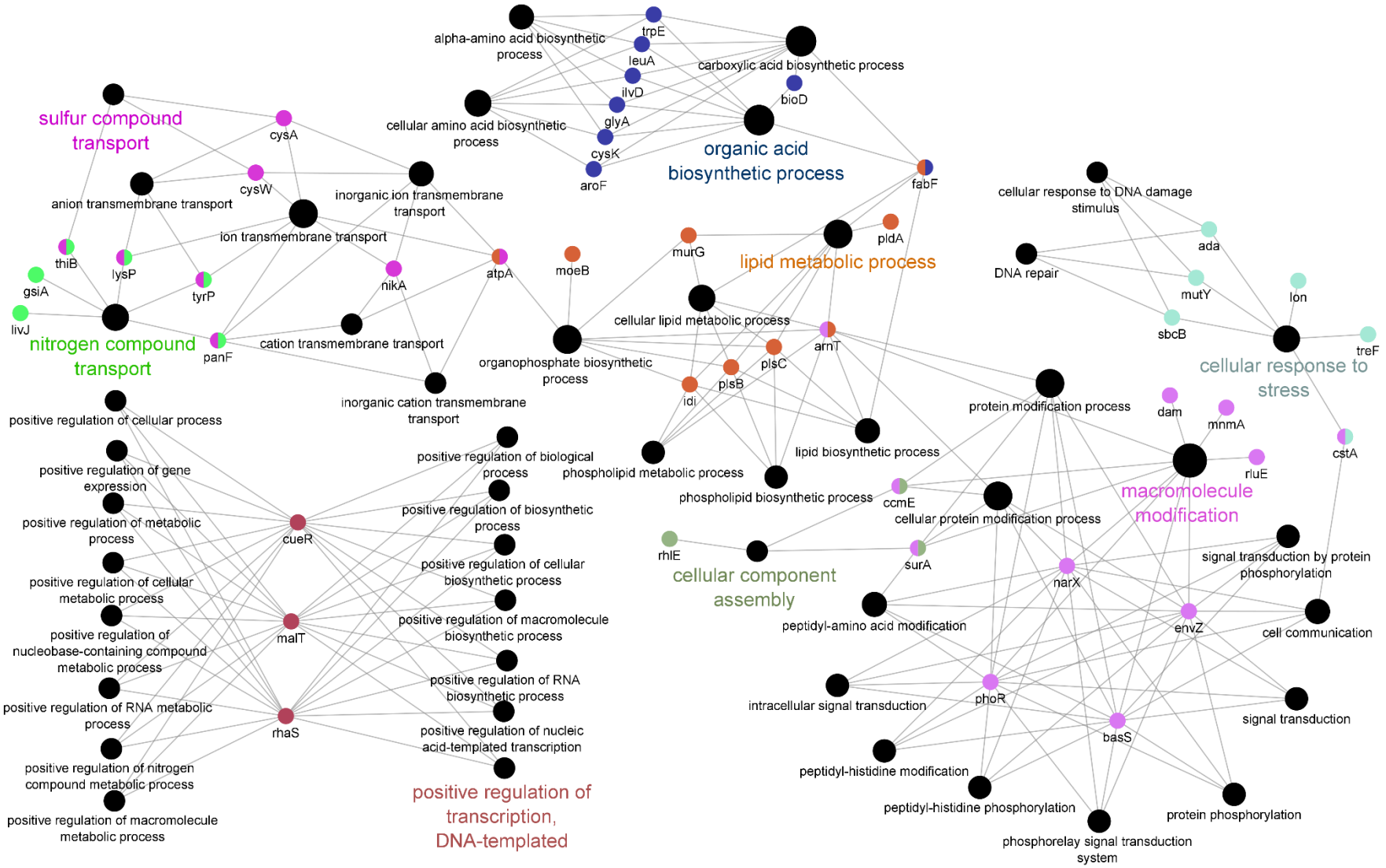

Figure 24. Network diagram of genes that contain mutations in *Klebsiella pneumoniae* NCTC 13443 benzalkonium chloride-tolerant samples Bz1, Bz2 and Bz3. Genes are indicated by the coloured dots, arranged according to gene ontology biological process annotation. Colours indicate biological process annotation. Black dots indicate biological process annotations, as labelled. Lines connect genes to their annotations. This network map was generated by Cytoscape v3.9.1 using the ClueGO v2.5.9 plugin.

5.4.1.3.1.2. Didecyldimethylammonium chloride-tolerant samples

The refined mutation list for DDAC-tolerant samples contained 225 genes, of which 14 and 23 were frameshift deletions and insertions, respectively (Table 26), while 3 and 1 were non-frameshift deletions and insertions, respectively (Table 26). 174 were non-synonymous SNPs, while 7 and 3 were stop gain and stop loss mutations (Table 26). Of these, 104 were functionally annotated and placed into a network map using the ClueGO v2.5.9 plugin [358] within the Cytoscape v3.9.1 programme [359], as shown in Figure 25.

DDAC-tolerant samples contained mutations in common with BAC-tolerant samples. This includes genes coding for histidine kinase *basS*, nitrate sensor protein *narX*, osmotic stress protein *treF*, maltose transcriptional regulator *malT* and nucleotide repair proteins *ada* and *mutY* (Figure 24, Figure 25). The mutations in these genes are identical in all biological replicates of both BAC and DDAC-tolerant samples, indicating that these mutations are beneficial for *K. pneumoniae* survival to both disinfectants. This overlap is likely due to the seminal MOAs of these disinfectants (Table 2). Specifically, the mutation in *basS* is conserved across both DDAC and BAC-tolerant samples, and causes a reduction of the net-negative charge of the outer membrane, as described previously in Chapter 5.4.1.3.1.1. This decreases the affinity of cationic surfactants BAC and DDAC to the bacterial cell surface and thus confers a degree of tolerance.

However, despite these similarities in MOA and acquired mutations, many of the mutations developed by *K. pneumoniae* tolerant samples varied significantly between the 2 sets of disinfectant-tolerant samples (Table 11), which is reflected in the variation between the two networks (Figure 24, Figure 25) and the genetic distances between the tolerant samples when phylogeny was inferred (Figure 20). While both sets of tolerant samples gain mutations associated with lipid metabolic processes and macromolecular modification, the other biological processes are unique to each disinfectant treatment (Figure 24, Figure 25).

DDAC-tolerant samples accumulate mutations in various metabolic processes, including metabolism of monosaccharides and carboxylic acids (Figure 25). The number of mutated genes associated with lipid metabolism is increased in comparison to BAC-tolerant samples, and notably does not include mutations in the gene coding for lipid A modification protein ArnT (Figure 24, Figure 25).

In addition, DDAC-tolerant samples contain mutations in genes associated with ion transport, including *nikC*, a nickel permease protein of the plasma membrane (Figure 25). BAC-tolerant

samples also contained a mutation associated with nickel uptake in the gene coding for protein NikA, which binds nickel ions in the periplasm [360]. Furthermore, both BAC and DDAC-tolerant samples contain mutations that likely reduce *copA* functionality, a protein that is responsible for the efflux of copper ions into the periplasm [360]. The proteins may have pleiotropic affects that may impact BAC and DDAC tolerance, although it is unclear if or how these mutations contribute to *K. pneumoniae* tolerance based on these data. DDAC-tolerant samples seem to display conserved mutations associated with lipid-A modification, as with BAC-tolerant samples (Chapter 5.4.1.3.1.1). Other adaptations observed in DDAC-tolerant samples are associated with metabolic processes, lipid metabolism and ion transport.

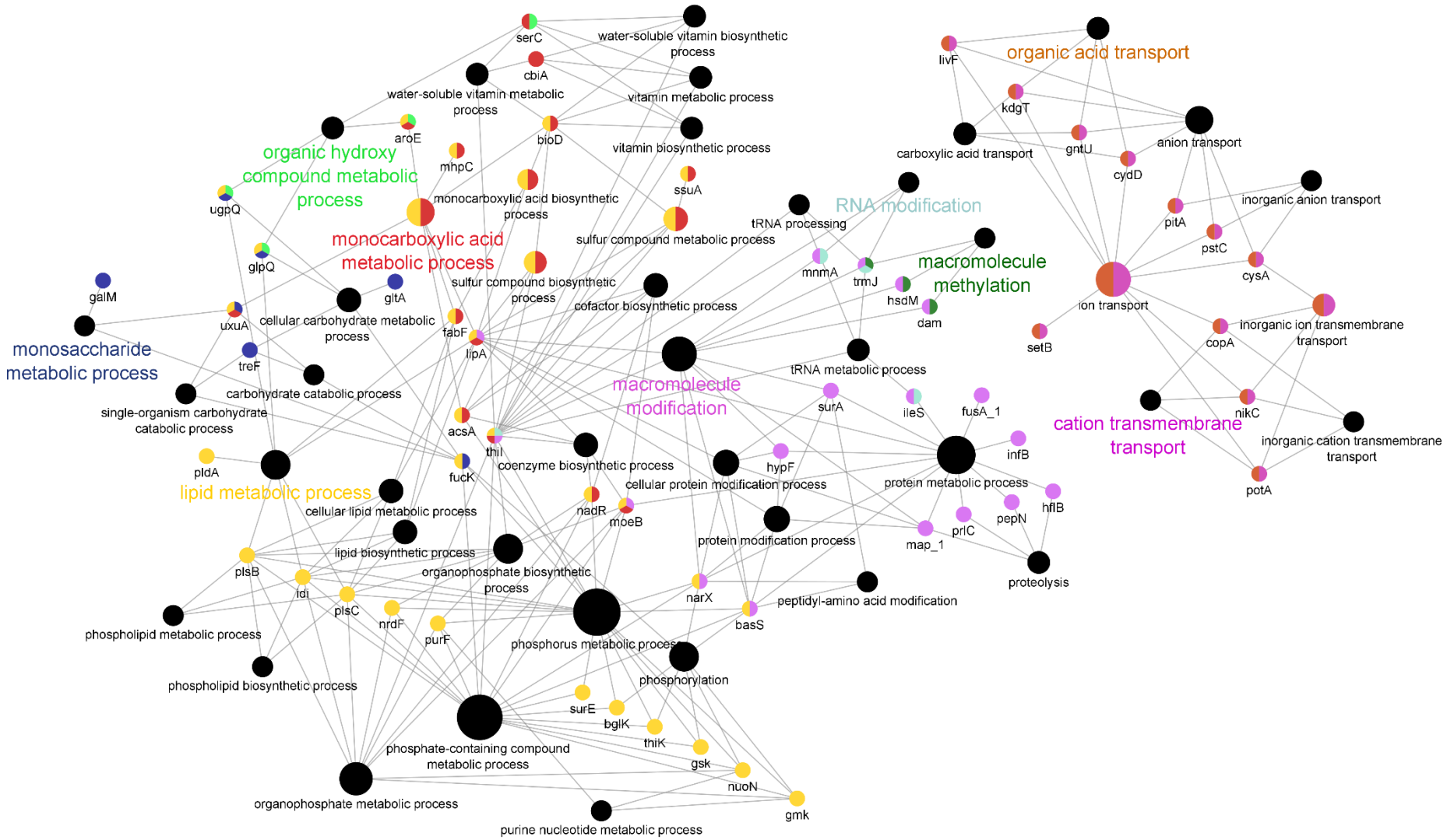

Figure 25. Network diagram of genes that contain mutations in *Klebsiella pneumoniae* NCTC 13443 didecyldimethylammonium chloride-tolerant samples Dd1, Dd2 and Dd3. Genes are indicated by the coloured dots, arranged according to gene ontology biological process annotation. Colours indicate biological process annotation. Black dots indicate biological process annotations, as labelled. Lines connect genes to their annotations. This network map was generated by Cytoscape v3.9.1 using the ClueGO v2.5.9 plugin.

5.4.1.3.1.3. Polyhexamethylene biguanide-tolerant samples

PHMB-tolerant samples gained between 19 and 119 mutations compared to the respective parent strains (Figure 19a, c). Of these mutations, only 2 were conserved across all biological replicates (Table 11). This may be a result of the variation in the MOA of PHMB (Table 2) allowing multiple possible mechanisms of tolerance development and explaining the inconsistencies between the biological replicates observed in terms of the number of mutations (Figure 19) and cross-tolerance profiles (Figure 18).

BasS is also referred to as PmrB, which is responsible for lipid A modification [376] as previously discussed. The non-synonymous SNP causes the substitution of a threonine to a proline at position 157. This region of the protein is highly conserved across species [377], and contains a conserved histidine residue at position 153, which is the site of autophosphorylation upon activation of the protein. This mutation has been reported previously in *K. pneumoniae* clinical strains, and is associated with a decreased susceptibility to polymyxin [381], [382] through activation of the *arnABCDEFT* genes.

Similar mutations in this gene are also present in all biological replicates of BAC and DDAC, indicating that these mutations confer a beneficial adaptation to all cationic membrane-active disinfectants. Notably, mutations in this gene are not present in any of the other disinfectant-tolerant samples, likely due to these genes not being cationic surfactants (Table 2). This collectively indicates that lipid A modification is a key mechanism underpinning *K. pneumoniae* tolerance to the cationic disinfectants BAC, DDAC and PHMB.

The PHMB tolerance observed is therefore a result of constitutive activation of BasS, leading to increased modification of lipid A with L-Ara4N and a reduced affinity of PHMB to the outer surface of the bacterial cell. This mechanism is also seen to be associated with tolerance to the other cationic disinfectants BAC (Chapter 5.4.1.3.1.1) and DDAC (Chapter 5.4.1.3.1.2).

5.4.1.3.1.4. Bronopol-tolerant samples

Bronopol contained mutations in the *yjcC* and *cpdA* genes (Table 11). *yjcC* is synonymous with the *pdeC* gene in *E. coli*, which is a phosphodiesterase that hydrolyses cyclic-di-GMP (c-di-GMP) [360]. It has previously been demonstrated that overexpression of this protein leads to reduced biofilm formation in *E. coli* [383]. In addition, a study by Huang *et al.* (2013) demonstrated that *K. pneumoniae* YjcC negatively regulates type 3 fimbriae expression and biofilm formation via the manipulation of c-di-GMP levels [384]. It is therefore possible that mutations that impede YjcC function may result in increased c-di-GMP levels, and thus enhanced biofilm formation and type 3 fimbriae expression.

Previously, increased intracellular c-di-GMP levels have been observed via mass spectrometry analysis of *P. aeruginosa* samples exposed to hypochlorite [385]. This was associated with increased expression of a putative diguanylate cyclase (DGC) (responsible for c-di-GMP synthesis) and an increased initial attachment of *P. aeruginosa* cells [385]. This suggests that elevated c-di-GMP levels are associated with biofilm formation and adaptation to hypochlorite [385]. In addition, oxidative stress-inducing molecule tellurite has been shown to induce biofilm formation through increased intracellular concentrations of c-di-GMP in *P. aeruginosa*, which was once again associated with elevated activity of DGCs SadC and SiaD [386]. Knockouts of these DGCs displayed an elevated susceptibility to tellurite [386], collectively indicating a link between c-di-GMP concentration, biofilm formation and bacterial tolerance to oxidative stress-inducing antimicrobials.

Bronopol, hypochlorite and tellurite are all known to induce oxidative stress, so it is unsurprising that the observed bacterial mechanisms of adaptation are similar. As a result, the increased intracellular concentration of c-di-GMP caused by a loss of function mutation in YjcC is therefore likely to contribute to bronopol tolerance in *K. pneumoniae*. This correlates with the observed EPS formation seen in *K. pneumoniae* samples exposed to bronopol when imaged via SEM (Figure 5i, j).

The CpdA protein hydrolyses cyclic adenosine monophosphate (cAMP) to 5'- adenosine monophosphate (AMP) [360]. Once again, mutations in this protein may impede protein functionality and thus result in elevated levels of cAMP, a known promoter of biofilm formation in *K. pneumoniae* via type 3 fimbriae production [387]–[389].

A mutation in the *pur* operon repressor *pur*R was seen in bronopol-tolerant samples (Table 11). The *pur* operon is responsible for inosine monophosphate (IMP) biosynthesis [390], which is a precursor to guanosine monophosphate (GMP) and AMP. Therefore, mutations in *pur*R may lead to greater availability of AMP and GMP, thus further allowing for biofilm formation.

Collectively, this indicates that mutations associated with the regulation of secondary messengers c-di-GMP and cAMP contribute to the disinfectant tolerance seen in bronopol-tolerant samples through promoting biofilm formation. The mechanisms by which biofilms are associated with an increased tolerance to disinfectants are discussed in Chapter 1.4.2.2.1.

5.4.1.3.1.5. Chlorocresol-tolerant samples

Chlorocresol-tolerant samples displayed mutations in the *yjcC* and *cpdA* genes (Table 11), as with bronopol-tolerant samples (Chapter 5.4.1.3.1.4). These charges are likely to be associated with an

increase in concentrations of c-di-GMP and cAMP respectively, which leads to increased biofilm formation and disinfection tolerance through mechanisms described in Chapter 1.4.2.2.1.

Chlorocresol-tolerant samples contained mutations in the *marR_1* and *acrB_5* genes (Table 11). MarR is a repressor of the *marRAB* operon, which is responsible for changes in expression associated with AMR including the down-regulation of outer membrane porin OmpF [391], increased expression of multidrug efflux complex AcrAB-TolC [392], [393] and tolerance to oxidative stress via transcriptional activator SoxS [393]. Mutations in this repressor have been shown to induce these changes of gene expression in *E. coli* [394], and confer resistance to disinfectants including pine oil [225] and triclosan [395]. Thus, the frameshift insertion seen across all chlorocresol-tolerant biological replicates likely impedes the ability for *marR* to repress the *marRAB* operon, resulting in the down-regulation of OmpF and increased expression of AcrAB-TolC and SoxS, and thus collectively contributing to chlorocresol tolerance.

The *acrB* gene encodes part of the AcrAB-TolC multidrug efflux pump complex. Previous evidence has linked AcrAB-TolC expression to the resistance of multiple disinfectants including BAC and DDAB in *K. pneumoniae* [223]. In addition, the deletion of AcrAB-TolC efflux system has been linked to increased *E. coli* susceptibility to phenol derivate chloroxylenol [225]. As noted previously, the increased expression of AcrAB-TolC has been attributed to tolerance to pine oil [225] and triclosan [395]. As a result, the *acrB* gene has been directly linked to disinfectant tolerance. The conserved mutation seen across all chlorocresol-tolerant samples is a non-synonymous SNP that changes an aspartate to an alanine. It is unclear what benefit, if any, this mutation has in terms of chlorocresol tolerance. It is possible that mutations may allow for a broader substrate range, or may increase affinity of chlorocresol to the efflux pump.

Collectively, mutations in chlorocresol-tolerant samples indicate that the underpinning mechanism of tolerance is a result of multiple factors including reduced expression of porins, modifications to the AcrAB-TolC complex, increased biofilm formation and transcriptional activation of the superoxide response regulon.

5.4.1.3.1.6. SQ53-tolerant samples

SQ53-tolerant samples contained a variety of mutations across all biological replicates. Of note, the *relA* gene encodes for guanosine triphosphate (GTP) pyrophosphokinase [360]. This enzyme synthesises (p)ppGpp in response to amino acid starvation, which is then hydrolysed to form guanosine tetraphosphate (ppGpp) and induces the "stringent response", causing the down-regulation of RNA synthesis and up-regulation of stress-related genes [396]. In addition, ppGpp supresses biofilm formation [383]. The mutation caused a valine to be substituted with a

methionine at position 351. It is possible that if the non-synonymous SNP in *relA* compromises RelA functionality, it may reduce the formation of ppGpp, removing the suppression of biofilm formation. Alternatively, RelA point mutations have been documented to give rise to the accumulation of ppGpp, and permanent induction of the stringent response and associated stress-related genes [397], [398]. The specific mutations documented in the literature are not observed here, so it is therefore uncertain the specific effect the non-synonymous SNP has upon RelA functionality, and how this influences SQ53 tolerance. A single point mutation was also observed in *relA* in sample Bz2g, but this resulted in a synonymous substitution so is unlikely to be associated with tolerance to BAC. Otherwise, no other disinfectant-tolerant samples displayed mutations associated with *relA*.

The MutL protein is a key DNA mismatch repair protein [360]. Function-compromising mutations in this protein would lead to an increase in DNA damage, and have previously been associated with hypermutable phenotypes in *K. pneumoniae* [379]. The mutation acquired was a stop gain at position 576, which is leads to a compromised, truncated protein. As a result, this mutation may have assisted in the emergence of mutations that conferred tolerance to SQ53. A non-synonymous SNP was also observed in *mutL* in Dd3; however, this mutation was not conserved across DDAC-tolerant samples so is unlikely to be critical to DDAC tolerance. No other disinfectant-tolerant samples displayed mutations associated with *mutL*.

Overall, the disinfectant-tolerant samples display mutations in a wide range of genes with varying levels of significance in terms of antimicrobial tolerance. Many potential functionally-compromising mutations can be found in seemingly critical antimicrobial tolerance genes. Other mutations can be found in expression regulatory proteins that may contribute to the activation or suppression of pathways relevant to the tolerance of disinfectant action. The quantification of protein content of the tolerant samples will be required to further shed light upon how these mutations may give rise to the characteristic disinfectant tolerance displayed by these samples.

Table 11. Conserved mutations detected in all biological replicates of *Klebsiella pneumoniae* NCTC 13443 disinfectant-tolerant samples. Table categories as follows. Tolerant sample: The disinfectant-tolerant sample. Gene: mutated gene. Mutation type: type of mutation. Par. Seq: original nucleic acid sequence in the parent strain. Alt. Seq: mutated nucleic acid sequence in the respective tolerant sample. Protein product: product of the listed gene. Ph: polyhexamethylene biguanide-tolerant samples. Br: bronopol-tolerant samples. Cc: chlorocresol-tolerant samples. SQ: disinfectant formulation "SQ53"-tolerant samples. DNA: deoxyribonucleic acid. RND: resistance-nodulation-division. NADP: nicotinamide adenine dinucleotide phosphate. GTP: guanosine triphosphate.

Tolerant Samples	Gene	Mutation Type	Par. Seq	Alt. Seq	Protein product
Ph	*basS*	non-synonymous SNP	T	G	Sensor protein BasS/PmrB
	*kdg*R	non-synonymous SNP	T	C	Transcriptional regulator KdgR
Br	*cpdA_2*	non-synonymous SNP	T	C	3',5'-cyclic-nucleotide phosphodiesterase
	htrE	non-synonymous SNP	T	G	Fimbriae usher protein StcC
	NCTC13443 _06216	non-synonymous SNP	A	C	Fimbrial-like protein
	*pur*R_2	non-synonymous SNP	G	T	Purine nucleotide synthesis repressor
	putA_3	non-synonymous SNP	T	G	PutA and PutP / proline dehydrogenase transcriptional repressor
	rhaS_2	non-synonymous SNP	C	G	Negative transcriptional regulator of cel operon
	yjcC_2	non-synonymous SNP	G	A	Cyclic-guanylate-specific phosphodiesterase
	fim_1	non-frameshift deletion	TGC CCA CCA CCA	-	Fimbrial protein
Cc	*mar*R_1	frameshift insertion	-	A	DNA-binding transcriptional repressor MarR
	yicC	frameshift insertion	-	C	Protein YicC
	acrB_5	non-synonymous SNP	T	G	RND efflux system
	cpdA_2	non-synonymous SNP	T	C	3',5'-cyclic-nucleotide phosphodiesterase
	fnr	non-synonymous SNP	C	T	Fumarate and nitrate reduction regulatory protein
	htrE	non-synonymous SNP	T	G	Fimbriae usher protein StcC
	NCTC13443 _06216	non-synonymous SNP	A	C	Fimbrial-like protein
	NCTC13443 _06725	non-synonymous SNP	C	A	Membrane protein
	yjcC_2	non-synonymous SNP	G	A	Cyclic-guanylate-specific phosphodiesterase
	fim_1	non-frameshift deletion	TGC CCA CCA CCA	-	Fimbrial protein
SQ	*dapL_1*	frameshift insertion	-	CC	Aspartate aminotransferase
	*mae*B	non-synonymous SNP	T	C	NADP-dependent malic enzyme
	mipA	non-synonymous SNP	G	A	MltA-interacting protein MipA
	NCTC13443 _06461	non-synonymous SNP	G	A	Transmembrane protein
	relA	non-synonymous SNP	C	T	GTP pyrophosphokinase
	scrY_3	non-synonymous SNP	G	A	Maltoporin
	ugpC_2	non-synonymous SNP	G	A	ABC sugar transporter
	yjiY	non-synonymous SNP	A	G	Carbon starvation protein A
	mutL	stop gain	C	A	DNA mismatch repair protein MutL

5.4.1.3.2. Analysis of mutations in antimicrobial resistance genes

The second methodology of data refinement utilised the AMRF tool [354]. The genomes of all disinfectant-tolerant samples were screened for AMR genes. The compiled AMR gene lists were cross-referenced with the SNP and InDel mutations detected in each sample, the result of which are presented in Table 12. Analysis of gene and protein function of the refined list of genes related to AMR was conducted using the UniProt database [360]. If functional information was not available for the gene or protein in *K. pneumoniae* NCTC 13443, the search was broadened to include all *K. pneumoniae* strains and then to *E.coli* K12, as noted in each case.

The cationic surfactants BAC, DDAC and PHMB all developed non-synonymous SNP mutations in *basS*, which is synonymous with PmrB [360]. As previously noted, mutations in this gene lead to activation of the PmrA regulon and subsequent lipid A modification [376]. This has been demonstrated to contribute to polymyxin and cationic peptide resistance in *E. coli* and *S.* Typhimurium [231], [374], so is likely to also contribute to cationic disinfectant tolerance.

DDAC-tolerant samples also contained conserved frameshift insertion mutations in copper resistance efflux protein *copA* (Table 12), responsible for exporting copper ions from the cytoplasm to the periplasm [399]. As this mutation is a frameshift insertion, it is likely to result in the loss of *copA* functionality. However, the exact significance of this mutation in terms of DDAC tolerance cannot be fully elucidated from these data.

Synonymous SNP mutations can be seen in *cusA_6* in DDAC-tolerant samples and in *cusC* gene in BAC-tolerant samples (Table 12). These genes are both involved in copper/silver efflux [360], however the synonymous nature of the mutations mean that protein function is not likely to be impacted, so these mutations are not likely to contribute to antimicrobial tolerance.

DDAC-tolerant samples contained a conserved non-synonymous mutation in *bepE* (Table 12), which encodes a resistance-nodulation-division (RND) multidrug efflux pump [360]. *Brucella suis bepE* knockouts were observed to have greater susceptibility to ethidium bromide, crystal violet and deoxycholate so were inferred to be responsible for broad-spectrum efflux of dyes and detergents [400]. Due to the critical nature of broad-spectrum efflux pumps and the established role of BepE in the removal of detergents from bacteria, it is unlikely that this non-synonymous SNP has a negative impact on protein functionality. The mutation may broaden substrate specificity or enhance substrate affinity. However, from these data it is unclear exactly how the non-synonymous mutation contributes to the tolerance of *K. pneumoniae* to DDAC.

Mutations in the *merR_1* gene were seen in all disinfectant-tolerant samples except SQ2 and SQ3 (Table 12). Mercuric resistance operon regulatory protein is capable of both activating and repressing the *mer* operon, depending on the presence or absence of mercury, respectively [401]. The frameshift insertion likely prevents *merR* functionality, preventing it from acting as a promoter for the *mer* operon. The operon contains genes associated with mercury regulation and removal [402], so once again it is unclear what impact the conserved mutation in *merR_1* may have upon disinfectant tolerance. As mutations were observed across most disinfectant-tolerant samples it is likely that these proteins have pleiotropic functions that are beneficial to disinfectant tolerance, potentially associated with oxidative stress. However, at present the nature of these potential functions are not understood.

Finally, a conserved non-synonymous SNP was detected in uncharacterised protein NCTC13443_07417 across all BAC-tolerant samples. A protein Basic Local Alignment Search Tool (pBLAST) search against the database reveals the encoded protein sequence shares a 100% homology with APH(6)-I family aminoglycoside O-phosphotransferase in *K. pneumoniae* and *E. coli*, encoded by the *strB* gene [403], [404]. This protein confers resistance by modifying and inactivating streptomycin via the addition of a phosphate [405]. It is unclear what impact the SNP has on the function of the protein and what benefit, if any, this confers to the BAC-tolerant samples.

Table 12. Mutations detected in antimicrobial resistance genes in *Klebsiella pneumoniae* NCTC 13443 disinfectant-tolerant samples. Antimicrobial resistance genes detected via Antimicrobial Resistance Finder plus programme. Table categories as follows. Gene: mutated gene. Mutation type: type of mutation. Ref. Seq.: original nucleic acid sequence in the parent strain. Alt. Seq.: mutated nucleic acid sequence in the respective tolerant sample. Protein product: product of the listed gene. Mutation distribution: 1 = tolerant samples that carried the mutation. Bz: benzalkonium chloride-tolerant sample. Dd: didecyldimethylammonium chloride-tolerant sample. Ph: polyhexamethylene biguanide-tolerant sample. Br: bronopol-tolerant sample. Cc: chlorocresol-tolerant sample. SQ: Disinfectant formulation "SQ53" -tolerant sample. SNP: single nucleotide polymorphism. RND: resistance-nodulation-division.

Gene	Mutation Type	Ref. Seq.	Alt. Seq.	Protein product	Mutation distribution																	
					Bz1G	Bz1D	Bz2G	Bz2D	Bz3	Dd1	Dd2	Dd3	Ph1	Ph2	Ph3	Br1	Br2	Br3	Cc1	Cc2	Cc3	SQ1	SQ2	SQ3
basS	non-synonymous SNP	G	A	Sensor protein BasS/PmrB	1	1	1	1	1	1	1	1											
basS	non-synonymous SNP	T	G	Sensor protein BasS/PmrB									1	1	1								
bepE_3	non-synonymous SNP	T	C	RND multidrug efflux transporter						1	1	1											
copA_5	frameshift insertion	-	GG	Copper resistance protein A						1	1	1											
copA_5	frameshift insertion	-	C	Copper resistance protein A						1	1	1											
merR_1	frameshift insertion	-	C	Mercuric resistance operon regulatory protein	1	1	1	1	1	1	1	1	1	1	1	1	1	1	1	1	1	1	
NCTC13443_07417	non-synonymous SNP	C	T	3'-kinase StrB	1	1	1	1	1														
silC	synonymous SNP	T	C	Copper/silver efflux system outer membrane protein CusC/SilC	1	1	1	1	1														

5.4.2. Comparative global proteomic analysis

5.4.2.1. Proteome statistics

The protein content of each disinfectant-tolerant sample was quantified using area under the curve label-free global proteomic analysis. For a comprehensive overview of the methodology used during the experimental procedure and during the data analysis steps, please refer to Chapter 5.3.2.

The proteomic analysis statistics are shown in Table 13. Volcano plots of differentially expressed proteins can be found in Chapter 8. Appendix, Figure 45. The number of differentially expressed proteins ranges from 507 to 726 (Table 13). In addition, the majority of differentially expressed proteins showed a decreased expression across all tolerant samples. The reduction of protein expression [138], [165] and degradation of protein [138] are known general stress responses in bacteria. This overall reduction in protein abundance is therefore likely a result of the *K. pneumoniae* cells consolidating and conserving resources in order to adapt to the respective disinfectant treatment (Table 13).

The distribution of up-regulated and down-regulated proteins across the tolerant samples are shown in Figure 26a and b respectively. A Venn diagram was not used as there were 6 samples that needed simultaneous comparison. Instead, bar graphs were used to show the number of proteins that were found to be in common in any given combination of disinfectant-tolerance samples, arranged from highest to lowest (Figure 26a, b). The associated matrices below each bar graph display the combination of disinfectant-tolerance samples that contained the number of proteins in the corresponding bar (Figure 26a, b). Each protein is only represented once in the figure.

A total of 122 proteins were unique to SQ53-tolerant *K. pneumoniae* samples, 82 of which were up-regulated, and 40 were down down-regulated (Figure 26a, b). Previously it has been observed that the SQ53-tolerant samples were genetically distant from the other samples when phylogeny was inferred (Figure 20), indicating that the selection pressure applied by the disinfectants in combination is unique and distinct from the selection pressures of each component individually. The 122 unique differentially expressed proteins in SQ53-tolerant samples supports this observation (Figure 26a, b).

BAC-tolerant samples contained 76 and 99 unique up- and down-regulated proteins respectively (Figure 26a, b), despite BAC having a similar MOA to DDAC (Table 2). In addition, the samples tolerant to these two disinfectants only shared 22 and 14 unique up and down-regulated proteins

respectively (Figure 26a, b). Once again, these disinfectant-tolerant samples were observed to be genetically distant from each other when phylogeny was inferred (Figure 20). Collectively this further indicates that that although the MOAs of BAC and DDAC are similar, the underlying mechanisms of tolerance to these disinfectants in *K. pneumoniae* are unique.

Bronopol-tolerant samples contained 149 unique down-regulated proteins, the most of any of the tolerant samples (Figure 26a). While the MOA of bronopol varies in comparison to the other disinfectants, the large number of unique up-regulated proteins does not reflect the short genetic distance between bronopol, chlorocresol and PHMB-tolerant samples (Figure 20). This is likely a result of mutations in proteins responsible for the regulation of protein expression, causing individual mutations to impact the expression of a large number of proteins. Furthermore, the short genetic distance (Figure 20) contrasted by the large number of unique variations in protein expression may be indicative of the observed bronopol-tolerance being a result of phenotypical changes, not solely a result of genetic variation.

The 12 and 54 up- and down-regulated proteins in common across all tolerant samples (Figure 26a, b) likely represent the centralised *K. pneumoniae* stress response pathways. It is also possible that these expression changes are due to changes to metabolism that occur consistently as a result of the uniform experimental procedure. This could have been avoided by conducting the serial passage procedure on the control samples, without exposing them to any disinfectant treatment.

Table 13. Label-free global proteomics analysis sample statistics of *Klebsiella pneumoniae* NCTC 13443 disinfectant-tolerant samples. Table categories as follows. Tolerant sample: disinfectant-tolerant sample analysed. Proteins detected: number of proteins that were detected in every biological replicate and parent strains. Total proteome coverage (%): the percentage coverage of the total proteome of the reference strain (7186 proteins). Differentially expressed proteins: the number of proteins that were differentially expressed. Increased/decreased expression: The number and percentage of proteins that increased or decreased expression. Percentage presented as a percentage of the differentially expressed proteins. Bz: benzalkonium chloride-tolerant samples. Dd: didecyldimethylammonium chloride-tolerant samples. Ph: polyhexamethylene biguanide-tolerant samples. Br: bronopol-tolerant samples. Cc: chlorocresol-tolerant samples. SQ: disinfectant formulation "SQ53" -tolerant samples.

Tolerant samples	Proteins detected (No.)	Total proteome coverage (%)	Differentially expressed proteins (No.)	Expression			
				Decreased		Increased	
				(No.)	(%)	(No.)	(%)
Bz	2036	28.3	649	480	74.0	169	26.0
Dd	1851	25.8	585	470	80.3	115	19.7
Ph	1981	27.6	527	431	81.8	96	18.2
Br	1859	25.9	726	636	87.6	90	12.4
Cc	2035	28.3	573	395	68.9	178	31.1
SQ	2074	28.9	507	325	64.1	182	35.9

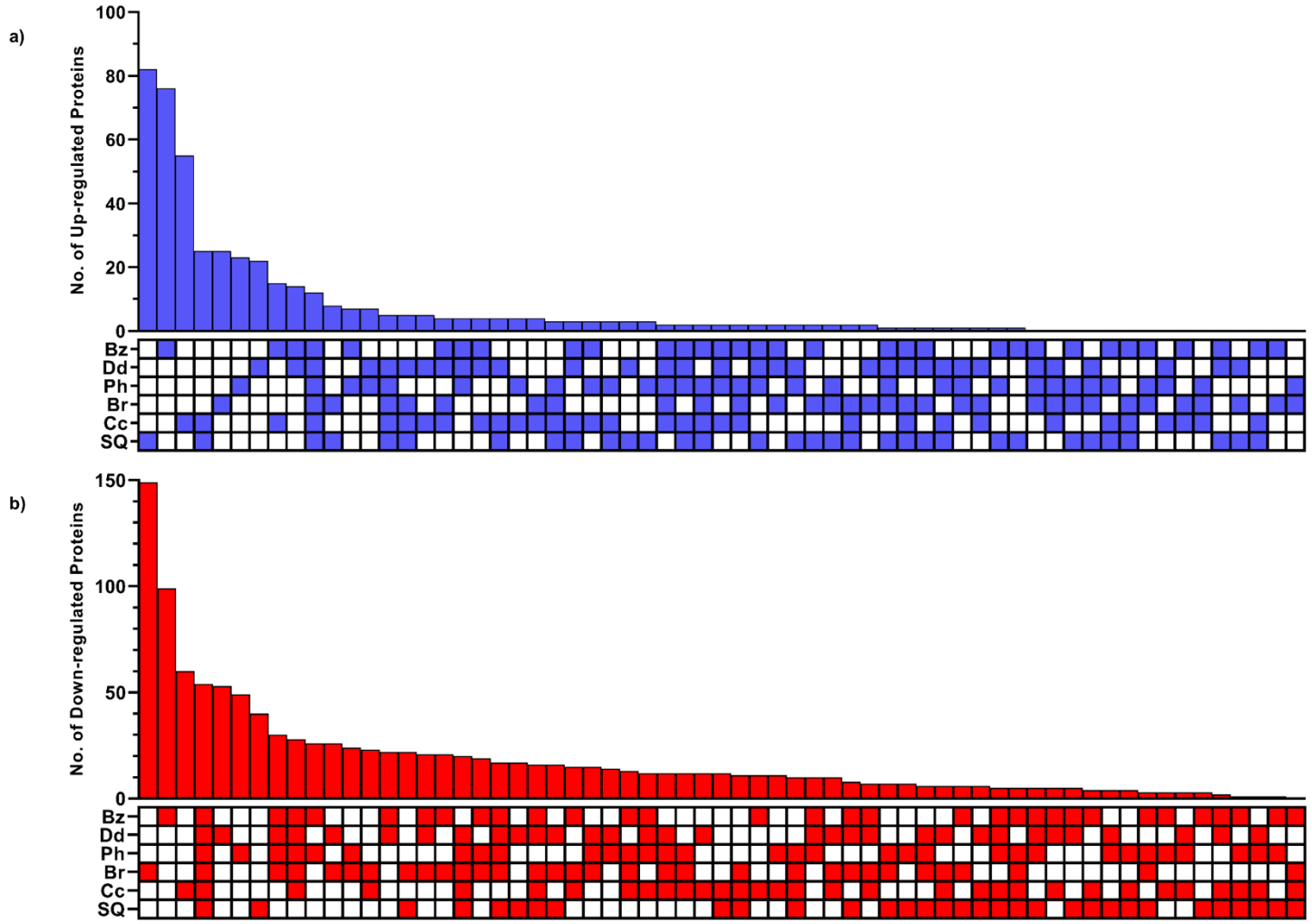

Figure 26. Graph showing the number of differentially expressed proteins that were in common between disinfectant-tolerant *Klebsiella pneumoniae* NCTC 13443 samples. The matrix indicates the combination of disinfectant-tolerant samples and the corresponding bar on the graph above the matrix indicates the number of proteins found to be uniquely found in that combination of samples. Each protein is only represented once. a) Up-regulated proteins. b) Down-regulated proteins. Bz: benzalkonium chloride-tolerant samples. Dd: didecyldimethylammonium chloride-tolerant samples. Ph: polyhexamethylene biguanide-tolerant samples. Br: bronopol-tolerant samples. Cc: chlorocresol-tolerant samples. SQ: disinfectant formulation "SQ53" -tolerant samples.

5.4.2.2. Examination of differentially expressed proteins

The analysis of differentially expressed proteins affords us insight into the molecular differences between the disinfectant-tolerant samples and the parent samples. This gives us an indication of how the samples have adapted to be able to survive concentrations of disinfectant that the parent samples cannot. It can also be useful to investigate the proteins that are not differentially expressed, as this gives an indication of which proteins are not influenced or related to disinfectant tolerance.

However, with up to 2074 proteins detected and up to 726 that are differentially expressed in each sample (Table 13), it is not possible to manually examine and consider the relative expression of each protein detected within the timescales of this project. As a result, data refinement strategies needed to be utilised to distil the data and elucidate potential molecular mechanisms of disinfectant tolerance.

Three strategies were employed. Firstly, the top 10 up-regulated proteins detected in each disinfectant-tolerant sample were examined manually. Secondly, gene ontology (GO) enrichment analysis was conducted on differentially expressed proteins to view patterns in the biological processes and cellular components of each sample. Finally, to visualise the changes in expression at the proteome level, the underlying genes of differentially expressed proteins were mapped into a network based on their involvement in biological pathways.

Once data refinement had been conducted, analysis of protein function was conducted via the UniProt database [360]. If functional information was not available for the protein in *K. pneumoniae* NCTC 13443, the search was broadened to include other *K. pneumoniae* strains and then to *E. coli* K12, as noted in each case.

The results and discussion presented here represents a preliminary analysis that focused on genes of immediate interest based on previous literature and experimental work. A more comprehensive analysis of these data is required in future, as discussed in Chapter 7.2.

5.4.2.2.1. Manual examination of the top 10 up-regulated proteins in each tolerant sample

In order to refine the extensive lists of differentially expressed proteins, the top 10 up-regulated proteins from each sample were compiled (Table 14). The functions of these proteins were manually examined. This list represents the proteins that had the most significant up-regulation in each of the disinfectant-tolerant samples, and thus may give an indication of the underpinnings of the respective disinfectant tolerance mechanisms.

BAC-tolerant samples displayed a significant up-regulation of bifunctional polymyxin resistance protein ArnA [360] (Table 14). This enzyme forms uridine diphosphate-L-4-formamido-arabinose (UDP-L-Ara4FN) which is bound to lipid A by ArnT, neutralising negative charge [372]. This modification of lipid A has recently been shown to underpin *Pseudomonas aeruginosa* [233] and *E. coli* [339] resistance to BAC. This up-regulation is likely a result of the constitutive activation of the upstream regulator BasS caused by a nonsynonymous SNP mutation in the transmembrane region of the protein, as explained in Chapter 5.4.1.3.1.1.

AcrAB proteins were also up-regulated in BAC-tolerant samples (Table 14), which are part of the AcrAB-TolC multidrug efflux complex [360]. A recent study on *K. pneumoniae* efflux pumps and their contribution to disinfectant tolerance has found a ≥4-fold increase in BAC and DDAB susceptibility in *K. pneumoniae* mutants that lack a functional AcrAB-TolC multidrug efflux pump [223]. As a result, these data suggest that *K. pneumoniae* is able to regulate AcrAB-TolC expression in order to tolerate BAC. Interestingly, DDAC-tolerant samples did not demonstrate significant differential expression of either of the AcrAB proteins, and a reduction in TolC expression. This indicates that AcrAB-TolC efflux pump up-regulation is not involved the mechanisms that underpin DDAC tolerance, further indicating variations in the mechanisms of QAC-tolerance, despite the similarities in disinfectant MOAs. This may be due to AcrAB-TolC being unable to efflux DDAC.

YfdX protein was detected as up-regulated in all disinfectant-tolerant samples (Table 14), indicating that it may be of potential significance. However, this protein is poorly characterised [360]. In *E. coli*, YfdX expression is positively regulated by EvgA, which also controls the expression of the multidrug efflux proteins EmrKY [406]. A study on YfdX functionality in *Salmonella enterica* demonstrated an association with reduced virulence, growth rate and antibiotic susceptibility [407]. In addition, YfdX has been demonstrated to be a periplasmic chaperone and involved in the acid stress response in *K. pneumoniae* [408]. However, further details regarding the molecular function and mechanisms of this protein remain to be elucidated, so the extent of this protein's involvement in the tolerance to the tested disinfectants is unknown.

Bronopol-tolerant samples displayed in increased level of expression of various proteins associated with oxidation and reduction, including NCTC13443_03659 and NCTC13443_01223 [360] (Table 14). These unidentified proteins are predicted to be a putative nicotinamide adenine dinucleotide (NADH):flavin oxidoreductase and thioredoxin-like protein respectively [360]. Bronopol causes the formation of disulphide bonds [99], alter the redox state and releases ROS

[100], as explained previously (Table 2). It is therefore unsurprising that the bronopol-tolerant samples express higher quantities of proteins relating to redox stress mitigation.

Thioredoxin proteins are disulphide oxidoreductases, which are capable of reducing the disulphide bonds [409], [410] formed by the MOA of bronopol. In addition, flavin oxidoreductase mutants show a high susceptibility to oxidative stress in both *E. coli* [411] and *Streptococcus pneumoniae* [412], so up-regulation of this putative NADH:flavin oxidoreductase may contribute to *K. pneumoniae* tolerance to bronopol-induced oxidative stress. This protein also appeared in the top 10 up-regulated proteins in all disinfectant-tolerant samples except BAC, of which the protein was not detected at all. This is likely a result of oxidative stress being a common result of the MOAs of these disinfectants.

In addition, NCTC13443_01223 (thioredoxin-like protein) was expressed higher in both the BAC-tolerant and PHMB-tolerant samples in comparison to the respective parent samples (Table 14). This further indicates that these disinfectants induce oxidative stress, likely as a result of membrane perturbation.

Bronopol-tolerant samples also displayed an increased expression of the flavin-dependant reductase N-ethylmaleimide reductase NemA [360] (Table 14). This protein has previously been shown to be capable of breaking down 2,4,6-trinitrotoluene (TNT) [413], [414] and more broadly involved in electrophile reduction [415] in *E. coli*. Bronopol, like TNT, contains the nitro electrophilic group. It is therefore possible that NemA is able to break down bronopol, and the up-regulation of NemA contributes to the bronopol tolerance seen in the samples. In addition, NemA requires a flavin cofactor in order to function, which may link to the up-regulation of NCTC13443_03659 NADH:flavin oxidoreductase.

Chlorocresol-tolerant samples displayed a heightened expression of multidrug efflux protein MdtC (Table 14), part of the MdtABC complex [360]. BepD is synonymous with MdtA [360], which also showed elevated expression (Table 14). This efflux complex has been shown to decrease *E. coli* susceptibility to novobiocin and deoxycholate [416]. These data suggest that broad-spectrum drug efflux may contribute to *K. pneumoniae* chlorocresol tolerance. This aligns with previous reports that indicate that the AcrAB-TolC broad-spectrum efflux pump complex contributes to tolerance to chloroxylenol [225], and efflux pump activity correlates with *S. enterica* susceptibility to phenol [226].

The universal stress protein UspG is up-regulated in chlorocresol-tolerant samples (Table 14). This protein has not been directly characterised [360], so it is not clear how this protein specifically contributes to chlorocresol tolerance.

An increase in expression of NCTC13443_03659 Putative NADH:flavin oxidoreductase can be seen in SQ53-tolerant samples, alongside YfdX-like protein as noted previously (Table 14).

An initial analysis of these data does not give a clear indication of the specific mechanisms of SQ53-tolerance demonstrated by the samples. These samples displayed a large genetic distance between each other when phylogeny was inferred, and the biological replicates were distributed across multiple clades (Figure 20). Additionally, these samples demonstrated varying cross-tolerance profiles to other disinfectants (Figure 18). This collectively may be a result of variation between the biological replicates in the underlying mechanisms of tolerance to SQ53. Therefore, the lack of clear mechanism of action of tolerance observed via quantitative proteomics may be a result of the analysis being conducted across all three of the biological replicates, rather than comparing the biological replicates individually. To explore this limitation, analysis would have to be repeated comparing each of the replicates individually to the respective parent samples. This would be interesting to consider in future studies.

Manual examination of the top 10 up-regulated proteins in each sample provides a narrow snapshot of how the samples may have adapted to the disinfectant treatments. However, much information is being missed across the rest of the dataset. To fully elucidate the mechanisms that underpin disinfectant tolerance it is important to consider the broader proteome.

Table 14. The 10 proteins that demonstrated the highest average increased expression change detected via label-free global proteomics analysis. Samples consisted of disinfectant-tolerant *Klebsiella pneumoniae* NCTC 13443, and were compared to untreated parent samples. Table categories as follows. Tolerant sample: disinfectant-tolerant sample analysed. Expression change: the log_2 fold change of the protein in comparison to the untreated parent samples. Protein: The identifier and full name of the differentially expressed protein. Bz: benzalkonium chloride-tolerant samples. Dd: didecyldimethylammonium chloride-tolerant samples. Ph: polyhexamethylene biguanide-tolerant samples. Br: bronopol-tolerant samples. Cc: chlorocresol-tolerant samples. SQ: disinfectant formulation "SQ53" - tolerant samples. NADH: Nicotinamide adenine dinucleotide. RNA: ribonucleic acid. n=3, except for Bz-tolerant samples, where n=5.

Tolerant samples	Expression change (log_2 fold change)	Protein identifier	Full protein name
Bz	5.64	BudB	Acetolactate synthase
	5.64	ArnA	Bifunctional polymyxin resistance protein ArnA
	5.64	YfdX	YfdX-like protein
	5.06	NCTC13443_01223	Thioredoxin-like protein
	4.64	MalZ	Maltodextrin glucosidase
	4.32	FruB	Multiphosphoryl transfer protein
	3.84	FruB	Multiphosphoryl transfer protein
	3.64	AcrB	Efflux pump membrane transporter AcrB
	3.64	FrlD	Fructosamine kinase FrlD
	3.47	AcrA	Efflux pump membrane transporter AcrA
Dd	5.64	YfdX	YfdX-like protein
	5.64	GlpK	Glycerol kinase
	5.64	BudC	Diacetyl reductase [(S)-acetoin forming]
	4.64	NCTC13443_03659	Putative NADH:flavin oxidoreductase
	4.06	FruB	Multiphosphoryl transfer protein
	4.06	ValS	Valine--tRNA ligase
	3.84	ScrY	Sucrose porin
	3.32	DmlA	D-malate dehydrogenase (decarboxylating)
	3.32	LysA	Diaminopimelate decarboxylase
	3.18	AldB	Alpha-acetolactate decarboxylase
Ph	5.64	GlpK	Glycerol kinase
	5.64	NCTC13443_03659	Putative NADH:flavin oxidoreductase
	5.64	YfdX	YfdX-like protein
	5.64	NCTC13443_02382	Putative L-fucose isomerase, C-terminal
	5.64	NCTC13443_02379	Putative L-fucose isomerase, C-terminal
	5.64	BudC	Diacetyl reductase [(S)-acetoin forming]
	5.06	NCTC13443_01223	Thioredoxin-like protein
	5.06	SacA	Sucrose-6-phosphate hydrolase
	4.64	ThiC	Phosphomethylpyrimidine synthase
	4.64	NCTC13443_02381	Putative L-fucose isomerase, C-terminal
Br	5.64	BudB	Acetolactate synthase
	5.64	YfdX	YfdX-like protein
	5.64	DDJ638005	-
	4.32	NCTC13443_03659	Putative NADH:flavin oxidoreductase
	4.06	NCTC13443_01223	Thioredoxin-like protein
	3.64	FruB	Multiphosphoryl transfer protein
	3.47	FrlD	Fructokinase
	3.47	FadB	Fatty acid oxidation complex subunit alpha
	3.32	NemA	N-ethylmaleimide reductase
	3.32	DkgB	2,5-didehydrogluconate reductase DkgB
Cc	5.64	YebE	Inner membrane protein YebE
	5.64	MdtC	Multidrug resistance protein MdtC
	5.06	YfdX	YfdX-like protein
	5.06	BudC	Diacetyl reductase [(S)-acetoin forming]
	4.64	AldB	Alpha-acetolactate decarboxylase
	4.64	BepD	Multidrug resistance protein MdtA
	4.64	UspG	Universal stress protein G
	4.32	NCTC13443_03659	Putative NADH:flavin oxidoreductase
	4.06	HutU	Urocanate hydratase
	3.84	FdhF	Formate dehydrogenase
SQ	5.64	GabD	NADP-dependent succinate-semialdehyde dehydrogenase
	5.64	NCTC13443_03659	Putative NADH:flavin oxidoreductase
	5.64	YfdX	YfdX-like protein
	5.06	AstD	N-succinylglutamate 5-semialdehyde dehydrogenase
	5.06	GabD	NADP-dependent succinate-semialdehyde dehydrogenase
	5.06	HutH	Histidine ammonia-lyase
	5.06	RidA	2-iminobutanoate/2-iminopropanoate deaminase
	4.64	HutU	Urocanate hydratase
	4.64	NCTC13443_04408	ABC transporter, periplasmmic iron binding protein
	4.32	ArgT	Histidine ABC transporter

5.4.2.2.2. Gene ontology annotation

In order to examine the impacts of disinfectant adaptation on the entire proteome, gene ontology enrichment analysis was performed. The biological process and cellular component terms were identified for the differentially expressed proteins, and enrichment analysis was performed using the DAVID online tool [362], [363] with *K. pneumoniae* MGH 78578 used as the background list. All enriched terms with a p-value ≤ 0.05 are displayed via heatmap in Figure 27. The raw values outputted by the DAVID online tool can be found in Chapter 8. Appendix, Table 27.

'De novo' inosine monophosphate (IMP) biosynthetic process shows a negative enrichment in bronopol-tolerant samples (Figure 27a), despite observing a conserved SNP polymorphism mutation in *pur* operon repressor *pur*R (Table 11). However, as *purB*, *purC*, *purE*, *purH*, *purL* and *purM* were all detected as down-regulated across all bronopol-tolerant biological replicates, the *pur*R mutation seems to enhance the repression of the *pur* operon, possibly through permanent activation of the repressor. In addition, a negative enrichment was also observed in BAC, DDAC and Cc-tolerant samples (Figure 27a), despite no observed mutations in *pur*R in any of these samples. Negative enrichment was also observed in the 'de novo' uridine monophosphate (UMP) biosynthetic process tag in DDAC, PHMB and Br-tolerant samples (Figure 27a). This collectively undermines the previous hypothesis that increased availability of c-di-GMP and c-AMP, and thus increased biofilm formation, may contribute to the bronopol and chlorocresol-tolerance observed.

The Gram-negative-bacterium-type outer membrane assembly gene ontology tag shows a decreased fold-enrichment in BAC, bronopol, chlorocresol and SQ53-tolerant samples (Figure 27a). The proteins associated with this tag include the LptA and LptC-E proteins, responsible for transporting LPS from the outer leaflet of the inner membrane to the outer leaflet of the outer membrane [417]. The BamA-E proteins are also included with this gene ontology tag, which form the beta-barrel insertion complex in the outer membrane [418].

The down-regulation of outer membrane assembly machinery is surprising for BAC, Cc and SQ53-tolerant samples, as these disinfectants operate via membrane disruption and increasing membrane permeability. LptD was originally designated imp, after the increased membrane permeability caused by mutations that disrupted its functionality [419]. It is therefore difficult to rationalise how decreasing the expression of LptD and associated LPS-assembly proteins will enable a higher tolerance to BAC, Cc, or SQ53.

Previous evidence suggests that BAC, DDAC and PHMB-tolerant samples contain conserved mutations in genes associated with the modification of lipid A via the addition of the L-Ara4N moiety (Figure 24, Figure 25, Table 11), resulting in the neutralization of the negative charge of the lipid A 4 '-phosphate group [231], [374]. This modification takes place on the outer leaflet of the inner membrane [372], before the transfer of the modified lipid A to the outer membrane where it may have an impact on the efficacy of the cationic surfactants. Therefore, the down-regulation of the LptA and LptC-E proteins in BAC-tolerant samples is additionally paradoxical. Based on the current understanding of these data, this may lead to the accumulation of modified lipid A on the outer leaflet of the inner membrane, projecting into the periplasm. This may be desirable, as it would ensure that all lipid A that is transferred to the outer membrane is not negatively charged. Alternatively, it is possible that the LptA-E machinery is not the bottleneck of the LPS biosynthesis and assembly pathways, so the down-regulation of these proteins that is observed may not necessarily impact outer membrane assembly.

Further experimentation and analysis of these data would be required to investigate the impact LptA and LptC-E down-regulation may have on BAC-tolerance.

It is important to note that the Gram-negative-bacterium-type outer membrane assembly gene ontology tag did not have a decreased enrichment in DDAC and PHMB-tolerant samples (Figure 27a). Initially, this may further highlight variation in the tolerance mechanisms of *K. pneumoniae* to these disinfectants. However, in these tolerant samples down-regulation was observed in LptD but not LptC. LptA, B, E, F and G were not detected, likely due to the 25.8% and 27.6% protein coverage of these two samples (Table 13). It is therefore not possible to conclusively state whether the observed decrease in Lpt proteins seen in BAC-tolerant samples is also common to DDAC and PHMB-tolerant samples of account of their similar disinfectant MOAs.

Bronopol-tolerant samples also displayed a reduction in LptD. As a result, this reduction in expression was seen across all tolerant samples, including all biological replicates. As the parent samples were not subject to the serial passage protocol, it is possible that the down-regulation observed in all disinfectant-tolerant samples is not a result of the individual disinfection treatments at all, instead simply a result of the serial passage treatment itself. Additional controls would need to be undertaken, whereby the parent strains are subjected to the serial passage experiment but exposed to dH_2O in lieu of any disinfectant treatment.

The fold enrichment of cellular component GO terms for each of the disinfectant-tolerant samples are shown in Figure 27b. Proteins localised to the cell outer membrane are negatively

enriched in bronopol, chlorocresol and SQ53-tolerant samples, but not BAC, DDAC and PHMB-tolerant samples (Figure 27b). This down-regulation in bronopol-tolerant samples may be a result of bronopol not operating directly via membrane disruption, therefore membrane proteins are not required to be replaced. In addition, the MOA of bronopol requires penetration into the cytoplasm [99], [100], so the negative enrichment of outer membrane proteins may be represented by porins and other proteins that promote bronopol uptake.

The negative enrichment of outer membrane proteins in chlorocresol and SQ53-tolerant samples is unexpected, as these disinfectants operate via membrane disruption and solubilisation of membrane proteins (Table 2, Table 3), which would need replacing to maintain membrane integrity. The proteins down-regulated include OmpX, nucleoside-specific channel-forming protein Tsx and iron uptake proteins FepA and FhuA [360].

The gene ontology enrichment analysis presented here provides a very broad overview of the regulation of proteins associated with biological processes, and their distribution within the bacterial cell. This enables us to build up a picture of the impact that prolonged exposure to the respective disinfectants have had. A more in-depth analysis method is required to visualise the protein interactions and pathways that may underpin the tolerance displayed by each of the tolerant samples.

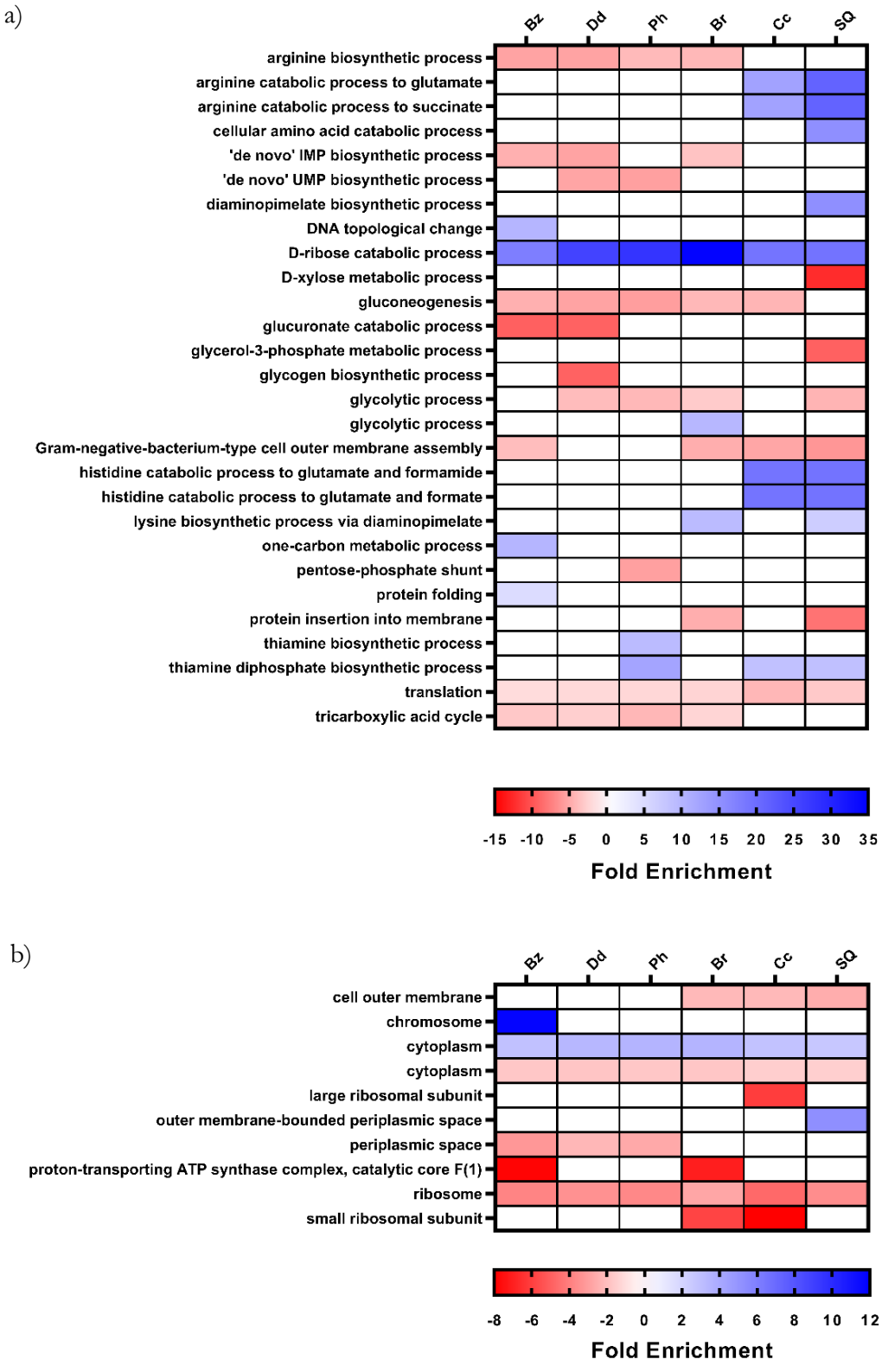

Figure 27. Heatmaps showing gene ontology (GO) enrichment analysis of *Klebsiella pneumoniae* NCTC 13443 disinfectant-tolerant samples. a) Fold enrichment of biological process GO terms. b) Fold enrichment of cellular component GO terms. Blue indicates a higher expression of proteins associated with the term, and red indicates a lower expression of proteins associated with the term, as depicted in the key. Bz: benzalkonium chloride-tolerant samples. Dd: didecyldimethylammonium chloride-tolerant samples. Ph: polyhexamethylene biguanide-tolerant samples. Br: bronopol-tolerant samples. Cc: chlorocresol-tolerant samples. SQ: disinfectant formulation "SQ53" -tolerant samples. The "glycolytic process" and "cytoplasm" GO terms are repeated due to individual samples showing both higher and lower expression of proteins associated with these terms.

5.4.2.2.3. Visualisation of differentially expressed proteins via expression networks

For detailed visualisation of the changes in expression of proteins in disinfectant-tolerant samples in comparison to parent samples, gene networks were generated using the ClueGO v2.5.9 plugin [358] within the Cytoscape v3.9.1 programme [359], as shown in Figure 28, Figure 29, Figure 30, Figure 31, Figure 32 and Figure 33. The genes that encode the differentially expressed proteins were arranged according to their KEGG database annotations [364], [365], showing the biological pathways the genes are associated with. *Klebsiella pneumoniae* strain 342 was used as the reference gene list, as this was the closest relative to *K. pneumoniae* NCTC 13443 available in the software. As indicated in the figure legends, the red and blue colouration indicates the degree of down or up regulation of the protein, respectively.

The underlying genes corresponding to differentially expressed proteins in BAC-tolerant samples are mapped according to KEGG pathway annotation in Figure 28. Based on previous observations, it is clear that proteins of the "Lipopolysaccharide biosynthesis" KEGG pathway are down-regulated, with the exception of HldE, a bifunctional protein involved in 2 of 4 steps of the synthesis of adenosine 5'-diphosphate -L-glycero-beta-D-manno-heptose, a precursor to LPS [360]. Interestingly, GmhA and HldD form the other 2 steps of this pathway in *E. coli* [420], so the overall regulatory impact on this pathway is unclear. Despite this, overall, the proteins detected that are associated with LPS biosynthesis seem to be down-regulated (Figure 28, "Lipopolysaccharide biosynthesis" KEGG pathway annotation). In addition, the proteins ArnA and ArnB can be seen to be up-regulated (Figure 28, "Amino sugar and nucleotide sugar metabolism" KEGG pathway annotation), which are known to be involved in the formation of UDP-L-Ara4N [376] which is then added to lipid A by ArnT [372], as described previously. This is likely a result of the observed mutations in *basS* (Figure 24), which have previously been demonstrated to induce lipid A modification [231], [374].

The same can be observed in the differential expression map of DDAC and PHMB-tolerant samples (Figure 29, Figure 30), with down-regulation of genes associated with the "Lipopolysaccharide biosynthesis" KEGG pathway annotation and the up-regulation of ArnA, and ArnB in PHMB-tolerant samples. It should be noted that ArnB was detected in DDAC samples as up-regulated, but the significance value was below the FDR cut-off so was not included in further analysis.

It is assumed that this mechanism of LPS modification is in common between the cationic surfactants, as this reduces the negative charge of the outer leaflet of the outer membrane, which reduces the affinity of the cationic disinfectants to their target site [231], [374]. As a result of this,

a higher concentration of disinfectant would be required to induce an inhibitory effect, as shown previously (Table 8). The modification of lipid A has been previously demonstrated as a mechanism of resistance of *P. aeruginosa* [421], [422] and *E. coli* [232], [423] to polymyxin and cationic peptides, and more recently *P. aeruginosa* [233] and *E. coli* [339] to BAC. Provisionally these data suggest that *K. pneumoniae* is able to demonstrate similar mechanisms to develop tolerance to the cationic surfactants BAC, DDAC and PHMB.

ArnA was found to have been down-regulated in chlorocresol and SQ53-tolerant samples (Figure 32, Figure 33 - "Amino sugar and nucleotide sugar metabolism" KEGG pathway annotation). Chlorocresol has a membrane-active MOA but is not cationic (Table 2), so the efficacy will not be impacted by outer membrane charge changes via lipid A modifications, so thus ArnAB is down-regulated. SQ53 is a formulation containing all of the other disinfectants, including the cationic surfactants (Table 3). The down-regulation of ArnA indicates that the mechanism of SQ53 tolerance is not reliant on lipid A modification. The implication is that there is another alternative mechanism for tolerating the cationic surfactants present within the SQ53 formulation. Alternatively, *K. pneumoniae* does not need to develop tolerance to these disinfectants as they are not the key active components within the formulation. The lack of similarity between SQ53 and QAC tolerance mechanisms opposes previous consistencies observed between the cross-resistance profiles of DDAC-tolerant and SQ53-tolerant samples (Table 9, Figure 18).

BAC and DDAC-tolerant samples displayed a down-regulation in proteins associated with "Base exisicion repair" and "Mismatch repair" KEGG pathway annotations in comparison to the parent strains that were not exposed to any disinfectants (Figure 28, Figure 29). This observed down-regulation in DNA repair mechanisms may be a result of the *K. pneumoniae* tolerant samples attempting to promote a hypermutable phenotype in order to develop potential tolerance mechanisms. This has been seen previously in *K. pneumoniae* samples with mutations in MutL [379], shown down-regulated in DDAC-tolerant samples (Figure 29).

Interestingly, PHMB and bronopol were the only tolerant-samples to not display a down-regulation in some form of DNA repair mechanisms (Figure 30, Figure 31). This suggests that DNA repair mechanisms may be of more importance to *K. pneumoniae* survivability when tolerating PHMB and bronopol. This aligns with the MOAs of these disinfectants, as PHMB has been suggested to have a secondary DNA-active mechanism [73], [74], and bronopol generates ROS which cause DNA damage [100].

All tolerant samples down-regulated catalase-peroxidase KatE (Figure 28-14, "Glyoxylate and dicarboxylate metabolism" KEGG pathway annotation). Bronopol-tolerant samples also down-regulated catalase KatG (Figure 31, "Tryptophan metabolism" KEGG pathway annotation). This indicates that protection from ROS via these proteins is not required in the disinfectant-tolerant samples. This is particularly surprising for the bronopol-tolerant samples, as bronopol produces ROS in aerobic conditions [100] as a by-product in a secondary mechanism as described previously (Table 2). Furthermore, after manually searching the bronopol-tolerant proteome results, superoxide dismutase SodB is down-regulated in these samples too. This indicates that the mechanism by which *K. pneumoniae* is able to tolerate bronopol relies upon the prevention of ROS generation. For example, if the environment is anaerobic or bronopol is prevented from reaching the target sites then ROS will not be generated and thus catalases will not be required.

GTP pyrophosphokinase (RelA) expression is also decreased in bronopol (Figure 31, "Purine metabolism" KEGG pathway annotation). This protein is responsible for mediating the stringent response through generation of (p)ppGpp [396]. A decrease in RelA expression indicates that the samples are limiting the stringent response. Similar changes in expression can be seen in chlorocresol-tolerant samples (Figure 30, "Purine metabolism" KEGG pathway annotation), with an up-regulation in the quantity of GppA, which converts (p)ppGpp to ppGpp [360], and a decrease in SpoT expression, which also mediates the stringent response via the synthesis and degradation of ppGpp [396]. It is unclear what function the limitation of the stringent response provides in terms of disinfectant-tolerance. Once again, further analysis would be required which is outside the scope of this thesis.

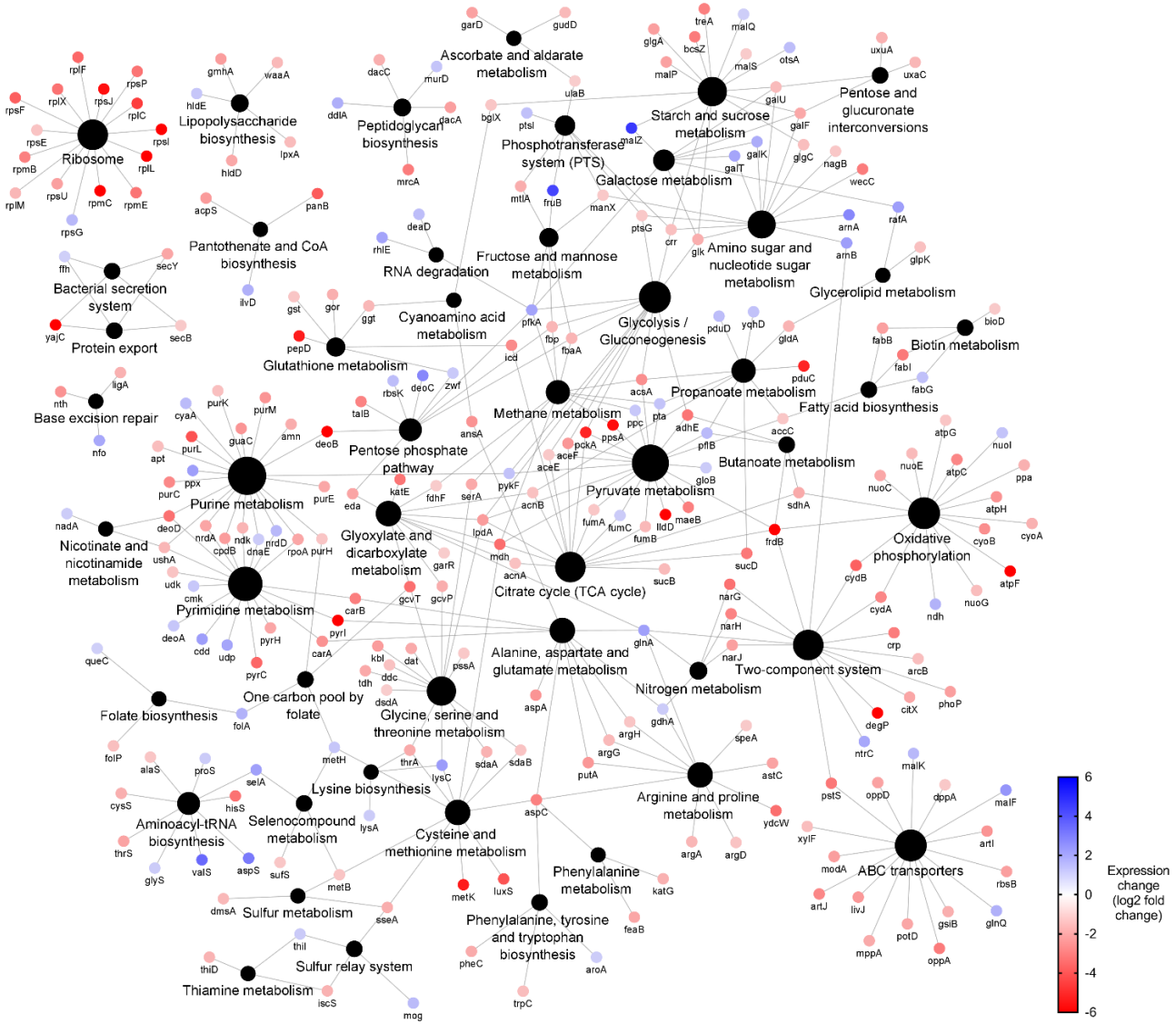

Figure 28. Network diagram of differentially expressed proteins in benzalkonium chloride-tolerant *Klebsiella pneumoniae* NCTC 13443 samples (Bz1G, Bz1D, Bz2G, Bz2D and Bz3). Differentially expressed proteins are indicated by the coloured dots, arranged according to Kyoto Encyclopedia of Genes and Genomes (KEGG) pathway annotation. Blue and red colouration indicates up or down expression, respectively. Black dots indicate KEGG pathway annotations, as labelled. Lines connect proteins to their annotations. This network map was generated by Cytoscape v3.9.1 using the ClueGO v2.5.9 plugin.

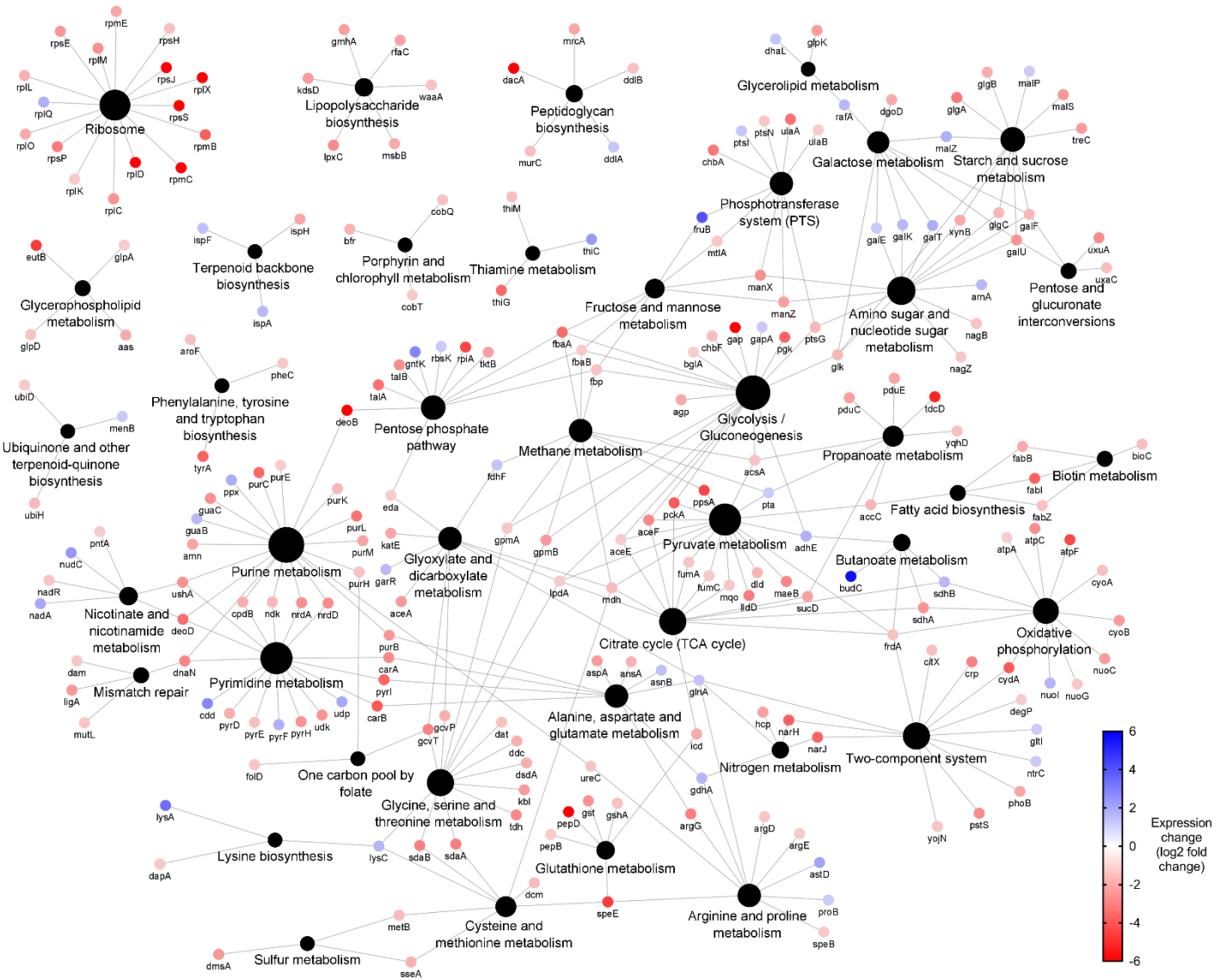

Figure 29. Network diagram of differentially expressed proteins in didecyldimethylammonium chloride-tolerant *Klebsiella pneumoniae* NCTC 13443 samples (Dd1, Dd2 and Dd3). Differentially expressed proteins are indicated by the coloured dots, arranged according to Kyoto Encyclopedia of Genes and Genomes (KEGG) pathway annotation. Blue and red colouration indicates up or down expression, respectively. Black dots indicate KEGG pathway annotations, as labelled. Lines connect proteins to their annotations. This network map was generated by Cytoscape v3.9.1 using the ClueGO v2.5.9 plugin.

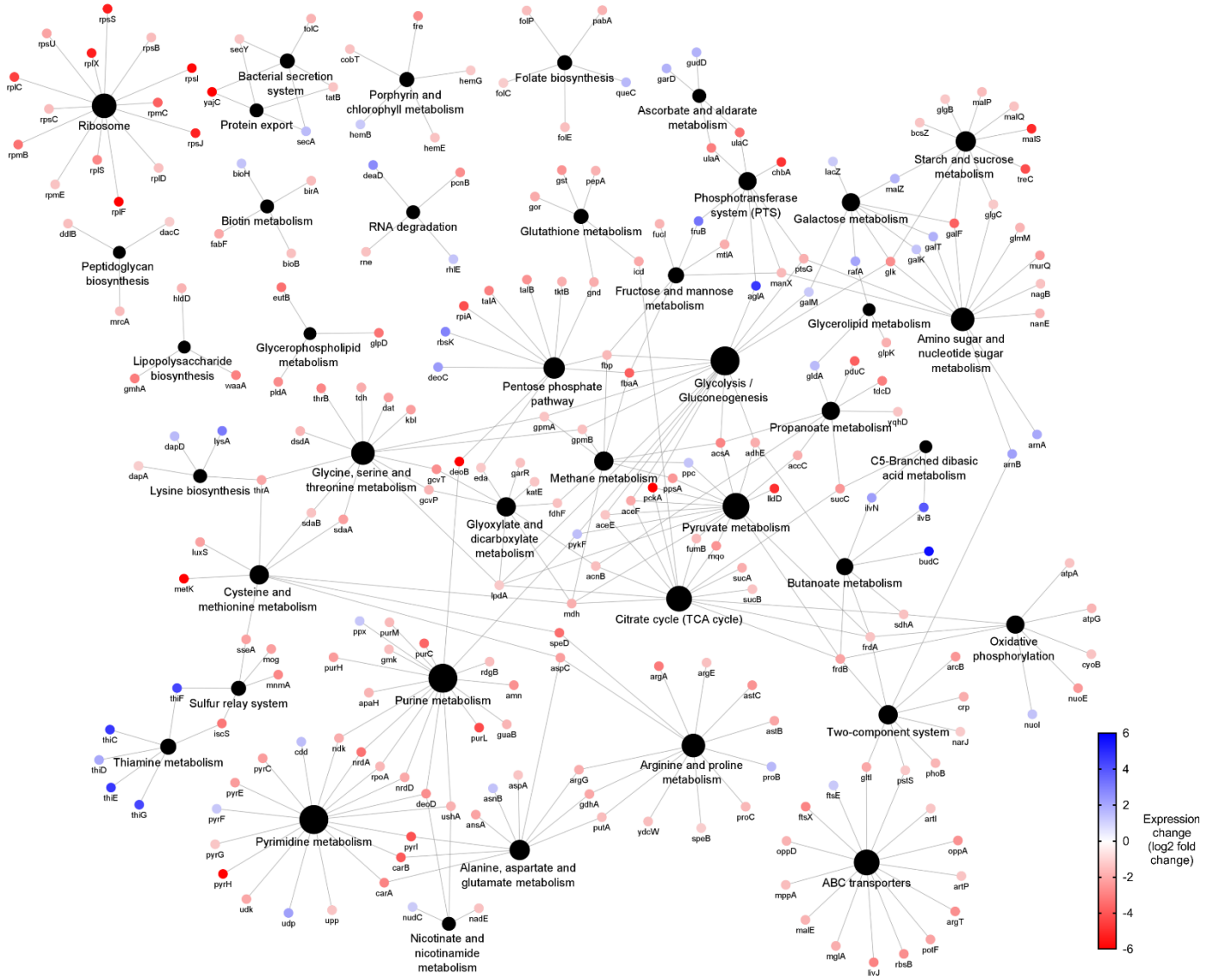

Figure 30. Network diagram of differentially expressed proteins in polyhexamethylene biguanide-tolerant *Klebsiella pneumoniae* NCTC 13443 samples (Ph1, Ph2 and Ph3). Differentially expressed proteins are indicated by the coloured dots, arranged according to Kyoto Encyclopedia of Genes and Genomes (KEGG) pathway annotation. Blue and red colouration indicates up or down expression, respectively. Black dots indicate KEGG pathway annotations, as labelled. Lines connect proteins to their annotations. This network map was generated by Cytoscape v3.9.1 using the ClueGO v2.5.9 plugin.

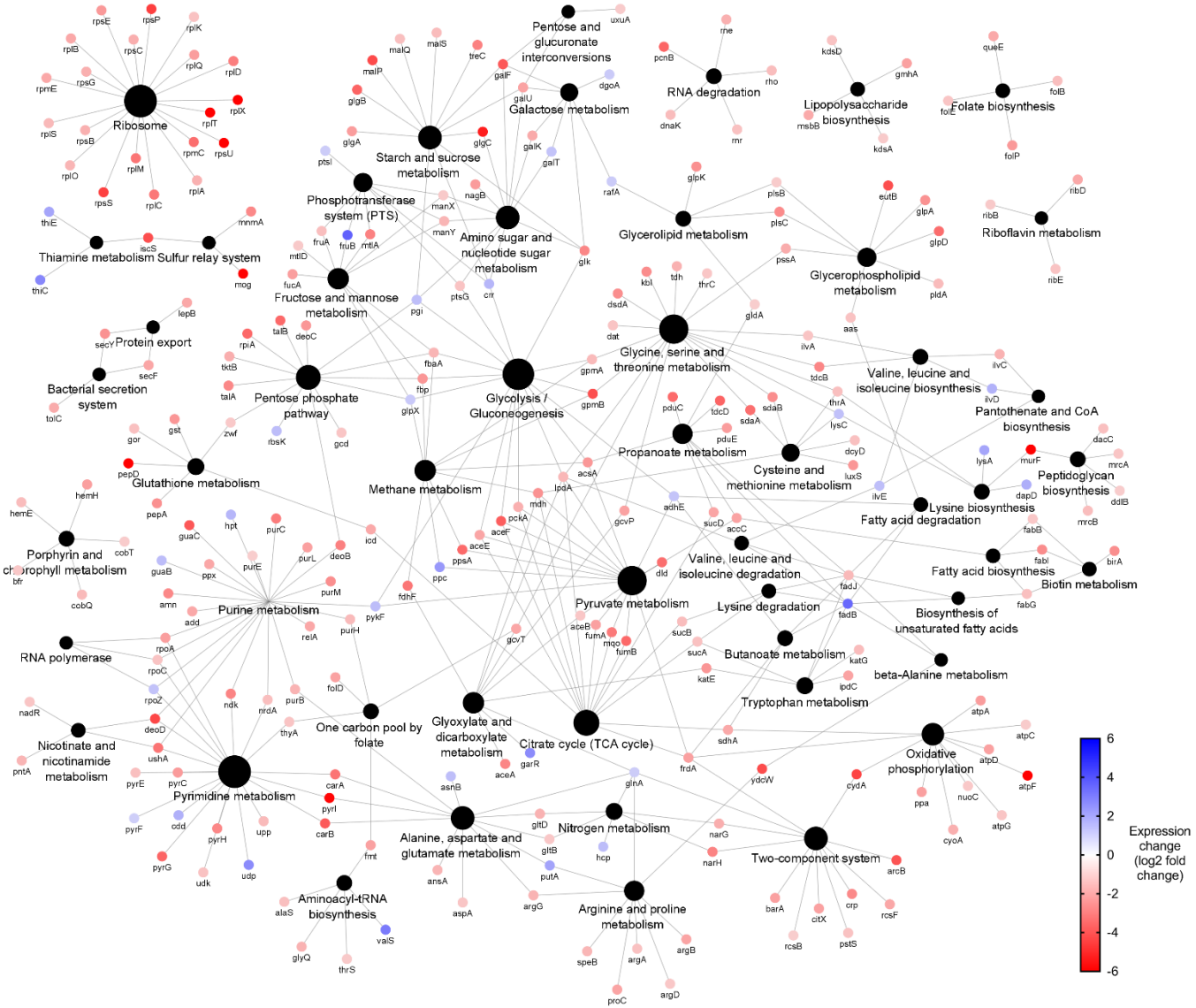

Figure 31. Network diagram of differentially expressed proteins in bronopol-tolerant *Klebsiella pneumoniae* NCTC 13443 samples (Br1, Br 2 and Br3). Differentially expressed proteins are indicated by the coloured dots, arranged according to Kyoto Encyclopedia of Genes and Genomes (KEGG) pathway annotation. Blue and red colouration indicates up or down expression, respectively. Black dots indicate KEGG pathway annotations, as labelled. Lines connect proteins to their annotations. This network map was generated by Cytoscape v3.9.1 using the ClueGO v2.5.9 plugin.

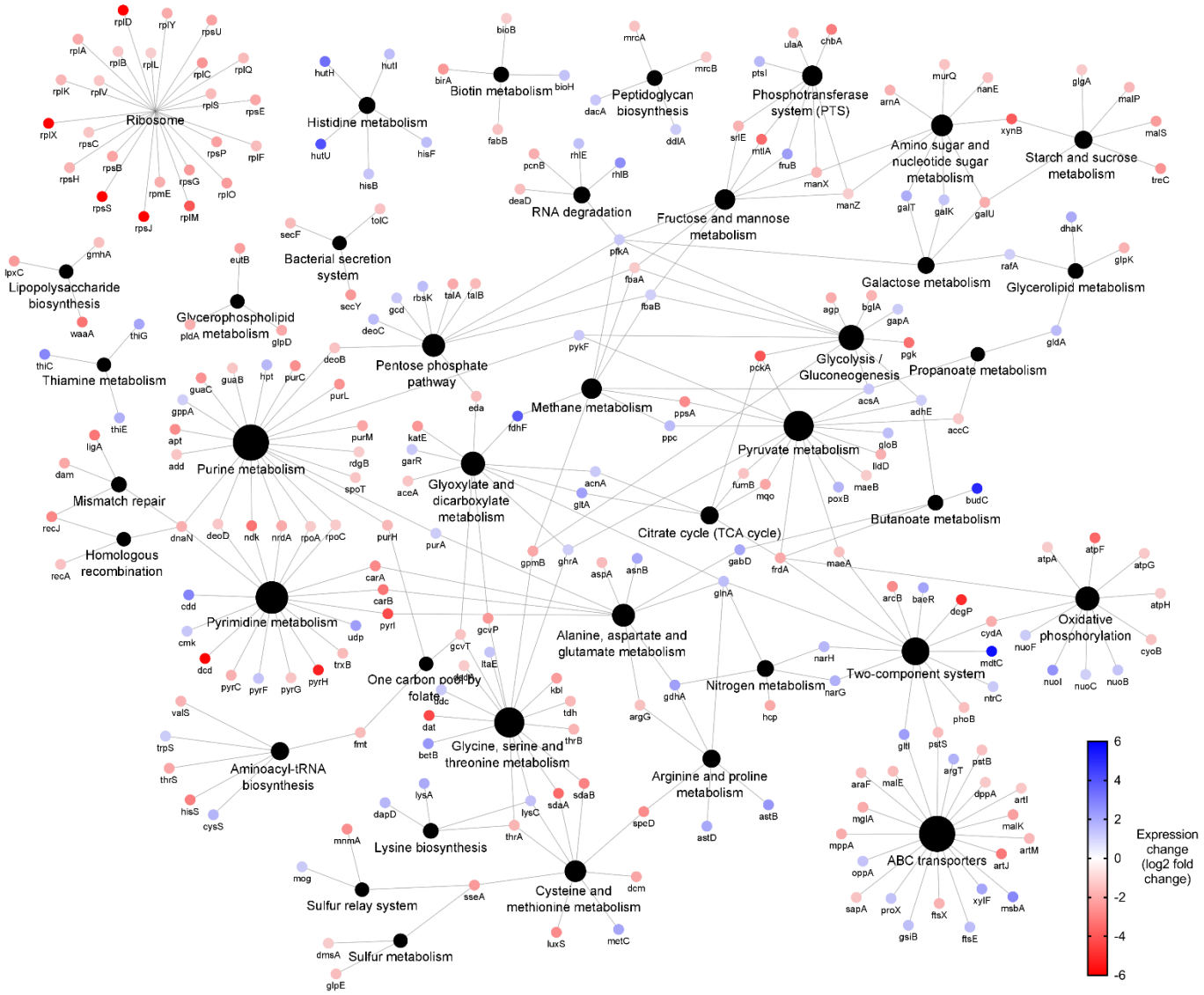

Figure 32. Network diagram of differentially expressed proteins in chlorocresol-tolerant *Klebsiella pneumoniae* NCTC 13443 samples (Cc1, Cc2 and Cc3). Differentially expressed proteins are indicated by the coloured dots, arranged according to Kyoto Encyclopedia of Genes and Genomes (KEGG) pathway annotation. Blue and red colouration indicates up or down expression, respectively. Black dots indicate KEGG pathway annotations, as labelled. Lines connect proteins to their annotations. This network map was generated by Cytoscape v3.9.1 using the ClueGO v2.5.9 plugin.

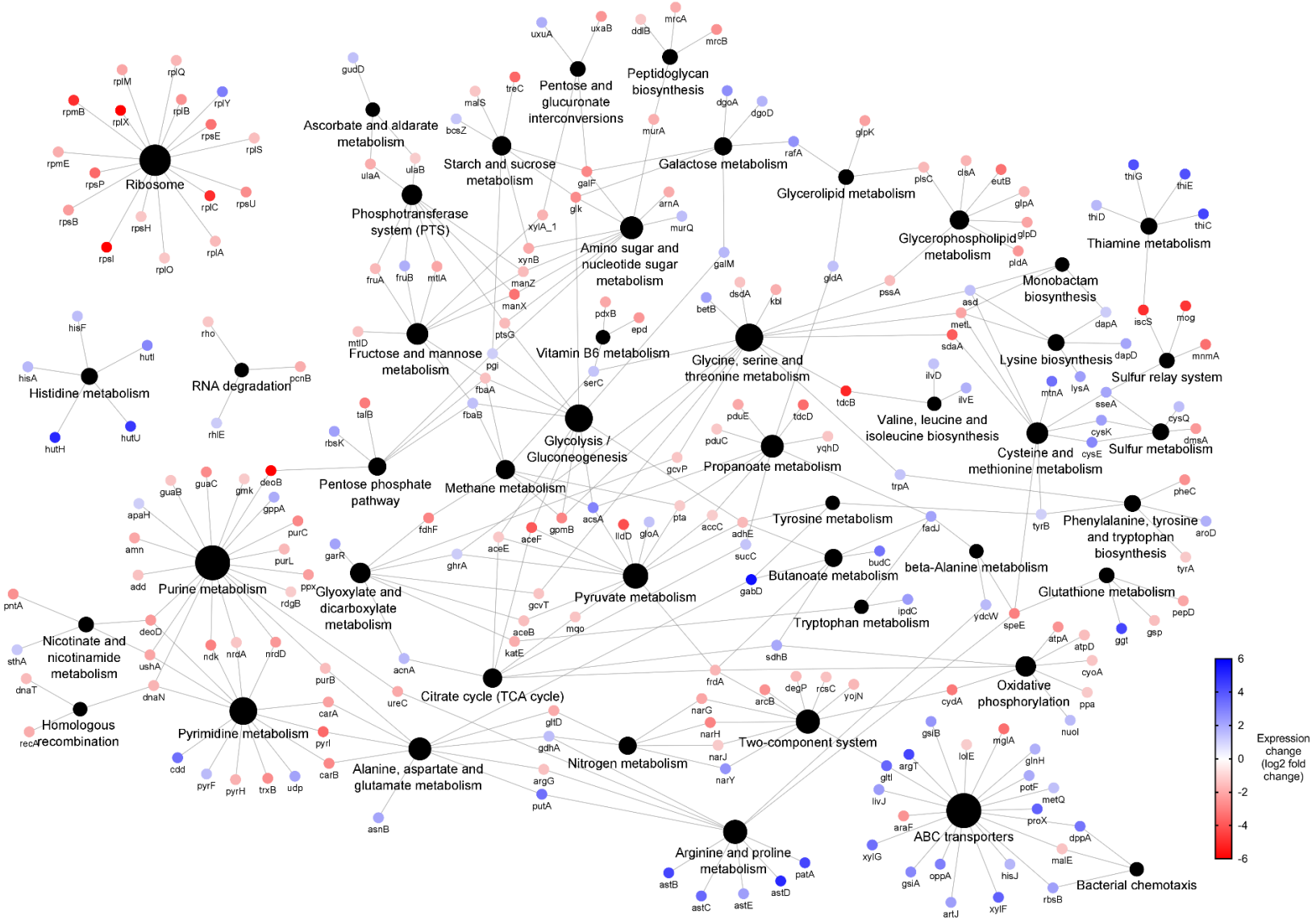

Figure 33. Network diagram of differentially expressed proteins in disinfectant formulation "SQ53"-tolerant *Klebsiella pneumoniae* NCTC 13443 samples (SQ1, SQ2 and SQ3). Differentially expressed proteins are indicated by the coloured dots, arranged according to Kyoto Encyclopedia of Genes and Genomes (KEGG) pathway annotation. Blue and red colouration indicates up or down expression, respectively. Black dots indicate KEGG pathway annotations, as labelled. Lines connect proteins to their annotations. This network map was generated by Cytoscape v3.9.1 using the ClueGO v2.5.9 plugin.

5.5. Conclusions

This chapter aimed to elucidate the underpinning mechanisms of tolerance observed in disinfectant tolerant *K. pneumoniae* samples. Whole genome sequencing was conducted to identify genetic variation between the untreated parent samples and each of the disinfectant-tolerant samples, and to establish if tolerance resulted from genetically acquired adaptations or phenotypical variation.

Each sample gained from 5 to 506 SNPs, and between 5 and 142 InDels (Figure 19a, c), indicating that samples may have acquired adaptations that enable tolerance to disinfectants. The variation in the number of SNPs and InDels between the disinfectant-tolerant samples suggest differences in the strength of the selection pressure applied or the level of adaptation required by *K. pneumoniae* to develop tolerance to the respective disinfectant treatments.

Phylogenetic analysis reveals that disinfectant-tolerant samples often displayed conserved mutations, and were grouped into clades based on the disinfectant treatment applied (Figure 20). This indicates that the mutations observed were not necessarily due to random chance, but were selected for by the disinfectant treatments.

In addition, the genetic distances between the disinfectant-tolerant sample clades did not correlate with similarities and differences between the MOAs of the disinfectants (Figure 20). This may be due to unique methods of tolerance to each of the disinfectants, or due to the same molecular mechanisms manifesting from different mutation sites. Furthermore, BAC, PHMB and SQ53-tolerant samples displayed large genetic distances between each other (Figure 20). Once again this may be due to varying mechanisms of tolerance development to the same disinfectant treatment, or variation in the mutation sites that generate the same molecular mechanisms of disinfectant tolerance.

The underpinning molecular mechanisms of the tolerance phenotypes were investigated by examining the locations of mutations that were likely to impact function and elucidating the relative expression of proteins via label-free quantitative proteomics.

BAC, DDAC and PHMB-tolerant samples demonstrate mutations in *basS* (Figure 24, Figure 25, Table 11), which has previously been demonstrated to induce lipid-A modification and result in tolerance to polymyxin and cationic peptides [231], [374]. This is accompanied by an up-regulation of proteins associated with lipid-A modification with L-Ara4N, alongside a down-regulation of proteins associated with LPS formation (Table 14, Figure 28, Figure 29, Figure 30). Collectively this results in a reduction in the net negative charge of the outer leaflet of the outer

membrane, causing cationic surfactants to display a lower affinity to the outer surface of bacterial cells. This results in a higher concentration of disinfectant being required to induce an antimicrobial effect. This aligns with previous reports that have linked this mechanism to BAC resistance in *P. aeruginosa* [233] and *E.coli* [339]. To our knowledge this mechanism has not been previously reported with regards to *K. pneumoniae* tolerance to BAC, or been demonstrated to be linked with bacterial tolerance to DDAC or PHMB.

In addition, BAC-tolerant samples up-regulated expression of proteins associated with the AcrAB-TolC efflux pump (Table 14, Figure 28), which aligns with recent reports noting an increased susceptibility of *K. pneumoniae* mutants lacking a functional AcrAB-TolC to BAC [223]. These data suggest a link between the up-regulation of this efflux complex and reduced *K. pneumoniae* susceptibility to BAC.

Bronopol-tolerant samples displayed a high up-regulation of NemA, a protein previously shown to be associated with oxidative stress mitigation and be capable of enzymatically breaking down electrophilic compounds [415], and more specifically nitro group-containing compounds such as TNT [413], [414]. Bronopol is an electrophilic nitro group-containing compound so this protein may be involved in the enzymatic breakdown of bronopol. This is therefore the possible mechanism of bronopol-tolerance displayed by *K. pneumoniae*. This potential mechanism of bronopol tolerance has not been reported in the literature before.

The underlying mechanisms of chlorocresol also seem to involve the up-regulation of efflux pumps, specifically the MdtABC complex (Table 14). This complex has been previously demonstrated to contribute to a reduction in *E. coli* susceptibility to novobiocin and deoxycholate [416]. More broadly, phenol and phenol-derivative chloroxylenol susceptibility has been associated with efflux pump activity in *S. enterica* [226] and *E.coli* [225] respectively.

The underpinning mechanisms of disinfectant formulation SQ53-tolerance remain unclear. The samples gained a conserved stop gain mutation in MutL DNA mismatch repair protein, the impediment of which has been previously associated with the development of hypermutable phenotypes [379]. As the biological replicates were exposed to a disinfectant formulation containing all of the other disinfectants, it is possible that the multiple disinfectant mechanisms of the components applied a strong selection pressure which requires more severe levels of adaptation. Thus, a hypermutable phenotype was preferential, resulting in the large genetic variation displayed between the SQ53-tolerant samples (Figure 20).

This strong selection pressure, paired with the hypermutable phenotype likely gave rise to varying mechanisms of SQ53 tolerance that vary between the biological replicates. The proteomic analysis methodology compares the proteins detected across all SQ53-tolerant samples to the proteins detected in all parent samples. As a result, any mechanisms of tolerance displayed by individual biological replicates are unlikely to be elucidated. More detailed analysis is required to further examine the underlying molecular mechanisms of SQ53-tolerance displayed by the samples, including repeating the analysis on each of the biological replicates individually.

Despite this chapter only representing an initial analysis, these data have already clearly demonstrated the breadth of mechanisms that a single bacterial strain is able to develop in order to adapt to otherwise lethal concentrations of disinfectants. This work represents a crucial step toward understanding the complex mechanisms of bacterial tolerance to disinfectants.

6. The Induction of the Viable but Nonculturable State via Exposure to Common Disinfectants

6.1. Introduction

Bacteria are capable of many phenotypic behaviours in order to overcome and adapt to stressful conditions. A common series of stress-induced behavioural changes include the reduction of cell size [133], [424], lowering of cellular metabolism [425] and cell surface reorganisation [140], [142], ultimately leading to the cell adapting a dormant state. Cells in this state are observed to be metabolically active but incapable of growing on standard growth medium [130], and thus the state is termed "viable but nonculturable", or VBNC. At least 101 bacterial species have been documented as able to enter the VBNC state [144], which is suggested to allow bacteria to outlast the stressor [426]. An overview of our current understanding of the VBNC state can be found in Chapter 1.4.2.2.2.

K. pneumoniae has been demonstrated to enter the VBNC state [135], [427]. Furthermore, various disinfectants including BAC [154], non-ionic surfactants [155], peracetic acid [156], sodium hypochlorite [156], [159] and hydrogen peroxide [157] are capable of VBNC induction, alongside disinfectant formulations containing DDAC and PHMB [158]. Research conducted by Robben *et al.* (2019) demonstrated that *E. coli, B. cereus, P. aeruginosa,* and *L. monocytogenes* VBNC cells display a reduced susceptibility to various antibiotics, disinfectants and preservatives, including BAC and bronopol [160].

However, the ability for BAC, DDAC and PHMB exposure to induce the VBNC state in *K. pneumoniae* has not been established. In addition, bronopol and chlorocresol have not been demonstrated to induce the VBNC state in any species.

The most common methods of VBNC quantification include LIVE/DEAD™ BacLight™ (live/dead) staining, PMA qPCR, DVC, CTC with 4',6-diamidino-2-phenylindole (DAPI) double staining and CFDA staining [175]. These methods are discussed further in Chapter 1.4.2.2.2.3. All of these methods rely upon differentiating between live and dead bacterial cells utilising physiological biomarkers such as membrane integrity [175], [176], respiration [180], growth [179] or enzymatic activity [175], [182]. This therefore provides an estimation of the total number of viable cells, including both culturable cells and VBNCs. Quantifying the number of colony

forming units via plate-counts and taking this value away from the total number of viable cells leaves an estimation of the number of VBNCs [143], [175]. Thus, all of these methods are an indirect estimation of the number of VBNCs within a population. To our knowledge, there are currently no methodologies that directly quantify the number of VBNC cells within a population.

The various stains and dyes used currently are only capable of differentiating between viable and non-viable bacterial cells. Direct enumeration of VBNCs would require the ability to differentiate between culturable cells and VBNC cells, despite both cell populations being viable. The main characteristic that varies between the two populations is simply the ability to proliferate in standard growth medium [130].

Cell proliferation dye eFlour™ 670 (CPD) is a dye that reacts with primary amines, resulting in non-specific labelling of any primary amine-containing structures on the surface of cells [428]. As stained bacterial cells proliferate, the dye is divided approximately equally among daughter cells, causing the fluorescence intensity to approximately half with each division [428]. This change is quantifiable, potentially allowing for bacterial cells that proliferate (culturable cells) to be distinguished from those that do not (VBNCs and non-viable cells). By combining CPD with any viability stain, it may be possible to distinguish VBNC cells from both dead and culturable cells. If such an assay were paired with flow cytometry, the VBNC population within a culture could be quantified directly, without relying on estimations of total viable cells and colony counts. Fluorescence-activated cell sorting (FACS) could then be used to isolate the VBNC population for further analysis.

The use of proliferation dyes is well established in eukaryotic cell biology, but their use has not been as widely established in bacteriology. Nebe von-Caron *et al.* (1995) successfully demonstrated the use of chloro-CFDA-succinimidyl ester to track the reproductive viability of *Listeria innocua* via flow cytometric analysis [429]. In addition, CF succinimidyl ester (CFSE) has been utilised to examine the lag times of *Lactobacillus plantarum* after heat stress and exposure to antimicrobial peptide nisin, and was even suggested to be able to distinguish bacteria based on the number of cell divisions undertaken since staining [430]. CPD has been utilised to demonstrate the proliferation of *S. aureus* within phagocytes, and was shown to be applicable to the staining of Gram-negative bacteria including *E. coli* [428].

Experiments investigating persister cell resuscitation have been conducted using various fluorescence markers such as GFP [431], *mCherry* [432] and CFSE [433]. Notably, Orman *et al.* utilised *mCherry* to enumerate and isolate *E. coli* persister and VBNC/dead populations using flow cytometry and FACS, although VBNC numbers were only able to be elucidated after

subsequent growth steps [174]. However, this methodology requires the bacteria to be transformed and expression of the protein to be induced, which is an invasive process that has been demonstrated to cause stress and act as a selection pressure [434]. The use of proliferation stains would therefore provide a non-invasive alternative that may allow for the quantification and isolation of VBNC populations without needing to transform and induce expression in the sample. To our knowledge, there are no previous studies that have explored this possibility.

The hypothesised novel methodology is as follows. The bacterial culture to be examined is stained with a cell proliferation stain such as CPD, CFSE or a CellTrace™ Cell Proliferation Kit, before incubation in liquid culture medium. Once culturable cells are given sufficient time to proliferate, the sample is stained with a viability marker, such as PI or 2-Deoxy-2-[(7-nitro-2,1,3-benzoxadiazol-4-yl)amino]-D-glucose (2-NBDG), before being examined by flow cytometry. A dot plot showing hypothetical model data as generated via this methodology is shown in Figure 34. Bacterial cells that have proliferated will be distinguishable from those that have not due to variations in cell proliferation stain fluorescence intensity, while VBNCs will be distinguishable from dead cells as a result of the viability stain (Figure 34).

The core principle is the direct quantification of VBNCs through the exclusion of proliferating bacterial cells, so the methodology is thus provisionally termed "proliferation exclusion" (PE).

Direct identification of VBNC populations may allow for the isolation of VBNCs via FACS, and subsequent molecular interrogation of purified VBNC cultures. Decreasing proliferation dye fluorescence intensity also provides a tool for the examination of VBNC resuscitation.

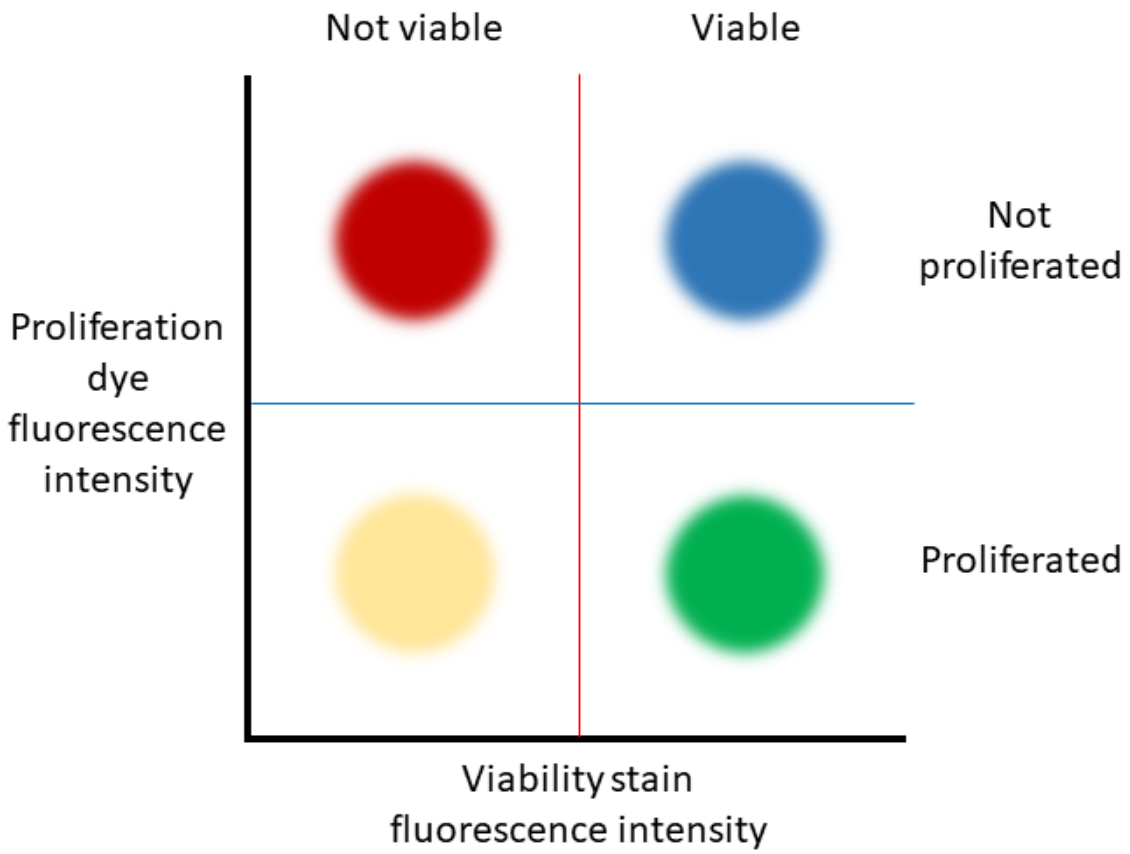

Figure 34. A dot plot displaying hypothetical model data as produced by the proliferation exclusion methodology. The fluorescence intensities of the proliferation dye and viability stain are plotted on the Y and X axes, respectively. Quadrants separating the cell populations are depicted by the red and blue lines. The red vertical line shows the threshold separating viable from non-viable bacterial populations, as identified using the viability stain. The blue horizontal line separates bacterial populations that have and have not proliferated, as identified using the cell proliferation dye. The resulting cell populations are depicted by the coloured circles. The red population is located in the quadrant showing bacterial cells that are not viable and have not proliferated, so considered to be "dead". The green population is localised to the quadrant showing bacterial cells that are viable and have proliferated, so are considered to be "alive". The blue population consists of cells that are viable but have not proliferated, so are therefore considered to be viable but nonculturable (VBNC). Therefore, the number of VBNCs can be directly enumerated by counting the number of events in the top right quadrant. Any cells in the bottom left quadrant (depicted by the yellow circle) are hypothesised to be few in number. Bacterial cells in this quadrant have proliferated but are no longer viable, so have therefore died during the incubation period in the experimental procedure.

6.2. Chapter aims

A novel methodology of quantifying VBNCs has been hypothesised, provisionally named "proliferation exclusion" (PE). The aim of this chapter was to validate PE as a viable method of quantifying VBNCs, with the view of applying this to FACS in order to isolate VBNC cells from cultures containing mixed viability states.

In addition, this chapter aimed to evaluate the ability for common disinfectants to induce the VBNC state in *K. pneumoniae* utilising the novel PE methodology.

6.3. Materials and methods

Klebsiella pneumoniae NCTC 13443 was cultured as described in Chapter 2.3.1. The justification for the use of this strain is also described in Chapter 2.3.1. *K. pneumoniae* NCTC 9633 was selected for PE validation experiments for its antibiotic susceptibility, ensuring visible elongation during DVC. This strain was cultured using the method as described in Chapter 2.3.1.

The specific disinfectant-tolerant *K. pneumoniae* NCTC 13443 samples to be examined were generated during disinfectant adaptation experiments conducted in Chapter 4. For details on the biological replicates selected and a schematic diagram of the experimental workflow, see Chapter 4.3.3 and Figure 15, respectively.

Details on the disinfectants utilised and the justification for their use are overviewed in Chapter 2.3.2.

6.3.1. Proliferation exclusion validation

For ease of reference, the methodology for validation experiments will be overviewed here. As the validation of this novel methodology was an aim of the chapter, each step of the methodology is also discussed further in Chapter 6.4.1.

6.3.1.1. Establishing flow cytometry gates

6.3.1.1.1. Bacterial cell and singlet gates

One ml aliquots of *K. pneumoniae* NCTC 13443 overnight stock cultures were spun down at 5400 G for 10 minutes and re-suspended in PBS. This PBS wash step was repeated twice more, before stocks were serially diluted 10-fold in PBS. These samples were analysed by flow cytometric analysis to generate dot plots plotting forward scatter pulse height (FSC H) against side scatter pulse height (SSC H) on the X and Y axis, respectively. An additional dot plot that plots SSC H against side scatter pulse area (SSC A) was utilised. All axes were plotted using a base-10 logarithmic scale. From these dot plots the cell and singlet gates were established, as described in Chapter 6.4.1.1.1.

In addition, to establish whether events visible within the gates are a result of intact bacterial cells, an additional *K. pneumoniae* NCTC 13443 sample from the prior experiment containing 1 x 10^6 CFU/ml was filtered through a 0.22 µm filter and examined via flow cytometric analysis. This was compared to an aliquot from the same sample that did not undergo filtration.

6.3.1.1.2. Proliferation exclusion stain controls and quadrant positioning

K. pneumoniae NCTC 13443 cultures were generated as previously described (Chapter 2.3.1), before being spun down at 5400 G for 10 minutes and re-suspended in PBS. This PBS wash step was repeated twice more, before pellets were re-suspended in either PBS or 4% (w/v) formaldehyde and incubated at 4°C for 30 minutes. The samples were subjected to 3 more spin and PBS wash steps before being re-suspended in 1 ml PBS pre-warmed to 37°C that contained either 2.5 μM CPD, 10 μM 2-NBDG, or no stain, and mixed thoroughly by vortexing. Samples were then incubated at 37°C for 25 minutes in the dark. Stain was neutralised by a 1:500 dilution in PBS and the samples were analysed via flow cytometric analysis. In addition, the number of CFUs in each sample after staining were elucidated by serial dilution and plate counting. To establish the significance of any observed variation in the CFU/ml counts between staining treatments and the unstained control, unpaired t tests were conducted using GraphPad Prism 9.4.1.

A table displaying the excitation and emission values of each fluorophore, and the corresponding excitation laser and filter used can be found in Table 15. Histograms were generated with fluorescence intensity on the X axis, and number of events on the Y axis. Dot plots were generated with green fluorescence on the X axis and red fluorescence on the Y axis, both in base-10 logarithmic scale. Gates were established as described in Chapter 6.4.1.1.2.

6.3.1.1.3. LIVE/DEAD™ BacLight™ stain controls

K. pneumoniae NCTC 13443 cultures were generated as previously described (Chapter 2.3.1), before being spun down at 5400 G for 10 minutes and re-suspended in PBS. This PBS wash step was repeated twice more, before pellets were re-suspended in either PBS or 4% (w/v) formaldehyde and incubated at 4°C for 30 minutes. The samples were subjected to 3 more spin and PBS wash steps before being re-suspended in 1 ml PBS pre-warmed to 37°C that contained either 5 μM SYTO 9, 10 μM PI, both stains or no stain, and mixed thoroughly by vortexing. Samples were then incubated at room temperature for 10 minutes in the dark. Stain was neutralised by a 1:500 dilution in PBS and the samples were analysed via flow cytometric analysis. A table displaying the excitation and emission values of each fluorophore, and the corresponding excitation laser and filter used can be found in Table 15. Dot plots were generated with green fluorescence on the X axis and red fluorescence on the Y axis, both in base-10 logarithmic scale. Gates were established as described in Chapter 6.4.1.1.3.

Table 15. The excitation and emission characteristics of the stains used, alongside corresponding excitation laser and emission filter wavelengths used. SYTO9: SYTO™ 9 Green Fluorescent Nucleic Acid Stain. PI: propidium iodide. 2-NBDG: 2-(N-(7-Nitrobenz-2-oxa-1,3-diazol-4-yl)Amino)-2-Deoxyglucose. CPD: Cell Proliferation Dye eFluor™ 670.

Stain	Peak excitation wavelength (nm)	Peak emission wavelength (nm)	Wavelength of excitation laser used (nm)	Wavelength of emission filter used (nm)
SYTO9	485	498	488	525/30
PI	493	636	488	695/50
2-NBDG	465	540	488	525/30
CPD	647	670	642	661/15

6.3.1.2. Proliferation exclusion validation experiment

The MIC values of BAC, DDAC and PHMB when challenged with *K. pneumoniae* NCTC 9633 were elucidated via the broth microdilution methodology, as described previously in Chapter 2.3.3.

Based on these data, *K. pneumoniae* NCTC 9633 samples were exposed to varying concentrations of either BAC, DDAC or PHMB at concentrations ranging above and below the respective MICs. Samples exposed to BAC were exposed to either 0 μg/ml, 4 μg/ml, 8 μg/ml, 12 μg/ml, 16 μg/ml or 20 μg/ml BAC. DDAC-exposed samples were exposed to either 0 μg/ml, 4 μg/ml, 8 μg/ml or 12 μg/ml DDAC. Samples exposed to PHMB were exposed to 0 μg/ml, 3 μg/ml, 6 μg/ml or 9 μg/ml PHMB. All samples were exposed to the respective disinfectant treatment for 24-hours at 37°C in MHB, upon which 1 ml aliquots of each sample were centrifuged at 5400 G for 10 minutes and washed in PBS, repeated three times. Samples were then re-suspended in Dey-Engley neutralising broth (DEB) to neutralise residual disinfectant before being washed a further 3 times with PBS. Before the final wash step the 1 ml aliquots were split equally into 4 for subsequent CFU enumeration, DVC, live/dead and PE treatments, respectively.

Samples taken for CFU enumeration were serially diluted in PBS and plated out onto MHA before being incubated at 37°C for 24-hours. The number of CFUs were quantified manually to estimate the total number of culturable bacteria in each sample.

The aliquots taken for DVC were made up to 1 ml PBS, before being added to 4 ml dH_2O, 5 ml R2 broth and 10 μg/ml pipemidic acid. Samples were then incubated for 24-hours at room temperature in darkness before 1 ml aliquots were stained with 5 μM SYTO 9 for 10 minutes in the dark. The samples were then vacuum filtered onto a 0.22 μm Nuclepore™ Track-Etched Membrane filter (Whatman®), before the number of viable cells were enumerated via manual counting on a fluorescence microscope. Cells that had visibly elongated by at least 2 x their

normal length were counted on 30 FOVs. The counts were then used to estimate the total number of viable cells in each of the samples using the following equation.

$$\text{Total no. of viable cells per ml} = \frac{\left(A \times \left(\frac{f}{F}\right)\right)}{(v \times d)}$$

A = average no. of elongated cells per FOV
f = total filter surface area (mm)
F = individual FOV surface area (mm)
v = volume of culture filtered (ml)
d = dilution factor

The respective CFU count estimates calculated previously were then taken away from the total viable cells, leaving an estimate of the number of VBNCs via the DVC methodology.

Aliquots taken for live/dead analysis were stained with 5 μM SYTO 9 and 30 μM PI for 10 minutes at room temperature in the dark. The stain was then neutralised via 1:500 dilution in PBS and the samples were analysed via flow cytometric analysis using the gates established in the gating control experiments. The number of events captured in the "R6LiveCells" gate were quantified and used to estimate the total number of viable cells in each sample. The respective CFU count estimates calculated previously were then taken away from the total viable cells, leaving an estimate of the number of VBNCs via the live/dead methodology.

The aliquots taken for PE treatment were stained with 2.5 μM CPD for 25 minutes at 37°C. A 2 μl aliquot was quenched via dilution in 998 μl PBS, before being analysed via flow cytometric analysis to validate initial CPD uptake (0-hour time point). Excess CPD in the remaining sample was quenched via the addition of 9 ml of MHB pre-warmed to 37°C, before a 24-hour incubation at 37°C. At the 6-hour and 24-hour incubation time points, 1 ml aliquots of each sample were taken, washed in PBS 3 times and stained with 10 μM 2-NBDG viability stain for 25 minutes at 37°C. The stain was quenched via a 1:500 dilution in PBS and the samples were analysed via flow cytometry using the gates established in the control experiments previously. The number of events captured in the upper right quadrant after 6 and 24-hours were used to quantify the number of VBNCs in each sample.

6.3.2. Induction into the viable but nonculturable state via disinfectant exposure

The PE methodology was used to investigate the ability for common disinfectants to induce the VBNC state in the disinfectant-tolerant *K. pneumoniae* NCTC 13443 samples developed in Chapter 4. Three biological replicates from each disinfectant treatment were selected for further analysis, as described in Chapter 4.3.3 and displayed in Figure 15. Unique phenotypes were observed in 2 of the biological replicates of the BAC-tolerant samples ("green" and "dark", as described in Chapter 4.4.1), which were each isolated and subject to molecular characterisation. As a result, 5 BAC-tolerant samples were analysed from 3 BAC-tolerant biological replicates. The disinfectant-tolerant samples were cultured overnight at 37°C in 10 ml MHB containing varying disinfectant concentrations above and below the adapted MICs as shown in Table 16.

One ml aliquots were taken from each culture and pelleted via centrifugation at 5400 G for 10 minutes before re-suspension in PBS. This wash step was repeated a further 2 times before resuspension in 1 ml DEB. Samples were then incubated at room temperature for 10 minutes before undergoing a further 3 PBS wash steps. Samples were stained with 1ml PBS containing 2.5 μM CPD for 25 minutes at 37°C. Excess CPD was quenched via the addition of 9 ml of MHB pre-warmed to 37°C, before being incubated for 6 hours at 37°C in the dark. After incubation, a 1 ml aliquot of each sample was taken, washed in PBS 3 times and stained with 1ml PBS containing 10 μM 2-NBDG viability stain for 25 minutes at 37°C. The stain is quenched via a 1:500 dilution in PBS and the samples are analysed via flow cytometry using the gates established in the gating control experiments. The number of events captured in the upper right quadrant was used to quantify the number of VBNCs in each sample, which were plotted into bar charts using GraphPad Prism 9.4.1. One-way analysis of variance (ANOVA) tests were conducted to determine statistically significant differences in the number of VBNCs between conditions.

Table 16. The concentrations of the respective disinfectants that disinfectant-tolerant *Klebsiella pneumoniae* NCTC 13443 samples were exposed to before viable but nonculturable quantification through proliferation exclusion. Bz: benzalkonium chloride. Dd: didecyldimethylammonium chloride. Ph: polyhexamethylene biguanide. Br: bronopol. Cc: chlorocresol SQ: disinfectant formulation "SQ53". * highlights disinfectant concentrations that are equal to the respective minimum inhibitory concentration.

Tolerant sample and disinfectant treatment	Concentration 1 (µg/ml)	Concentration 2 (µg/ml)	Concentration 3 (µg/ml)	Concentration 4 (µg/ml)
Bz	0	25	55*	85
Dd	0	7	13*	19
Ph	0	4	8*	12
Br	0	20	40*	60
Cc	0	110	220*	330
SQ	0	120	240*	360

6.4. Results and discussion

6.4.1. Proliferation exclusion validation

The first set of experiments aimed to investigate if PE is a viable methodology of VBNC quantification. The first step was to conduct appropriate control experiments.

6.4.1.1. Control experiments

Before establishing if PE is able to quantify the number of VBNC cells within a population via flow cytometric analysis, appropriate gates must be set up to ensure that only individual *K. pneumoniae* cells are identified.

6.4.1.1.1. Establishing cell gates

The first gate must isolate *K. pneumoniae* cells from other debris within the sample. This is especially important as the experiment conditions to be investigated will cover a range of disinfectant concentrations that have previously been shown to cause total loss of bacterial cell integrity (Chapters 2.4.3, 2.4.4 and 2.4.5). Intact *K. pneumoniae* cells were identified by comparing dot plots of FSC H vs SSC H generated via flow cytometric analysis of 10-fold sequentially diluted samples of *K. pneumoniae* NCTC 13443. The results of this, and the resulting gate ("R4Cell"), can be seen in (Figure 35). As the samples become increasingly dilute, the likelihood of droplets containing >1 bacterial cell decreases, causing the distribution of data points to cluster together at a single location. The "R4Cell" gate was placed around this consistent population of single *K. pneumoniae* cells (Figure 35). The gate was placed to allow for a reduction in bacterial cell size as a result of stressful conditions, as established in the literature [137].

Additional events surrounding the observable cell population can be seen around the gate and within it. These events are diluted along with the *K. pneumoniae* cells (Figure 35). This indicates that these events are not a result of the medium and are likely to be cellular debris associated with *K. pneumoniae* culture. The "R4Cell" gate filters out the majority of these events, but some pass through. To investigate the nature of these events, a *K. pneumoniae* sample was filtered through a 0.22 μm filter and examined via flow cytometric analysis, as presented in Figure 36. The events can still be seen after filtration (Figure 36), indicating that they are a result of debris smaller than 0.22 μm, and are therefore not *K. pneumoniae* cells. As these events are not cells, they will not test positive for viability. Therefore, these events will not influence the detection of VBNC cells.

A second gate is required to filter out data collected from droplets containing multiple *K. pneumoniae* cells, called "multiplets". Multiplets will generate a single set of fluorescence intensity

values despite being detected from multiple cells, leading to inaccurate results. To ensure that only droplets containing a single cell ("singlets") are included in subsequent analysis, *K. pneumoniae* samples were measured via flow cytometric analysis and dot plots were generated comparing the SSC H and SSC A. The side scatter pulse height and area values of droplets containing single cells will be proportional, and droplets containing >1 bacterial cell will not be proportional, as shown in Figure 35. As the concentration of *K. pneumoniae* cells decreases, the likelihood of a droplet containing >1 cell also decreases, causing the observed proportional relationship of singlets to become more evident, allowing the placement of a singlet gate (Figure 35). Based on these data, the "R4Cell" and "R5SingletsLog" gates are applied to all subsequent flow cytometric analyses of *K. pneumoniae* samples.

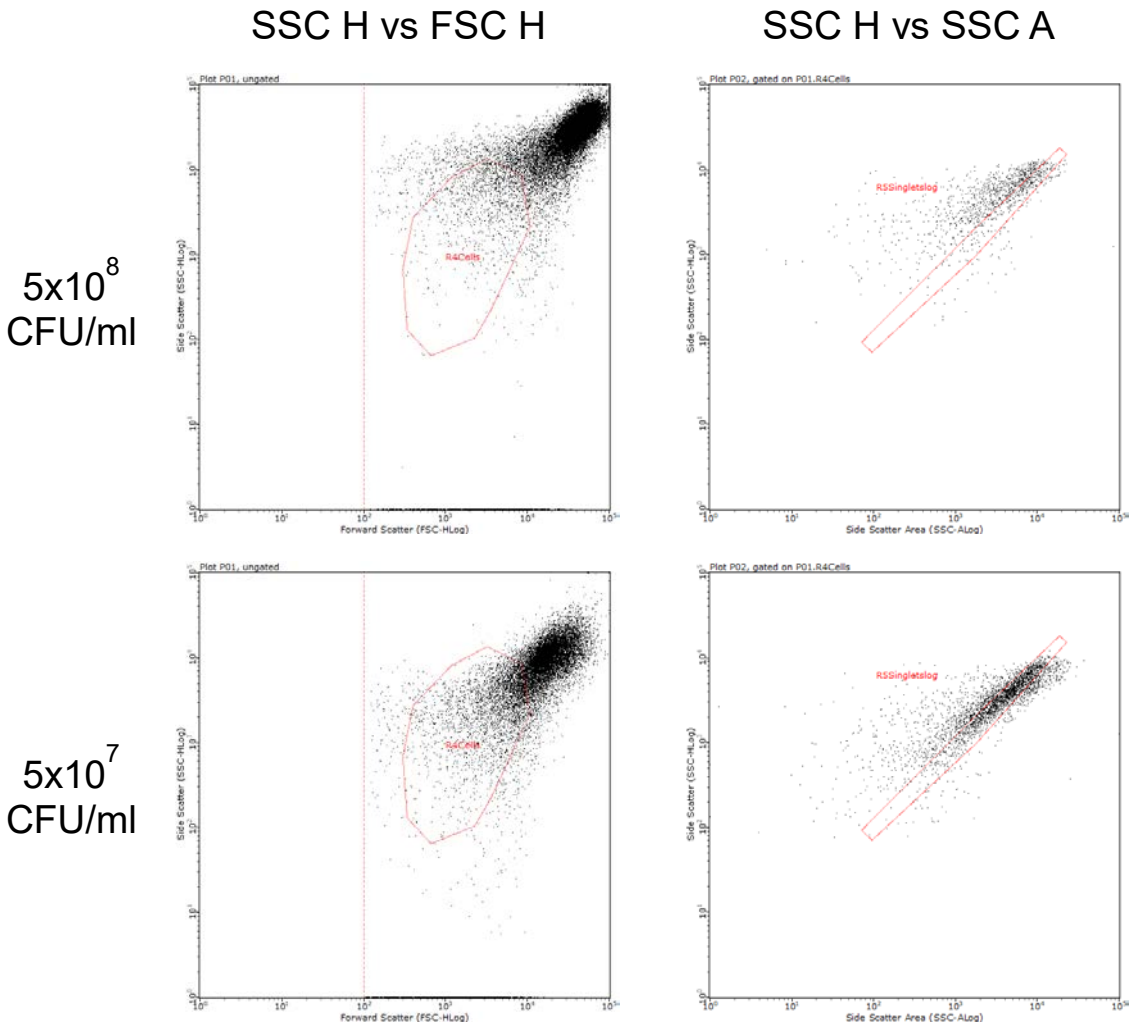

Figure 35. Flow cytometric analysis of *Klebsiella pneumoniae* NCTC 13443 cells at varying concentrations, as deduced via plate counts. Dot plots on the left side: Y axis, SSC H: Side scatter pulse height. X axis, FSC H: Forward scatter pulse height. Dot plots on the right side: Y axis, SSC H: Side scatter pulse height. X axis, SSC A: Side scatter pulse area. Red areas show gates. Left side: Gate "R4 Cells" isolates pulse readings corresponding to bacterial cells. Right side: Gate "R5 Singlets Log" isolates pulse readings corresponding to single cells. Figure continued on the next page.

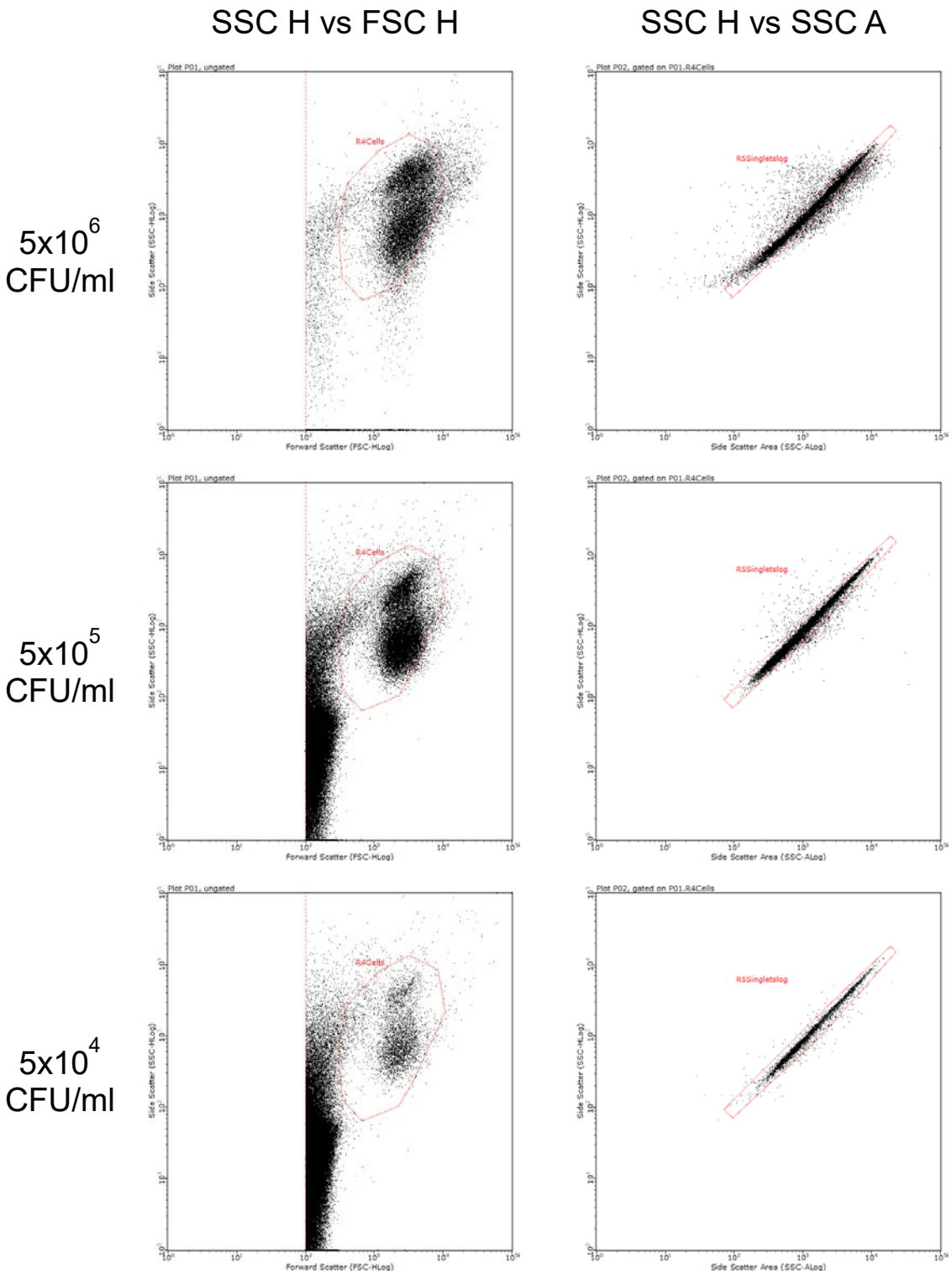

Figure 35 (continued).

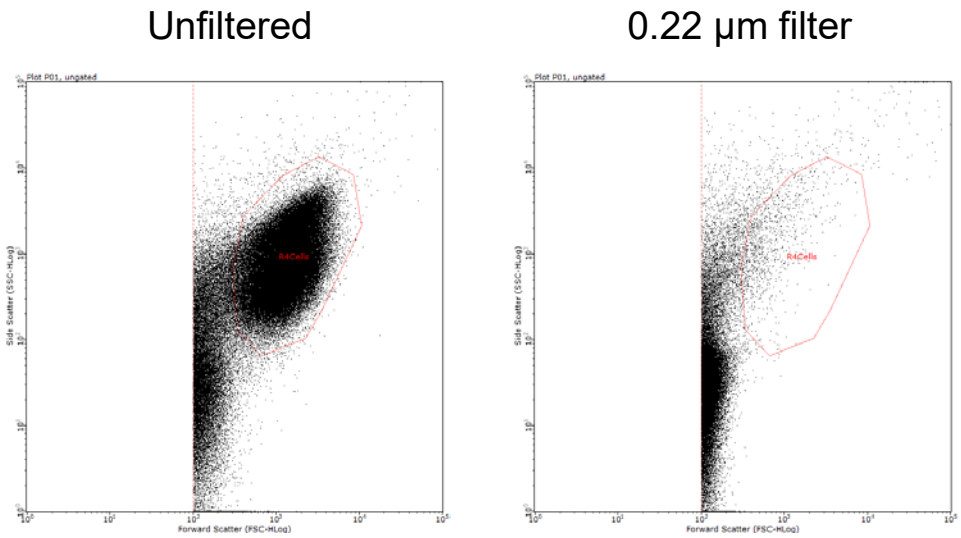

Figure 36. Flow cytometric analysis of *Klebsiella pneumoniae* NCTC 13443 samples containing 1 x 10^6 cells/ml that are untreated, or have been passed through a 0.22 µm filter, as described. Y axis, SSC H: Side scatter pulse height. X axis, FSC H: Forward scatter pulse height. Red gate "R4 Cells" isolates events corresponding to bacterial cells.

6.4.1.1.2. Proliferation exclusion stain controls and quadrant positioning

Once individual *K. pneumoniae* cells could be reliably identified, the fluorescent stains to be used required validation. The ability for *K. pneumoniae* cells to take up the stains was determined, alongside whether the stains can be used to distinguish between cell populations. For a comprehensive overview of the methodology used, please refer to Chapter 6.3.1.1.2.

In brief, *K. pneumoniae* NCTC 13443 cells were exposed to PBS or inactivated via exposure to 4% (w/v) formaldehyde and incubated at 4°C for 30 minutes. Both untreated and fixed cells were then stained with 2-NBDG or CPD before flow cytometric analysis.

2-NBDG is glucose covalently bound to a 7-nitrobenzofurazan fluorophore, and has been shown to be selectively taken up by viable *E. coli* cells [435], and is not toxic [436]. CPD binds to protein primary amines on the surface of bacterial cells [428], which are then distributed to daughter cells as division occurs. This causes a reduction in fluorescent intensity that is detectable via flow cytometry.

Colony counts were also conducted after fixation and staining to ensure the fixation protocol caused loss of culturability in cells, and to establish if the staining procedure resulted in a loss of *K. pneumoniae* culturability. The CFU counts of the various staining treatments for both strains can be seen in Table 17 and Table 18. Untreated and unstained *K. pneumoniae* NCTC 13443 cells remained culturable (Table 17, Table 18), while fixed cells were no longer culturable, as expected (data not shown).

Samples that underwent staining treatments demonstrated a statistically insignificant reduction in the number of culturable cells compared to the unstained controls for both *K. pneumoniae* strains (Table 17, Table 18). The statistically insignificant decrease in CFUs demonstrates that the use of these stains is likely to be less invasive and stress-inducing than other VBNC quantification methods.

The flow cytometric data of a representative *K. pneumoniae* NCTC 13443 biological replicate exposed to various treatments and staining procedures is shown via histograms in Figure 37 and via dot plots in Figure 38. The X axis of the histograms show green or red fluorescence intensity in parts a and b respectively (Figure 37). For the dot plots green and red fluorescence intensity are plotted on the X and Y axis, respectively (Figure 38). These measurements correspond to the fluorescence intensity of the two stains, with 2-NBDG (green) on the X axis and CPD (red) on the Y axis. The excitation lasers and filters used, alongside the excitation/emission peaks of the stains is summarised in Table 15. The experiment was conducted in triplicate.

Unstained cells showed no autofluorescence in either channel, with the exception of a small number of readings detected with higher green fluorescence values in the fixed, unstained sample (Figure 37a, Figure 38). This is a result of user error, as the flow cytometer was erroneously set to begin measurements within the first 10 seconds of the flow rate being established. This can result in cells from the previous sample contaminating the next one. Chronologically, the unstained fixed sample was measured directly after the untreated 2-NBDG-stained sample, accounting for the high green fluorescence values in the unstained sample. This error was noticed immediately and corrected for all subsequent samples and experiments.

Untreated, viable *K. pneumoniae* samples showed an increased green fluorescence intensity when stained with 2-NBDG (Figure 37a, Figure 38). In contrast, fixed samples showed a lower green fluorescence intensity, such that the two populations were discrete (Figure 38). This validates that 2-NBDG is selectively taken up by viable *K. pneumoniae*, in accordance with previous reports regarding selective uptake in viable *E. coli* [435]. The variation in fluorescence intensity allowed for the vertical line of the quadrant gate to distinguish between the two populations at 2×10^1 RLU, as shown in Figure 38. As a result, *K. pneumoniae* cells detected with a green fluorescence intensity greater than 2×10^1 RLU are considered viable, and those with a fluorescence intensity below this cut off are considered not viable. A small number of cells were detected as not viable in untreated *K. pneumoniae* samples, which result from the small minority of dead cells that naturally occur within bacterial populations (Figure 38).

Both untreated and fixed *K. pneumoniae* cells stained with CPD showed an increased red fluorescence intensity in comparison to the respective unstained samples (Figure 37b, Figure 38). This validates that *K. pneumoniae* cells are stained by CPD. This variation in red fluorescence integrity between stained and unstained cells allows for the populations to be distinguished. The horizontal line of the quadrant is therefore placed at 2×10^1 RLU, distinguishing between *K. pneumoniae* cells that have taken up CPD, and those that have not (Figure 38).

Interestingly, the level of increase in red fluorescence intensity consistently varied between fixed and untreated cells, with viable cells showing a reduced uptake in comparison to fixed cells (Figure 37b, Figure 38). Hoefel *et al.* (2003) noted that fixed *E. coli* stained with CFDA/SE demonstrated a higher fluorescence intensity than viable cells, which was attributed to variable dye uptake between the populations [437]. The variation in staining observed is therefore likely to be a result of differential stain uptake resulting from characteristics such as variations in membrane integrity.

Unfortunately, due to viable cells taking up a lower concentration of CPD, the unstained cell populations and CPD-stained viable cell population are not completely discrete (Figure 38). As a result, a small number of CPD-stained viable *K. pneumoniae* cells fall below the 2×10^1 RLU threshold, and thus will be classified as "proliferated" (Figure 38). This may result in false-negative results, with individual viable cells not taking up enough CPD to ever be classed as stained, so thus will always count as having proliferated, even if they have not. However, this is preferable to moving the threshold lower, potentially causing false-positive results. To potentially address this issue in future, further optimisation of the CPD *K. pneumoniae* staining procedure will be required.

Once the ability for *K. pneumoniae* NCTC 13443 to take up each of the stains had been validated, the same controls were conducted for *K. pneumoniae* NCTC 9633 (Figure 39, Figure 40) to establish any variability between strains. In addition, to validate that CPD drops as a result of cells proliferating, CPD-stained *K. pneumoniae* NCTC 9633 cells underwent flow cytometric analysis at 2 separate time points, once at time 0 (immediately after staining), and once after a 24-hour incubation in MHB at 37°C (Figure 39, Figure 40).

The flow cytometric analysis results did not significantly vary between *K. pneumoniae* strains (Figure 38, Figure 40), so for the purposes of the following experiments all procedures and gating was assumed to be interchangeable between the two strains. After a 24-hour incubation in MHB at 37°C, the red fluorescence intensity values of viable *K. pneumoniae* cells can be seen to have dropped down from a maximum fluorescence intensity of 1×10^2 RLU directly after

staining to 4 x 10^1 RLU after 24-hours (Figure 39b, Figure 40). This is higher than the previous horizontal gate set at 2 x 10^1 RLU, due to the cells containing more CPD than unstained cells, even after 24-hours. As a result, the horizontal gate is hereby moved to 4 x 10^1 RLU to differentiate between CPD-stained *K. pneumoniae* cells that have proliferated and those that have not. The vast majority of fixed *K. pneumoniae* cells stained with CPD do not demonstrate a decrease in red fluorescence intensity after a 24-hour incubation period (Figure 39b, Figure 40), indicating that CPD is able to distinguish between *K. pneumoniae* cells that have proliferated and those that have not.

A minority of events in the fixed *K. pneumoniae* sample display a low red fluorescence intensity after the 24-hour incubation period. The samples displayed no visible increase in turbidity, indicating that the fixed cells within the culture have not undergone proliferation. The emergence of a low-CPD-stained population without an increase in turbidity may be a result of CPD photo bleaching, loss of stain or cellular debris that is being detected within the cell gates.

Photo bleaching of the fluorophore would result in an overall decrease in fluorescence intensity across the entire sample, which was not seen. Similarly, loss of stain through enzymatic activity would also result in a more consistent sample-wide reduction in fluorescence intensity. Therefore, the observed events are likely to be a result of cellular debris that has formed over the 24-hour incubation period, which are being detected within the gates as seen in the filter control in Figure 36, and described in Chapter 6.3.1.1.1.

As a result of these controls, the quadrants presented were demonstrated to be able to differentiate between various cell populations. Viable *K. pneumoniae* cells that have undergone proliferation are located in the lower right quadrant. Non-viable cells that have not undergone proliferation (dead cells) are located in the upper left quadrant. Viable cells that have not proliferated (or in a literal sense, "viable but nonculturable cells"), are located in the upper right quadrant. The remaining lower left quadrant shows cellular debris and aggregates, or cells that have proliferated during the experiment but have since died. A hypothetical example of these quadrants and the resulting bacterial cell populations are shown in Figure 34.

Table 17. The number of *Klebsiella pneumoniae* NCTC 9633 culturable cells in samples after various staining procedures. CFU/ml: colony forming units per millilitre. P value: generated via unpaired t test comparing CFU/ml values of staining condition to CFU/ml values of unstained control. Both p values were greater than 0.05, so the variation is deemed not significant.

Staining condition	*Klebsiella pneumoniae* NCTC 9633 culturable cells (CFU/ml)			Mean average (CFU/ml)	Standard deviation	P value
	1	2	3			
Unstained	2.25E+06	3.30E+06	4.15E+06	3.23E+06	9.52E+05	-
CPD	3.05E+06	4.20E+06	1.10E+06	2.78E+06	1.57E+06	0.6926
2-NBDG	1.20E+06	2.25E+06	3.35E+06	2.27E+06	1.08E+06	0.3084

Table 18. The number of *Klebsiella pneumoniae* NCTC 13443 culturable cells in samples after various staining procedures. CFU/ml: colony forming units per millilitre. P value: generated via unpaired t test comparing CFU/ml values of staining condition to CFU/ml values of unstained control. Both p values were greater than 0.05, so the variation is deemed not significant

Staining condition	*Klebsiella pneumoniae* NCTC 13443 culturable cells (CFU/ml)			Mean average (CFU/ml)	Standard deviation	P value
	1	2	3			
Unstained	1.05E+09	9.00E+08	6.00E+08	8.50E+08	2.29E+08	-
CPD	6.00E+08	6.00E+08	8.00E+08	6.67E+08	1.15E+08	0.2835
2-NBDG	8.00E+08	1.05E+09	6.00E+08	8.17E+08	2.25E+08	0.8662

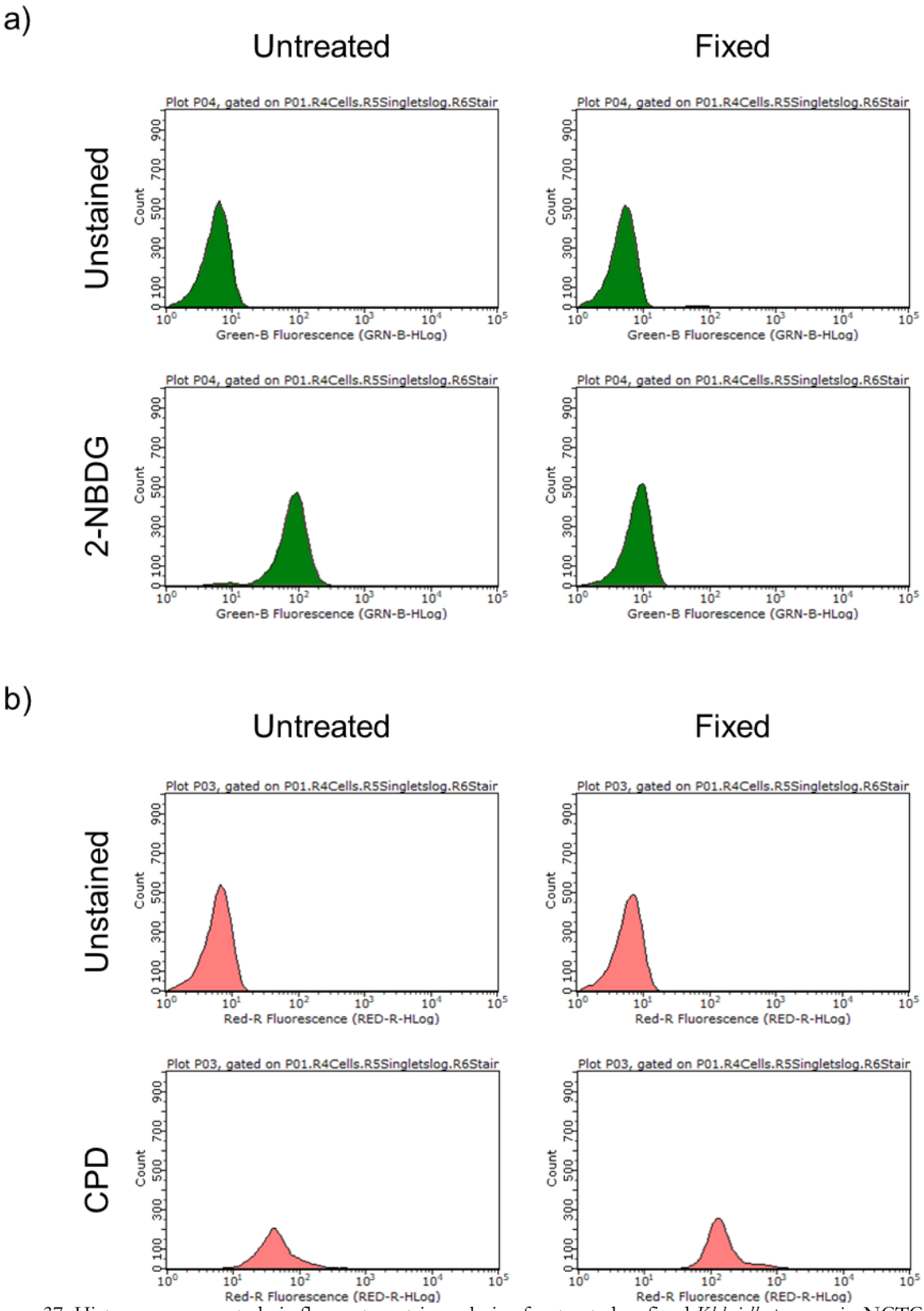

Figure 37. Histograms generated via flow cytometric analysis of untreated or fixed *Klebsiella pneumoniae* NCTC 13443 cells that have been stained with 2-Deoxy-2-[(7-nitro-2,1,3-benzoxadiazol-4-yl)amino]-D-glucose (2-NBDG), Cell Proliferation Dye eFluor 670 (CPD), or no stain. a) Histograms showing 2-NBDG fluorescence intensity on the X axis, and the number of measured events on the Y axis. b) Histograms showing CPD fluorescence intensity on the X axis, and the number of measured events on the Y axis. Fixed: Cells treated with 4% (w/v) formaldehyde for 30 minutes. Untreated: Cells exposed to phosphate-buffered saline for 30 minutes. Unstained: Cells did not undergo a staining procedure. 2-NBDG: Cells stained with 2-NBDG viability stain. CPD: Cells stained with CPD.

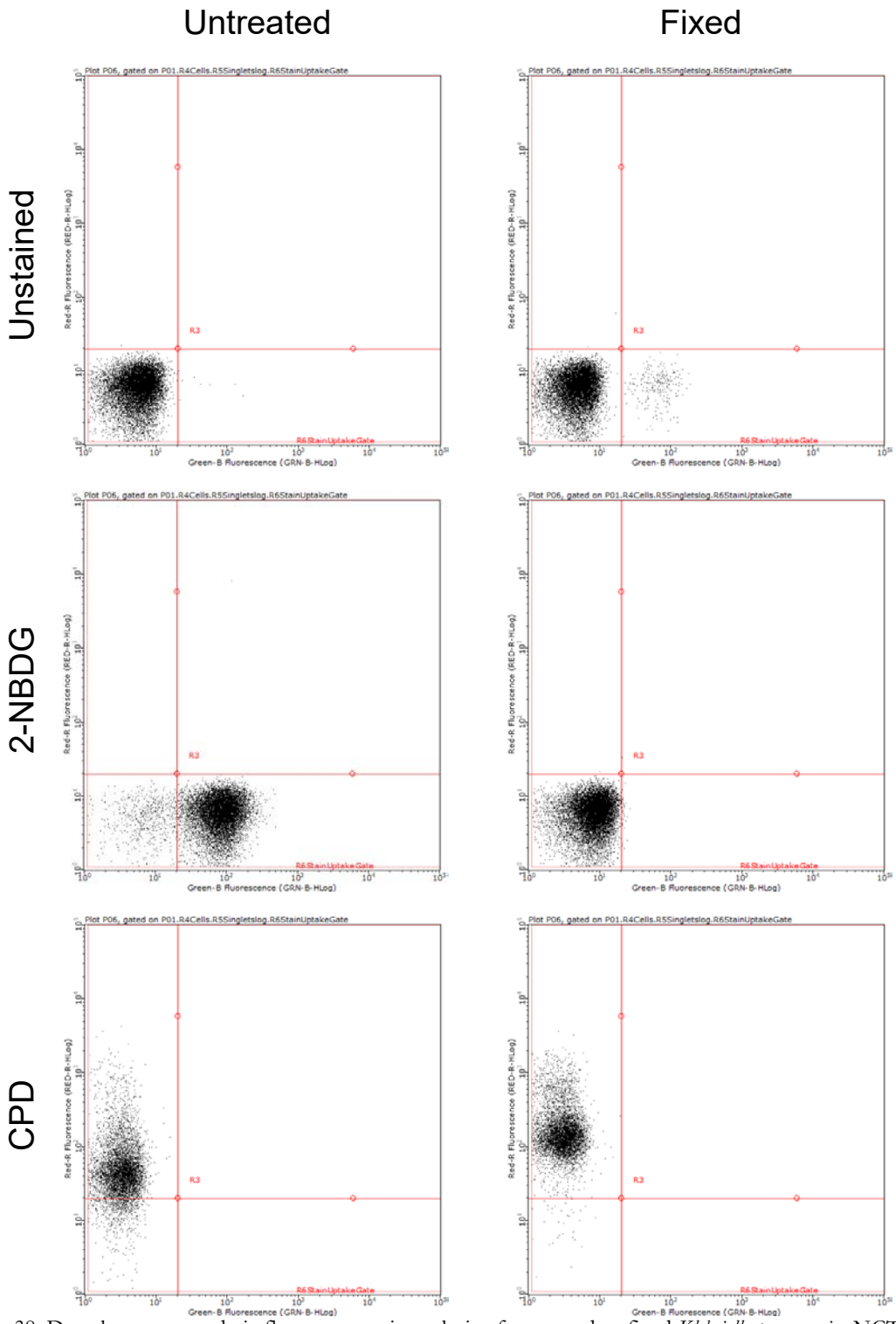

Figure 38. Dot plots generated via flow cytometric analysis of untreated or fixed *Klebsiella pneumoniae* NCTC 13443 cells that have been stained with 2-Deoxy-2-[(7-nitro-2,1,3-benzoxadiazol-4-yl)amino]-D-glucose (2-NBDG), Cell Proliferation Dye eFluor 670 (CPD), or no stain. All dot plots depict 2-NBDG fluorescence intensity on the X axis, and CPD fluorescence intensity on the Y axes. Fixed: Cells treated with 4% (w/v) formaldehyde for 30 minutes. Untreated: Cells exposed to phosphate-buffered saline for 30 minutes. Unstained: Cells did not undergo a staining procedure. 2-NBDG: Cells stained with 2-NBDG viability stain. CPD: Cells stained with CPD. Red gates show differentiation between cell populations as differentiated by the stains.

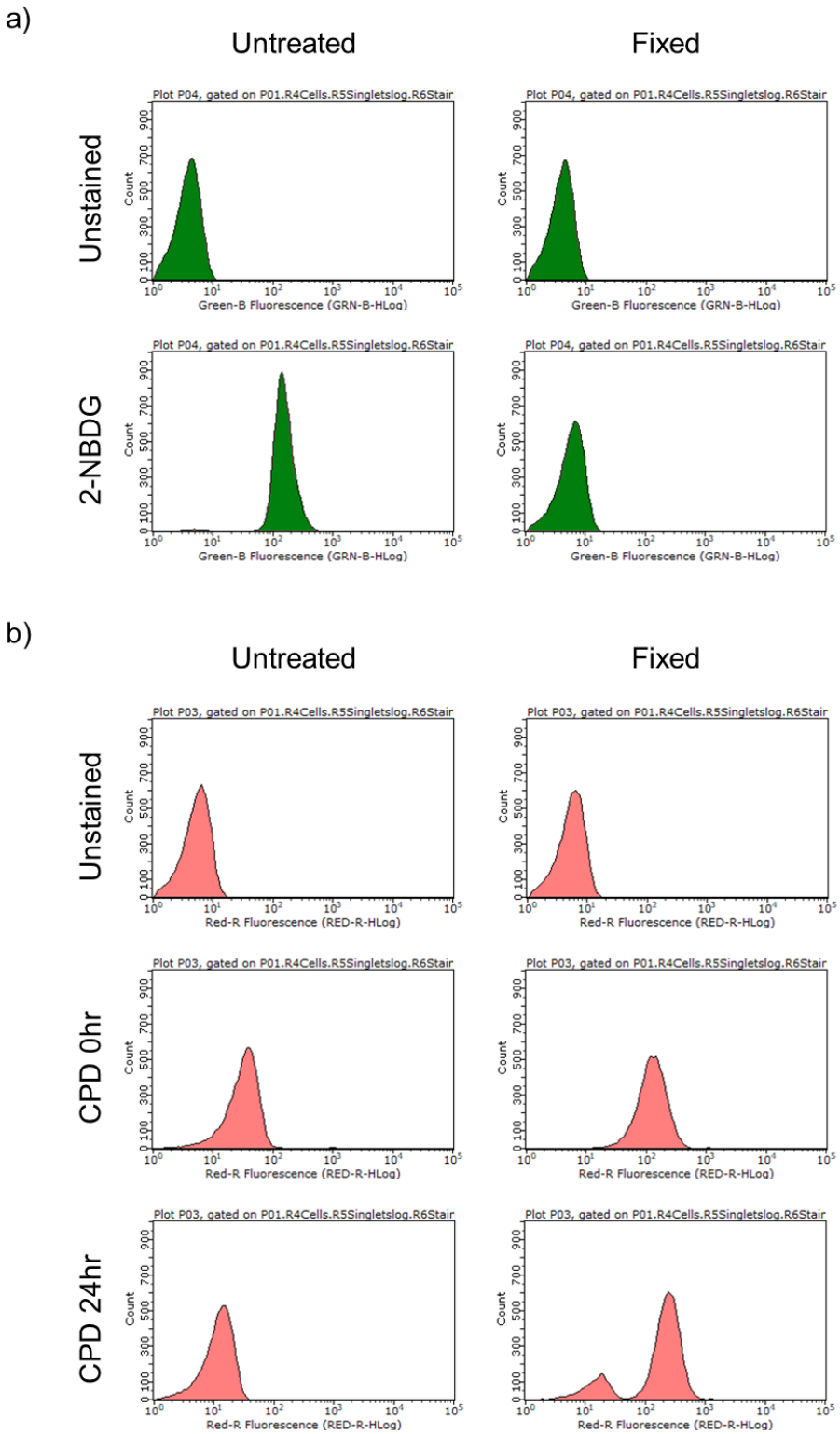

Figure 39. Histograms generated via flow cytometric analysis of untreated of fixed *Klebsiella pneumoniae* NCTC 9633 cells that have been stained with 2-Deoxy-2-[(7-nitro-2,1,3-benzoxadiazol-4-yl)amino]-D-glucose (2-NBDG), Cell Proliferation Dye eFluor 670 (CPD), or no stain. a) Histograms showing 2-NBDG fluorescence intensity on the X axis, and the number of measured events on the Y axis. b) Histograms showing CPD fluorescence intensity on the X axis, and the number of measured events on the Y axis. Fixed: Cells treated with 4% (w/v) formaldehyde for 30 minutes. Untreated: Cells exposed to phosphate-buffered saline for 30 minutes. Unstained: Cells did not undergo a staining procedure. 2-NBDG: Cells stained with 2-NBDG. CPD: Cells stained with CPD. Times indicate post-staining incubation time in hours, in Mueller Hinton broth at 37°C, before flow cytometric analysis.

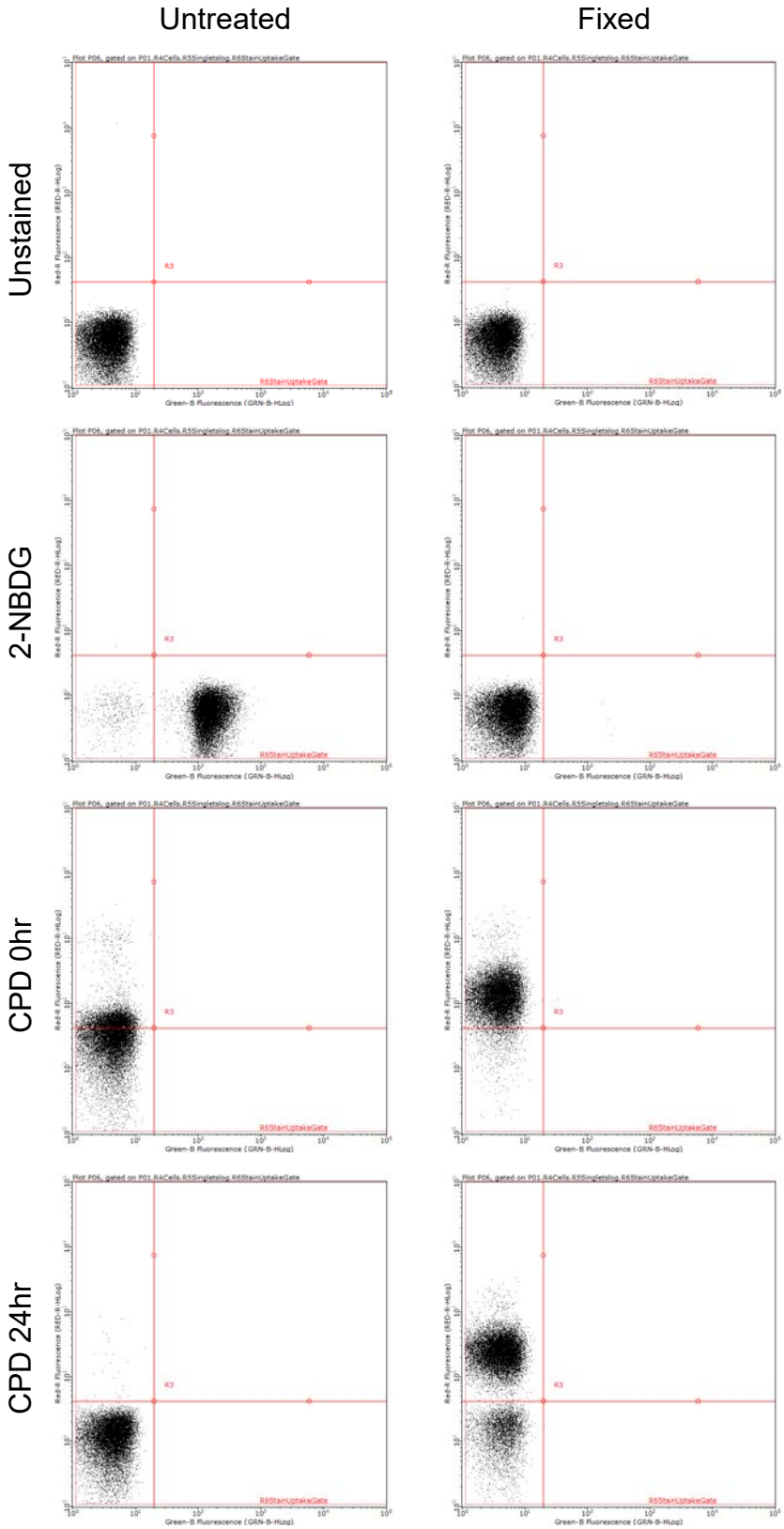

Figure 40. Dot plots generated via flow cytometric analysis of untreated of fixed *Klebsiella pneumoniae* NCTC 9633 cells that have been stained with 2-Deoxy-2-[(7-nitro-2,1,3-benzoxadiazol-4-yl)amino]-D-glucose (2-NBDG), Cell Proliferation Dye eFluor 670 (CPD), or no stain. All dot plots depict 2-NBDG fluorescence intensity on the X axis, and CPD fluorescence intensity on the Y axes. Fixed: Cells treated with 4% (w/v) formaldehyde for 30 minutes. Untreated: Cells exposed to phosphate-buffered saline for 30 minutes. Unstained: Cells did not undergo a staining procedure. 2-NBDG: Cells stained with 2-NBDG. CPD: Cells stained with CPD. Times indicate post-staining incubation time in hours, in Mueller Hinton broth at 37°C, before flow cytometric analysis. Red gates show differentiation between cell populations as differentiated by the stains.

6.4.1.1.3. LIVE/DEAD™ BacLight™ stain controls

To establish if PE is an accurate and reliable methodology of VBNC detection it must be compared to existing methods. One of the methods employed utilises the SYTO 9 and PI stains to differentiate between viable and non-viable cells. To establish regions for these stains, *K. pneumoniae* NCTC 9633 cells were once again left untreated or fixed with 4% (w/v) formaldehyde, before being stained with SYTO 9, PI, both or neither, as described in Chapter 6.3.1.1.3, before analysis via flow cytometric analysis.

The resulting dot plots can be seen in Figure 41, with green fluorescence intensity plotted on the X axis, and red fluorescence intensity on the Y axis, corresponding to SYTO 9 and PI staining respectively. The excitation lasers and filters used, alongside the excitation/emission peaks of the stains is summarised in Table 15. Unstained *K. pneumoniae* cells were located in the lower left quadrant and showed no auto-fluorescence, irrespective of viability (Figure 41). Viable cells exposed to PI demonstrated an increase in red fluorescence intensity peaking at $1x10^2$ RLUs (Figure 41), likely as a result of unwashed residual stain. The populations of unstained cells and PI-stained viable cells formed the boundaries for the "R6LiveCells" and "R7DeadCells" gates (Figure 41). Fixed cells exposed to PI demonstrated a high red fluorescence intensity, peaking at $1\text{-}2x10^3$ RLUs (Figure 41). This population is discrete from the PI-stained viable cell population, allowing a gate to be set to distinguish between the two populations at $1x10^2$ RLUs (Figure 41). A large number of non-viable cells did not display a red fluorescence above $1x10^2$ RLUs as a result of a lack of PI staining (Figure 41). This is likely a result of PI not being membrane permeable, so these cells likely represent non-viable *K. pneumoniae* that have maintained membrane integrity, so are erroneously detected as viable [178].

SYTO 9 is membrane-permeable to stains all cells, irrespective of whether they are viable or not. As a result, both viable and fixed cells show an increase in green fluorescence intensity (Figure 41). The teardrop shape of these populations is likely a result of SYTO 9 fluorescence being detected in the red channel, known as spectral overlap [438], [439]. The resulting population demonstrates a proportional increase in fluorescence intensity along both axes, as SYTO 9 emissions are being detected in both green and red filters. However, as the stains are only required to distinguish between viable and non-viable *K. pneumoniae* subpopulations and these populations do not overlap, compensation is not required. Instead, the spectral overlap is accounted for in the shape of the gates, with a diagonal line differentiating between the "R6LiveCells" and "R7DeadCells" gates (Figure 41).

When both stains are combined, viable cell populations fall within the "R6LiveCells" gate, and the majority of fixed cells fall within the "R7DeadCells" gate (Figure 41). However, due to non-viable cells that maintain their membrane integrity, a number of cells exclude PI and demonstrate a lower red fluorescence intensity, as seen in the PI-stained fixed cell dot plot (Figure 41). These cells are detected as within the "R6LiveCells" gate. This is a known issue with the use of SYTO 9 and PI as an indicator of bacterial cell viability [178], [440], and will likely result in an over-estimation in the number of viable cells, and thus an over-estimation in the number of VBNC cells detected via the live/dead methodology in later experiments.

The gates and quadrants established through these control experiments are used across all experiments going forward.

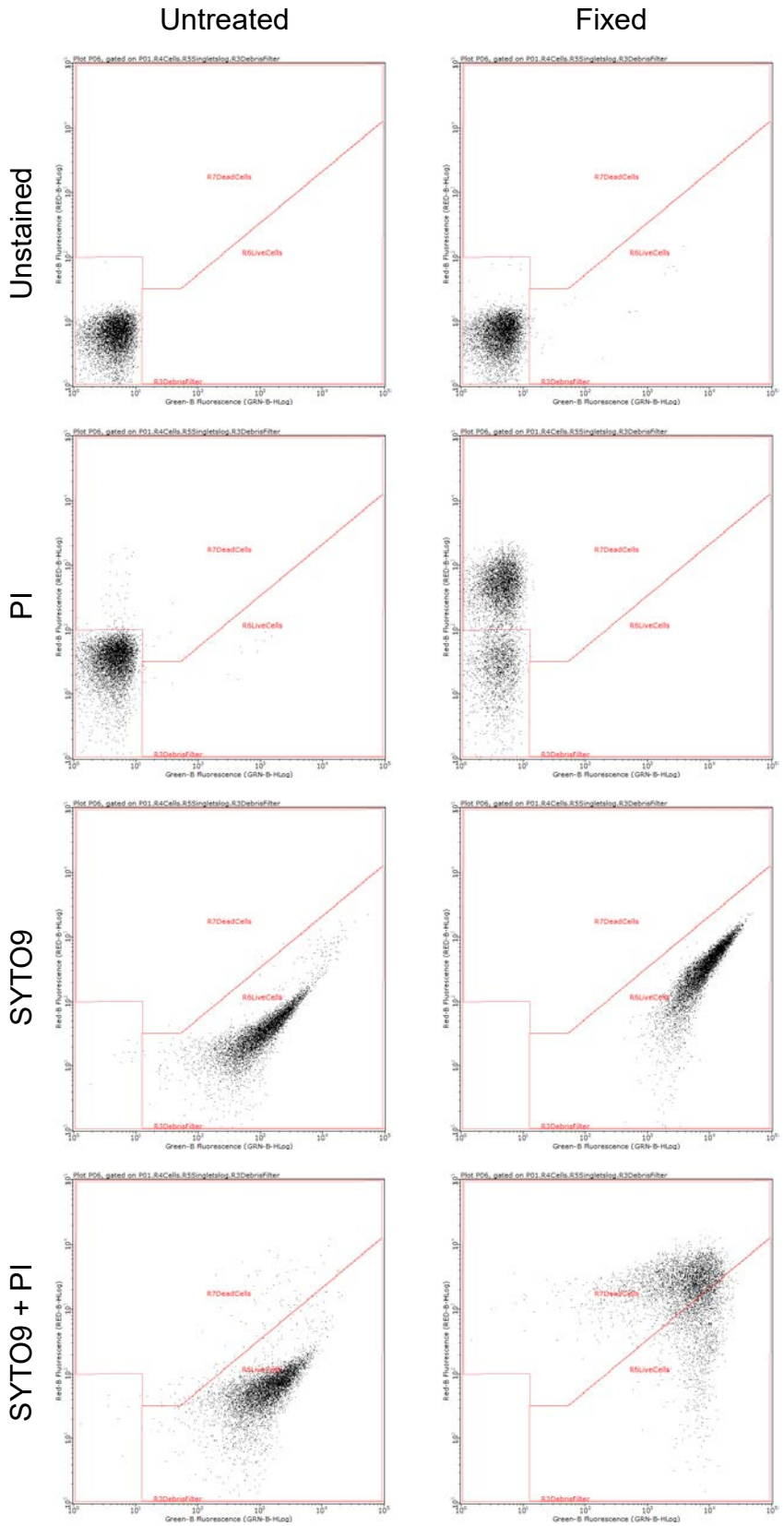

Figure 41. Dot plots generated via flow cytometric analysis of untreated or fixed *Klebsiella pneumoniae* NCTC 9633 cells that are unstained or stained with either SYTO 9, propidium iodide (PI) or both. All dot plots depict SYTO 9 fluorescence intensity on the X axis and PI fluorescence intensity on the Y axes. Fixed: Cells treated with 4% (w/v) formaldehyde for 30 minutes. Untreated: Cells exposed to phosphate-buffered saline for 30 minutes. Unstained: Cells did not undergo a staining procedure. SYTO 9: Cells stained with SYTO 9 stain. PI: Cells stained with PI stain. SYTO 9 + PI: Cells stained with both SYTO 9 and PI.

6.4.1.2. Proliferation exclusion validation

Once *K. pneumoniae* stain uptake controls and flow cytometry gates had been established, the PE methodology of VBNC enumeration could be tested and compared to existing VBNC quantification methods. Specifically, the DVC and live/dead VBNC quantification methods were used, as outlined previously (Chapter 1.4.2.2.2.3).

The PE methodology used is comprehensively overviewed in Chapter 6.3.1.2, but will also be briefly overviewed here. Prior to the experiment, the MIC values of BAC, DDAC and PHMB against *K. pneumoniae* NCTC 9633 were determined via microbroth dilution. The MICs were found to be 12 μg/ml, 8 μg/ml, and 6 μg/ml for BAC, DDAC and PHMB respectively.

Based on these data, *K. pneumoniae* NCTC 9633 samples were exposed to varying concentrations of either BAC, DDAC or PHMB at concentrations ranging above and below the respective MICs for 24 hours. All samples were exposed to the respective disinfectant treatment for 24-hours at 37 °C in MHB, upon which 1 ml aliquots of each sample were neutralised using DEB before being washed 3 times with PBS. Before the final wash step the 1 ml aliquots were split into 4 for subsequent CFU enumeration, DVC, live/dead and PE treatments, respectively.

Samples taken for CFU enumeration were serially diluted in PBS and plated out onto MHA before being incubated at 37 °C for 24-hours. The number of CFUs were quantified manually to estimate the total number of culturable bacteria in each sample.

The aliquots taken for DVC were made up to 1 ml PBS, before being added to 4 ml dH_2O, 5 ml R2 broth and 10 μg/ml pipemidic acid. Samples were then incubated for 24-hours at room temperature in darkness before staining with 5 μM SYTO 9 for 10 minutes in the dark. The samples were then vacuum filtered on to 0.22 μm filters, before the number of viable cells were enumerated via manual counting on a fluorescence microscope. Cells that had visibly elongated by at least 2 x their normal length were counted on 30 FOVs. The counts were then used to estimate the total number of viable cells in each of the samples using the formula described in Chapter 6.3.1.2. The respective CFU count estimates were then taken away from the total viable cells, leaving an estimate of the number of VBNCs via the DVC methodology as displayed in Figure 43. The raw data can be found in Chapter 8. Appendix, Table 28, Table 29 and Table 30.

Aliquots taken for live/dead analysis were stained with 5 μM SYTO 9 and 30 μM PI for 10 minutes at room temperature in the dark. The stain was then neutralised via 1:500 dilution in PBS and the samples were analysed via flow cytometric analysis using the gates established in the previous control experiments (Figure 41). The number of events captured in the "R6LiveCells"

gate were quantified and used to estimate the total number of viable cells in each sample. The respective CFU count estimates were then taken away from the total viable cells, leaving an estimate of the number of VBNCs via the live/dead methodology as displayed in Figure 43. The data can also be found in Chapter 8. Appendix, Table 28, Table 29 and Table 30.

The aliquots taken for PE treatment were stained with 2.5 μM CPD for 25 minutes at 37 °C. A 2 μl aliquot was quenched via dilution in 998 μl PBS, before being analysed via flow cytometric analysis to validate CPD uptake (0-hour time point). Excess CPD in the remaining sample was quenched via the addition of 9 ml of MHB pre-warmed to 37 °C, before a 24-hour incubation at 37 °C. At the 6-hour and 24-hour incubation time points, 1 ml aliquots of each sample were taken, washed in PBS 3 times and stained with 10 μM 2-NBDG viability stain for 25 minutes at 37 °C. The stain was quenched via a 1:500 dilution in PBS and the samples were analysed via flow cytometry using the gates established in the control experiments previously. The number of events captured in the upper right quadrant after 6 and 24-hours were used to quantify the number of VBNCs in each sample, as displayed in Figure 43. A dot plot showing representative data can be seen in Figure 42. The data can also be found in Chapter 8. Appendix, Table 28, Table 29 and Table 30.

Figure 42 shows representative dot plots of PE flow cytometric data. At the 0-hour time point, all *K. pneumoniae* samples can be seen to have taken up CPD. The samples exposed to higher concentrations of disinfectant demonstrating a higher red fluorescence intensity (Figure 42), indicating that *K. pneumoniae* cells in these samples have taken up higher quantities of CPD. This is in accordance with observations made during the control experiments, whereby fixed samples demonstrated a high fluorescence intensity than untreated samples (Figure 38). In accordance with previous observations [437], this is likely due to the cell populations demonstrating variations in characteristics such as membrane integrity as a result of disinfectant exposure. However, as the majority of cells are above the 4×10^1 RLU threshold, the experiment was continued (Figure 42). The low green fluorescence intensity across all 0-hour time point measurements is due to lack of 2-NBDG staining (Figure 42).

After a 6-hour incubation at 37°C, the main *K. pneumoniae* cell population in samples exposed to 0, 4 and 8 μg/ml BAC all demonstrated a reduction in red fluorescence intensity (Figure 42). This is a result of the *K. pneumoniae* cells having proliferated during this time. The majority of the events detected fall in the lower right quadrant, indicating that the cells are viable and have proliferated, so are alive. This reflects the 12 μg/ml BAC MIC. The concentration of BAC in

these samples was insufficient to impede growth, so the *K. pneumoniae* cells in these samples were able to proliferate.

A small number of events can be seen that have both a low red and green fluorescence after a 6-hour incubation period at BAC concentrations below 12 μg/ml (Figure 42). These likely represent the small number of events containing cellular debris that makes it through the initial filters, as described previously. The events in the upper left quadrant represent cells that have not proliferated over the 6-hour incubation and are not viable, so are dead (Figure 42). Interestingly, there are a larger number of events in the upper left quadrant of 4 μg/ml BAC than 8 μg/ml BAC (Figure 42), a trend that was consistent across all biological replicates. This is due to fewer dead *K. pneumoniae* cells remaining intact after exposure to the higher disinfectant concentration, causing fewer events in this quadrant. Finally, there are a greater number of events in the upper right quadrant of samples exposed to 4 μg/ml BAC than 0 μg/ml BAC (Figure 42), indicating that the stress induced via low-level disinfectant exposure leads to the induction of the VBNC state in *K. pneumoniae* NCTC 9633 cells. Interestingly, the number of events in the upper right quadrant then steadily decreases as the concentration continues above 4 μg/ml BAC (Figure 42

). This indicates that higher disinfectant concentrations do not induce the VBNC state, or more likely that VBNC cells still succumb to the antimicrobial action of the disinfectants at higher concentrations, reducing the total number of VBNC cells.

The green fluorescence intensity of samples after a 24-hour incubation period was reduced in comparison to samples incubated for 6-hours (Figure 42). This indicates that these samples take up a lower quantity of 2-NBDG. This is a result of samples being in different growth phases at these time points, so will take up differing quantities of glucose analogue 2-NBDG. Culturable *K. pneumoniae* cells that have been incubated for 6-hours will be within the log phase and will have high energy requirements, so will take up a high amount of 2-NBDG and display a higher fluorescence intensity. In contrast, cells that have been cultured for 24-hours will be within the stationary phase, so will not take up a lower quantity of 2-NBDG and will therefore show a lower green fluorescence intensity. In addition, a greater number of cells will have died as a result of nutrient starvation as the culture enters the death phase, explaining the greater number of events detected that fall within the lower left quadrant (Figure 42).

Furthermore, the longer incubation time allows for a greater number of VBNC cells to potentially resuscitate and proliferate, leading to the reduction of red fluorescence intensity below 4×10^1 RLU. This would cause these cells to no longer be identified as VBNCs, potentially leading to an under-estimation of the original number of VBNCs present in the

original culture. For this reason, alongside the lower uptake of 2-NBDG after 24-hours, all future experiments were conducted using a 6-hour time incubation time only.

K. pneumoniae cultures exposed to BAC concentrations of 12 μg/ml and above did not display an increased turbidity after a 6-hour incubation (Figure 42). When examined by flow cytometric analysis, the samples displayed a lower number of events than the same sample at time point 0 (Figure 42). This is a result of the samples being diluted in 1:10 in 9 ml MHB between the time 0 measurement and the beginning of the incubation, and then the cells not proliferating during the 6-hour incubation. This leaves the same number dead cells at a higher dilution, which then appears as fewer events when the sample is analysed via flow cytometric analysis.

Events were detected within the lower left quadrant in *K. pneumoniae* samples of 12 μg/ml BAC and above after a 6-hour incubation, despite the same samples overwhelmingly displaying a fluorescence intensity greater than 4×10^1 RLU at time point 0 (Figure 42). This is unlikely to be due to processes such as enzymatic degradation or photo bleaching, as any resulting reduction in fluorescence intensity would be expected to be uniform across all events in the samples. This population is likely to have arisen as a result of stained, dead cells losing structural integrity throughout the 6-hour incubation period, leading to the presence of cellular debris that display a lower fluorescence intensity so appear in the lower left quadrant. A similar observation was made during the control experiments (Figure 40), whereby events were detected within the bottom left quadrant of a sample consisting of fixed *K. pneumoniae* cells stained with CPD analysed after a 24-hour incubation. Therefore, the presence of these events has no influence on the detection of VBNCs within the upper right quadrant and are henceforth not considered further.

Interestingly, all samples exposed to 12 μg/ml BAC or above displayed a large population in the lower right quadrant once incubated for 24-hours, consistent with live cells present in the lower concentrations of BAC (Figure 42). This population is unlikely to be a result of spontaneous resistance developing as the population is consistently observed across all biological replicates (Figure 42). This population would be consistent with contamination introduced at the 6-hour time point; however, this again is unlikely due to it being ubiquitously present across all samples and biological replicates. The presence of this population remains unexplained.

Figure 43 displays the number of VBNCs detected within *K. pneumoniae* samples after 24-hour exposure to vary concentrations of common disinfectants, as detected via the live/dead, DVC and PE methodologies. Across all experiments the live/dead and DVC methodologies were unable to enumerate the number of VBNCs within untreated samples, or samples exposed to low concentrations of disinfectant (Figure 43). This is a result of these methods indirectly

inferring the number of VBNCs within a population by estimating the total number of bacteria and the number of proliferating bacteria within a population. The number of VBNCs is assumed to be the difference between these two values, with the number proliferating bacteria taken away from the total number of bacteria. Conditions without bars (Figure 43) are a result of these methodologies estimating the number of proliferating bacteria to be higher than the total number of viable bacteria, which is not possible. This results in a negative difference between the two, resulting in a negative number of VBNCs, thus no bars are shown.

These impossible results are due to the total number of cells and CFU counts being merely estimations, both relying on methodologies that utilise large dilution factors, causing minor discrepancies during the enumeration stages to be magnified into large differences in the final values. This can result in large errors, even when experiments are performed in triplicate and repeated on multiple experiment conditions as illustrated here (Figure 43). This demonstrates a fundamental limitation with the use of DVC and live/dead methodologies, alongside other indirect methods of VBNC quantification.

At best, if it is assumed that these estimations are somewhat accurate, then these data imply that the number of VBNCs detected via these methodologies is 0 in these conditions.

In contrast, PE does not rely upon indirectly quantifying VBNCs via estimating the difference between cell populations, and instead directly quantifies the number of cells that are alive and have not proliferated within a culture. As a result, fewer assumptions have to be made when elucidating the number VBNCs by PE, allowing for a more accurate result.

The lack of VBNCs detected at low concentrations of disinfectant when measured via live/dead and DVC implies that *K. pneumoniae* VBNC induction does not occur until cells are exposed to a critical concentration of disinfectant, whereby large VBNC populations form (Figure 43). This supports the long-established view that VBNCs form in response to stress [135], [426], [441]. However, these data are undermined by recent research that suggests that VBNCs also occur stochastically within cultures, providing a pre-emptive level of protection from future stressors [164], [174], [442].

Furthermore, there is disparity between the concentrations of DDAC and PHMB required to spontaneously induce VBNC formation when examined by the live/dead and DVC methodologies. DVC infers the presence of ~$3x10^8$ and ~$1x10^8$ VBNC cells/ml when *K. pneumoniae* is exposed to 4 μg/ml DDAC and 3 μg/ml PHMB, respectively (Figure 43b, c). In contrast, live/dead estimates that there are no *K. pneumoniae* cells in the VBNC state in these

conditions, instead indicating that 8 μg/ml DDAC and 6 μg/ml PHMB are required for VBNC formation to spontaneously occur (Figure 43b, c).

This disparity between the live/dead and DVC methodologies paired with the aforementioned limitations of estimating cell population numbers raises the question of whether these methodologies produce valid and accurate results when attempting to quantify VBNCs, especially in low-stress conditions.

The number of VBNCs quantified by PE indicates that there are a basal number of VBNCs within a population, as supported by the literature [164], [174], [442]. Exposure to 4 μg/ml of BAC or DDAC caused an increased number of VBNCs to form (Figure 43a, b), likely due to stress inflicted by the antimicrobial activity of the disinfectants, in accordance with previous reports [154], [155]. Exposure to higher concentrations of these disinfectants caused a decrease in the number of VBNCs detected by both PE and DVC (Figure 43a, b), due to the higher concentrations of disinfectants lysing cells. When exposed to PHMB, the number of VBNCs quantified via PE remained consistent until the MIC was exceeded, upon which the number of VBNCs decreased (Figure 43c), again because of the increased disinfectant concentration.

When VBNCs are detected by all methodologies used, a disparity can be seen in the number of VBNC cells inferred by live/dead and the other VBNC quantification methods (Figure 43). Live/dead generally overestimates the number of VBNCs present by approximately 2 orders of magnitude in comparison to DVC and PE, which are relatively consistent throughout (Figure 43). This is likely a result of non-viable cells that have maintained membrane integrity excluding PI and being detected within the "R6LiveCells" gate, as observed in the control experiments (Figure 41). This causes an overestimation in the number of total live cells, and thus accounts for the overestimation in the number of VBNCs observed [178]. For this reason, the number of VBNCs as inferred via the live/dead methodology is deemed to have low validity.

As PE directly quantifies viable but non-proliferating cells within a population, fewer estimations are made to enumerate VBNCs. Therefore, PE is more likely to accurately represent the number of VBNCs within a population in comparison to the estimations produced via live/dead and DVC, especially when used to enumerate cultures exposed to low-stress conditions. Even so, in the conditions where DVC was able to infer the number of VBNCs within the population, the values generated were all relatively comparable with PE. This further indicates that PE may produce a valid and accurate representation of the number of VBNCs within these conditions, even at the lower concentrations that the other methodologies could not quantify.

Provisionally, these data indicate that PE provides an accurate alternative to DVC and live/dead that is capable of directly enumerating VBNCs within a population, even in low-stress conditions where the other methods could not (Figure 43). In addition, these data suggests that the PE and DVC methodologies are likely more accurate at enumerating *K. pneumoniae* VBNCs than the widely used live/dead methodology. If PE can be demonstrated to identify and gate VBNC populations within cultures containing mixed culturability states, it may be possible to apply the methodology to FACS to isolate VBNCs.

However, the full validation of the PE methodology will require comparison to other established VBNC detection methods, such as PMA-qPCR. Furthermore, the methodology will need to be tested upon a wider range of species and other established conditions that are known to induce the VBNC state. This experiment represents an initial successful "proof of concept", and indicates that PE works and is worth investigating further.

Irrespective of the methodology used, VBNCs were detected at concentrations of disinfectant above the MIC (Figure 43). Therefore, *K. pneumoniae* NCTC 9633 in the VBNC state are able to survive at concentrations that culturable bacteria cannot. This is in accordance with Robben *et al.* (2019), who demonstrated that VBNC *L. monocytogenes, E. coli, B. cereus* and *P. aeruginosa* display a higher tolerance to BAC, trioctylmethylammonium chloride, bronopol and sodium azide than their culturable counterparts [160].

In addition, PE results indicate an increase in the number of bacteria in the VBNC state when *K. pneumoniae* NCTC 9633 is exposed to 4 μg/ml BAC or DDAC respectively, implying that low concentrations of these disinfectants can induce the VBNC state (Figure 43a, b). Previously, a study has reported an increased prevalence of VBNC *L. monocytogenes* in food processing plants after routine disinfection, concluding that VBNC induction occurs in response to stress-induced via industrial disinfectants [443]. More broadly, non-ionic surfactants have been shown to induce the VBNC state across a range of Gram-negative and Gram-positive bacteria [155]. These data presented here expand on the work established in the literature and indicate that cationic surfactants are able to induce the VBNC state in *K. pneumoniae* NCTC 9633 (Figure 43a, b), and cells in this state can demonstrate an increased tolerance to BAC, DDAC and PHMB (Figure 43).

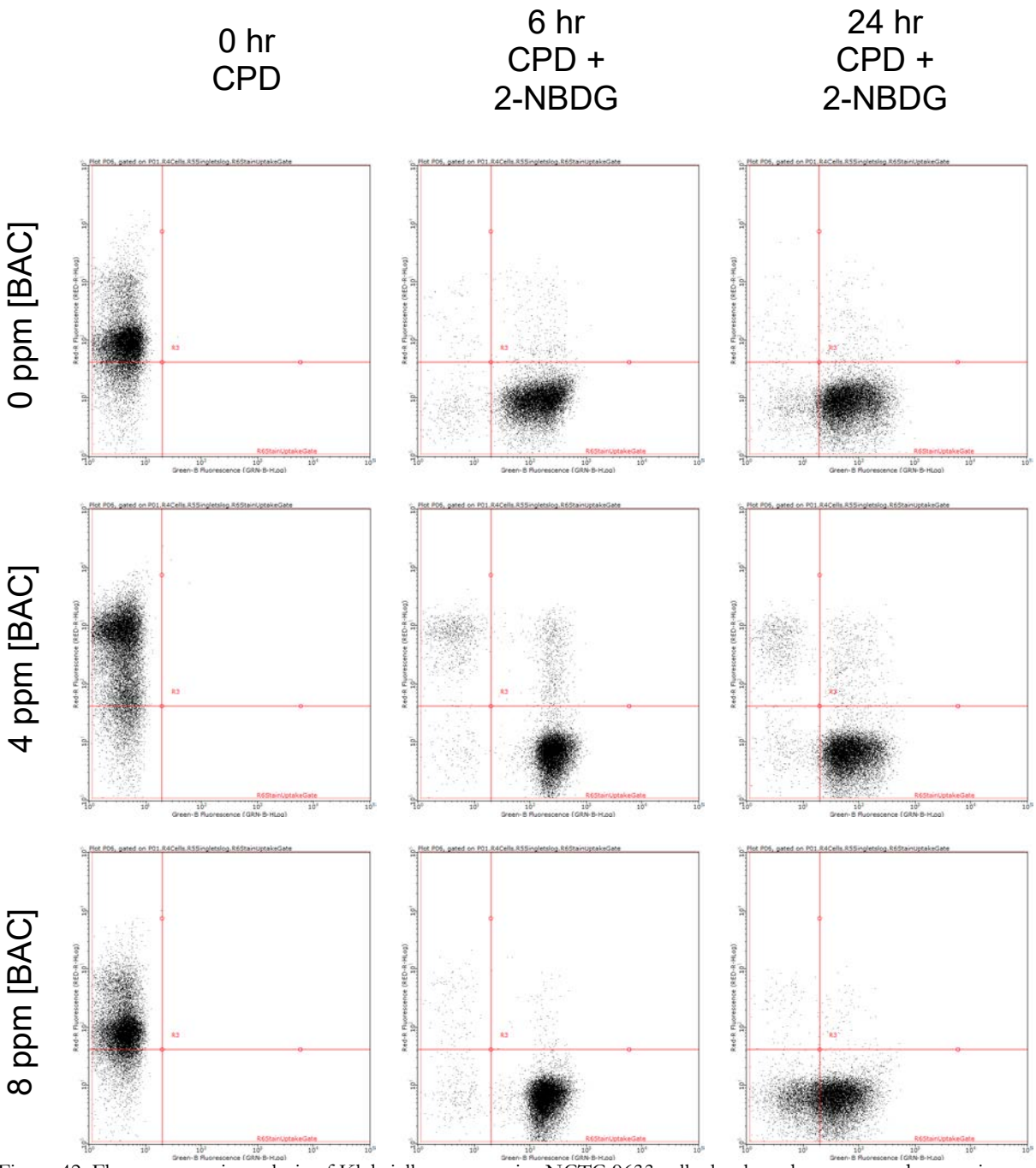

Figure 42. Flow cytometric analysis of Klebsiella pneumoniae NCTC 9633 cells that have been exposed to varying concentrations of benzalkonium chloride (BAC) before undergoing varying staining procedures, as described. All dot plots depict 2-Deoxy-2-[(7-nitro-2,1,3-benzoxadiazol-4-yl)amino]-D-glucose (2-NBDG) fluorescence intensity on the X axis, and Cell Proliferation Dye eFluor 670 (CPD) fluorescence intensity on the Y axes. Red gates show differentiation between cell populations as determined by control experiments. Times indicate post-staining incubation time in hours, in Mueller Hinton broth at 37°C before flow cytometric analysis. [BAC]: Concentration of BAC that the cells were exposed to for 24-hours prior to staining. Samples analysed at time 0 were not stained with 2-NBDG. Figure continued on the next page.

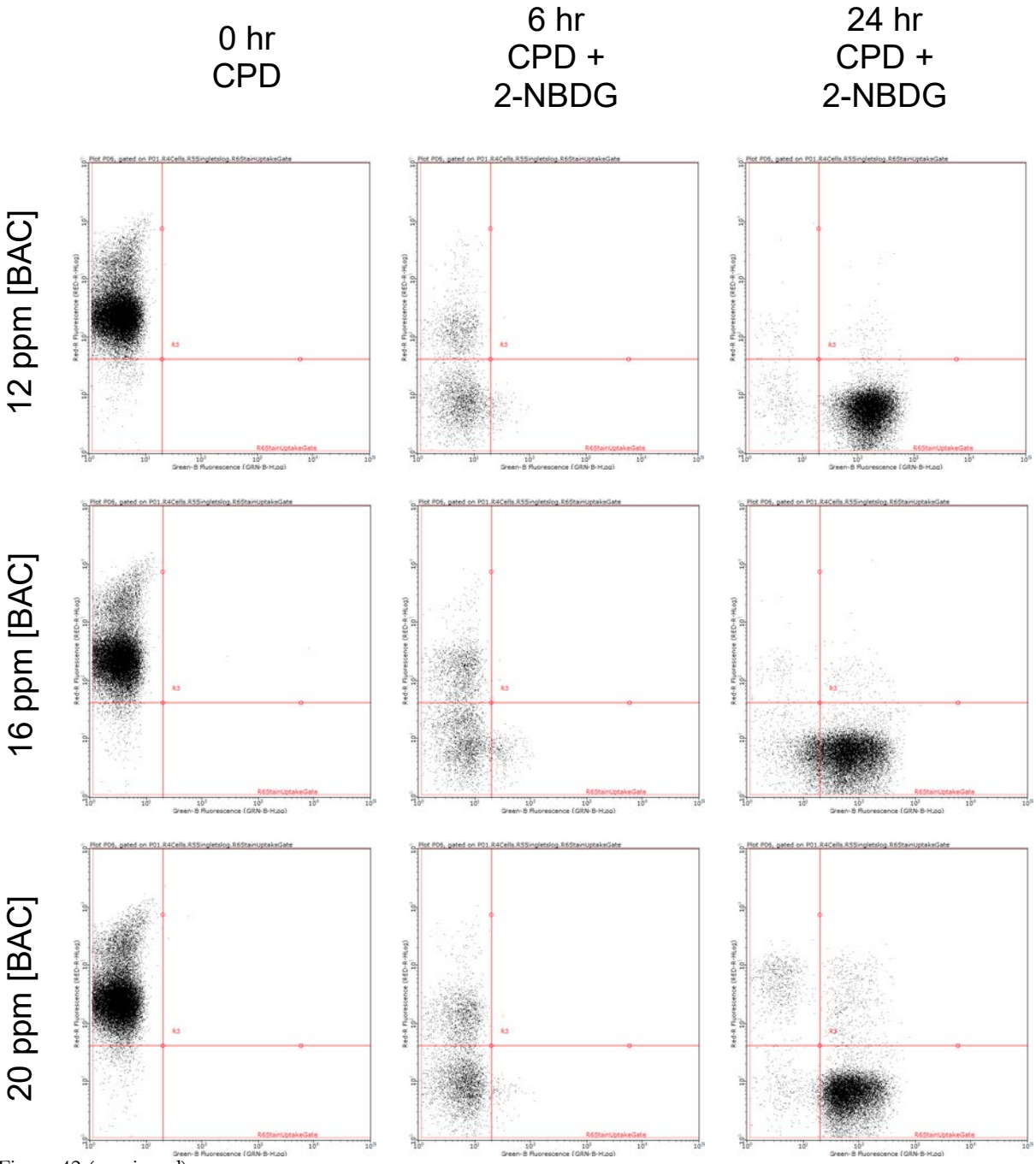

Figure 42 (continued).

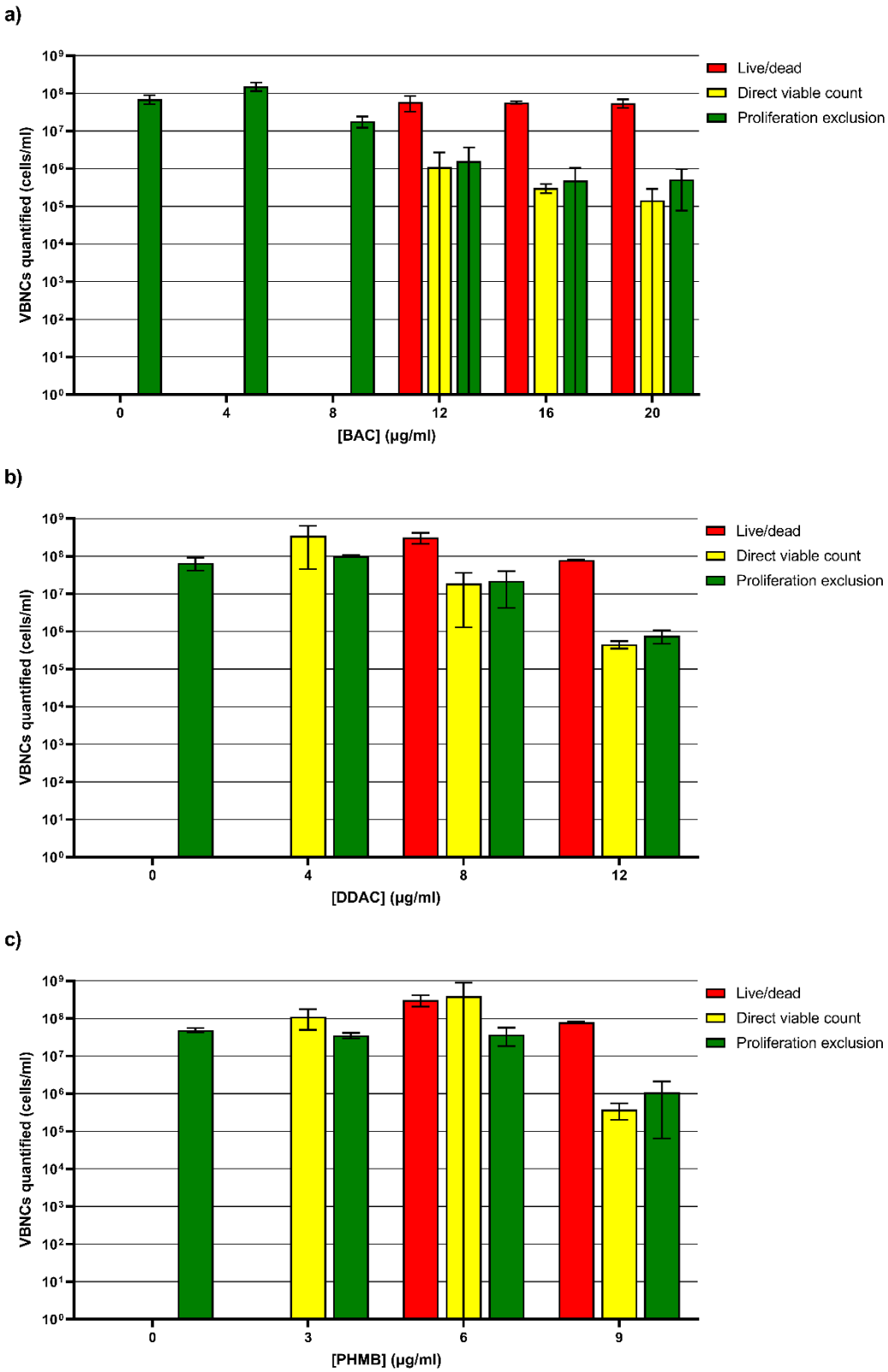

Figure 43. The number of *Klebsiella pneumoniae* NCTC 9633 cells that have entered the viable but nonculturable (VBNC) state after exposure to varying concentrations of common disinfectants, as identified by various VBNC quantification methods. a) *Klebsiella pneumoniae* NCTC 9633 VBNC cells quantified after 24-hour exposure to benzalkonium chloride (BAC). b) *Klebsiella pneumoniae* NCTC 9633 VBNC cells quantified after 24-hour exposure to didecyldimethylammonium chloride (DDAC). c) *Klebsiella pneumoniae* NCTC 9633 VBNC cells quantified after 24-hour exposure to polyhexamethylene biguanide (PHMB). n=3.

6.4.2. Induction into the viable but nonculturable state via disinfectant exposure

Initial experiments have indicated that PE is a viable methodology of directly enumerating *K. pneumoniae* NCTC 9633 in the VBNC state. Control experiments conducted on *K. pneumoniae* NCTC 9633 (Figure 40) and *K. pneumoniae* NCTC 13443 (Figure 38) produced synonymous results, therefore it was assumed that PE will enumerate VBNCs to the same standard in both strains. VBNC quantification via the live/dead methodology was found to overestimate the number of VBNCs in *K. pneumoniae* NCTC 9633, and both live/dead and DVC were unable to quantify VBNCs in low-stress conditions (Figure 43). As a result, these methodologies were not used further.

To elucidate if disinfectant-tolerant samples of *K. pneumoniae* NCTC 13443 are induced into the VBNC state as a result of disinfectant exposure, the PE protocol was conducted on the disinfectant-tolerant samples that were generated in Chapter 4, and examined via genomic and proteomic analysis in Chapter 5. Figure 15 shows a schematic diagram of the experimental workflow conducted on these samples. The disinfectant-tolerant samples were exposed to varying concentrations of the respective disinfectant that ranged above and below the tolerant MICs (Table 16), before being incubated at 37°C for 24-hours in MHB. PE analysis was conducted upon these samples, as described in Chapter 6.3.2.

The number of VBNCs identified via PE after the respective disinfectant treatments are displayed in Figure 44. BAC-tolerant samples exposed to 0 μg/ml, 25 μg/ml and 55 μg/ml BAC had equal VBNC cell populations, before the number of VBNCs decreases as samples were exposed to increasingly higher concentrations of BAC (Figure 44a). A visible decrease in VBNC population can also be seen as DDAC and PHMB-tolerant *K. pneumoniae* NCTC 13443 samples are exposed to increasing concentrations of the respective disinfectants (Figure 44b, c), although this decrease is not statistically significant. As there is no increase in VBNC numbers upon exposure to the respective treatment, these data indicate that these disinfectants do not induce the VBNC state. Alternatively, the disinfectant may be killing a higher quantity of VBNCs than those being formed in response to the stress of disinfectant exposure. The latter hypothesis is supported by research conducted by Bravo *et al.* (2018), which concluded that disinfectant formulations containing both DDAC and PHMB induce the VBNC state in *A. baumannii* samples [158].

In contrast, bronopol-tolerant *K. pneumoniae* samples exposed to concentrations ≤ MIC of the respective disinfectant display increasingly greater VBNC populations than untreated samples (Figure 44d). This indicates that non-lethal concentrations of bronopol induce the VBNC state in *K. pneumoniae*. This trend is reflected in the chlorocresol and SQ53-tolerant samples too.

This observed increase in VBNC cells is of particular interest when considering disinfectant formulation SQ53. The higher VBNC populations observed upon exposure to low concentrations of SQ53 may indicate that disinfectant formulations do not provide a discernible advantage over individual disinfectants in terms of mitigating VBNC induction, in accordance with previous investigations of *A. baumannii* VBNC induction by disinfectant formulations [158]. However, the observed increase in VBNC numbers for chlorocresol and SQ53-tolerant samples are statistically insignificant. Further biologically-independent replicates should be conducted to ascertain whether this observed increase is of statistical importance or just a product of random variation.

In addition, bacteria in the VBNC state demonstrate a reduced susceptibility to the respective disinfectants, as events in the upper right quadrant were detected at concentrations above the respective MICs (Figure 44). This is in accordance with previous experiments conducted on *K. pneumoniae* NCTC 9633 exposed to BAC, DDAC and PHMB (Figure 43). This is also supported by previous studies that have shown VBNC *L. monocytogenes, E. coli, B. cereus* and *P. aeruginosa* to have a reduced susceptibility to BAC and bronopol, alongside QAC trioctylmethylammonium chloride, and sodium azide [160].

However, it should be noted that exposure to concentrations of disinfectant above the MIC resulted in a statistically significant reduction in the number of VBNCs detected in BAC-tolerant and chlorocresol-tolerant samples. These data demonstrate that the VBNC populations only display a reduced susceptibility to the disinfectants, not complete resistance. This trend is reflected by statistically insignificant observable reductions in VBNC numbers when DDAC, bronopol and SQ53-tolerant samples were exposed to concentrations of disinfectant above the MIC (Figure 44).

Collectively, these data demonstrate that *K. pneumoniae* NCTC 13443 disinfectant-tolerant samples are capable of being induced into the VBNC state in response to bronopol, and potentially chlorocresol and disinfectant formulation SQ53. This therefore indicates that disinfectant formulations do not provide a discernible advantage in terms of mitigating VBNC induction. In addition, VBNC sub-populations display an increased tolerance to all disinfectants tested over the culturable populations.

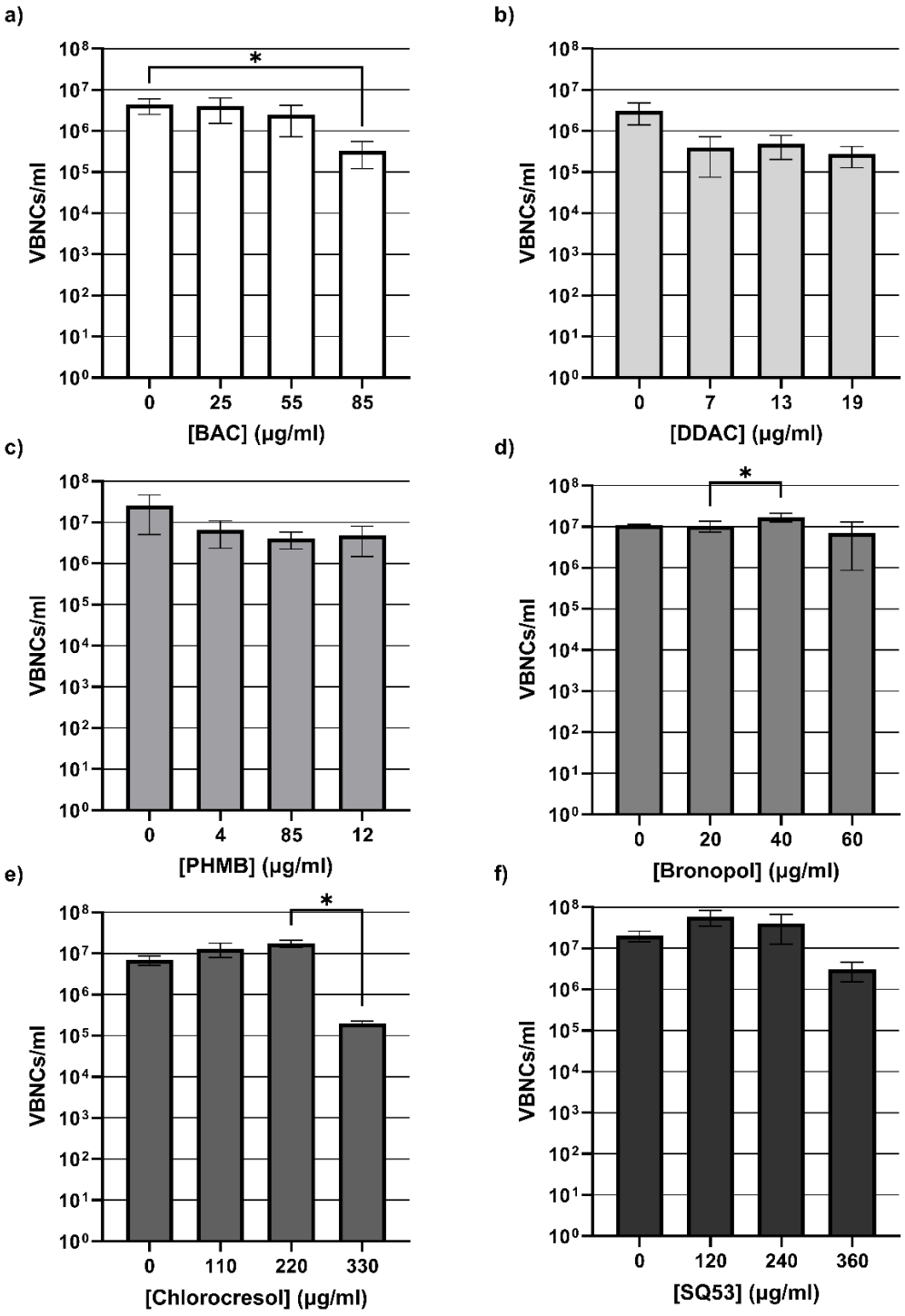

Figure 44. The number of *Klebsiella pneumoniae* NCTC 13443 cells that have entered the viable but nonculturable (VBNC) state after exposure to varying concentrations of common disinfectants, as identified by proliferation exclusion. a) VBNC cells in benzalkonium chloride (BAC)-tolerant samples after 24-hour exposure to varying concentrations of BAC. n=5. b) VBNC cells in didecyldimethylammonium chloride (DDAC)-tolerant samples after 24-hour exposure to varying concentrations of DDAC. n=3. c) VBNC cells in polyhexamethylene biguanide (PHMB)-tolerant samples after 24-hour exposure to varying concentrations of PHMB. n=3. d) VBNC cells in bronopol-tolerant samples after 24-hour exposure to varying concentrations of bronopol. n=3. e) VBNC cells in chlorocresol-tolerant samples after 24-hour exposure to varying concentrations of chlorocresol. n=3. f) VBNC cells in disinfectant formulation "SQ53" (SQ53)-tolerant samples after 24-hour exposure to varying concentrations of SQ53. * denotes significant difference in VBNC numbers between the highlighted conditions as identified by the one-way analysis of variation (ANOVA) statistical test. n=3.

6.5. Conclusions

A novel method of VBNC quantification is presented whereby cell populations are stained using a proliferation dye and a viability dye, allowing the populations to be differentiated according to their viability and culturability via flow cytometric analysis. The method enumerates bacteria that are identified as both viable and having not proliferated (VBNCs), while excluding bacteria that proliferate during the incubation period (Figure 42). The method is provisionally referred to as the proliferation exclusion (PE) methodology.

Proof of concept validation of PE was conducted via comparing the methodology against other VBNC quantification methods, namely live/dead and DVC. The number of VBNCs quantified by PE was found to be comparable to DVC, while the live/dead methodology was seen to overestimate the number of VBNCs within the sample (Figure 43). In addition, as PE provides a method of directly quantifying VBNC numbers, it is able to identify the number of VBNCs more reliably within low-stress conditions (Figure 43). These data suggest that PE provides a method to directly identify and quantify VBNCs within a population, with the view of being able to isolate VBNCs if applied to FACS. Further validation steps need to be taken, including comparing the methodology to a greater range of VBNC quantification methods and applying PE to a broader range of bacterial species and VBNC-induction conditions. No standardised methodology currently exists to directly quantify and isolate VBNCs.

Based on the initial proof of concept data, PE was used to enumerate VBNCs within *K. pneumoniae* NCTC 13443 samples that have been shown to display tolerance to common disinfectants (Figure 44). VBNC populations within *K. pneumoniae* cultures displayed an increased tolerance to all disinfectants tested in comparison to culturable bacteria in the same culture (Figure 44). In addition, samples exposed to low concentrations of bronopol demonstrated a statistically significant increase in VBNC population (Figure 44). Samples exposed to chlorocresol and disinfectant formulation SQ53 also displayed a visible increase in VBNC population, indicating that low-level stress as a result of these disinfectants may actively induce the VBNC state in *K. pneumoniae* (Figure 44). This indicates that disinfectant formulations do not provide an advantage over individual disinfectants in terms of preventing VBNC induction.

7. Conclusions and Future Directions

7.1. Conclusions

The average HAI prevalence on any given day is 7.1% in European acute care hospitals [4], rising to 15.5% in developing countries [2]. Bacteria are the underlying cause of the majority of HAIs [5], with *S. aureus* and *K. pneumoniae* being among the most prevalent [2], [7]–[9]. The threat of HAIs is only likely to worsen with the increasing prevalence of antimicrobial resistant bacteria [4]. As of 2018, it is estimated that between 35% and 55% of all HAIs are preventable with the application of evidence-based infection control strategies [18], demonstrating that continual improvements to infection control measures are necessary to save lives.

The use of chemical disinfectants as an infection control measure is critical, as demonstrated by our reliance on them during the COVID-19 pandemic. This dependence on disinfectants is only likely to be reinforced with the continually rising prevalence of AMR. The escalating chances of AMR-related treatment failure will likely result in a renewed focus on infection prevention and control.

In order to make improvements to the use of disinfectants as an infection control measure, we must first identify shortcomings associated with their use. This study aimed to elucidate and address various limitations associated with the use of chemical disinfectants as an infection control measure.

The first potential limitation to be investigated was regarding the use of formulations consisting of multiple disinfectant agents. These products are often marketed under the guise of increased efficacy, alongside liberal use of the "synergistic" buzzword. However, little scientific evidence exists regarding the antimicrobial interactions between disinfectants. As such, the interactions between disinfectants commonly utilised in formulations were elucidated using a stringent method, tested against clinically-relevant bacterial species.

The results indicated that synergistic interactions were possible between BAC and chlorocresol, and PHMB and chlorocresol, but FICI values were on the threshold of the synergy classification. In addition, the synergy classification was circumstantial depending on the bacterial species tested upon. The observed scarcity of synergy and abundance of additive interactions is hereby suggested to be a result of the broad range of cellular components targeted by the MOAs of the disinfectants. As a result, the widespread impact of each disinfectant on bacterial cells provides

little opportunity for multiple disinfectants to ever amount to an activity that is greater than the sum of their individual efficacies.

These data indicate that the interactions that underpin disinfectant formulations may be being inappropriately characterised, leading to potential issues regarding the correct use of the formulation. Furthermore, the correct classification of antimicrobial activity dictates the viability of substituting disinfectants for a functional analogue in the event of regulatory changes.

In addition, we question the need for the current emphasis in academic and commercial fields on synergistic disinfectant interactions at the expense of all others. Synergistic interactions are not likely to provide any discernible benefit to disinfectant formulation over additive interactions.

The second limitation associated with the use of disinfectants is the development of tolerance mechanisms leading to ineffective use as an infection control measure. The investigation of the ability for clinically-relevant *K. pneumoniae* and *S. aureus* strains to develop tolerance to common disinfectants and a disinfectant formulation was conducted. Samples were exposed to concentrations of disinfectant below their respective MICs before being serially passaged in increasing disinfectant concentrations until growth inhibition was observed.

In contrast to previous reports [266], [323]–[325], [334], [444], *S. aureus* was unable to develop tolerance to BAC, DDAC or PHMB, in addition to any of the other disinfectants tested. This discrepancy is likely a result of experimental variations both in terms of methodologies utilised and strains examined. Furthermore, the lack of prior evidence of *S. aureus* tolerance to bronopol, chlorocresol or disinfectant formulation SQ53 indicate that *S. aureus* is unable to develop tolerance to these disinfectants, even at low concentrations. Therefore, the risk of *S. aureus* developing tolerance to these disinfectants when exposed to "at use" concentrations is minimal.

However, *K. pneumoniae* was able to develop tolerance to all of the disinfectant examined, including the disinfectant formulation SQ53. Final MIC values were 30%-413% higher than the MICs of the parent samples, indicating that the ability for bacteria to develop tolerance varies between disinfectants. The presence of multiple disinfectants within a single formulation did not completely mitigate the development of tolerance. However, the MIC increase was limited to 30%; the same MIC increase as seen by chlorocresol-adapted *K. pneumoniae*. This indicates that the ability for bacteria to develop tolerance to a disinfectant formulation is limited by the ability for the bacteria to develop tolerance to each of the other components individually. This demonstrates that tolerance to disinfectant formulations is possible, although the extent to which tolerance was able to develop is somewhat mitigated.

The cross-tolerance profiles of disinfectant-tolerant *K. pneumoniae* indicate that cross-tolerance to other disinfectants is dependent on order of exposure, and is not automatically mutual. Furthermore, the majority of tolerant samples displayed higher susceptibilities to other disinfectants, indicating that the samples overspecialise in tolerating one disinfectant, leaving them vulnerable to others. This collectively indicates that there are significant differences in the underlying mechanistic requirements of disinfectant tolerance displayed by *K. pneumoniae* when comparing between different disinfectant treatments. In addition, the cross-tolerance profiles were not always consistent between biological replicates, with variations seen between biological replicates of PHMB and bronopol-tolerant *K. pneumoniae*. The implication is that these disinfectants may give rise to multiple varying methods of disinfection tolerance, likely as a result of the varying MOAs used by these disinfectants.

Whole-genome sequencing of the tolerant *K. pneumoniae* samples revealed significant genetic variation between the samples. Phylogenetic analysis indicates that disinfectant-tolerant samples display conserved mutations across biological replicates, as most samples were grouped into clades based on disinfectant treatment. This indicates that the observed mutations were a result of the selection pressure applied by the respective disinfectant treatments, rather than due to random chance. BAC, DDAC and SQ53-tolerant samples displayed a large genetic distance from the rest of the samples, indicating that these disinfectant treatments exert a stronger selection pressure, and more adaptations are required to develop tolerance to these treatments.

The sequencing data was combined with quantitative proteomic analysis in order to determine the underpinning molecular mechanisms of disinfectant tolerance in the respective *K. pneumoniae* samples. BAC, DDAC and PHMB-tolerant samples all demonstrated genetic and phenotypic changes associated with increasing the modification of lipid A with L-Ara4N, alongside the down-regulation of proteins associated with LPS production. This collectively results in a net decrease in the negative charge of the outer leaflet of the outer surface of *K. pneumoniae* cells, leading to cationic surfactants having a decreased affinity to the outer membrane, resulting in an increased tolerance. This mechanism of tolerance to BAC has previously been reported for *E. coli* [339] and *P. aeruginosa* [233] samples, but has not previously been demonstrated in *K. pneumoniae*. In addition, this mechanism has not been demonstrated to be associated with DDAC or PHMB tolerance in any bacterial species. BAC tolerance was also associated with an increased regulation of proteins associated with the AcrAB-TolC efflux pump, aligning with previous reports [223].

A novel mechanism of bronopol tolerance was identified via the increased expression of N-ethylmaleimide reductase, NemA. This protein is capable of enzymatically breaking down electrophiles [415] and nitro group-containing compounds such as TNT [413], [414]. As bronopol contains the nitro electrophilic group, this protein is suggested to enzymatically break down bronopol, preventing it from reacting with exposed thiol groups of proteins and producing ROS. It is therefore suggested that *K. pneumoniae* increases expression of NemA in response to bronopol exposure, resulting in the increased tolerance observed. This enzymatic degradation also explains the observed decrease in expression of catalase and superoxide dismutase that would otherwise be expected, as these proteins are not required if the second stage of the MOA of bronopol is unable to occur.

In accordance with previous reports linking efflux pump activity with phenolic disinfectant tolerance [225], [226], chlorocresol tolerance is likely to be associated with the increased expression of efflux pumps such as the MdtABC complex.

Finally, the exact mechanisms underpinning SQ53 tolerance were unable to be fully elucidated, likely due to the disinfectant formulation consisting of multiple disinfectants with multiple MOAs leading to a strong selection pressure. All samples gained a conserved stop gain mutation in MutL, a mismatch-repair protein associated with hypermutable strains [379]. This loss-of-function mutation resulted in a high variability in tolerance mechanisms demonstrated by the *K. pneumoniae* samples. As the proteomic analysis was conducted across all biological replicates, the individual tolerance mechanisms of each biological replicate were unable to be identified.

Previously, it had been assumed that the addition of multiple disinfectants leads to the mitigation of tolerance as samples would have to develop tolerance to multiple antimicrobials simultaneously, limiting the number of potential mechanisms by which tolerance can occur. However, these data indicate that an increased number of MOAs present within the formulation may provide a strong selection pressure that gives rise to hypermutable phenotypes.

Overall, the presence of multiple disinfectants does not outright prevent the development of tolerance in *K. pneumoniae*. Tolerance was likely to have been developed through the adaptation of a hypermutable phenotype, giving rise to multiple varying mechanisms. However, the multiple disinfectants present in the formulation were able to limit the extent to which tolerance was able to develop, so the use of disinfectant formulations may provide a minor benefit over individual disinfectants in terms of tolerance mitigation.

The ability for disinfectants to induce the VBNC state in *K. pneumoniae* cells was elucidated using a novel methodology. Samples exposed to sub-MIC concentrations of bronopol, chlorocresol and SQ53 demonstrated an increased number of VBNC cells, indicating that these disinfectants are able to induce the VBNC state in *K. pneumoniae*. In addition, VBNC populations were detected when *K. pneumoniae* samples were exposed to concentrations of disinfectant higher than the respective MICs. Therefore, *K. pneumoniae* cells in the VBNC state are able to tolerate higher concentrations of BAC, DDAC, PHMB, bronopol, chlorocresol and SQ53 than their culturable counterparts. It is therefore possible that *K. pneumoniae* is able to survive disinfection treatments if inappropriate concentrations or exposure times are used, presenting a potential HAI risk.

Overall, the ability for *K. pneumoniae* to readily develop up to a 413% higher tolerance to disinfectants commonly associated with HAIs is concerning, and represents a limitation of disinfectants as an infection control measure. In addition, disinfectants were also shown to induce the VBNC state in *K. pneumoniae* cells, even when the disinfectants were used together in a single formulation. It could be argued that the at-use concentrations of these disinfectants are significantly higher than those examined here, so these issues are of little concern. However studies have repeatedly shown that in practice bacteria are regularly able to survive disinfection treatments [107], [111], [238], [239], so are thus being exposed to non-lethal concentrations. Their survival provides an opportunity to develop adaptations to the disinfectants, such as those demonstrated by these data presented within this thesis.

Ultimately, these limitations demonstrate a significant infection risk that likely contribute to the high prevalence of preventable HAIs seen across the world. These data illustrate that disinfectants are not an infallible infection control method. The current understanding and attitudes towards disinfectant use and efficacy needs addressing in order for improvements to be made.

Finally, a proof-of-concept validation experiment of the novel methodology (PE) demonstrated that PE quantifies VBNCs to a similar accuracy to DVC, even in low-stress conditions. These data suggest that PE may provide a novel methodology to directly quantify VBNC populations, which is not currently possible. In addition, PE may be able to be applied to FACS, enabling VBNCs to be isolated for further experimentation. No standardised methodology currently exists to directly quantify or isolate VBNCs from cultures containing mixed viability states.

7.2. Future directions

Each results chapter of this thesis contained a discussion of the data and the findings, during which the limitations of the work were discussed and various potential avenues for future enquiry were presented. These will be overviewed and discussed further here.

The early experiments elucidating the properties of the disinfectants used individually and in combination were conducted upon *A. baumannii* NCTC 12156, *E. faecalis* NCTC 13379, *K. pneumoniae* NCTC 13443 and *S. aureus* NCTC 13143. Unfortunately, due to the scale of the remaining work the tolerance and VBNC-induction experiments were narrowed to focus on *K. pneumoniae* NCTC 13443 and *S. aureus* NCTC 13143 as a result of time constraints. Although *K. pneumoniae* and *S. aureus* are among the most prevalent HAIs globally [2], [7]–[9], the various limitations of disinfectants should be explored on a wider group of HAIs.

This is especially relevant considering that a repeating theme throughout the thesis was the variability between the bacterial species and strains that were examined. These data demonstrate that the efficacy and limitations of the use of disinfectants varies depending on the HAI-causing pathogen being experimented on. As such, future research should expand upon this work to elucidate the limitations of the use of disinfectants as an infection control measure on spore-forming bacterial pathogens such as *C. difficile* or mycobacteria such as *Mycobacterium tuberculosis*.

Similarly, great variation in efficacy and limitations were displayed by the various disinfectants examined, even between disinfectants of the same classification (QACs). Therefore future research should focus on elucidating the interactions, tolerance and VBNC-induction related limitations of other disinfectants commonly associated with healthcare environments, such as hypochlorites, other phenolic compounds and peroxygens [29].

More specific future works include the elucidation of the MOA of PHMB, which is currently disputed. These data presented in this thesis suggests that PHMB relies both on membrane perturbation and the condensing of DNA, although this is likely to vary between bacterial species. As a result, further experimentation should be conducted to elucidate PHMB mechanistic variation between species. High resolution TEM microscopy presents an opportunity to interrogate the intracellular effects of varying concentrations of PHMB on various bacterial species. Any PHMB-induced condensing of DNA will result in a more electron-dense region, thus being easily visible via TEM.

The interactions between common disinfectants were elucidated within this work, demonstrating that disinfectant combinations are rarely synergistic. However, many disinfectant formulations

are not limited to pairs of disinfectants, instead containing many more. Indeed, SQ53 itself contains 5 different active disinfectants. The addition of a greater number of disinfectants leads to complex interaction networks within formulations, potentially greatly impacting efficacy. As a result, the interactions between more complex disinfectant formulations should be explored. Stein *et al.* (2015) published a study documenting synergy between three antibiotics against *K. pneumoniae*, as demonstrated by a checkerboard methodology applied to three-dimensions [445]. This methodology could be applied to disinfectant formulations to elucidate how the addition of a third disinfectant impacts the efficacy of the final formulation. In addition, disinfectant formulations contain 'inactive' ingredients such as solvents, surfactants, emulsion stabilisers and fragrance enhancers, which are also likely to impact efficacy. The impact of these chemicals on the disinfectant interactions and overall product efficacy has never been specifically examined. The results presented within this thesis provide a starting point to start exploring these interactions, which may provide opportunities to improve the efficacy of disinfectant formulations used in infection control and beyond.

K. pneumoniae was able to develop an increased tolerance to all disinfectants tested, including disinfectant formulation SQ53. Samples that developed tolerance to chlorocresol demonstrated the lowest increase in MIC, alongside SQ53-tolerant samples. This was attributed to *K. pneumoniae* being limited in its ability to tolerate chlorocresol, which is also present in SQ53. This limiting of tolerance development presents a potential benefit of the use of disinfectant formulations. However, the ability for *K. pneumoniae* to develop tolerance to more chlorocresol-containing combinations of disinfectants should be conducted to explore this further.

In addition, it is unclear if the presence of a synergistic interaction between two components may further limit the ability for bacterial species to develop tolerance. Therefore, the impact of potential synergistic interactions between disinfectants on tolerance development should be investigated. For example, is the ability for *E. faecalis* to develop tolerance to BAC, PHMB and chlorocresol impacted by combining them into their synergistic pairwise combinations?

A multi-omics approach was employed to elucidate the underpinning molecular mechanisms of disinfectant tolerance observed in *K. pneumoniae* samples. The analysis conducted within this thesis represents an initial overview of genes and proteins of immediate interest and established importance with regards to antimicrobial and stress tolerance in bacteria. A full analysis of these data is ongoing, which includes the following.

Full analysis of mutations that were "lost" by the tolerant samples in comparison to the parent samples potentially represent mutations that were necessary to lose to promote disinfection

tolerance. Mutations in non-coding regions of DNA may include mutations in promotor, repressor or other regulatory DNA regions that influence the recruitment of transcription machinery and so on. Many of these mutations are likely to be critical to disinfection tolerance.

In addition, manual analysis of the functionality of all differentially expressed proteins identified via proteomic analysis of tolerant samples will allow for further investigations into potential novel mechanisms of disinfectant tolerance.

Lastly, each of the SQ53-tolerant samples were suspected to have developed unique tolerance mechanisms, so the analysis steps should be repeated on the individual biological replicates in isolation to further investigate this.

In Chapter 6, various disinfectants were found to induce the VBNC state in *K. pneumoniae*. These VBNC cells also demonstrated an increased tolerance to the respective disinfectant treatments. Provisionally, the ability for SQ53 to induce the VBNC state in *K. pneumoniae* indicates that formulations of disinfectants do not provide a discernible advantage over individual disinfectants when considering VBNC induction. However, no combination of the SQ53 components were found to be synergistic. As such, synergistic combinations with a unique combined mechanism may be able, to prevent formation and impede survivability of bacteria in the VBNC state. Investigation of this would require further VBNC quantification experiments on *S. aureus* and *E. faecalis* exposed to synergistic pairwise combinations of BAC, PHMB and chlorocresol.

Finally, an initial proof of concept experiment has validated PE as a potential method of direct VBNC identification and enumeration. Full validation of this method requires comparison to other VBNC quantification methods including CTC-DAPI dual staining and PMA qPCR. In addition, validation experiments need to be conducted on a broad range of species and VBNC induction stressors, in order to assess the applicability of the method to other species. Examples include *Vibrio cholerae, E. coli* and *S. aureus*. The potential for VBNCs to be isolated using FACS will require further experimental validation.

Furthermore, different cell proliferation dyes are available that utilise a range of fluorophores with varying excitation/emission spectra. This allows researchers to select a viability dye based on experiment requirements rather than excitation/emission spectra, as a proliferation dye with minimal spectral overlap can be chosen as required. This affords a level of modularity and flexibility not available through other VBNC detection methods. However, the use of other proliferation dyes requires validation.

7.3. Concluding statement

This project aimed to elucidate the limitations of the use of disinfectants as an infection control measure. To this end, a series of experiments were conducted utilising HAI pathogenic bacterial strains and a range of common disinfectants used for infection control.

The MOA of common disinfectant PHMB was found to be species-dependant and likely involves both membrane-active and DNA-binding mechanisms. Synergistic interactions between disinfectants were found to be uncommon, species-dependant and on the threshold of the synergism classification, while *K. pneumoniae* was found to be able to develop tolerance to individual disinfectants and a combined disinfectant formulation through the acquisition of adaptations and induction into the VBNC state. Molecular mechanisms of tolerance to these disinfectants were then identified through a multi-omics approach, allowing the identification of novel mechanisms of disinfectant tolerance demonstrated by *K. pneumoniae*.

These data indicate HAI-associated pathogenic bacteria are able to adapt to low-level disinfectant exposure. In addition, disinfectant formulations were found provide minimal benefits over disinfectants used individually when considering the development of tolerance and VBNC induction, ultimately undermining the axiom that the addition of more disinfectants must be beneficial to the final product. These data suggest that this is not necessarily true.

The results presented within this thesis highlight limitations in the use of disinfectants as an infection control measure that likely contribute to the high prevalence of preventable HAIs seen across the world. This work represents a crucial step towards addressing gaps in our knowledge in order for these limitations to be tackled, and highlights potential shortcomings in our current attitudes towards the efficacy and use of chemical disinfectants.

This project has also resulted in the initial development of a novel methodology of direct VBNC quantification and isolation, which is not currently possible with established methodologies. Currently, VBNC research is limited and restricted by the heavily flawed methods used, so further development of this promising novel methodology may provide new opportunities to expand our understanding of the VBNC state as a whole.

8. Appendix

Table 19. Quality control analysis of disinfectant-tolerant *Klebsiella pneumoniae* NCTC13443 samples before whole genome sequencing. Tolerant sample: disinfectant-tolerant sample analysed. A260: sample absorbance at 260 nm. A280: sample absorbance at 280 nm. OD 260/280 (AU): Optical density of sample, in arbitrary units. DNA: deoxyribonucleic acid. Bz: benzalkonium chloride-tolerant sample. Dd: didecyldimethylammonium chloride-tolerant sample. Ph: polyhexamethylene biguanide-tolerant sample. Br: bronopol-tolerant sample. Cc: chlorocresol-tolerant sample. SQ: disinfectant formulation "SQ53" -tolerant sample.

Tolerant sample	Concentration of DNA (ng/µl)	A260	A280	OD 260/280 (AU)
Ps1	26.04	0.521	0.285	1.83
Ps2	29.53	0.591	0.324	1.82
Ps3	26.15	0.523	0.29	1.81
Bz1G	38.08	0.762	0.405	1.88
Bz1D	41.58	0.832	0.463	1.8
Bz2G	21.6	0.432	0.227	1.9
Bz2D	17.56	0.351	0.188	1.86
Bz3	23.31	0.466	0.246	1.9
Dd1	25.14	0.503	0.274	1.83
Dd2	20.46	0.409	0.228	1.8
Dd3	16.58	0.332	0.182	1.83
Ph1	11.1	0.222	0.116	1.91
Ph2	43.84	0.877	0.487	1.8
Ph3	14.16	0.283	0.158	1.8
Br1	46.72	0.934	0.515	1.81
Br2	48.23	0.965	0.536	1.8
Br3	51.37	1.027	0.565	1.82
Cc1	13.04	0.261	0.142	1.84
Cc2	15.66	0.313	0.171	1.83
Cc3	16.94	0.339	0.183	1.85
SQ1	18.25	0.365	0.195	1.87
SQ2	13.89	0.278	0.153	1.81
SQ3	11.97	0.239	0.131	1.82

Table 20. Sequence insertion or deletions gained by disinfectant-tolerant *Klebsiella pneumoniae* NCTC 13443 samples in comparison to their respective untreated parent samples. Each event refers to an insertion or deletion (InDel) of ≤ 50 bp. Details of the annotation statistics are as follows. Upstream: InDels located within 1 kb upstream of a gene start site. Exonic: InDels located in protein-coding sequence. Stop gain/loss: InDel leads to introduction or deletion of a stop codon. Frameshift: InDel changes the open reading frame. Non-frameshift: InDel does not change the open reading frame. Downstream: InDel located within 1 kb downstream of gene region. Upstream/Downstream: InDel located between 2 genes that are ≤ 2kb apart. Intergenic: InDel located in the > 2 kb intergenic region. Bz: benzalkonium chloride-tolerant sample. Dd: didecyldimethylammonium chloride-tolerant sample. Ph: polyhexamethylene biguanide-tolerant sample. Br: bronopol-tolerant sample. Cc: chlorocresol-tolerant sample. SQ: Disinfectant formulation "SQ53" -tolerant sample.

Sample	Up-stream	Exonic						Intronic	Splicing	Down-stream	Up-stream/ Down-stream	Intergenic	Total Insertion	Total Deletion	Total
		Stop gain	Stop loss	Frameshift		Non-frameshift									
				Deletion	Insertion	Deletion	Insertion								
Bz1G	2	0	1	29	74	2	6	0	0	4	21	0	97	42	139
Bz1D	4	0	1	31	73	2	4	0	0	3	24	0	98	45	142
Bz2G	2	0	1	20	50	2	3	0	0	4	9	0	62	29	91
Bz2D	2	0	0	19	42	2	2	0	0	4	13	0	56	29	84
Bz3	2	0	1	22	48	2	3	0	0	4	10	0	61	31	92
Dd1	5	1	1	20	28	3	1	0	0	9	18	0	41	45	86
Dd2	5	0	1	20	34	3	2	0	0	10	19	0	50	44	94
Dd3	6	0	1	17	32	3	1	0	0	8	21	0	46	43	89
Ph1	2	0	0	4	0	0	0	0	0	1	3	0	3	7	10
Ph2	3	1	0	2	1	0	0	0	0	2	2	0	5	6	11
Ph3	2	0	0	4	2	0	2	0	0	2	2	0	8	6	14
Br1	1	0	0	1	0	3	0	0	0	0	0	0	0	5	5
Br2	2	0	0	0	1	1	0	0	0	1	0	0	3	2	5
Br3	1	0	0	1	0	1	0	0	0	2	2	0	0	7	7
Cc1	1	0	0	1	3	1	0	0	0	1	1	0	4	4	8
Cc2	1	1	0	1	3	1	2	0	0	0	1	0	7	3	10
Cc3	1	0	0	2	2	1	0	0	0	1	1	0	3	5	8
SQ1	2	0	0	10	22	0	1	0	0	6	10	0	37	14	51
SQ2	1	2	0	13	13	0	1	0	0	3	6	0	20	19	39
SQ3	2	0	0	1	2	0	0	0	0	3	5	0	9	4	13

Table 21. Sequence insertion or deletions in *Klebsiella pneumoniae* NCTC 13443 parent strains that were not detected in the respective disinfectant-tolerant samples. Each event refers to an insertion or deletion (InDel) of ≤ 50 bp. Details of the annotation statistics are as follows. Upstream: InDels located within 1 kb upstream of a gene start site. Exonic: InDels located in protein-coding sequence. Stop gain/loss: InDel leads to introduction or deletion of a stop codon. Frameshift: InDel changes the open reading frame. Non-frameshift: InDel does not change the open reading frame. Downstream: InDel located within 1 kb downstream of gene region. Upstream/Downstream: InDel located between 2 genes that are ≤ 2kb apart. Intergenic: InDel located in the > 2 kb intergenic region. Bz: benzalkonium chloride-tolerant sample. Dd: didecyldimethylammonium chloride-tolerant sample. Ph: polyhexamethylene biguanide-tolerant sample. Br: bronopol-tolerant sample. Cc: chlorocresol-tolerant sample. SQ: Disinfectant formulation "SQ53" -tolerant sample.

Sample	Up-stream	Exonic						Intronic	Splicing	Down-stream	Up-stream/ Down-stream	Intergenic	Total Insertion	Total Deletion	Total
		Stop gain	Stop loss	Frameshift		Non-frameshift									
				Deletion	Insertion	Deletion	Insertion								
Bz1G	3	0	0	51	30	0	0	0	0	6	47	0	51	86	137
Bz1D	3	0	0	45	28	0	0	0	0	5	51	0	52	80	132
Bz2G	3	0	0	47	28	0	0	0	0	5	51	0	51	83	134
Bz2D	4	0	0	47	26	0	0	0	0	5	51	0	49	84	133
Bz3	6	0	0	52	29	0	0	0	0	8	55	0	55	95	150
Dd1	5	1	0	48	27	0	0	0	0	6	51	0	51	87	138
Dd2	5	1	0	45	26	0	0	0	0	5	51	0	51	82	133
Dd3	10	1	0	86	39	0	0	0	0	11	79	0	76	150	226
Ph1	3	0	0	47	23	0	0	0	0	6	45	0	43	81	124
Ph2	3	0	0	50	25	0	0	0	0	12	48	0	48	90	138
Ph3	3	0	0	43	21	0	0	0	0	5	46	0	41	77	118
Br1	3	0	0	46	24	0	0	0	0	6	46	0	45	80	125
Br2	4	0	0	47	23	0	0	0	0	5	48	0	45	82	127
Br3	3	0	0	43	22	0	0	0	0	5	48	0	44	77	121
Cc1	7	0	0	47	24	0	0	0	0	7	48	1	48	86	134
Cc2	9	0	0	52	27	0	0	0	0	6	60	1	58	97	155
Cc3	9	0	0	46	21	0	0	0	0	6	50	1	48	85	133
SQ1	4	0	0	50	26	0	0	0	0	6	50	0	47	89	136
SQ2	0	0	0	7	1	0	0	0	0	0	3	0	1	10	11
SQ3	1	1	0	3	4	0	0	0	0	0	4	0	7	6	13

Table 22. Single nucleotide polymorphisms (SNPs) gained by disinfectant-tolerant *Klebsiella pneumoniae* NCTC 13443 samples in comparison to their respective untreated parent samples. Details of the annotation statistics are as follows. Upstream: SNPs located within 1 kb upstream of a gene start site. Exonic: SNPs located in protein-coding sequence. Stop gain/loss: SNP leads to introduction or removal of a stop codon. Synonymous: SNP does not lead to change in amino acid sequence. Downstream: SNP located within 1 kb downstream of gene region. Upstream/Downstream: SNP located between 2 genes that are ≤ 2kb apart. Intergenic: SNP located in the > 2 kb intergenic region. Bz: benzalkonium chloride-tolerant sample. Dd: didecyldimethylammonium chloride-tolerant sample. Ph: polyhexamethylene biguanide-tolerant sample. Br: bronopol-tolerant sample. Cc: chlorocresol-tolerant sample. SQ: Disinfectant formulation "SQ53" -tolerant sample.

Sample	Up-stream	Exonic				Intronic	Splicing	Down-stream	Up-stream/ Down-stream	Intergenic	Total
		Stop gain	Stop loss	Synonymous	Non-synonymous						
Bz1G	20	5	0	128	280	0	0	12	55	0	500
Bz1D	16	6	0	131	288	0	0	13	52	0	506
Bz2G	12	4	0	87	197	0	0	10	43	0	353
Bz2D	11	4	0	80	195	0	0	5	39	0	334
Bz3	13	3	0	94	192	0	0	10	40	0	352
Dd1	10	7	2	103	204	0	0	7	32	0	365
Dd2	9	7	2	102	202	0	0	7	38	0	367
Dd3	10	8	2	128	230	0	0	7	39	0	424
Ph1	0	0	0	3	4	0	0	0	2	0	9
Ph2	0	0	0	59	36	0	0	1	9	0	105
Ph3	0	0	0	9	4	0	0	1	3	0	17
Br1	1	0	0	5	13	0	0	0	1	0	20
Br2	1	0	0	6	10	0	0	0	1	0	18
Br3	0	0	0	4	7	0	0	1	0	0	12
Cc1	0	1	0	2	8	0	0	1	0	0	12
Cc2	0	0	0	1	8	0	0	1	0	0	10
Cc3	0	0	0	1	7	0	0	1	0	0	9
SQ1	9	7	0	80	143	0	0	6	26	0	271
SQ2	2	3	0	51	76	0	0	3	10	0	145
SQ3	4	7	0	42	88	0	0	4	15	1	161

Table 23. Single nucleotide polymorphisms (SNPs) in *Klebsiella pneumoniae* NCTC 13443 parent strains that were not detected in the respective disinfectant-tolerant samples. Details of the annotation statistics are as follows. Upstream: SNPs located within 1 kb upstream of a gene start site. Exonic: SNPs located in protein-coding sequence. Stop gain/loss: SNP leads to introduction or removal of a stop codon. Synonymous: SNP does not lead to change in amino acid sequence. Downstream: SNP located within 1 kb downstream of gene region. Upstream/Downstream: SNP located between 2 genes that are ≤ 2kb apart. Intergenic: SNP located in the > 2 kb intergenic region. Bz: benzalkonium chloride-tolerant sample. Dd: didecyldimethylammonium chloride-tolerant sample. Ph: polyhexamethylene biguanide-tolerant sample. Br: bronopol-tolerant sample. Cc: chlorocresol-tolerant sample. SQ: Disinfectant formulation "SQ53" -tolerant sample.

Sample	Up-stream	Exonic				Intronic	Splicing	Down-stream	Up-stream/ Down-stream	Intergenic	Total
		Stop gain	Stop loss	Synonymous	Non-synonymous						
Bz1G	0	0	0	0	0	0	0	1	1	0	2
Bz1D	0	0	0	0	0	0	0	0	1	0	1
Bz2G	0	0	0	0	0	0	0	2	1	0	3
Bz2D	0	0	0	0	0	0	0	0	1	0	1
Bz3	0	0	0	0	1	0	0	2	1	0	4
Dd1	0	0	0	0	0	0	0	5	2	0	7
Dd2	0	0	0	1	0	0	0	0	2	0	3
Dd3	0	0	0	0	0	0	0	0	2	0	2
Ph1	0	0	0	0	0	0	0	3	1	0	4
Ph2	0	0	0	1	0	0	0	3	1	0	5
Ph3	0	0	0	0	0	0	0	2	1	0	3
Br1	0	0	0	0	0	0	0	1	1	0	2
Br2	0	0	0	1	0	0	0	0	1	0	2
Br3	0	0	0	0	0	0	0	2	1	0	3
Cc1	0	0	0	0	0	0	0	2	1	0	3
Cc2	0	0	0	1	0	0	0	1	2	0	4
Cc3	0	0	0	0	0	0	0	1	2	0	3
SQ1	0	0	0	0	0	0	0	0	2	0	2
SQ2	0	0	0	1	0	0	0	1	0	0	2
SQ3	0	0	0	0	0	0	0	0	0	0	0

Table 24. Mutations detected in *Klebsiella pneumoniae* NCTC 13443 benzalkonium chloride-tolerant samples (Bz1G, Bz1D, Bz2G, Bz2D, and Bz3). Table categories as follows. Mutation type: type of mutation. Reference sequence: original nucleic acid sequence in the parent strain. Mutated sequence: mutated nucleic acid sequence in the respective tolerant sample. Gene: mutated gene. Protein product: product of the listed gene. SNP: single nucleotide polymorphism. Table contines on the next 2 pages.

Mutation Type	Reference Sequence	Mutated Sequence	Gene	Protein Product
frameshift deletion	T	-	*ascG_4*	LacI family transcriptional regulator
frameshift deletion	A	-	*cydA_5*	Cytochrome bd2
frameshift deletion	A	-	*entF_7*	enterobactin synthase subunit F
frameshift deletion	T	-	*intA_3*	integrase family protein
frameshift deletion	G	-	NCTC13443_02922	SD repeat-containing cell surface protein
frameshift deletion	G	-	NCTC13443_03262	antibiotic biosynthesis monooxygenase
frameshift deletion	GC	-	NCTC13443_04386	gluconate 2-dehydrogenase subunit gamma
frameshift deletion	A	-	NCTC13443_05638	Uncharacterised protein
frameshift deletion	C	-	NCTC13443_06478	Tail fibre protein
frameshift deletion	C	-	*prlC*	oligopeptidase A
frameshift deletion	C	-	*puo*	Putrescine oxidase
frameshift deletion	AC	-	*traI_2*	conjugal transfer nickase/helicase TraI
frameshift insertion	-	A	*ada_2*	ADA regulatory protein / Methylated-DNA-protein-cysteine methyltransferase
frameshift insertion	-	C	*bglH_2*	maltoporin
frameshift insertion	-	C	*ccmE*	cytochrome c-type biogenesis protein
frameshift insertion	-	T	*codB_1*	cytosine/purine/uracil/thiamine/allantoin permease family protein
frameshift insertion	-	G	*cstA_1*	Carbon starvation protein A
frameshift insertion	-	A	*cueR*	HTH-type transcriptional regulator cueR
frameshift insertion	-	C	*dus_1*	tRNA dihydrouridine synthase A
frameshift insertion	-	A	*eamA*	drug/metabolite transporter permease
frameshift insertion	-	G	*eutD*	phosphate acetyltransferase
frameshift insertion	-	A	*gmuB_4*	PTS system protein
frameshift insertion	-	T	*gmuD_2*	beta-glucosidase
frameshift insertion	-	C	*livJ_1*	hydrophobic amino acid ABC transporter periplasmic amino acid-binding protein
frameshift insertion	-	G	*moeB_2*	molybdopterin biosynthesis protein MoeB
frameshift insertion	-	A	NCTC13443_02541	B12-dependent methionine synthase
frameshift insertion	-	A	NCTC13443_03143	putative enzyme
frameshift insertion	-	T	NCTC13443_03206	Uncharacterised protein
frameshift insertion	-	C	NCTC13443_05033	thiamine biosynthesis protein ThiF
frameshift insertion	-	C	NCTC13443_05034	Uncharacterised protein
frameshift insertion	-	T	NCTC13443_05801	NAD(P)H-flavin oxidoreductase
frameshift insertion	-	GG	NCTC13443_07163	diguanylate cyclase
frameshift insertion	-	G	*panF_3*	sodium/panthothenate symporter
frameshift insertion	-	C	*qmcA*	stomatin/prohibitin-family membrane protease subunit YbbK
frameshift insertion	-	GG	*treF_2*	cytoplasmic trehalase
frameshift insertion	-	G	*tyrP_1*	tyrosine-specific transporter
frameshift insertion	-	C	*ves*	Various environmental stresses-induced protein
frameshift insertion	-	G	*ycfS_2*	LysM domain/ErfK/YbiS/YcfS/YnhG family protein
frameshift insertion	-	C	*yeaN_6*	cyanate transport protein CynX
frameshift insertion	-	C	*yfcA*	membrane protein YfcA
non-frameshift deletion	CGG	-	*mnmA*	thiouridylase
non-frameshift deletion	CTC CGC CCA ACA	-	*malT*	transcriptional regulator MalT
non-synonymous SNP	C	T	*acrB_6*	RND efflux system
non-synonymous SNP	T	C	*arnT*	4-amino-4-deoxy-L-arabinose transferase
non-synonymous SNP	C	T	*aroF*	phospho-2-dehydro-3-deoxyheptonate aldolase
non-synonymous SNP	C	T	*astB_1*	succinylarginine dihydrolase
non-synonymous SNP	C	T	*atpA_3*	ATP synthase subunit alpha
non-synonymous SNP	G	A	*basS*	sensor protein BasS/PmrB
non-synonymous SNP	A	G	*bioD_1*	dithiobiotin synthetase
non-synonymous SNP	G	A	*bsaA_2*	glutathione peroxidase
non-synonymous SNP	G	A	*btr*	4-hydroxyphenylacetate catabolism regulatory protein HpaA
non-synonymous SNP	T	C	*cmpB_2*	nitrate ABC transporter
non-synonymous SNP	C	G	*codB_1*	cytosine/purine/uracil/thiamine/allantoin permease family protein
non-synonymous SNP	G	A	*crp*	cyclic AMP receptor protein
non-synonymous SNP	T	C	*cusC_1*	copper/silver efflux system outer membrane protein CusC
non-synonymous SNP	G	A	*cysA_2*	sulphate and thiosulphate import ATP-binding protein CysA
non-synonymous SNP	A	G	*cysK_1*	cysteine synthase B
non-synonymous SNP	G	A	*cysW_1*	ABC transporter membrane protein
non-synonymous SNP	C	A	*cytR_3*	sugar-binding domain protein

Table 24 (continued).

Mutation Type	Reference Sequence	Mutated Sequence	Gene	Protein Product
non-synonymous SNP	C	T	*dadX*	alanine racemase
non-synonymous SNP	A	G	*dam_1*	methyl-directed repair DNA adenine methylase
non-synonymous SNP	A	G	*degP_1*	HtrA protease/chaperone protein
non-synonymous SNP	C	T	*deoC_1*	deoxyribose-phosphate aldolase
non-synonymous SNP	T	C	*dmlA_1*	tartrate dehydrogenase
non-synonymous SNP	C	T	*dppA_5*	antimicrobial peptide ABC transporter substrate-binding protein SapA
non-synonymous SNP	C	T	*entF_4*	enterobactin synthase subunit F
non-synonymous SNP	C	T	*envZ_2*	Osmolarity sensory histidine kinase EnvZ
non-synonymous SNP	A	G	*eptA_1*	putative cell division protein
non-synonymous SNP	A	G	*fabF_1*	3-oxoacyl-(acyl carrier protein) synthase II
non-synonymous SNP	C	T	*fepB*	Ferric enterobactin-binding periplasmic protein FepB
non-synonymous SNP	G	A	*fimD_9*	outer membrane protein for export and assembly of type 1 fimbriae
non-synonymous SNP	G	A	*fimD_9*	outer membrane protein for export and assembly of type 1 fimbriae
non-synonymous SNP	G	A	*fis*	DNA-binding protein Fis
non-synonymous SNP	C	T	*ganB*	galactosidase
non-synonymous SNP	C	T	*gbh*	Agmatinase
non-synonymous SNP	C	T	*gcvA_2*	glycine cleavage system transcriptional activator
non-synonymous SNP	C	T	*glnE*	glutamate-ammonia-ligase adenylyltransferase
non-synonymous SNP	G	A	*gloA*	Lactoylglutathione lyase
non-synonymous SNP	G	A	*glyA*	glycine hydroxymethyltransferase
non-synonymous SNP	C	T	*gsiA_9*	peptide transport system ATP-binding protein SapD
non-synonymous SNP	G	A	*hcpA_3*	Hcp family type VI secretion system effector
non-synonymous SNP	C	T	*icaB*	polysaccharide deacetylase
non-synonymous SNP	G	A	*idi_2*	isopentenyl-diphosphate delta-isomerase
non-synonymous SNP	C	T	*ilvD_3*	phosphogluconate dehydratase
non-synonymous SNP	T	C	*kdg*R	transcriptional regulator KdgR
non-synonymous SNP	T	C	*lacE_1*	PTS system protein
non-synonymous SNP	C	T	*lamB_4*	maltoporin
non-synonymous SNP	G	A	*leuA_3*	2-isopropylmalate synthase
non-synonymous SNP	T	C	*lolE*	outer membrane-specific lipoprotein transporter subunit LolE
non-synonymous SNP	G	A	*lon_2*	DNA-binding ATP-dependent protease La
non-synonymous SNP	T	C	*lptB_2*	lipopolysaccharide ABC transporter
non-synonymous SNP	C	T	*luxS*	S-ribosylhomocysteine lyase
non-synonymous SNP	T	C	*lysP_1*	Lysine-specific permease
non-synonymous SNP	C	T	*malH*	maltose-6'-phosphate glucosidase
non-synonymous SNP	G	T	*mipA*	MltA-interacting protein MipA
non-synonymous SNP	A	G	*msbA_2*	lipid A export ATP-binding/permease MsbA
non-synonymous SNP	G	A	*murG_2*	UDP-N-acetylglucosamine-N-acetylmuramyl-(pentapeptide) pyrophosphoryl-undecaprenol N-acetylglucosamine transferase
non-synonymous SNP	G	A	*mutY*	adenine DNA glycosylase
non-synonymous SNP	G	A	NCTC13443_00226	Uncharacterised protein
non-synonymous SNP	T	C	NCTC13443_00323	lipoprotein
non-synonymous SNP	C	T	NCTC13443_01284	5-keto-2-deoxygluconokinase
non-synonymous SNP	C	T	NCTC13443_01360	amine oxidase
non-synonymous SNP	A	G	NCTC13443_01431	transposase
non-synonymous SNP	C	T	NCTC13443_01522	phospholipase
non-synonymous SNP	G	A	NCTC13443_01557	inner membrane protein CreD
non-synonymous SNP	G	A	NCTC13443_02085	fumarate reductase/succinate dehydrogenase flavoprotein domain-containing protein
non-synonymous SNP	C	T	NCTC13443_02244	Uncharacterised protein
non-synonymous SNP	C	T	NCTC13443_02252	Uncharacterised protein
non-synonymous SNP	C	T	NCTC13443_02928	glycosyl transferase
non-synonymous SNP	C	T	NCTC13443_03209	terminase
non-synonymous SNP	C	T	NCTC13443_03672	auxin efflux carrier
non-synonymous SNP	T	C	NCTC13443_03977	AraC family transcriptional regulator
non-synonymous SNP	C	T	NCTC13443_03985	GntR family transcriptional regulator
non-synonymous SNP	T	C	NCTC13443_04134	alpha-L-rhamnosidase
non-synonymous SNP	G	A	NCTC13443_04491	3-beta hydroxysteroid dehydrogenase/isomerase family protein
non-synonymous SNP	G	A	NCTC13443_04522	selenoprotein O-like protein
non-synonymous SNP	G	A	NCTC13443_04782	phosphogluconate dehydratase
non-synonymous SNP	A	G	NCTC13443_04839	gp9
non-synonymous SNP	T	C	NCTC13443_04849	Lysozyme
non-synonymous SNP	C	T	NCTC13443_04850	Uncharacterised protein
non-synonymous SNP	G	A	NCTC13443_04875	TolA protein
non-synonymous SNP	T	C	NCTC13443_04971	membrane protein
non-synonymous SNP	T	C	NCTC13443_05458	Uncharacterised protein

Table 24 (continued).

Mutation Type	Reference Sequence	Mutated Sequence	Gene	Protein Product
non-synonymous SNP	T	C	NCTC13443_05650	2-polyprenylphenol hydroxylase related flavodoxin oxidoreductase
non-synonymous SNP	C	T	NCTC13443_06074	ImpA family type VI secretion-associated protein
non-synonymous SNP	A	G	NCTC13443_06079	Uncharacterised protein
non-synonymous SNP	A	G	NCTC13443_06203	Oligogalacturonate lyase
non-synonymous SNP	T	C	NCTC13443_06478	Tail fibre protein
non-synonymous SNP	A	C	NCTC13443_06601	hemolysin
non-synonymous SNP	C	T	NCTC13443_06709	putative cation transporter
non-synonymous SNP	T	G	NCTC13443_06725	membrane protein
non-synonymous SNP	C	T	NCTC13443_06725	membrane protein
non-synonymous SNP	A	G	NCTC13443_07298	type-F conjugative transfer system mating-pair stabilization protein TraN
non-synonymous SNP	C	T	NCTC13443_07417	StrB
non-synonymous SNP	G	A	*nfdA_1*	exoenzymes regulatory protein AepA
non-synonymous SNP	C	T	*nfnB_1*	Oxygen-insensitive NAD(P)H nitroreductase
non-synonymous SNP	A	G	*nikA_2*	nickel ABC transporter
non-synonymous SNP	C	T	*norG*	GntR family transcriptional regulator
non-synonymous SNP	G	A	*nuoM_1*	NADH-ubiquinone oxidoreductase subunit M
non-synonymous SNP	A	G	*phoC_2*	acid phosphatase
non-synonymous SNP	A	G	*phoR_4*	osmosensitive K+ channel histidine kinase KdpD
non-synonymous SNP	C	T	*pldA*	phospholipase A1
non-synonymous SNP	C	T	*plsB*	glycerol-3-phosphate acyltransferase
non-synonymous SNP	A	G	*plsC*	1-acyl-sn-glycerol-3-phosphate acyltransferase
non-synonymous SNP	C	T	*ppsA_1*	phosphoenolpyruvate synthase
non-synonymous SNP	T	C	*priC*	primosomal replication protein N"
non-synonymous SNP	C	T	*pulB*	pullulanase-specific type II secretion system component B
non-synonymous SNP	A	G	*rhaS_3*	AraC family transcriptional regulator
non-synonymous SNP	A	G	*rhlE*	ATP-dependent RNA helicase RhlE
non-synonymous SNP	T	C	*rluE*	ribosomal large subunit pseudouridine synthase E
non-synonymous SNP	G	A	*rnfG*	electron transport complex protein RnfG
non-synonymous SNP	C	T	*rplN*	50S ribosomal protein L14
non-synonymous SNP	A	G	*rpsD_1*	30S ribosomal protein S4
non-synonymous SNP	C	T	*rutG*	Uracil permease
non-synonymous SNP	G	A	*sbcB*	exodeoxyribonuclease I
non-synonymous SNP	A	G	*sbcD_2*	exonuclease SbcD
non-synonymous SNP	G	A	*setB*	sugar efflux transporter B
non-synonymous SNP	G	A	*setB*	sugar efflux transporter B
non-synonymous SNP	C	T	*surA*	survival protein SurA precursor (Peptidyl-prolyl cis-trans isomerase SurA)
non-synonymous SNP	G	A	*surE_1*	stationary phase survival protein SurE
non-synonymous SNP	T	C	*thiB*	thiamin ABC transporter
non-synonymous SNP	A	G	*tktA_1*	transketolase
non-synonymous SNP	T	C	*tonB*	transporter
non-synonymous SNP	C	T	*trpE_1*	anthranilate synthase
non-synonymous SNP	A	G	*tusE*	tRNA 2-thiouridine synthesizing protein E
non-synonymous SNP	C	T	*tvaI*	maltodextrin glucosidase
non-synonymous SNP	T	C	*ybhS_2*	ABC transporter
non-synonymous SNP	C	T	*ydcR_1*	GntR family transcriptional regulator
non-synonymous SNP	G	A	*yejB*	Oligopeptide transport system permease OppB
non-synonymous SNP	C	T	*ygbM_2*	hydroxypyruvate isomerase
non-synonymous SNP	G	A	*yggG_1*	exported zinc metalloprotease YfgC
stop gain	G	A	*afr_1*	Myo-inositol 2-dehydrogenase
stop gain	G	A	*narX_2*	nitrate/nitrite sensor protein
stop gain	G	A	*ssuB_5*	alkanesulfonates ABC transporter ATP-binding protein / Sulfonate ABC transporter

Table 25. Mutations detected in *Klebsiella pneumoniae* NCTC 13443 didecyldimethylammonium chloride-tolerant samples (Dd1, Dd2 and Dd3). Table categories as follows. Mutation type: type of mutation. Reference sequence: original nucleic acid sequence in the parent strain. Mutated sequence: mutated nucleic acid sequence in the respective tolerant sample. Gene: mutated gene. Protein product: product of the listed gene. SNP: single nucleotide polymorphism. Table continued on the next 3 pages.

Mutation Type	Reference Sequence	Mutated Sequence	Gene	Protein Product
frameshift deletion	G	-	*ampE*	AmpE protein
frameshift deletion	G	-	*traI_3*	conjugal transfer nickase/helicase TraI
frameshift deletion	G	-	NCTC13443_07068	conserved hypothetical signal peptide protein
frameshift deletion	G	-	*yjcC_2*	cyclic diguanylate phosphodiesterase (EAL) domain-containing protein
frameshift deletion	T	-	*ydcR_2*	GntR family transcriptional regulator
frameshift deletion	C	-	*galS*	Mgl repressor and galactose ultrainduction factor GalS
frameshift deletion	C	-	*tetA_2*	multidrug-efflux transporter, major facilitator superfamily (MFS)
frameshift deletion	C	-	*prlC*	oligopeptidase A
frameshift deletion	G	-	NCTC13443_02326	outer membrane protein romA
frameshift deletion	T	-	*artM_1*	phosphate transport ATP-binding protein PstB
frameshift deletion	G	-	*fusA_1*	translation elongation factor G
frameshift deletion	A	-	NCTC13443_05638	Uncharacterised protein
frameshift deletion	G	-	NCTC13443_04371	Uncharacterised protein
frameshift deletion	C	-	NCTC13443_04880	Uncharacterised protein
frameshift insertion	-	CC	*mhpC*	2-hydroxy-6-ketonona-2,4-dienedioic acid hydrolase
frameshift insertion	-	A	*ada_2*	ADA regulatory protein / Methylated-DNA-protein-cysteine methyltransferase
frameshift insertion	-	G	*feaB_1*	aldehyde dehydrogenase
frameshift insertion	-	T	*artI*	arginine ABC transporter substrate-binding protein
frameshift insertion	-	G	*ctfA*	bifunctional putative acetyl-CoA:acetoacetyl-CoA transferase: alpha subunit/beta subunit
frameshift insertion	-	GG	*copA_5*	copper resistance protein A
frameshift insertion	-	C	*copA_5*	copper resistance protein A
frameshift insertion	-	GG	*treF_2*	cytoplasmic trehalase
frameshift insertion	-	A	*repB*	DNA replication
frameshift insertion	-	A	*yfcG*	glutathione S-transferase
frameshift insertion	-	G	*ycfS_2*	LysM domain/ErfK/YbiS/YcfS/YnhG family protein
frameshift insertion	-	C	*bglH_2*	maltoporin
frameshift insertion	-	G	*moeB_2*	molybdopterin biosynthesis protein MoeB
frameshift insertion	-	G	*nikC_2*	nickel transport system permease protein NikC
frameshift insertion	-	C	NCTC13443_04866	Origin specific replication binding factor
frameshift insertion	-	A	NCTC13443_03229	phage protein
frameshift insertion	-	A	*gmuB_4*	PTS system protein
frameshift insertion	-	C	NCTC13443_05427	putative kinase
frameshift insertion	-	GG	*nepI_3*	putative MFS-family transport protein
frameshift insertion	-	C	*narZ*	respiratory nitrate reductase subunit alpha
frameshift insertion	-	C	*qseF*	sensory histidine kinase YfhA
frameshift insertion	-	A	NCTC13443_06493	terminase, endonuclease subunit (GpM)
frameshift insertion	-	A	NCTC13443_01315	Uncharacterised protein
non-frameshift deletion	CGG	-	*mnmA*	thiouridylase
non-frameshift deletion	CTC CGC CCA ACA	-	*malT*	transcriptional regulator MalT
non-frameshift deletion	CTG CTA CTG CTA CTG CTA	-	NCTC13443_07015	Uncharacterised protein
non-frameshift insertion	-	AAC AGC CAC	*traD_1*	conjugal transfer protein TraD
non-synonymous SNP	G	A	*hypD*	[NiFe] hydrogenase metallocenter assembly protein HypD
non-synonymous SNP	A	G	*plsC*	1-acyl-sn-glycerol-3-phosphate acyltransferase
non-synonymous SNP	A	G	*kdgT*	2-keto-3-deoxygluconate permease
non-synonymous SNP	G	A	*sra*	30S ribosomal subunit S22
non-synonymous SNP	G	A	NCTC13443_04491	3-beta hydroxysteroid dehydrogenase/isomerase family protein
non-synonymous SNP	A	G	*fabF_1*	3-oxoacyl-(acyl carrier protein) synthase II
non-synonymous SNP	C	T	*rplN*	50S ribosomal protein L14
non-synonymous SNP	C	T	NCTC13443_01284	5-keto-2-deoxygluconokinase
non-synonymous SNP	C	T	*ybhE*	6-phosphogluconolactonase
non-synonymous SNP	T	C	*potA_3*	ABC transporter
non-synonymous SNP	T	C	NCTC13443_02904	ABC transporter ATPase

Table 25 (continued).

Mutation Type	Reference Sequence	Mutated Sequence	Gene	Protein Product
non-synonymous SNP	G	A	*gsiA_17*	ABC transporter ATP-binding protein
non-synonymous SNP	A	G	*acs_2*	acetyl-CoA synthetase
non-synonymous SNP	G	A	*mutY*	adenine DNA glycosylase
non-synonymous SNP	C	T	*galM*	aldose 1-epimerase
non-synonymous SNP	G	A	NCTC13443_03908	alpha/beta hydrolase
non-synonymous SNP	T	C	NCTC13443_04134	alpha-L-rhamnosidase
non-synonymous SNP	G	A	NCTC13443_04134	alpha-L-rhamnosidase
non-synonymous SNP	C	T	*purF*	Amidophosphoribosyltransferase
non-synonymous SNP	G	A	*araC_3*	Arabinose operon regulatory protein
non-synonymous SNP	A	G	*artI*	arginine ABC transporter substrate-binding protein
non-synonymous SNP	G	A	NCTC13443_00262	AsmA family protein
non-synonymous SNP	C	T	NCTC13443_00263	AsmA family protein
non-synonymous SNP	C	T	NCTC13443_03571	ATP-dependent helicase hrpA
non-synonymous SNP	T	C	*hflB_2*	ATP-dependent metalloprotease
non-synonymous SNP	T	C	*uvrY*	BarA-associated response regulator UvrY (GacA, SirA)
non-synonymous SNP	T	C	*dmsA_1*	biotin sulfoxide reductase
non-synonymous SNP	A	G	*livF_1*	branched chain amino acid ABC transporter ATPase
non-synonymous SNP	C	T	NCTC13443_06939	branched-chain amino acid transport system permease LivM
non-synonymous SNP	C	T	*gltA_2*	Citrate synthase (si)
non-synonymous SNP	G	A	*cbiA*	cobyrinic acid a,c-diamide synthase
non-synonymous SNP	A	G	*trbB_1*	conjugal transfer protein TrbB
non-synonymous SNP	C	T	*yabI_2*	DedA-family integral membrane protein
non-synonymous SNP	A	G	*bioD_1*	dithiobiotin synthetase
non-synonymous SNP	G	A	*dam_3*	DNA adenine methylase
non-synonymous SNP	G	A	*yccS*	efflux (PET) family inner membrane protein YccS
non-synonymous SNP	G	A	*rnfG*	electron transport complex protein RnfG
non-synonymous SNP	C	T	*ksdD_2*	FAD-dependent oxidoreductase
non-synonymous SNP	C	T	*fepB*	Ferric enterobactin-binding periplasmic protein FepB
non-synonymous SNP	C	T	*ydcU_2*	Ferric iron ABC transporter
non-synonymous SNP	G	A	*fimA_3*	fimbrial protein
non-synonymous SNP	T	C	*ycgG_7*	fimbrial protein
non-synonymous SNP	C	T	*fsaB*	fructose-6-phosphate aldolase
non-synonymous SNP	C	T	*tcyC_4*	glutamine ABC transporter ATP-binding protein
non-synonymous SNP	C	T	*yxeN*	glutamine ABC transporter ATP-binding protein
non-synonymous SNP	C	T	*plsB*	glycerol-3-phosphate acyltransferase
non-synonymous SNP	G	A	*glpQ_3*	glycerophosphoryl diester phosphodiesterase
non-synonymous SNP	T	C	*ugpQ_2*	glycerophosphoryl diester phosphodiesterase
non-synonymous SNP	T	C	*gcvA_8*	glycine cleavage system transcriptional activator
non-synonymous SNP	T	A	*hflX_1*	GTP-binding protein HflX
non-synonymous SNP	C	T	*gmk*	guanylate kinase
non-synonymous SNP	A	C	NCTC13443_06601	hemolysin
non-synonymous SNP	G	A	*yycG*	histidine kinase
non-synonymous SNP	G	A	*hypF*	hydrogenase metallocenter assembly protein HypF
non-synonymous SNP	G	A	NCTC13443_06084	ImcF domain-containing protein
non-synonymous SNP	C	T	NCTC13443_06074	ImpA family type VI secretion-associated protein
non-synonymous SNP	G	A	NCTC13443_03769	inner membrane protein
non-synonymous SNP	G	A	*yicL*	inner membrane transporter yicL
non-synonymous SNP	C	T	*gsk_1*	inosine-guanosine kinase
non-synonymous SNP	T	A	*ppsE*	irp1
non-synonymous SNP	A	G	*ileS*	isoleucyl-tRNA synthetase
non-synonymous SNP	G	A	*idi_2*	isopentenyl-diphosphate delta-isomerase
non-synonymous SNP	G	A	*fucO_1*	Lactaldehyde reductase
non-synonymous SNP	C	T	*ansA_2*	L-asparaginase
non-synonymous SNP	A	G	*msbA_2*	lipid A export ATP-binding/permease MsbA
non-synonymous SNP	A	G	*lipA*	lipoate synthase
non-synonymous SNP	T	C	*gntU_2*	Low-affinity gluconate/H+ symporter GntU
non-synonymous SNP	T	C	*pitA_1*	Low-affinity inorganic phosphate transporter
non-synonymous SNP	T	C	*proW_1*	L-proline glycine betaine ABC transport system permease protein ProW
non-synonymous SNP	C	T	*cadA*	lysine decarboxylase 1
non-synonymous SNP	G	A	*gltR_2*	LysR family transcriptional regulator
non-synonymous SNP	T	C	*oxyR_2*	LysR family transcriptional regulator
non-synonymous SNP	T	C	*uxuA_1*	mannonate dehydratase
non-synonymous SNP	A	G	*pepN*	membrane alanine aminopeptidase N
non-synonymous SNP	T	G	NCTC13443_06725	membrane protein
non-synonymous SNP	C	T	NCTC13443_06725	membrane protein
non-synonymous SNP	T	C	*metI_4*	methionine ABC transporter permease
non-synonymous SNP	C	T	*metQ_2*	methionine ABC transporter substrate-binding protein
non-synonymous SNP	A	G	*map_1*	methionine aminopeptidase
non-synonymous SNP	C	T	NCTC13443_05221	methyltransferase
non-synonymous SNP	G	T	*mipA*	MltA-interacting protein MipA
non-synonymous SNP	C	T	*moeB_2*	molybdopterin biosynthesis protein MoeB

Table 25 (continued).

Mutation Type	Reference Sequence	Mutated Sequence	Gene	Protein Product
non-synonymous SNP	T	C	*acrR_2*	multidrug efflux pump acrAB operon transcription repressor
non-synonymous SNP	G	A	*mdtC_1*	multidrug transporter MdtB
non-synonymous SNP	C	T	*afr_2*	Myo-inositol 2-dehydrogenase
non-synonymous SNP	A	G	*bglK*	N-acetylmannosamine kinase
non-synonymous SNP	C	T	*ywnH*	N-acetyltransferase-like protein
non-synonymous SNP	C	T	*nuoN*	NADH-ubiquinone oxidoreductase subunit N
non-synonymous SNP	G	A	*narX_1*	nitrate/nitrite sensor protein
non-synonymous SNP	G	A	*ssuA_3*	nitrate/sulfonate/bicarbonate ABC transporter periplasmic protein
non-synonymous SNP	T	C	*mazG*	Nucleoside triphosphate pyrophosphohydrolase MazG
non-synonymous SNP	G	A	*yejB*	Oligopeptide transport system permease OppB
non-synonymous SNP	G	A	*fimD_9*	outer membrane protein for export and assembly of type 1 fimbriae
non-synonymous SNP	T	C	*fimD_9*	outer membrane protein for export and assembly of type 1 fimbriae
non-synonymous SNP	A	G	*pqiB*	paraquat-inducible protein B
non-synonymous SNP	A	G	*ampH*	penicillin-binding protein AmpH
non-synonymous SNP	G	A	*hmuT_2*	Periplasmic hemin-binding protein
non-synonymous SNP	G	A	*lptG*	Permease
non-synonymous SNP	G	A	NCTC13443_05444	phage portal protein
non-synonymous SNP	G	A	*pstC*	phosphate ABC transporter permease
non-synonymous SNP	G	A	NCTC13443_04782	phosphogluconate dehydratase
non-synonymous SNP	C	T	*pldA*	phospholipase A1
non-synonymous SNP	C	T	*phnD_1*	phosphonate ABC transporter substrate-binding protein
non-synonymous SNP	A	G	*serC*	phosphoserine aminotransferase
non-synonymous SNP	T	C	*kefA_3*	potassium efflux system KefA protein / Small-conductance mechanosensitive channel
non-synonymous SNP	A	G	NCTC13443_03204	Predicted ATP-binding protein involved in virulence
non-synonymous SNP	T	C	NCTC13443_06163	prepilin peptidase dependent protein B
non-synonymous SNP	T	C	*ddrA_3*	propanediol dehydratase reactivation factor large subunit
non-synonymous SNP	G	A	NCTC13443_05752	protein acetyltransferase
non-synonymous SNP	A	G	NCTC13443_00552	Protein of uncharacterised function (DUF3748)
non-synonymous SNP	G	A	*yhjK*	protein yhjK
non-synonymous SNP	T	C	*lacE_1*	PTS system protein
non-synonymous SNP	A	G	*hrsA*	PTS system transporter subunit IIA
non-synonymous SNP	C	T	NCTC13443_06709	putative cation transporter
non-synonymous SNP	A	G	*eptA_1*	putative cell division protein
non-synonymous SNP	G	T	*yhbX*	putative dehydrogenase
non-synonymous SNP	T	C	*pflA_2*	pyruvate formate-lyase activating enzyme
non-synonymous SNP	G	A	*yhdH*	quinone oxidoreductase
non-synonymous SNP	T	C	*narZ*	respiratory nitrate reductase subunit alpha
non-synonymous SNP	G	A	*ltrA_5*	Retron-type reverse transcriptase
non-synonymous SNP	C	T	*ltrA_7*	Retron-type reverse transcriptase
non-synonymous SNP	T	C	*yesR*	Rhamnogalacturonides degradation protein RhiN
non-synonymous SNP	C	T	*rna_1*	ribonuclease I
non-synonymous SNP	G	A	*rihA*	ribonucleoside hydrolase 1
non-synonymous SNP	G	A	*nrdA_4*	ribonucleotide reductase of class Ia
non-synonymous SNP	A	G	*nrdF_1*	ribonucleotide-diphosphate reductase subunit beta
non-synonymous SNP	A	G	NCTC13443_01516	ribosomal-protein-S18p-alanine acetyltransferase
non-synonymous SNP	C	T	*acrB_6*	RND efflux system
non-synonymous SNP	T	C	*bepE_3*	RND multidrug efflux transporter, Acriflavin resistance protein
non-synonymous SNP	A	G	NCTC13443_02920	SD repeat-containing cell surface protein
non-synonymous SNP	A	G	NCTC13443_02923	SD repeat-containing cell surface protein
non-synonymous SNP	G	A	NCTC13443_04522	selenoprotein O-like protein
non-synonymous SNP	G	A	*basS*	sensor protein BasS/PmrB
non-synonymous SNP	G	A	*pkn1_2*	serine/threonine kinase
non-synonymous SNP	G	A	*aroE_6*	shikimate 5-dehydrogenase
non-synonymous SNP	G	A	*surE_1*	stationary phase survival protein SurE
non-synonymous SNP	G	A	*setB*	sugar efflux transporter B
non-synonymous SNP	C	A	*cytR_3*	sugar-binding domain protein
non-synonymous SNP	G	A	*cysA_2*	sulphate and thiosulphate import ATP-binding protein CysA
non-synonymous SNP	G	A	*yedY_1*	sulfite oxidase subunit YedY
non-synonymous SNP	A	G	NCTC13443_01208	surface antigen
non-synonymous SNP	C	T	surA	survival protein SurA precursor (Peptidyl-prolyl cis-trans isomerase SurA)
non-synonymous SNP	T	C	NCTC13443_06478	Tail fibre protein
non-synonymous SNP	C	A	NCTC13443_06493	terminase, endonuclease subunit (GpM)
non-synonymous SNP	C	T	*thiI*	thiamine biosynthesis protein thiI
non-synonymous SNP	C	T	*thiK_2*	thiamine kinase
non-synonymous SNP	G	A	NCTC13443_04875	TolA protein
non-synonymous SNP	T	C	*soxS_3*	transcriptional activator RamA

Table 25 (continued).

Mutation Type	Reference Sequence	Mutated Sequence	Gene	Protein Product
non-synonymous SNP	C	T	*soxS_3*	transcriptional activator RamA
non-synonymous SNP	G	A	*ydcR_3*	transcriptional regulator of pyridoxine metabolism
non-synonymous SNP	T	C	NCTC13443_04116	transcriptional regulator TetR family
non-synonymous SNP	C	T	*tktB_4*	transketolase
non-synonymous SNP	T	C	*infB_1*	translation initiation factor 2
non-synonymous SNP	A	G	NCTC13443_01882	transpeptidase
non-synonymous SNP	T	C	*cydD*	transport ATP-binding protein CydD
non-synonymous SNP	T	C	*tonB*	transporter
non-synonymous SNP	T	C	NCTC13443_07086	transposase
non-synonymous SNP	T	A	NCTC13443_07459	transposase
non-synonymous SNP	T	C	*tnsB_3*	Transposon Tn7 transposition protein tnsB
non-synonymous SNP	T	C	NCTC13443_01559	TrmH family RNA methyltransferase
non-synonymous SNP	A	G	*trmJ_3*	tRNA:Cm32/Um32 methyltransferase
non-synonymous SNP	A	G	*hsdM_5*	type I restriction-modification system, M subunit
non-synonymous SNP	G	A	NCTC13443_00226	Uncharacterised protein
non-synonymous SNP	C	T	NCTC13443_02252	Uncharacterised protein
non-synonymous SNP	C	T	NCTC13443_03783	Uncharacterised protein
non-synonymous SNP	G	A	NCTC13443_04838	Uncharacterised protein
non-synonymous SNP	T	C	NCTC13443_04995	Uncharacterised protein
non-synonymous SNP	C	T	NCTC13443_04995	Uncharacterised protein
non-synonymous SNP	T	C	NCTC13443_05683	Uncharacterised protein
non-synonymous SNP	C	T	NCTC13443_02429	Uncharacterized conserved protein
non-synonymous SNP	T	C	*yqiC*	Uncharacterized protein conserved in bacteria
non-synonymous SNP	G	A	*vanB*	vanillate O-demethylase oxidoreductase
non-synonymous SNP	G	A	NCTC13443_06845	YccS/YhfK family integral membrane protein
non-synonymous SNP	T	C	*ratB*	yfjF
stop gain	G	A	NCTC13443_03908	alpha/beta hydrolase
stop gain	G	A	*fucK_2*	L-fuculokinase
stop gain	G	A	*ydiM*	MFS family transporter
stop gain	G	A	*narX_2*	nitrate/nitrite sensor protein
stop gain	C	T	NCTC13443_03443	OpgC protein
stop gain	C	T	NCTC13443_02172	transposase
stop gain	C	T	NCTC13443_03481	type VI secretion protein
stop loss	A	-	NCTC13443_07404	antirestriction protein
stop loss	A	G	*nadR_2*	NadR transcriptional regulator / Nicotinamide-nucleotide adenylyltransferase
stop loss	T	C	*scoA*	succinyl-CoA:3-ketoacid-coenzyme A transferase subunit A

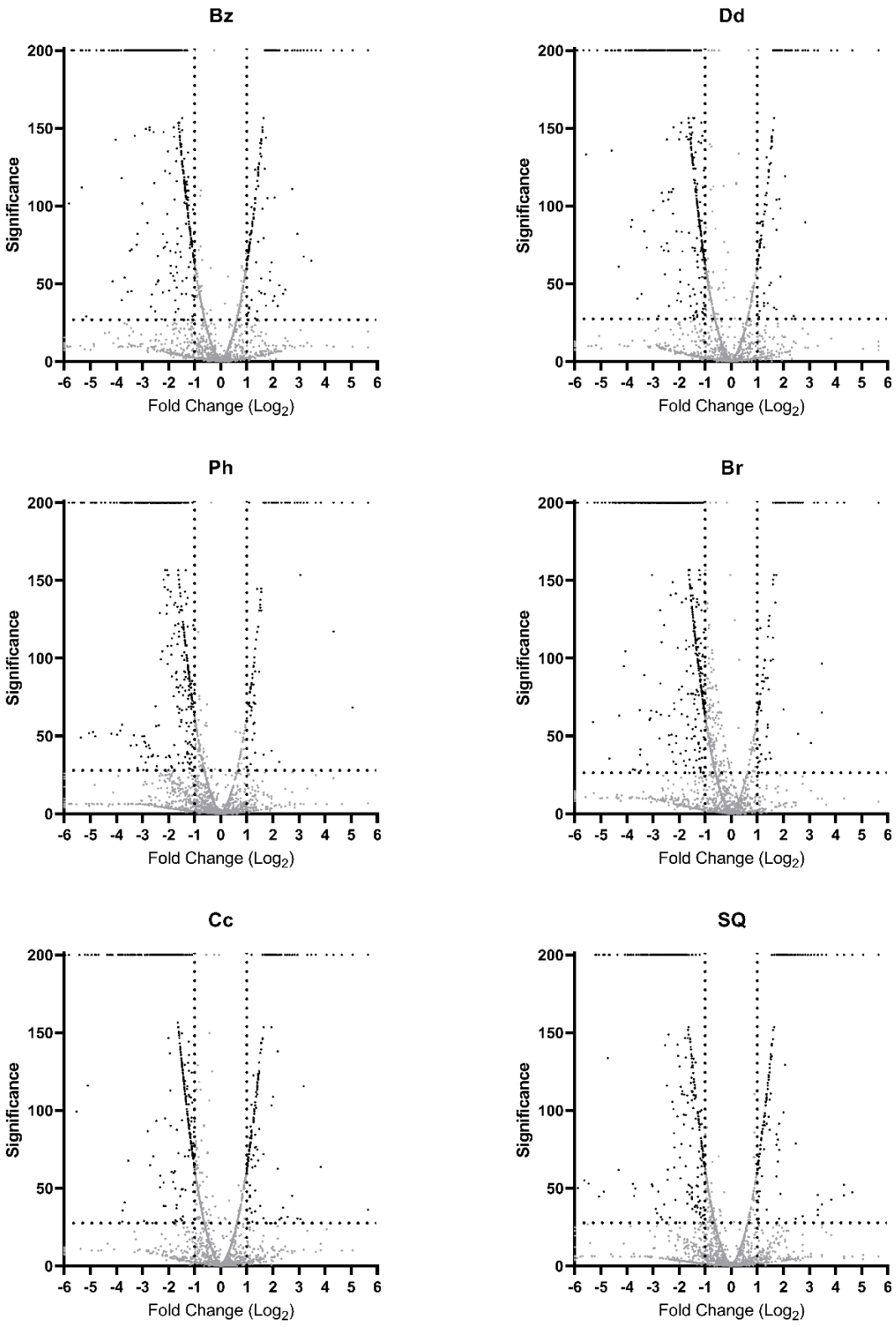

Figure 45. Volcano plots showing differentially expressed proteins between various disinfectant-tolerant *Klebsiella pneumoniae* NCTC 13443 samples and the untreated parent *Klebsiella pneumoniae* NCTC 13443 samples. Black dots denote differentially expressed proteins, and grey dots denote proteins without marked differences in expression. Bz: benzalkonium chloride-tolerant samples. Dd: didecyldimethylammonium chloride-tolerant samples. Ph: polyhexamethylene biguanide-tolerant samples. Br: bronopol-tolerant samples. Cc: chlorocresol-tolerant samples. SQ: disinfectant formulation "SQ53"-tolerant samples. Significance scores are equal to the $-10\log_{10}$ of the significance testing p-value, which was calculated via a paired T test in the PEAKS Studio Xpro software (Bioinformatics Solutions Inc.).

Table 26. Biological process gene ontology (GO) term enrichment analysis of differentially expressed proteins in *Klebsiella pneumoniae* NCTC 13443 disinfectant-tolerant samples. Conducted using the Database for Annotation, Visualization and Integrated Discovery (DAVID) online tool, with *K. pneumoniae* MGH 78578 used as the background annotated gene list. Input genes: number of genes that match the GO term from inputted list of genes. Total genes: total number of genes matching the GO term from the background gene list. Fold enrichment: measurement of the magnitude of enrichment of corresponding GO term.

Disinfectant treatment	Biological process GO term	Input genes	Total genes	Fold enrichment	Fold enrichment (log2)	P-value
Bz	D-ribose catabolic process	3	98	17.61	4.14	0.00998
Bz	DNA topological change	3	98	10.06	3.33	0.03216
Bz	one-carbon metabolic process	3	98	10.06	3.33	0.03216
Bz	protein folding	4	98	4.70	2.23	0.04919
Bz	translation	14	246	-2.11	-1.08	0.01142
Bz	tricarboxylic acid cycle	8	246	-3.25	-1.70	0.00780
Bz	Gram-negative-bacterium-type cell outer membrane assembly	5	246	-3.90	-1.96	0.03115
Bz	gluconeogenesis	6	246	-4.68	-2.23	0.00555
Bz	'de novo' IMP biosynthetic process	6	246	-4.68	-2.23	0.00555
Bz	arginine biosynthetic process	7	246	-5.46	-2.45	0.00073
Bz	glucuronate catabolic process	3	246	-9.35	-3.23	0.03150
Dd	D-ribose catabolic process	3	67	25.76	4.69	0.00468
Dd	translation	15	248	-2.24	-1.17	0.00473
Dd	tricarboxylic acid cycle	7	248	-2.82	-1.50	0.03018
Dd	glycolytic process	6	248	-3.98	-1.99	0.01213
Dd	'de novo' UMP biosynthetic process	4	248	-5.30	-2.41	0.03082
Dd	gluconeogenesis	7	248	-5.41	-2.44	0.00076
Dd	'de novo' IMP biosynthetic process	7	248	-5.41	-2.44	0.00076
Dd	arginine biosynthetic process	7	248	-5.41	-2.44	0.00076
Dd	glycogen biosynthetic process	3	248	-9.28	-3.21	0.03200
Dd	glucuronate catabolic process	3	248	-9.28	-3.21	0.03200
Ph	D-ribose catabolic process	3	62	27.83	4.80	0.00401
Ph	thiamine diphosphate biosynthetic process	3	62	12.37	3.63	0.02208
Ph	thiamine biosynthetic process	3	62	9.28	3.21	0.03847
Ph	translation	15	234	-2.38	-1.25	0.00275
Ph	arginine biosynthetic process	5	234	-4.10	-2.03	0.02637
Ph	glycolytic process	6	234	-4.21	-2.08	0.00949
Ph	tricarboxylic acid cycle	10	234	-4.28	-2.10	0.00022
Ph	pentose-phosphate shunt	4	234	-5.62	-2.49	0.02636
Ph	'de novo' UMP biosynthetic process	4	234	-5.62	-2.49	0.02636
Ph	gluconeogenesis	7	234	-5.74	-2.52	0.00055
Br	D-ribose catabolic process	3	50	34.51	5.11	0.00259
Br	glycolytic process	3	50	9.86	3.30	0.03435
Br	lysine biosynthetic process via diaminopimelate	3	50	9.20	3.20	0.03910
Br	tricarboxylic acid cycle	8	321	-2.49	-1.32	0.03150
Br	translation	22	321	-2.54	-1.35	0.00004
Br	glycolytic process	6	321	-3.07	-1.62	0.03456
Br	'de novo' IMP biosynthetic process	6	321	-3.58	-1.84	0.01730
Br	gluconeogenesis	7	321	-4.18	-2.06	0.00305
Br	arginine biosynthetic process	7	321	-4.18	-2.06	0.00305
Br	Gram-negative-bacterium-type cell outer membrane assembly	8	321	-4.78	-2.26	0.00040
Br	protein insertion into membrane	4	321	-4.78	-2.26	0.03855
Cc	D-ribose catabolic process	3	91	18.96	4.25	0.00862
Cc	histidine catabolic process to glutamate and formamide	3	91	18.96	4.25	0.00862
Cc	histidine catabolic process to glutamate and formate	3	91	18.96	4.25	0.00862
Cc	arginine catabolic process to glutamate	3	91	12.64	3.66	0.02048
Cc	arginine catabolic process to succinate	3	91	12.64	3.66	0.02048
Cc	thiamine diphosphate biosynthetic process	3	91	8.43	3.08	0.04554
Cc	translation	25	218	-4.26	-2.09	0.00000
Cc	gluconeogenesis	5	218	-4.40	-2.14	0.02075
Cc	Gram-negative-bacterium-type cell outer membrane assembly	6	218	-5.28	-2.40	0.00325
SQ	arginine catabolic process to glutamate	5	90	21.31	4.41	0.00003
SQ	arginine catabolic process to succinate	5	90	21.31	4.41	0.00003
SQ	D-ribose catabolic process	3	90	19.17	4.26	0.00844
SQ	histidine catabolic process to glutamate and formamide	3	90	19.17	4.26	0.00844
SQ	histidine catabolic process to glutamate and formate	3	90	19.17	4.26	0.00844
SQ	cellular amino acid catabolic process	3	90	15.34	3.94	0.01371
SQ	diaminopimelate biosynthetic process	3	90	15.34	3.94	0.01371
SQ	thiamine diphosphate biosynthetic process	3	90	8.52	3.09	0.04462
SQ	lysine biosynthetic process via diaminopimelate	4	90	6.82	2.77	0.01816
SQ	translation	16	185	-3.21	-1.68	0.00006
SQ	glycolytic process	5	185	-4.44	-2.15	0.02094
SQ	Gram-negative-bacterium-type cell outer membrane assembly	6	185	-6.22	-2.64	0.00154
SQ	protein insertion into membrane	4	185	-8.29	-3.05	0.00840
SQ	glycerol-3-phosphate metabolic process	3	185	-9.33	-3.22	0.03426
SQ	D-xylose metabolic process	4	185	-12.44	-3.64	0.00190

Table 27. Cellular component gene ontology (GO) term enrichment analysis of differentially expressed proteins in *Klebsiella pneumoniae* NCTC 13443 disinfectant-tolerant samples. Conducted using the Database for Annotation, Visualization and Integrated Discovery (DAVID) online tool, with *K. pneumoniae* MGH 78578 used as the background annotated gene list. Input genes: number of genes that match the GO term from inputted list of genes. Total genes: total number of genes matching the GO term from the background gene list. Fold enrichment: measurement of the magnitude of enrichment of corresponding GO term.

Disinfectant treatment	Cellular component GO term	Input genes	Total genes	Fold enrichment	Fold enrichment (log2)	P-value
Bz	chromosome	3	75	11.81	3.56	0.02365
Bz	cytoplasm	49	75	2.90	1.53	0.00000
Bz	cytoplasm	63	157	-1.78	-0.83	0.00000
Bz	periplasmic space	14	157	-3.29	-1.72	0.00017
Bz	ribosome	13	157	-3.89	-1.96	0.00006
Bz	proton-transporting ATP synthase complex, catalytic core F(1)	3	157	-7.90	-2.98	0.04868
Dd	cytoplasm	32	42	3.38	1.76	0.00000
Dd	cytoplasm	67	162	-1.83	-0.87	0.00000
Dd	periplasmic space	10	162	-2.28	-1.19	0.02651
Dd	ribosome	12	162	-3.48	-1.80	0.00037
Ph	cytoplasm	26	33	3.49	1.80	0.00000
Ph	cytoplasm	60	150	-1.77	-0.83	0.00000
Ph	periplasmic space	11	150	-2.71	-1.44	0.00558
Ph	ribosome	12	150	-3.76	-1.91	0.00018
Br	cytoplasm	23	29	3.52	1.81	0.00000
Br	cytoplasm	95	234	-1.80	-0.85	0.00000
Br	cell outer membrane	18	234	-2.21	-1.14	0.00192
Br	ribosome	14	234	-2.81	-1.49	0.00072
Br	small ribosomal subunit	4	234	-5.89	-2.56	0.02186
Br	proton-transporting ATP synthase complex, catalytic core F(1)	4	234	-7.06	-2.82	0.01191
Cc	cytoplasm	38	59	2.86	1.51	0.00000
Cc	cytoplasm	59	169	-1.55	-0.63	0.00015
Cc	cell outer membrane	13	169	-2.21	-1.14	0.01150
Cc	ribosome	17	169	-4.72	-2.24	0.00000
Cc	large ribosomal subunit	4	169	-6.11	-2.61	0.02179
Cc	small ribosomal subunit	4	169	-8.15	-3.03	0.00879
SQ	outer membrane-bounded periplasmic space	4	49	5.27	2.40	0.03642
SQ	cytoplasm	29	49	2.62	1.39	0.00000
SQ	cytoplasm	49	144	-1.51	-0.59	0.00117
SQ	cell outer membrane	13	144	-2.59	-1.37	0.00313
SQ	ribosome	11	144	-3.59	-1.84	0.00059

Table 28. Number of viable but nonculturable (VBNC) bacteria in *Klebsiella pneumoniae* NCTC 9633 samples after exposure to varying concentrations of benzalkonium chloride (BAC), as enumerated via different VBNC quantification methods. To calculate the number of VBNCs by the direct viable count (DVC) and live/dead methodologies, the number of culturable cells are taken away from the number of total viable cells as enumerated via the respective methodology. DVC: direct viable count. PE: proliferation exclusion. CFU: colony forming units. * : Negative values arise through there being a greater number of culturable cells than viable cells.

BAC concentration (µg/ml)	Biological replicate	Culturable cells (CFU/ml)	DVC total viable cells (cells/ml)	Live/dead total viable cells (cells/ml)	DVC VBNCs (cells/ml)	Live/dead VBNCs (cells/ml)	PE VBNCs (cells/ml)	Mean Average (cells/ml)			Standard deviation		
								DVC VBNCs	Live/dead VBNCs	PE VBNCs	DVC VBNCs	Live/dead VBNCs	PE VBNCs
0	1	6.07E+09	5.56E+09	2.23E+09	-5.09E+08*	-3.83E+09*	4.89E+07	-5.18E+08*	-2.44E+09*	7.12E+07	2.30E+08	1.22E+09	1.94E+07
	2	4.07E+09	3.77E+09	2.48E+09	-2.94E+08*	-1.58E+09*	8.31E+07						
	3	3.93E+09	3.18E+09	2.04E+09	-7.53E+08*	-1.90E+09*	8.17E+07						
4	1	3.07E+09	2.86E+09	1.49E+09	-2.07E+08*	-1.58E+09*	1.11E+08	-5.91E+08*	-1.28E+09*	1.56E+08	4.37E+08	3.37E+08	4.10E+07
	2	2.33E+09	1.83E+09	1.42E+09	-5.00E+08*	-9.15E+08*	1.64E+08						
	3	2.60E+09	1.53E+09	1.25E+09	-1.07E+09*	-1.35E+09*	1.92E+08						
8	1	2.47E+09	1.71E+09	1.25E+09	-7.53E+08*	-1.22E+09*	1.16E+07	-8.84E+08*	-8.24E+08*	1.84E+07	1.19E+08	3.44E+08	6.02E+06
	2	1.60E+09	6.88E+08	9.87E+08	-9.12E+08*	-6.13E+08*	2.04E+07						
	3	1.73E+09	7.48E+08	1.10E+09	-9.86E+08*	-6.38E+08*	2.32E+07						
12	1	6.00E+02	3.53E+04	3.67E+07	3.47E+04	3.67E+07	6.06E+04	1.10E+06	5.92E+07	1.73E+06	1.59E+06	2.64E+07	2.13E+06
	2	6.80E+03	3.39E+05	5.26E+07	3.32E+05	5.25E+07	1.00E+06						
	3	6.27E+03	2.93E+06	8.82E+07	2.93E+06	8.82E+07	4.12E+06						
16	1	3.27E+03	2.33E+05	5.70E+07	2.29E+05	5.70E+07	2.02E+05	3.10E+05	5.75E+07	6.13E+05	8.54E+04	4.32E+06	6.26E+05
	2	3.20E+03	3.03E+05	5.35E+07	3.00E+05	5.35E+07	1.33E+06						
	3	2.60E+03	4.02E+05	6.21E+07	3.99E+05	6.21E+07	3.03E+05						
20	1	1.00E+03	2.89E+05	5.33E+07	2.88E+05	5.33E+07	1.41E+05	1.45E+05	5.52E+07	6.35E+05	1.47E+05	1.42E+07	4.42E+05
	2	4.67E+03	0.00E+00	4.20E+07	-4.67E+03*	4.20E+07	9.94E+05						
	3	3.60E+03	1.55E+05	7.03E+07	1.52E+05	7.03E+07	7.68E+05						

Table 29. Number of viable but nonculturable (VBNC) bacteria in *Klebsiella pneumoniae* NCTC 9633 samples after exposure to varying concentrations of didecyldimethylammonium chloride (DDAC), as enumerated via different VBNC quantification methods. To calculate the number of VBNCs by the direct viable count (DVC) and live/dead methodologies, the number of culturable cells are taken away from the number of total viable cells as enumerated via the respective methodology. DVC: direct viable count. PE: proliferation exclusion. CFU: colony forming units. * : Negative values arise through there being a greater number of culturable cells than viable cells.

DDAC concentration (µg/ml)	Biological replicate	Culturable cells (CFU/ml)	DVC total viable cells (cells/ml)	Live/dead total viable cells (cells/ml)	DVC VBNCs (cells/ml)	Live/dead VBNCs (cells/ml)	PE VBNCs (cells/ml)	Mean Average (cells/ml)			Standard deviation		
								DVC VBNCs	Live/dead VBNCs	PE VBNCs	DVC VBNCs	Live/dead VBNCs	PE VBNCs
0	1	4.13E+09	3.53E+09	2.22E+09	-6.00E+08*	-1.92E+09*	3.84E+07	-2.9E+08*	-1.06E+09*	6.77E+07	2.71E+08	7.44E+08	2.54E+07
	2	2.67E+09	2.55E+09	2.10E+09	-1.14E+08*	-5.69E+08*	8.13E+07						
	3	2.93E+09	2.78E+09	2.24E+09	-1.51E+08*	-6.94E+08*	8.35E+07						
4	1	2.20E+09	2.48E+09	1.92E+09	2.75E+08	-2.75E+08*	9.59E+07	3.47E+08	-3.49E+07*	1.04E+08	3.02E+08	7.77E+08	7.26E+06
	2	2.73E+09	2.82E+09	2.07E+09	8.77E+07	-6.63E+08*	1.05E+08						
	3	8.67E+08	1.54E+09	1.70E+09	6.78E+08	8.34E+08	1.10E+08						
8	1	1.33E+06	3.73E+07	1.98E+08	3.60E+07	1.97E+08	3.28E+07	1.90E+07	3.17E+08	2.40E+07	1.77E+07	1.04E+08	1.87E+07
	2	1.67E+07	1.73E+07	3.92E+08	6.83E+05	3.76E+08	2.43E+06						
	3	6.67E+06	2.70E+07	3.86E+08	2.03E+07	3.79E+08	3.67E+07						
12	1	0.00E+00	5.22E+05	8.03E+07	5.22E+05	8.03E+07	1.72E+06	4.53E+05	8.00E+07	1.44E+06	9.99E+04	1.86E+06	3.94E+05
	2	4.67E+02	3.39E+05	8.16E+07	3.38E+05	8.16E+07	9.90E+05						
	3	3.13E+03	5.01E+05	7.80E+07	4.98E+05	7.80E+07	1.62E+06						

Table 30. Number of viable but nonculturable (VBNC) bacteria in *Klebsiella pneumoniae* NCTC 9633 samples after exposure to varying concentrations of polyhexamethylene biguanide (PHMB), as enumerated via different VBNC quantification methods. To calculate the number of VBNCs by the direct viable count (DVC) and live/dead methodologies, the number of culturable cells are taken away from the number of total viable cells as enumerated via the respective methodology. PE: proliferation exclusion. CFU: colony forming units. X: contaminated, sample not used. * : Negative values arise through there being a greater number of culturable cells than viable cells.

PHMB concentration (µg/ml)	Biological replicate	Culturable cells (CFU/ml)	DVC total viable cells (cells/ml)	Live/dead total viable cells (cells/ml)	DVC VBNCs (cells/ml)	Live/dead VBNCs (cells/ml)	PE VBNCs (cells/ml)	Mean Average (cells/ml)			Standard deviation		
								DVC VBNCs	Live/dead VBNCs	PE VBNCs	DVC VBNCs	Live/dead VBNCs	PE VBNCs
0	1	4.00E+09	4.07E+09	2.22E+09	7.29E+07	-1.78E+09*	5.54E+07	-2.0E+07*	-1.30E+09*	4.94E+07	1.8E+08	4.25E+08	6.63E+06
	2	3.07E+09	2.84E+09	2.10E+09	-2.28E+08*	-9.69E+08*	5.05E+07						
	3	3.40E+09	3.49E+09	2.24E+09	9.46E+07	-1.16E+09*	4.23E+07						
3	1	2.73E+09	2.84E+09	1.92E+09	1.05E+08	-8.08E+08*	3.35E+07	1.13E+08	-3.24E+08*	3.57E+07	6.33E+07	5.92E+08	6.03E+06
	2	1.73E+09	1.79E+09	2.07E+09	5.45E+07	3.37E+08	3.11E+07						
	3	2.20E+09	2.38E+09	1.70E+09	1.80E+08	-5.00E+08*	4.25E+07						
6	1	7.33E+06	X	1.98E+08	X	1.91E+08	1.73E+07	3.96E+08	3.12E+08	3.76E+07	5.03E+08	1.05E+08	1.91E+07
	2	2.00E+07	5.99E+07	3.92E+08	3.99E+07	3.72E+08	5.54E+07						
	3	1.33E+07	7.65E+08	3.86E+08	7.52E+08	3.73E+08	4.00E+07						
9	1	1.60E+03	2.82E+05	8.03E+07	2.81E+05	8.03E+07	6.67E+05	3.79E+05	8.00E+07	1.09E+06	1.77E+05	1.86E+06	1.03E+06
	2	1.40E+03	5.85E+05	8.16E+07	5.84E+05	8.16E+07	2.26E+06						
	3	1.47E+03	2.75E+05	7.80E+07	2.74E+05	7.80E+07	3.44E+05						

References

[1] R. Girard *et al.*, "World Health Organization Prevention of hospital-acquired infections, a practical guide. 2nd edition," 2002.

[2] (WHO) World Health Organization, "Report on the Burden of Endemic Health Care-Associated Infection Worldwide," Geneva, 2011. [Online]. Available: https://www.ncbi.nlm.nih.gov/books/NBK144030/.

[3] J. Vincent, "Nosocomial infections in adult intensive-care units," *Lancet*, vol. 361, pp. 2068–2077, 2003.

[4] European Centre for Disease Prevention and Control, "Annual Epidemiological Report on Communicable Diseases in Europe 2008," 2008.

[5] H. A. Khan, F. K. Baig, and R. Mehboob, "Nosocomial infections: Epidemiology, prevention, control and surveillance," *Asian Pac. J. Trop. Biomed.*, vol. 7, no. 5, pp. 478–482, 2017, doi: 10.1016/j.apjtb.2017.01.019.

[6] S. . Wright and V. . Bieluch, "Selected nosocomial viral infections.," *Hear. Lung, J. Crit. Care.*, vol. 22, no. 2, pp. 183–187, 1993.

[7] S. S. Magill *et al.*, "Multistate Point-Prevalence Survey of Health Care-Associated Infections," *N. Engl. J. Med.*, vol. 370, no. 13, pp. 1198–1208, 2014, doi: 10.1056/NEJMoa1306801.

[8] S. S. Magill *et al.*, "Changes in Prevalence of Health Care–Associated Infections in U.S. Hospitals," *N. Engl. J. Med.*, vol. 379, no. 18, pp. 1732–1744, 2018, doi: 10.1056/NEJMoa1801550.

[9] B. Allegranzi *et al.*, "Burden of endemic health-care-associated infection in developing countries: systematic review and meta-analysis," *Lancet*, vol. 377, pp. 228–241, 2011, doi: 10.1016/S0140-6736(10)61458-4.

[10] Q. Zhu *et al.*, "Phylogenomics of 10,575 genomes reveals evolutionary proximity between domains Bacteria and Archaea," *Nat. Commun.*, vol. 10, 2019, doi: 10.1038/s41467-019-13443-4.

[11] M. R. J. Salton and K.-S. Kim, "Chapter 2. Structure," in *Medical Microbiology. 4th edition.*, Galveston (TX), 1996.

[12] J. W. Bartholomew and T. Mittwer, "The Gram Stain," *Bacteriol. Rev.*, vol. 16, no. 1, pp. 1–29, 1952.

[13] T. J. Silhavy, D. Kahne, and S. Walker, "The Bacterial Cell Envelope1 T. J. Silhavy, D. Kahne and S. Walker, .," *Cold Spring Harb. Perspect. Biol.*, vol. 2, no. 5, 2010, doi: 10.1101/cshperspect.a000414.

[14] F. C. Neuhaus and J. Baddiley, "A Continuum of Anionic Charge: Structures and Functions of D -Alanyl-Teichoic Acids in Gram-Positive Bacteria," *Microbiol. Mol. Biol. Rev.*, vol. 67, no. 4, pp. 686–723, 2003, doi: 10.1128/MMBR.67.4.686.

[15] A. H. Delcour, "Outer Membrane Permeability and Antibiotic Resistance," *Biochim Biophys Acta.*, vol. 1794, no. 5, pp. 808–816, 2009, doi: 10.1016/j.bbapap.2008.11.005.Outer.

[16] O. D. Novikova and T. F. Solovyeva, "Nonspecific porins of the outer membrane of

Gram-negative bacteria: Structure and functions," *Biochem. Suppl. Ser. A Membr. Cell Biol.*, vol. 3, no. 1, pp. 3–15, 2009, doi: 10.1134/s1990747809010024.

[17] L. Brown, J. M. Wolf, R. Prados-rosales, and A. Casadevall, "Through the wall: extracellular vesicles in Gram-positive bacteria , mycobacteria and fungi," *Nat. Rev. Microbiol.*, vol. 13, pp. 620–630, 2015, doi: 10.1038/nrmicro3480.

[18] P. W. Schreiber, H. S. Prof, A. Wolfensberger, L. Clack, S. P. Kuster, and Swissnoso, "The preventable proportion of healthcare-associated infections 2005–2016: Systematic review and meta-analysis," *Infect. Control Hosp. Epidemiol.*, vol. 39, pp. 1277–1295, 2018, doi: 10.1017/ice.2018.183.

[19] (WHO) World Health Organization, "WHO Guidelines on Hand Hygiene in Health Care," Geneva, 2017. doi: 10.1086/600379.

[20] (CDC) Centers of Disease Control and Prevention, "Morbidity and Mortality Weekly Report Guideline for Hand Hygiene in Health-Care Settings," 2002.

[21] World Health Organization, "Evidence of hand hygiene as the building block for infection prevention and control," 2017.

[22] K. V. Nguyen, P. T. M. Nguyen, and S. L. Jones, "Effectiveness of an alcohol-based hand hygiene programme in reducing nosocomial infections in the Urology Ward of Binh Dan Hospital, Vietnam," *Trop. Med. Int. Heal.*, vol. 13, no. 10, pp. 1297–1302, 2008, doi: 10.1111/j.1365-3156.2008.02141.x.

[23] L. T. A. Thu, M. J. Dibley, V. Van Nho, L. Archibald, W. R. Jarvis, and A. H. Sohn, "Reduction in Surgical Site Infections in Neurosurgical Patients Associated With a Bedside Hand Hygiene Program in Vietnam," *Infect. Control Hosp. Epidemiol.*, vol. 28, no. 05, pp. 583–588, 2007, doi: 10.1086/516661.

[24] V. D. Rosenthal, S. Guzman, and N. Safdar, "Reduction in nosocomial infection with improved hand hygiene in intensive care units of a tertiary care hospital in Argentina," *Am. J. Infect. Control*, vol. 33, no. 7, pp. 392–397, 2005, doi: 10.1016/j.ajic.2004.08.009.

[25] D. Pittet *et al.*, "Effectiveness of a hospital-wide programme to improve compliance with hand hygiene," *Lancet*, vol. 356, pp. 1307–1312, 2000.

[26] V. Erasmus *et al.*, "Systematic Review of Studies on Compliance with Hand Hygiene Guidelines in Hospital Care," *Infect. Control Hosp. Epidemiol.*, vol. 31, no. 3, pp. 283–294, 2000, doi: 10.1086/650451.

[27] Council of the European Union, "Regulation concerning the making available on the market and use of biocidal products," *Off. J. Eur. Union*, 2012, doi: 10.3000/19770677.L_2012.167.eng.

[28] Council of the European Union, "EU Guidelines for the prudent use of antimicrobials in human health (2017/C 212/01)," *Off. J. Eur. Union*, 2017, doi: 10.1097/ipc.0b013e318068b1c0.

[29] W. A. Rutala and D. J. Weber, "Guideline for Disinfection and Sterilization in Healthcare Facilities (2008)," Atlanta, 2008. [Online]. Available: https://www.cdc.gov/infectioncontrol/guidelines/disinfection/index.html.

[30] H. Lei, R. M. Jones, and Y. Li, "Exploring surface cleaning strategies in hospital to prevent contact transmission of methicillin-resistant Staphylococcus aureus," *BMC Infect. Dis.*, vol. 17, no. 85, 2017, doi: 10.1186/s12879-016-2120-z.

[31] K. Saka, A. Akanbi, T. Obasa, R. Raheem, and A. Oshodi, "Bacterial Contamination of Hospital Surfaces According to Material Make, Last Time of Contact and Last Time of Cleaning/Disinfection," *J. Bacteriol. Parasitol.*, vol. 08, no. 03, pp. 8–11, 2017, doi: 10.4172/2155-9597.1000312.

[32] A. A. Pochtovyi *et al.*, "Contamination of Hospital Surfaces with Bacterial Pathogens under the Current COVID-19 Outbreak," *Int. J. Environ. Res. Public Health*, vol. 18, 2021.

[33] V. Russotto, A. Cortegiani, S. M. Raineri, and A. Giarratano, "Bacterial contamination of inanimate surfaces and equipment in the intensive care unit," *J. Intensive Care*, vol. 3, no. 54, 2015, doi: 10.1186/s40560-015-0120-5.

[34] G. Grass, C. Rensing, and M. Solioz, "Metallic Copper as an Antimicrobial Surface," *Appl. Environ. Microbiol.*, vol. 77, no. 5, pp. 1541–1547, 2011, doi: 10.1128/aem.02766-10.

[35] M. Rai, A. Yadav, and A. Gade, "Silver nanoparticles as a new generation of antimicrobials," *Biotechnol. Adv.*, vol. 27, pp. 76–83, 2009, doi: 10.1016/j.biotechadv.2008.09.002.

[36] J. O. Noyce, H. Michels, and C. W. Keevil, "Potential use of copper surfaces to reduce survival of epidemic meticillin-resistant Staphylococcus aureus in the healthcare environment," *J. Hosp. Infect.*, vol. 63, no. 3, pp. 289–297, 2006, doi: 10.1016/j.jhin.2005.12.008.

[37] W. Sim, R. T. Barnard, and Z. M. Ziora, "Antimicrobial Silver in Medicinal and Consumer Applications : A Patent Review of the Past Decade (2007-2017)," *Antibiotics*, vol. 7, no. 93, 2018, doi: 10.3390/antibiotics7040093.

[38] C. Adlhart *et al.*, "Surface modifications for antimicrobial effects in the healthcare setting: a critical overview," *J. Hosp. Infect.*, vol. 99, no. 3, pp. 239–249, 2018, doi: 10.1016/j.jhin.2018.01.018.

[39] M. Cloutier, D. Mantovani, and F. Rosei, "Antibacterial Coatings: Challenges, Perspectives, and Opportunities," *Trends Biotechnol.*, vol. 33, no. 11, pp. 637–652, 2015, doi: 10.1016/j.tibtech.2015.09.002.

[40] Centers of Disease Control and Prevention, "Glossary, Guideline for Disinfection and Sterilization in Healthcare Facilities (2008)." .

[41] G. McDonnell and A. D. Russell, "Antiseptics and Disinfectants: Activity, Action, and Resistance," *Clin. Microbiol. Rev.*, vol. 12, no. 1, pp. 147–179, 1999, doi: 10.4135/9781412983907.n399.

[42] A. T. Kothekar and A. P. Kulkarni, "Basic Principles of Disinfection and Sterilization in Intensive Care and Anesthesia and Their Applications during COVID-19 Pandemic," *Indian J. Crit. Care Med.*, vol. 24, no. 11, pp. 1114–1124, 2020.

[43] S. P. Denyer, "Mechanisms of Action of Biocides," *Int. Biodeterior.*, vol. 26, pp. 89–100, 1990, doi: 10.1016/0265-3036(90)90050-H.

[44] E. B. Herman, G. J. Haas, W. H. Crosby, and C. J. Cante, "Antimicrobial action of short chain alcohols and glycols," *J. Food Saf.*, vol. 2, pp. 131–139, 1980.

[45] L. O. Ingram, "Adaptation of Membrane Lipids to Alcohols," *J. Bacteriol.*, vol. 125, no. 2, pp. 670–678, 1976.

[46] B. Berger, C. E. Carty, and L. O. Ingram, "Alcohol-Induced Changes in the Phospholipid

Molecular Species of Escherichia colit," *J. Bacteriol.*, vol. 142, no. 3, pp. 1040–1044, 1980.

[47] G. Sykes, "The influence of germicides on the dehydrogenase of Bact. coli 1. The succinic acid dehydrogenase of Bact. coli," *Epidemiol. Infect.*, vol. 39, no. 4, pp. 463–469, 1939.

[48] S. Dagley, E. A. Dawes, and G. A. Morrison, "Inhibition of growth of Aerobacter aerogenes: the mode of action of phenols, alcohols, acetone and ethyl acetate," *J. Bacteriol.*, vol. 60, no. 4, pp. 369–379, 1950.

[49] Y. Yasuda-Yasaki, S. Namiki-Kanie, and Y. Hachisuka, "Inhibition of Bacillus subtilis spore germination by various hydrophobic compounds: demonstration of hydrophobic character of the L-alanine receptor site," *J. Bacteriol.*, vol. 136, no. 2, pp. 484–490, 1978.

[50] R. Trujillo and N. Laible, "Reversible inhibition of spore germination by alcohols.," *Appl. Microbiol.*, vol. 20, no. 4, pp. 620–623, 1970.

[51] H. E. Morton, "The relationship of concentration and germicidal efficiency of ethyl alcohol," *Ann. N. Y. Acad. Sci.*, vol. 53, no. 1, pp. 191–196, 1950.

[52] L. W. Bush, L. M. Benson, and J. H. White, "Pig Skin as Test Substrate for Evaluating Topical Antimicrobial Activity," *J. Clin. Microbiol.*, vol. 24, no. 3, pp. 343–348, 1986.

[53] E. H. Spaulding, "Acohol as a surgical disinfectant. Pros and cons of a much discussed topic," *AORN J.*, vol. 2, no. 5, pp. 67–71, 1964.

[54] H. Fraenkel-Conrat and H. S. Olcott, "The Reaction of Formaldehyde with Proteins. V. Cross-linking between Amino and Primary Amide or Guanidyl Groups," *J. Am. Chem. Soc.*, vol. 70, no. 8, pp. 2673–2684, 1948, doi: 10.1021/ja01188a018.

[55] G. Voulgaridou, I. Anestopoulos, R. Franco, M. I. Panayiotidis, and A. Pappa, "Mutation Research / Fundamental and Molecular Mechanisms of Mutagenesis DNA damage induced by endogenous aldehydes : Current state of knowledge," *Mutat. Res. - Fundam. Mol. Mech. Mutagen.*, vol. 711, 2011, doi: 10.1016/j.mrfmmm.2011.03.006.

[56] T. J. Munton and A. D. Russell, "Effect of Glutaraldehyde on Cell Viability, Triphenyltetrazolium Reduction, Oxygen Uptake, and -Galactosidase Activity in Escherichia coli," *Appl. Microbiol.*, vol. 26, no. 4, pp. 508–511, 1973.

[57] P. V McGucken and W. Woodside, "Studies on the Mode of Action of Glutaraldehyde on Escherichia coli," *J. Appl. Bacteriol.*, vol. 36, no. 3, pp. 419–426, 1973.

[58] R. Tennen, B. Setlow, K. L. Davis, C. A. Loshon, and P. Setlow, "Mechanisms of killing of spores of Bacillus subtilis by iodine, glutaraldehyde and nitrous acid," *J. Appl. Microbiol.*, vol. 89, no. 2, pp. 330–338, 2000.

[59] H. Fraenkel-conrat, M. Cooper, and H. S. Olcott, "The Reaction of Formaldehyde with Proteins," *J. Am. Chem. Soc.*, vol. 67, no. 6, pp. 950–954, 1945.

[60] H. Fraenkel-conrat and H. S. Olcott, "Reaction of Formaldehyde with Proteins. II. Participation of the Guanidyl Groups and Evidence of Crosslinking," *J. Am. Chem. Soc.*, vol. 68, no. 1, pp. 34–37, 1946.

[61] N. K. Sarkar and A. L. Dounce, "A spectroscopic study of the reaction of formaldehyde with deoxyribonucleic and ribonucleic acids," *Biochim. Biophys. Acta*, vol. 49, no. 1, pp. 160–169, 1961.

[62] K. A. Fitzgerald, A. Davies, and A. D. Russell, "Uptake of 14C-chlorhexidine diacetate to Escherichia coli and Pseudomonas aeruginosa and its release by azolectin," *FEMS*

Microbiol. Lett., vol. 60, no. 3, pp. 327–332, 1989.

[63] P. Broxton, P. M. Woodcock, F. Heatley, and P. Gilbert, "Interaction of some polyhexamethylene biguanides and membrane phospholipids in Escherichia coli," *J. Appl. Bacteriol.*, vol. 57, no. 1, pp. 115–124, 1984, doi: 10.1111/j.1365-2672.1984.tb02363.x.

[64] P. Gilbert and L. E. Moore, "Cationic antiseptics: Diversity of action under a common epithet," *J. Appl. Microbiol.*, vol. 99, no. 4, pp. 703–715, 2005, doi: 10.1111/j.1365-2672.2005.02664.x.

[65] J. A. Chawner and P. Gilbert, "Interaction of the bisbiguanides chlorhexidine and alexidine with phospholipid vesicles: evidence for separate modes of action," *J. Appl. Bacteriol.*, vol. 66, no. 3, pp. 253–258, 1989.

[66] W. B. Hugo and A. R. Longworth, "Some aspects of the mode of action of chlorhexidine," *J. Pharm. Pharmacol.*, vol. 16, no. 10, pp. 655–662, 1964.

[67] W. B. Hugo and A. R. Longworth, "The effect of chlorhexidine on the electrophoretic mobility, cytoplasmic constituents, dehydrogenase activity and cell walls of Escherichia coli and Staphylococcus aureus," *J. Pharm. Pharmacol.*, vol. 18, no. 9, pp. 569–578, 1966.

[68] J. A. Chawner and P. Gilbert, "A comparative study of the bactericidal and growth inhibitory activities of the bisbiguanides alexidine and chlorhexidine," *J. Appl. Bacteriol.*, vol. 66, no. 3, pp. 243–252, 1989.

[69] T. Ikeda, S. Tazuke, and M. Watanabe, "Interaction of biologically active molecules with phospholipid membranes: I. Fluorescence depolarization studies on the effect of polymeric biocide bearing biguanide groups in the main chain," *Biochim. Biophys. Acta - Biomembr.*, vol. 735, no. 3, pp. 380–386, 1983, doi: 10.1016/0005-2736(83)90152-9.

[70] T. Ikeda, A. Ledwith, C. H. Bamford, and H. R. A, "Interaction of a Polymeric Biguanide Biocide with Phospholipid Membranes," *Biochim. Biophys. Acta*, vol. 769, no. 1, pp. 57–66, 1984.

[71] P. Broxton, P. M. Woodcock, and P. Gilbert, "A study of the antibacterial activity of some polyhexamethylene biguanides towards Escherichia coli ATCC 8739," *J. Appl. Bacteriol.*, vol. 54, no. 3, pp. 345–353, 1983, doi: 10.1111/j.1365-2672.1983.tb02627.x.

[72] T. Ikeda, S. Tazuke, C. H. Bamford, and A. Ledwith, "Spectroscopic Studies on the Interaction of Polymeric In-chain Biguanide Biocide with Phospholipid Membranes as Probed by 8-Anilinonaphthalene-l-sulfonate," *Bull. Chem. Soc. Jpn.*, vol. 58, no. 2, pp. 705–709, 1985.

[73] K. Chindera *et al.*, "The antimicrobial polymer PHMB enters cells and selectively condenses bacterial chromosomes," *Sci. Rep.*, vol. 6, no. March, 2016, doi: 10.1038/srep23121.

[74] S. Sowlati-Hashjin, S. Sowlati-Hashjin, P. Carbone, M. Karttunen, M. Karttunen, and M. Karttunen, "Insights into the Polyhexamethylene Biguanide (PHMB) Mechanism of Action on Bacterial Membrane and DNA: A Molecular Dynamics Study," *J. Phys. Chem. B*, vol. 124, no. 22, pp. 4487–4497, 2020, doi: 10.1021/acs.jpcb.0c02609.

[75] L. A. Shaker, J. R. Furr, and A. D. Russell, "Mechanism of resistance of Bacillus subtilis spores to chlorhexidine," *J. Appl. Bacteriol.*, vol. 64, no. 6, pp. 531–539, 1988.

[76] L. A. Shaker, B. N. Dancer, A. D. Russell, and J. R. Furr, "Emergence and development of chlorhexidine resistance during sporulation of Bacillus subtilis 168," *FEMS Microbiol.*

Lett., vol. 51, no. 1, pp. 73–76, 1988.

[77] S. M. McKenna and K. J. Davies, "The inhibition of bacterial growth by hypochlorous acid," *Biochem. J.*, vol. 254, no. 3, pp. 685–92, 1988, [Online]. Available: http://www.ncbi.nlm.nih.gov/pubmed/2848494%0Ahttp://www.pubmedcentral.nih.gov/articlerender.fcgi?artid=PMC1135139.

[78] A. K. Camper and G. A. Mcfeters, "Chlorine Injury and the Enumeration of Waterborne Coliform Bacteria," *Appl. Environ. Microbiol.*, vol. 37, no. 3, pp. 633–641, 1979.

[79] W. C. Barrette, D. M. Hannum, W. D. Wheeler, and J. K. Hurst, "General Mechanism for the Bacterial Toxicity of Hypochlorous Acid: Abolition of ATP Production," *Biochemistry*, vol. 28, no. 23, pp. 9172–9178, 1989.

[80] S. F. Bloomfield and M. Arthur, "Interaction of Bacillus subtilis spores with sodium hypochlorite, sodium dichloroisocyanurate and chloramine-T," *J. Appl. Bacteriol.*, vol. 72, no. 2, pp. 166–172, 1992.

[81] A. D. Russell, W. B. Hugo, and G. A. J. Ayliffe, "Peroxygens," in *Disinfection, Preservation and Sterilization, fourth edition*, 2004, p. 56.

[82] S. P. Denyer and G. S. A. B. Stewart, "Mechanism of action of disinfectants," *Int. Biodeterior. Biodegredation*, vol. 41, pp. 261–268, 1998.

[83] M. G. C. Baldry, "The bactericidal, fungicidal and sporicidal properties of hydrogen peroxide and peracetic acid," *J. Appl. Bacteriol.*, vol. 54, no. 3, pp. 417–423, 1983.

[84] D. Coates, "Sporicidal peroxygen activity of sodium and glutaraldehyde Bacillus disinfectants against subtilis," *J. Hosp. Infect.*, vol. 32, no. 4, pp. 283–294, 1996.

[85] J. Judis, "Studies on the mechanism of action of phenolic disinfectants I: Release of radioactivity from carbon14-labeled Escherichia coli," *J. Pharm. Sci.*, vol. 51, no. 3, pp. 261–265, 1962.

[86] J. Judis, "Studies on the mechanism of action of phenolic disinfectants II. Patterns of release of radioactivity from Escherichia coli labeled by growth on various compounds," *J. Pharm. Sci.*, vol. 52, no. 2, pp. 126–131, 1963.

[87] J. Judis, "Mechanism of Action of Phenolic Disinfectants III: Uptake of phenol-c-14, 2,4-dichlorophenol-c-14, and p-tert- amylphenol-c-14 by escherichia coli," *J. Pharm. Sci.*, vol. 53, no. 2, pp. 196–201, 1964.

[88] J. Judis, "Mechanism of Action of Phenolic Disinfectants IV: Effects on Induction of and Accessibility of Substrate to β-Galactosidase in Escherichia coli," *J. Pharm. Sci.*, vol. 54, no. 3, pp. 417–420, 1965.

[89] J. Judis, "Mechanism of Action of Phenolic Disinfectants V: Effect of 2,4-Dichlorophenol on the Incorporation of Labeled Substrates by Escherichia coli," *J. Pharm. Sci.*, vol. 54, no. 4, pp. 541–544, 1965.

[90] H. Commager and J. Judis, "Mechanism of Action of Phenolic Disinfectants VI: Effects on Glucose and Succinate Metabolism of Escherichia coli," *J. Pharm. Sci.*, vol. 54, no. 10, pp. 1436–1439, 1965.

[91] J. E. Starr and J. Judis, "Mechanism of Action of Phenolic Disinfectants VIII: Association of Phenolic Disinfectants With Proteins," *J. Pharm. Sci.*, vol. 57, no. 5, pp. 768–773, 1968.

[92] W. B. Hugo and S. F. Bloomfield, "Studies on the mode of action of the phenolic

antibacterial agent fentichlor against Staphylococcus aureus and Escherichia coli 3. The effect of fentichlor on the metabolic activities of Staphylococcus aureus and Escherichia coli," *J. Appl. Bacteriol.*, vol. 34, no. 3, pp. 579–591, 1971.

[93] S. F. Bloomfield, "The Effect of the Phenolic Antibacterial Agent Fentichlor on Energy Coupling in Staphylococcus aureus," *J. Appl. Bacteriol.*, vol. 37, pp. 117–131, 1974.

[94] S. P. Denyer, W. B. Hugo, and V. D. Harding, "The biochemical basis of synergy between the antibacterial agents, chlorocresol and 2-phenylethanol," *Int. J. Pharm.*, vol. 29, no. 1, pp. 29–36, 1986, doi: 10.1016/0378-5173(86)90196-1.

[95] S. Alkhalifa *et al.*, "Analysis of the Destabilization of Bacterial Membranes by Quaternary Ammonium Compounds: A Combined Experimental and Computational Study," *ChemBioChem*, vol. 21, no. 10, pp. 1510–1516, 2020, doi: 10.1002/cbic.201900698.

[96] S. P. Denyer and W. B. Hugo, "The Mode of Action of Tetradecyltrimethyl Ammonium Bromide (CTAB) on Staphylococcus aureus," *J. Pharm. Pharmacol.*, vol. 29, p. 66P, 1977.

[97] P. A. Lambert and S. M. Hammond, "Potassium fluxes, first indications of membrane damage in micro-organisms," *Biochem. Biophys. Res. Commun.*, vol. 54, no. 2, pp. 796–799, 1973.

[98] B. Croshaw, M. J. Groves, and B. Lessel, "Some properties of bronopol, a new antimicrobial agent active against," *J. Pharm. Pharmacol.*, vol. 16, pp. 127–130, 1964.

[99] R. J. Stretton and T. W. Manson, "Some Aspects of the Mode of Action of the Antibacterial Compound Bronopol (2-bromo-2-nitropropan-1,3-diol)," *J. Appl. Bacteriol.*, vol. 36, pp. 61–76, 1973.

[100] J. A. Shepherd, R. D. Waigh, and P. Gilbert, "Antibacterial Action of 2-Bromo-2-Nitropropane-1,3-Diol (Bronopol)," *Antimicrob. Agents Chemother.*, vol. 32, no. 11, pp. 1693–1698, 1988.

[101] D. M. Bryce, B. Croshaw, J. E. Hall, V. R. Holland, and B. Lessel, "The activity and safety of the antimicrobial agent Bronopol (2-bromo-2-nitropropan-1, 3-diol)," *J. Soc. Cosmet. Chem.*, vol. 29, pp. 3–24, 1978.

[102] T. R. Corner, "Synergism in the inhibition of Bacillus subtilis by combinations of lipophilic weak acids and fatty alcohols," *Antimicrob. Agents Chemother.*, vol. 19, no. 6, pp. 1082–1085, 1981, doi: 10.1128/AAC.19.6.1082.

[103] R. M. Epand and R. F. Epand, "Domains in bacterial membranes and the action of antimicrobial agents," *Mol. Biosyst.*, vol. 5, no. 6, pp. 580–587, 2009, doi: 10.1039/b900278m.

[104] M. Goff, "Nudging for Hand Hygiene: A Systematic Review and Meta- Analysis," Georgia State University, 2022.

[105] S. F. Bloomfield and E. A. Miller, "A comparison of hypochlorite and phenolic disinfectants for disinfection of clean and soiled surfaces and blood spillages," *J. Hosp. Infect.*, vol. 13, no. 3, pp. 231–239, 1989.

[106] D. J. Weber, S. L. Barbee, M. D. Sobsey, and W. A. Rutala, "The Effect of Blood on the Antiviral Activity of Sodium Hypochlorite, a Phenolic, and a Quaternary Ammonium Compound," *Infect. Control Hosp. Epidemiol.*, vol. 20, no. 12, pp. 821–827, 1999.

[107] A. M. West, P. J. Teska, C. B. Lineback, and H. F. Oliver, "Strain, disinfectant,

concentration and contact time quantitatively impact disinfectant efficacy," *Antimicrob. Resist. Infect. Control*, vol. 49, no. 7, 2018.

[108] GAMA Healthcare, "Universal Range Efficacy Data," 2022. .

[109] E. Shepherd, A. Leitch, E. Curran, and Infection Prevention and Control Team NHS Lanarkshire, "A quality improvement project to standardise decontamination procedures in a single NHS board in Scotland," *J. Infect. Prev.*, vol. 21, no. 6, pp. 241–246, 2020, doi: 10.1177/1757177420947477.

[110] E. DeVere and D. Purchase, "Effectiveness of domestic antibacterial products in decontaminating food contact surfaces," *Food Microbiol.*, vol. 24, no. 4, pp. 425–430, 2007, doi: 10.1016/j.fm.2006.07.013.

[111] A. M. West *et al.*, "Surface area wiped, product type, and target strain impact bactericidal efficacy of ready-to-use disinfectant Towelettes," *Antimicrob. Resist. Infect. Control*, vol. 7, 2018.

[112] J. B. Corliss *et al.*, "Submarine Thermal Sprirngs on the Galapagos Rift," *Science (80-.).*, vol. 203, no. 4385, pp. 1073–1083, 1979, doi: 10.1126/science.203.4385.1073.

[113] T. D. Brock and H. Freeze, "Thermus aquaticus gen. n. and sp. n., a Nonsporulating Extreme Thermophile," *J. Bacteriol.*, vol. 98, no. I, pp. 289–297, 1969.

[114] K. R. Redeker, J. P. J. Chong, A. Aguion, A. Hodson, and D. A. Pearce, "Microbial metabolism directly affects trace gases in (sub) polar snowpacks," *J. R. Soc. Interface*, vol. 14, 2017, doi: 10.1098/rsif.2017.0729.

[115] P. A. Vaishampayan, E. Rabbow, G. Horneck, and K. J. Venkateswaran, "Survival of Bacillus pumilus Spores for a Prolonged Period of Time in Real Space Conditions," *Astrobiology*, vol. 12, no. 5, 2012.

[116] P. Demchick and A. L. Koch, "The Permeability of the Wall Fabric of Escherichia coli and Bacillus subtilis," *J. Bacteriol.*, vol. 178, no. 3, pp. 768–773, 1996.

[117] N. Malanovic and K. Lohner, "Gram-positive bacterial cell envelopes: The impact on the activity of antimicrobial peptides," *Biochim. Biophys. Acta - Biomembr.*, pp. 936–946, 2016, doi: 10.1016/j.bbamem.2015.11.004.

[118] J. W. Costerton, "How Bacteria Stick," *Sci. Am.*, vol. 238, pp. 86–95, 1978.

[119] P. S. Stewart, "Mechanisms of antibiotic resistance in bacterial biofilms," *Int. J. Med. Microbiol.*, vol. 292, pp. 107–113, 2002, doi: 10.1128/9781555815554.ch14.

[120] R. M. Donlan and J. W. Coserton, "Biofilms: Survival Mechanisms of Clinically Relevant Microorganisms," *Clin. Microbiol. Rev.*, vol. 15, no. 2, pp. 167–189, 2002, doi: 10.1128/CMR.15.2.167.

[121] T. C. Mah and G. A. O. Toole, "Mechanisms of biofilm resistance to antimicrobial agents," *Trends Microbiol.*, vol. 9, no. 1, pp. 34–39, 2001.

[122] C. W. Hall and T. Mah, "Molecular mechanisms of biofilm-based antibiotic resistance and tolerance in pathogenic bacteria," *FEMS Microbiol. Rev.*, 2017, doi: 10.1093/femsre/fux010.

[123] P. S. Stewart, J. Rayner, F. Roe, and W. M. Rees, "Biofilm penetration and disinfection efficacy of alkaline hypochlorite and chlorosulfamates," *J. Appl. Microbiol.*, vol. 91, no. 3, pp. 525–532, 2001.

[124] C. Sandt, J. Barbeau, M.-A. Gagnon, and M. Lafleur, "Role of the ammonium group in the diffusion of quaternary ammonium compounds in Streptococcus mutans biofilms," *J. Antimicrob. Chemother.*, vol. 60, no. 6, pp. 1281–1287, 2007, doi: 10.1093/jac/dkm382.

[125] P. S. Stewart, "Antimicrobial Tolerance in Biofilms," *Microbiol. Spectr.*, vol. 3, no. 3, 2015, doi: 10.1128/microbiolspec.MB-0010-2014.Antimicrobial.

[126] H. Hu, K. Johani, I. B. Gosbell, A. S. W. Jacombs, and A. Almatroudi, "Intensive care unit environmental surfaces are contaminated by multidrug-resistant bacteria in biofilms: combined results of conventional culture, pyrosequencing, scanning electron microscopy, and confocal laser microscopy," *J. Hosp. Infect.*, vol. 91, pp. 35–44, 2015, doi: 10.1016/j.jhin.2015.05.016.

[127] K. Ledwoch *et al.*, "Beware biofilm! Dry biofilms containing bacterial pathogens on multiple healthcare surfaces; a multi-centre study," *J. Hosp. Infect.*, vol. 100, no. 3, pp. e47–e56, 2018, doi: 10.1016/j.jhin.2018.06.028.

[128] D. Chowdhury *et al.*, "Transfer of dry surface biofilm in the healthcare environment: the role of healthcare workers' hands as vehicles," *J. Hosp. Infect.*, vol. 100, no. 3, pp. e85–e90, 2018, doi: 10.1016/j.jhin.2018.06.021.

[129] A. Almatroudi, I. B. Gosbell, H. Hu, S. O. Jensen, and B. A. Espedido, "Staphylococcus aureus dry-surface biofilms are not killed by sodium hypochlorite: implications for infection control," *J. Hosp. Infect.*, vol. 93, no. 3, pp. 263–270, 2016, doi: 10.1016/j.jhin.2016.03.020.

[130] H. Xu, N. Roberts, F. Singleton, R. Attwell, D. Grimes, and R. Colwell, "Survival and viability of nonculturable Escherichia coli and Vibrio cholerae in the estuarine and marine environment.," *Microb. Ecol.*, vol. 8, no. 4, pp. 313–323, 1982.

[131] G. J. Medema, F. M. Schets, A. W. Van De Giessen, and A. H. Havelaar, "Lack of colonization of 1 day old chicks by viable , non-culturable Campylobacter jejuni," *J. Appl. Bacteriol.*, vol. 72, no. 6, pp. 512–516, 1992.

[132] D. Lloyd and J. Hayes, "Vigour, vitality and viability of microorganisms," *FEMS Microbiol. Lett.*, vol. 133, no. 1–2, pp. 1–7, 1995.

[133] I. Rahman, M. Shahamat, P. A. Kirchman, and R. R. Colwell, "Methionine Uptake and Cytopathogenicity of Viable but Nonculturable Shigella dysenteriae Type 1," *Appl. Environ. Microbiol.*, vol. 60, no. 10, pp. 3573–3578, 1994.

[134] M. del M. Lleò, S. Pierobon, M. C. Tafi, C. Signoretto, and P. Canepari, "mRNA Detection by Reverse Transcription-PCR for Monitoring Viability over Time in an Enterococcus faecalis Viable but Nonculturable Population Maintained in a Laboratory Microcosm," *Appl. Environ. Microbiol.*, vol. 66, no. 10, pp. 4564–4567, 2000.

[135] J. D. Oliver, "The viable but nonculturable state in bacteria.," *J. Microbiol.*, vol. 43, pp. 93–100, 2005, [Online]. Available: http://www.ncbi.nlm.nih.gov/pubmed/15765062.

[136] X. Zhao, J. Zhong, C. Wei, C. W. Lin, and T. Ding, "Current perspectives on viable but non-culturable state in foodborne pathogens," *Front. Microbiol.*, vol. 8, 2017, doi: 10.3389/fmicb.2017.00580.

[137] R. M. Baker, F. L. Singleton, and M. A. Hood, "Effects of Nutrient Deprivation on Vibrio cholerae," *Appl. Environ. Microbiol.*, vol. 46, no. 4, pp. 930–940, 1983.

[138] J. Porter, C. Edwards, and R. W. Pickup, "Rapid assessment of physiological status in

Escherichia coli using fluorescent probes," *J. Appl. Bacteriol.*, vol. 79, no. 4, pp. 399–408, 1995.

[139] D. S. Morton and J. D. Oliver, "Induction of Carbon Starvation-Induced Proteins in Vibrio vulnificus," *Appl. Environ. Microbiol.*, vol. 60, no. 10, pp. 3653–3659, 1994.

[140] A. P. Day and J. D. Oliver, "Changes in Membrane Fatty Acid Composition during Entry of Vibrio vulnificus into the Viable But Nonculturable State," *J. Microbiol.*, vol. 42, no. 2, pp. 69–73, 2004.

[141] C. Signoretto, M. del M. Lleo, M. C. Tafi, and P. Canepari, "Cell Wall Chemical Composition of Enterococcus faecalis in the Viable but Nonculturable State," *Appl. Environ. Microbiol.*, vol. 66, no. 5, pp. 1953–1959, 2000.

[142] C. Signoretto, M. del M. Lleò, and P. Canepari, "Modification of the Peptidoglycan of Escherichia coli in the Viable But Nonculturable State," *Curr. Microbiol.*, vol. 44, pp. 125–131, 2002, doi: 10.1007/s00284-001-0062-0.

[143] J. D. Oliver, "Recent findings on the viable but nonculturable state in pathogenic bacteria," *FEMS Microbiol. Rev.*, vol. 34, no. 4, pp. 415–425, 2010, doi: 10.1111/j.1574-6976.2009.00200.x.

[144] X.-H. Zhang, W. Ahmad, X.-Y. Zhu, J. Chen, and B. Austin, "Viable but nonculturable bacteria and their resuscitation: implications for cultivating uncultured marine microorganisms," *Mar. Life Sci. Technol.*, vol. 3, pp. 189–203, 2021, doi: 10.1007/s42995-020-00041-3.

[145] D. Pinto, M. A. Santos, and L. Chambel, "Thirty years of viable but nonculturable state research: Unsolved molecular mechanisms," *Crit. Rev. Microbiol.*, vol. 41, no. 1, pp. 61–76, 2015, doi: 10.3109/1040841X.2013.794127.

[146] K. L. Cook and C. H. Bolster, "Survival of Campylobacter jejuni and Escherichia coli in groundwater during prolonged starvation at low temperatures," *J. Appl. Microbiol.*, vol. 103, no. 3, pp. 573–583, 2007, doi: 10.1111/j.1365-2672.2006.03285.x.

[147] L. A. Pazos-Rojas *et al.*, "Desiccation-induced viable but nonculturable state in Pseudomonas putida KT2440 , a survival strategy," *PLoS One*, vol. 14, no. 7, 2019.

[148] H. Asakura *et al.*, "Gene expression profile of Vibrio cholerae in the cold stress-induced viable but non-culturable state," *Environ. Microbiol.*, vol. 9, no. 4, pp. 869–879, 2006, doi: 10.1111/j.1462-2920.2006.01206.x.

[149] R. A. Bovill and B. M. Mackey, "Resuscitation of 'non-culturable' cells from aged cultures of Campylobacter jejuni," *Microbiology*, vol. 143, no. 5, pp. 1575–1581, 1997.

[150] J. D. Oliver, M. Dagher, and K. Linden, "Induction of Escherichia coli and Salmonella typhimurium into the viable but nonculturable state following chlorination of wastewater.," *J. Water Health*, vol. 3, no. 3, pp. 249–257, 2005.

[151] C. J. Highmore, J. C. Warner, S. D. Rothwell, S. A. Wilks, and C. W. Keevil, "Viable-but-Nonculturable Listeria monocytogenes and Salmonella enterica Serovar Thompson Induced by Chlorine Stress Remain Infectious," *Am. Acad. Microbiol.*, 2018, [Online]. Available: https://doi.org/10.1128/ mBio.00540-18. Editor.

[152] X. Liao, W. Hu, D. Liu, and T. Ding, "Stress Resistance and Pathogenicity of Nonthermal-Plasma-Induced Viable-but-Nonculturable Staphylococcus aureus through Energy Suppression, Oxidative Stress Defense, and Immune-Escape Mechanisms," *Food*

Microbiol., vol. 87, no. 2, 2021.

[153] V. Besnard, M. Federighi, and J. M. Cappelier, "Evidence of Viable But Non-Culturable state in Listeria monocytogenes by direct viable count and CTC-DAPI double staining," *Food Microbiol.*, vol. 17, no. 6, pp. 697–704, 2000, doi: 10.1006/fmic.2000.0366.

[154] M. Noll *et al.*, "Benzalkonium chloride induces a VBNC state in Listeria monocytogenes," *Microorganisms*, vol. 8, no. 2, 2020, doi: 10.3390/microorganisms8020184.

[155] C. Robben, S. Fister, A. K. Witte, D. Schoder, P. Rossmanith, and P. Mester, "Induction of the viable but non-culturable state in bacterial pathogens by household cleaners and inorganic salts," *Sci. Rep.*, vol. 8, 2018, doi: 10.1038/s41598-018-33595-5.

[156] M. Arvaniti, P. Tsakanikas, V. Papadopoulou, A. Giannakopoulou, and P. Skandamis, "Listeria monocytogenes Sublethal Injury and Viable-but-Nonculturable State Induced by Acidic Conditions and Disinfectants," *Microbiol. Spectr.*, vol. 9, no. 3, pp. e01377-21, 2021.

[157] J. J. Alvear-daza, A. García-barco, P. Osorio-vargas, H. M. Gutiérrez-zapata, J. Sanabria, and J. A. Rengifo-herrera, "Resistance and induction of viable but non culturable states (VBNC) during inactivation of E. coli and Klebsiella pneumoniae by addition of H2O2 to natural well water under simulated solar irradiation," *Water Res.*, vol. 188, 2021, doi: 10.1016/j.watres.2020.116499.

[158] Z. Bravo *et al.*, "Analysis of Acinetobacter baumannii survival in liquid media and on solid matrices as well as effect of disinfectants," *J. Hosp. Infect.*, vol. 103, pp. e42–e52, 2019, doi: 10.1016/j.jhin.2019.04.009.

[159] S. Chen *et al.*, "Induction of Escherichia coli into a VBNC state through chlorination/chloramination and differences in characteristics of the bacterium between states," *Water Res.*, vol. 142, pp. 279–288, 2018, doi: 10.1016/j.watres.2018.05.055.

[160] C. Robben, A. K. Witte, D. Schoder, B. Stessl, P. Rossmanith, and P. Mester, "A fast and easy ATP-based approach enables MIC testing for non-resuscitating VBNC pathogens," *Front. Microbiol.*, vol. 10, 2019, doi: 10.3389/fmicb.2019.01365.

[161] M. Boaretti, M. Lleò, B. Bonato, C. Signoretto, and P. Canepari, "Involvement of rpoS in the survival of Escherichia coli in the viable but non-culturable state," *Environ. Microbiol.*, vol. 5, no. 10, pp. 986–996, 2003, doi: 10.1046/j.1462-2920.2003.00497.x.

[162] A. Kusumoto, H. Asakura, and K. Kawamoto, "General stress sigma factor RpoS influences time required to enter the viable but non-culturable state in Salmonella enterica," *Microbiol. Immunol.*, vol. 56, no. 4, pp. 228–237, 2012, doi: 10.1111/j.1348-0421.2012.00428.x.

[163] A. Mishra, N. Taneja, and M. Sharma, "Viability kinetics , induction , resuscitation and quantitative real-time polymerase chain reaction analyses of viable but nonculturable Vibrio cholerae O1 in freshwater microcosm," *J. Appl. Microbiol.*, vol. 112, no. 5, pp. 945–953, 2012, doi: 10.1111/j.1365-2672.2012.05255.x.

[164] M. Ayrapetyan, T. C. Williams, and J. D. Oliver, "Bridging the gap between viable but non-culturable and antibiotic persistent bacteria," *Trends Microbiol.*, vol. 23, no. 1, pp. 7–13, 2015, doi: 10.1016/j.tim.2014.09.004.

[165] M. F. Traxler *et al.*, "The global, ppGpp-mediated stringent response to amino acid starvation in Escherichia coli," *Mol. Microbiol.*, vol. 68, no. 5, pp. 1128–1148, 2008, doi: 10.1111/j.1365-2958.2008.06229.x.

[166] D. Gangaiah, I. I. Kassem, Z. Liu, and G. Rajashekara, "Importance of Polyphosphate Kinase 1 for Campylobacter jejuni Viable-but-Nonculturable Cell Formation, Natural Transformation, and Antimicrobial Resistance," *Appl. Environ. Microbiol.*, vol. 75, no. 24, pp. 7838–7849, 2009, doi: 10.1128/AEM.01603-09.

[167] D. B. Roszak, D. J. Grimes, and R. R. Colwell, "Viable but nonrecoverable stage of Salmonella enteritidis in aquatic systems," *Can. J. Microbiol.*, vol. 30, no. 3, pp. 334–338, 1984.

[168] D. Pinto, V. Almeida, M. A. Santos, and L. Chambel, "Resuscitation of Escherichia coli VBNC cells depends on a variety of environmental or chemical stimuli," *J. Appl. Microbiol.*, vol. 110, no. 6, pp. 1601–1611, 2011, doi: 10.1111/j.1365-2672.2011.05016.x.

[169] Public Health England, "Detection and enumeration of bacteria in swabs and other environmental samples National Infection Service Food Water and Environmental Microbiology Standard Method About Public Health England," London, 2017. [Online]. Available: https://assets.publishing.service.gov.uk/government/uploads/system/uploads/attachment_data/file/660648/Detection_and_enumeration_of_bacteria_in_swabs_and_other_environmental_samples.pdf.

[170] (CDC) Centers of Disease Control and Prevention, "Guidelines for Environmental Infection Control in Health-Care Facilities," Atlanta, 2003. [Online]. Available: https://www.cdc.gov/infectioncontrol/guidelines/environmental/background/sampling.html.

[171] L. Alleron, N. Merlet, C. Lacombe, and J. Frere, "Long-Term Survival of Legionella pneumophila in the Viable But Nonculturable State After Monochloramine Treatment," *Curr. Microbiol.*, vol. 57, no. 5, pp. 497–502, 2008, doi: 10.1007/s00284-008-9275-9.

[172] A. K. Bej, M. H. Mahbubani, and R. M. Atlas, "Detection of Viable Legionella pneumophila in Water by Polymerase Chain Reaction and Gene Probe Methods," *Appl. Environ. Microbiol.*, vol. 57, no. 2, pp. 597–600, 1991.

[173] B. Casini *et al.*, "Detection of viable but non-culturable legionella in hospital water network following monochloramine disinfection," *J. Hosp. Infect.*, vol. 98, no. 1, pp. 46–52, 2018, doi: 10.1016/j.jhin.2017.09.006.

[174] M. A. Orman and M. P. Brynildsen, "Establishment of a method to rapidly assay bacterial persister metabolism," *Antimicrob. Agents Chemother.*, vol. 57, no. 9, pp. 4398–4409, 2013, doi: 10.1128/AAC.00372-13.

[175] N. E. Wideman, J. D. Oliver, P. G. Crandall, and N. A. Jarvis, "Detection and Potential Virulence of Viable but Non-Culturable (VBNC) Listeria monocytogenes: A Review," *Microorganisms*, vol. 9, no. 1, 2021.

[176] A. Nocker and A. K. Camper, "Selective Removal of DNA from Dead Cells of Mixed Bacterial Communities by Use of Ethidium Monoazide," *Appl. Environ. Microbiol.*, vol. 72, no. 3, pp. 1997–2004, 2006, doi: 10.1128/AEM.72.3.1997.

[177] K. Rudi, K. Naterstad, S. M. Drømtorp, and H. Holo, "Detection of viable and dead Listeria monocytogenes on gouda-like cheeses by real-time PCR," *Lett. Appl. Microbiol.*, vol. 40, no. 4, pp. 301–306, 2005, doi: 10.1111/j.1472-765X.2005.01672.x.

[178] J. T. Trevors, "Can dead bacterial cells be defined and are genes expressed after cell death?," *J. Microbiol. Methods*, vol. 90, pp. 25–28, 2012, doi: 10.1016/j.mimet.2012.04.004.

[179] K. Kogure, U. Simidu, and N. Taga, "A tentative direct microscopic method for counting living marine bacteria," *Can. J. Microbiol.*, vol. 25, no. 3, pp. 415–420, 1979.

[180] G. G. Rodriguez, D. Phipps, K. Ishiguro, and H. F. Ridgway, "Use of a Fluorescent Redox Probe for Direct Visualization of Actively Respiring Bacteria," *Appl. Environ. Microbiol.*, vol. 58, no. 6, pp. 1801–1808, 1992.

[181] S. J. Lahtinen *et al.*, "Degradation of 16S rRNA and attributes of viability of viable but nonculturable probiotic bacteria," *Lett. Appl. Microbiol.*, vol. 46, no. 6, pp. 693–698, 2008, doi: 10.1111/j.1472-765X.2008.02374.x.

[182] B. Kramer and P. Muranyi, "Effect of pulsed light on structural and physiological properties of Listeria innocua and Escherichia coli," *J. Appl. Microbiol.*, vol. 116, pp. 596–611, 2013, doi: 10.1111/jam.12394.

[183] M. Ayrapetyan, T. Williams, and J. D. Oliver, "Relationship between the Viable but Nonculturable State and Antibiotic Persister Cells," *J. Bacteriol.*, vol. 200, no. 20, 2018.

[184] S. Fernandes, I. B. Gomes, S. F. Sousa, and M. Simões, "Antimicrobial Susceptibility of Persister Biofilm Cells of Bacillus cereus and Pseudomonas fluorescens," *Microorganisms*, vol. 10, no. 1, 2022.

[185] G. L. Hobby, K. Meyer, and E. Chaffee, "Observations on the Mechanism of Action of Penicillin," *Exp. Biol. Med.*, vol. 50, no. 2, pp. 281–285, 1942.

[186] J. W. Bigger, "Treatment of Staphylococcal Infections with Penicillin by Intermittent Sterilisation," *Lancet*, vol. 244, no. 6320, pp. 497–500, 1944.

[187] N. Q. Balaban, J. Merrin, R. Chait, L. Kowalik, and S. Leibler, "Bacterial Persistence as a Phenotypic Switch," *Science (80-.).*, vol. 305, no. 5690, pp. 1622–1625, 2004.

[188] Y. Pu *et al.*, "Enhanced Efflux Activity Facilitates Drug Tolerance in Dormant Bacterial Cells Article Enhanced Efflux Activity Facilitates Drug Tolerance in Dormant Bacterial Cells," *Mol. Cell*, vol. 62, no. 2, pp. 284–294, 2016, doi: 10.1016/j.molcel.2016.03.035.

[189] Y. Pu, Y. Ke, and F. Bai, "Active efflux in dormant bacterial cells – New insights into antibiotic persistence," *Drug Resist. Updat.*, vol. 30, pp. 7–14, 2017, doi: 10.1016/j.drup.2016.11.002.

[190] S. P. Bernier, D. Lebeaux, A. S. Defrancesco, A. Valomon, J. Ghigo, and C. Beloin, "Starvation, Together with the SOS Response, Mediates High Biofilm-Specific Tolerance to the Fluoroquinolone Ofloxacin," *PLOS Genet.*, vol. 9, no. 1, 2013, doi: 10.1371/journal.pgen.1003144.

[191] Y. Wu, M. Vulic, I. Keren, and K. Lewis, "Role of Oxidative Stress in Persister Tolerance," *Antimicrob. Agents Chemother.*, vol. 56, no. 9, pp. 4922–4926, 2012, doi: 10.1128/AAC.00921-12.

[192] T. Dörr, M. Vulić, and K. Lewis, "Ciprofloxacin Causes Persister Formation by Inducing the TisB toxin in Escherichia coli," *PLOS Biol.*, vol. 8, no. 2, 2010, doi: 10.1371/journal.pbio.1000317.

[193] N. Verstraeten *et al.*, "Obg and Membrane Depolarization Are Part of a Microbial Bet-Hedging Strategy that Leads to Article Obg and Membrane Depolarization Are Part of a Microbial Bet-Hedging Strategy that Leads to Antibiotic Tolerance," *Mol. Cell*, vol. 59, no. 2, pp. 9–21, 2015, doi: 10.1016/j.molcel.2015.05.011.

[194] S. M. Amato and M. P. Brynildsen, "Nutrient Transitions Are a Source of Persisters in Escherichia coli Biofilms," *PLoS One*, vol. 9, no. 3, 2014, doi: 10.1371/journal.pone.0093110.

[195] S. M. Amato and M. P. Brynildsen, "Persister Heterogeneity Arising from a Single Article Persister Heterogeneity Arising from a Single Metabolic Stress," *Curr. Biol.*, vol. 25, no. 16, pp. 2090–2098, 2015, doi: 10.1016/j.cub.2015.06.034.

[196] Y. Pu *et al.*, "ATP-Dependent Dynamic Protein Aggregation Regulates Bacterial Dormancy Depth Critical for Article ATP-Dependent Dynamic Protein Aggregation Regulates Bacterial Dormancy Depth," *Mol. Cell*, vol. 73, no. 1, pp. 143–156, 2019, doi: 10.1016/j.molcel.2018.10.022.

[197] R. A. Fisher, B. Gollan, and S. Helaine, "Persistent bacterial infections and persister cells," *Nat. Rev. Microbiol.*, vol. 15, no. 8, pp. 453–464, 2017, doi: 10.1038/nrmicro.2017.42.

[198] M. J. Kennedy and S. L. Reader, "Preservation records of micro-organisms: evidence of the tenacity of life," *Microbiology*, vol. 140, no. 10, pp. 2513–2529, 1994.

[199] M. J. Leggett, G. Mcdonnell, S. P. Denyer, P. Setlow, and J. Maillard, "Bacterial spore structures and their protective role in biocide resistance," *J. Appl. Microbiol.*, vol. 113, no. 3, pp. 485–498, 2012, doi: 10.1111/j.1365-2672.2012.05336.x.

[200] P. T. Mckenney, A. Driks, and P. Eichenberger, "The Bacillus subtilis endospore: Assembly and functions of the multilayered coat," *Nat. Rev. Microbiol.*, vol. 11, no. 1, pp. 33–44, 2013, doi: 10.1038/nrmicro2921.

[201] L. L. Matz, T. Cabrera Beanman, and P. Gerhardt, "Chemical Composition of Exosporium from Spores of Bacillus cereus," *J. Appl. Microbiol.*, vol. 101, no. I, pp. 196–201, 1970.

[202] W. L. Nicholson, N. Munakata, G. Horneck, H. J. Melosh, and P. Setlow, "Resistance of Bacillus endospores to extreme terrestrial and extraterrestrial environments.," *Microbiol. Mol. Biol. Rev.*, vol. 64, no. 3, pp. 548–72, 2000.

[203] P. Setlow, "Spores of Bacillus subtilis: Their resistance to and killing by radiation, heat and chemicals," *J. Appl. Microbiol.*, vol. 101, no. 3, pp. 514–525, 2006, doi: 10.1111/j.1365-2672.2005.02736.x.

[204] L. J. Rode, C. Willard Lewis, and J. W. Foster, "Electron Microscopy of Spores of Bacillus megaterium with Special Reference to the Effects of Fixation and Thin Sectioning," *J. Cell Biol.*, vol. 13, no. 3, pp. 423–435, 1962.

[205] B. Setlow and P. Setlow, "Measurements of the pH within dormant and germinated bacterial spores," *Biochemistry*, vol. 77, no. 5, pp. 2474–2476, 1980.

[206] P. Gerhardt, S. H. Black, A. Arbor, and S. H. B. Permeability, "Permeability of bacterial spores. II. Molecular variables affecting solute permeation.," *J. Bacteriol.*, vol. 82, pp. 750–760, 1961.

[207] C. Darwin, *The origin of species by means of natural selection*. New York: D. Appleton and Company, 1882.

[208] A. Shi, F. Fan, and J. R. Broach, "Microbial adaptive evolution," *J. Ind. Microbiol. Biotechnol.*, vol. 49, no. 2, 2022, doi: 10.1093/jimb/kuab076.

[209] L. Sandegren and D. I. Andersson, "Bacterial gene amplification: implications for the

evolution of antibiotic resistance," *Nat. Rev. Microbiol.*, vol. 7, pp. 578–588, 2009, doi: 10.1038/nrmicro2174.

[210] B. R. Levin and O. E. Cornejo, "The Population and Evolutionary Dynamics of Homologous Gene Recombination in Bacteria," *PLOS Genet.*, vol. 5, no. 8, 2009, doi: 10.1371/journal.pgen.1000601.

[211] T. M. Wassenaar, D. Ussery, L. N. Nielsen, and H. Ingmer, "Review and phylogenetic analysis of qac genes that reduce susceptibility to quaternary ammonium compounds in Staphylococcus species.," *Eur. J. Microbiol. Immunol. (Bp).*, vol. 5, no. 1, pp. 44–61, 2015, doi: 10.1556/EuJMI-D-14-00038.

[212] M. P. Jevons, "Celbenin-resistant Staphylococci," *Br. Med. J.*, vol. 1, pp. 123–125, 1961.

[213] D. Yong *et al.*, "Characterization of a new metallo-β-lactamase gene, bla NDM-1, and a novel erythromycin esterase gene carried on a unique genetic structure in Klebsiella pneumoniae sequence type 14 from India," *Antimicrob. Agents Chemother.*, vol. 53, no. 12, pp. 5046–5054, 2009, doi: 10.1128/AAC.00774-09.

[214] J. P. Flaherty and R. A. Weinstein, "Nosocomial Infection Caused by Antibiotic-Resistant Organisms in the Intensive-Care Unit," *Infect. Control Hosp. Epidemiol.*, vol. 17, no. 4, pp. 236–248, 1996.

[215] G. Kampf, "Challenging biocide tolerance with antiseptic stewardship," *J. Hosp. Infect.*, vol. 100, no. 3, pp. e37–e39, 2018, doi: 10.1016/j.jhin.2018.07.014.

[216] J. Maillard, G. Kampf, and R. Cooper, "Antimicrobial stewardship of antiseptics that are pertinent to wounds: the need for a united approach," *JAC - Antimicrob. Resist.*, vol. 3, no. 1, 2021, doi: 10.1093/jacamr/dlab027.

[217] U.S. Food and Drug Administration, *Safety and Effectiveness of Consumer Antiseptics; Topical Antimicrobial Drug Products for Over-the-Counter Human Use. Final rule*, vol. 81, no. 172. United States of America, 2016, pp. 61106–61130.

[218] U.S. Food and Drug Administration, "FDA Response to ACI July 2020 Progress Report (ethanol bzk pmcx bzec pi)," *FDA-1975-N-0012-0833*, 2020. .

[219] C. Tong, H. Hu, G. Chen, Z. Li, A. Li, and J. Zhang, "Disinfectant resistance in bacteria: Mechanisms, spread, and resolution strategies," *Environ. Res.*, vol. 195, 2021, doi: 10.1016/j.envres.2021.110897.

[220] M. T. Gillespie, J. W. May, and R. A. Skurray, "Plasmid-encoded resistance to acriflavine and quaternary ammonium compounds in methicillin-resistant Staphylococcus aureus," *FEMS Microbiol. Lett.*, vol. 34, no. 1, pp. 47–51, 1986.

[221] M. H. Brown and R. A. Skurray, "Staphylococcal Multidrug Efflux Protein QacA," *J. Mol. Microbiol. Biotechnol.*, vol. 3, no. 2, pp. 163–170, 2001.

[222] A. Abdelaziz, F. Sonbol, T. Elbanna, and E. El-ekhnawy, "Exposure to Sublethal Concentrations of Benzalkonium Chloride Induces Antimicrobial Resistance and Cellular Changes in Klebsiellae pneumoniae Clinical Isolates," *Microb. Drug Resist.*, vol. 00, no. 00, 2018, doi: 10.1089/mdr.2018.0235.

[223] M. E. Wand, E. M. Darby, J. M. A. Blair, and J. M. Sutton, "Contribution of the efflux pump AcrAB-TolC to the tolerance of chlorhexidine and other biocides in Klebsiella spp .," *J. Med. Microbiol.*, vol. 71, no. 3, 2022, doi: 10.1099/jmm.0.001496.

[224] G. Wu *et al.*, "Evaluation of agar dilution and broth microdilution methods to determine the disinfectant susceptibility," no. July 2014, pp. 661–665, 2015, doi: 10.1038/ja.2015.51.

[225] M. C. Moken, L. M. McMurry, and S. B. Levy, "Selection of Multiple-Antibiotic-Resistant (Mar) Mutants of Escherichia coli by Using the Disinfectant Pine Oil: Roles of the mar and acrAB Loci," *Antimicrob. Agents Chemother.*, vol. 41, no. 12, pp. 2770–2772, 1997.

[226] L. P. Randall *et al.*, "Commonly used farm disinfectants can select for mutant Salmonella enterica serovar Typhimurium with decreased susceptibility to biocides and antibiotics without compromising virulence," *J. Antimicrob. Chemother.*, vol. 60, pp. 1273–1280, 2007, doi: 10.1093/jac/dkm359.

[227] A. Abuzaid, A. Hamouda, and S. G. B. Amyes, "Klebsiella pneumoniae susceptibility to biocides and its association with cepA, qacE and qacE efflux pump genes and antibiotic resistance," *J. Hosp. Infect.*, vol. 81, pp. 87–91, 2012, doi: 10.1016/j.jhin.2012.03.003.

[228] E. A. Elekhnawy, F. I. Sonbol, T. E. Elbanna, and A. A. Abdelaziz, "Evaluation of the impact of adaptation of Klebsiella pneumoniae clinical isolates to benzalkonium chloride on biofilm formation," *Egypt. J. Med. Hum. Genet.*, vol. 22, no. 51, 2021.

[229] L. Guérin-Méchin, F. Dubois-Brissonnet, B. Heyd, and J. Y. Leveau, "Specific variations of fatty acid composition of Pseudomonas aeruginosa ATCC 15442 induced by Quaternary Ammonium Compounds and relation with resistance to bactericidal activity," *J. Appl. Microbiol.*, vol. 87, no. 5, pp. 735–742, 1999.

[230] I. M. Helander, I. Kilpelainen, and M. Vaara, "Increased substitution of phosphate groups in lipopoiysaccharides and lipid A of the polymyxin-resistant pmrA mutants of Salmonella typhimurium: a P-NMR study," *Mol. Microbiol.*, vol. 11, no. 3, pp. 481–487, 1994.

[231] Z. Zhou, A. A. Ribeiro, S. Lin, R. J. Cotter, S. I. Miller, and C. R. H. Raetz, "Lipid A Modifications in Polymyxin-resistant Salmonella typhimurium," *J. Biol. Chem.*, vol. 276, no. 46, pp. 43111–43121, 2001, doi: 10.1074/jbc.M106960200.

[232] C. M. Herrera, J. V Hankins, and M. S. Trent, "Activation of PmrA inhibits LpxT-dependent phosphorylation of lipid A promoting resistance to antimicrobial peptides," *Mol. Microbiol.*, vol. 76, no. 6, pp. 1444–1460, 2010, doi: 10.1111/j.1365-2958.2010.07150.x.

[233] M. Kim, J. K. Hatt, M. R. Weigand, R. Krishnan, S. G. Pavlostathis, and K. T. Konstantinidis, "Genomic and Transcriptomic Insights into How Bacteria Withstand High Concentrations of Benzalkonium Chloride Biocides," *Appl. Environ. Microbiol.*, vol. 84, no. 12, 2018.

[234] P. Bisbiroulas, M. Psylou, I. Iliopoulou, I. Diakogiannis, A. Berberi, and S. K. Mastronicolis, "Adaptational changes in cellular phospholipids and fatty acid composition of the food pathogen Listeria monocytogenes as a stress response to disinfectant sanitizer benzalkonium chloride," *Lett. Appl. Microbiol.*, vol. 52, no. 3, pp. 275–280, 2011, doi: 10.1111/j.1472-765X.2010.02995.x.

[235] H. Gao and C. Liu, "Biochemical and morphological alteration of Listeria monocytogenes under environmental stress caused by chloramine-T and sodium hypochlorite," *Food Control*, vol. 46, pp. 455–461, 2014, doi: 10.1016/j.foodcont.2014.05.016.

[236] M. Tandukar, S. Oh, U. Tezel, K. T. Konstantinidis, and S. G. Pavlostathis, "Long-Term Exposure to Benzalkonium Chloride Disinfectants Results in Change of Microbial Community Structure and Increased Antimicrobial Resistance," *Environ. Sci. Technol.*, vol.

47, no. 13, pp. 9730–9738, 2013.

[237] N. H. Chen, K. Y. Djoko, F. J. Veyrier, and A. G. Mcewan, "Formaldehyde Stress Responses in Bacterial Pathogens," *Front. Microbiol.*, vol. 7, 2016, doi: 10.3389/fmicb.2016.00257.

[238] W. A. Rutala, M. F. Gergen, M. T. Ascp, E. E. Sickbert-bennett, D. J. Anderson, and D. J. Weber, "Antimicrobial activity of a continuously active disinfectant against healthcare pathogens," *Infect. Control Hosp. Epidemiol.*, vol. 40, no. 11, pp. 1284–1286, 2019, doi: 10.1017/ice.2019.260.

[239] M. G. Schmidt, S. E. Fairey, and H. H. Attaway, "In situ evaluation of a persistent disinfectant provides continuous decontamination within the clinical environment," *Am. J. Infect. Control*, vol. 47, no. 6, pp. 732–734, 2019, doi: 10.1016/j.ajic.2019.02.013.

[240] R. J. W. Lambert, M. D. Johnston, G. W. Hanlon, and S. P. Denyer, "Theory of antimicrobial combinations: Biocide mixtures - Synergy or addition?," *J. Appl. Microbiol.*, vol. 95, no. 1, p. 202, 2003, doi: 10.1046/j.1365-2672.2003.02014.x.

[241] M. M. Sopirala *et al.*, "Synergy testing by etest, microdilution checkerboard, and time-kill methods for pan-drug-resistant Acinetobacter baumannii," *Antimicrob. Agents Chemother.*, vol. 54, no. 11, pp. 4678–4683, 2010, doi: 10.1128/AAC.00497-10.

[242] G. Orhan, A. Bayram, Y. Zer, and I. Balci, "Synergy tests by E test and checkerboard methods of antimicrobial combinations against Brucella melitensis," *J. Clin. Microbiol.*, vol. 43, no. 1, pp. 140–143, 2005, doi: 10.1128/JCM.43.1.140-143.2005.

[243] R. L. White, D. S. Burgess, M. Manduru, and J. A. Bosso, "Comparison of three different in vitro methods of detecting synergy: Time-kill, checkerboard, and E test," *Antimicrob. Agents Chemother.*, vol. 40, no. 8, pp. 1914–1918, 1996, doi: 10.1128/aac.40.8.1914.

[244] W. Grzybowska, M. Banaszczyk-Ruś, and S. Tyski, "Comparison of the checkerboard and E-test methods used for the analysis of two antibiotics combination," *Med. Dosw. Mikrobiol.*, vol. 57, no. 1, p. 65—75, 2005, [Online]. Available: http://europepmc.org/abstract/MED/16130296.

[245] C. R. Bonapace, J. A. Bosso, L. V. Friedrich, and R. L. White, "Comparison of methods of interpretation of checkerboard synergy testing," *Diagn. Microbiol. Infect. Dis.*, vol. 44, no. 4, pp. 363–366, 2002, doi: 10.1016/S0732-8893(02)00473-X.

[246] J. Chevalier, J. Corre, and A. Crémieux, "Evaluation of synergistic effects of three bactericidal agents associated in an antiseptic formulation," *Pharm. Acta Helv.*, vol. 70, no. 2, pp. 155–159, 1995, doi: 10.1016/0031-6865(95)00015-2.

[247] J. -L Pons, N. Bonnaveiro, J. Chevalier, and A. Crémieux, "Evaluation of antimicrobial interactions between chlorhexidine, quaternary ammonium compounds, preservatives and excipients," *J. Appl. Bacteriol.*, vol. 73, no. 5, pp. 395–400, 1992, doi: 10.1111/j.1365-2672.1992.tb04994.x.

[248] X. Xu, L. Xu, G. Yuan, Y. Wang, Y. Qu, and M. Zhou, "Synergistic combination of two antimicrobial agents closing each other's mutant selection windows to prevent antimicrobial resistance," *Sci. Rep.*, vol. 8, no. 1, pp. 1–7, 2018, doi: 10.1038/s41598-018-25714-z.

[249] Y. C. Lee, P. Y. Chen, J. T. Wang, and S. C. Chang, "A study on combination of daptomycin with selected antimicrobial agents: In vitro synergistic effect of MIC value of

1 mg/L against MRSA strains," *BMC Pharmacol. Toxicol.*, vol. 20, no. 1, pp. 4–9, 2019, doi: 10.1186/s40360-019-0305-y.

[250] F. C. Odds, "Synergy, antagonism, and what the chequerboard puts between them," *J. Antimicrob. Chemother.*, vol. 52, no. 1, 2003, doi: 10.1093/jac/dkg301.

[251] Journal of Antimicrobial Chemotherapy, "Instructions for Authors," *Journal of Antimicrobial Chemotherapy*. .

[252] Antimicrobial Agents and Chemotherapy, "Instructions to Authors," *Antimicrob. Agents Chemother.*, pp. 1–22, 2020.

[253] EUCAST, "Terminology relating to methods for the determination of susceptibility of bacteria to antimicrobial agents," *Clin. Microbiol. Infect.*, vol. 6, no. 9, 2000, doi: 10.1046/j.1469-0691.2000.00149.x.

[254] Y. L. Wu, E. M. Scott, A. L. W. Po, and V. N. Tariq, "Ability of azlocillin and tobramycin in combination to delay or prevent resistance development in," *J. Antimicrob. Chemother.*, vol. 44, no. 3, pp. 389–392, 1999.

[255] P. D. Lister and D. J. Wolter, "Levofloxacin-Imipenem Combination Prevents the Emergence of Resistance among Clinical Isolates of Pseudomonas aeruginosa," *Clin. Infect. Dis.*, vol. 40, no. Issue Supplement_2, pp. S105–S114, 2005.

[256] P. D. Lister, D. J. Wolter, P. A. Wickman, and M. D. Reisbig, "Levofloxacin/imipenem prevents the emergence of high-level resistance among Pseudomonas aeruginosa strains already lacking susceptibility to one or both drugs," *J. Antimicrob. Chemother.*, vol. 57, no. 5, pp. 999–1003, 2006, doi: 10.1093/jac/dkl063.

[257] C. Wiegand, M. Abel, P. Ruth, P. Elsner, and U.-C. Hiplet, "pH Influence on Antibacterial Efficacy of Common Antiseptic Substances," *Ski. Pharmacol. Physiology*, vol. 28, pp. 147–158, 2015, doi: 10.1159/000367632.

[258] S. L. Percival, S. Finnegan, G. Donelli, C. Vuotto, S. Rimmer, and B. A. Lipsky, "Antiseptics for treating infected wounds: Efficacy on biofilms and effect of pH," *Crit. Rev. Microbiol.*, vol. 42, no. 2, pp. 293–309, 2016, doi: 10.3109/1040841X.2014.940495.

[259] A. D. Russell, W. B. Hugo, and G. A. J. Ayliffe, "Factors influencing the efficacy of antimicrobial agents," in *Principles and Practice of Disinfection, Preservation and Sterilization*, 4th editio., A. P. Fraise, P. A. Lambert, and J. Y. Maillard, Eds. Blackwell Publishing Ltd, 2004, pp. 89–113.

[260] V. Drauch, C. Ibesich, C. Vogl, M. Hess, and C. Hess, "In-vitro testing of bacteriostatic and bactericidal efficacy of commercial disinfectants against Salmonella Infantis reveals substantial di ff erences between products and bacterial strains," *Int. J. Food Microbiol.*, vol. 328, 2020, doi: 10.1016/j.ijfoodmicro.2020.108660.

[261] A. Bridier, R. Briandet, V. Thomas, and F. Dubois-brissonnet, "Comparative biocidal activity of peracetic acid , benzalkonium chloride and ortho-phthalaldehyde on 77 bacterial strains," *J. Hosp. Infect.*, vol. 78, no. 3, pp. 208–213, 2011, doi: 10.1016/j.jhin.2011.03.014.

[262] M. Demirbilek and E. Evren, "Efficacy of Multipurpose Contact Lens Solutions Against ESBL-Positive Escherichia coli, MRSA, and Candida albicans clinical isolates," *Eyes Contact Lens*, vol. 40, no. 3, pp. 157–160, 2014, doi: 10.1097/ICL.0000000000000029.

[263] A. T. Köhler, A. C. Rodloff, M. Labahn, M. Reinhardt, U. Truyen, and S. Speck, "Efficacy

of sodium hypochlorite against multidrug-resistant Gram-negative bacteria," *J. Hosp. Infect.*, vol. 100, pp. 40–46, 2018, doi: 10.1016/j.jhin.2018.07.017.

[264] T. K. Anne, A. C. Rodloff, M. Labahn, M. Reinhardt, U. Truyen, and S. Speck, "Evaluation of disinfectant efficacy against multidrug-resistant bacteria: A comprehensive analysis of different methods," *Am. J. Infect. Control*, vol. 47, pp. 1181–1187, 2019, doi: 10.1016/j.ajic.2019.04.001.

[265] S. Langsrud and G. Sundheim, "Factors influencing a suspension test method for antimicrobial activity of disinfectants," *J. Appl. Microbiol.*, vol. 85, pp. 1006–1012, 1998.

[266] N. L. Cowley, S. Forbes, A. Amézquita, P. Mcclure, G. J. Humphreys, and A. J. McBain, "Effects of Formulation on Microbicide Potency and Mitigation of the Development of Bacterial Insusceptibility," *Appl. Environ. Microbiol.*, vol. 81, no. 20, pp. 7330–7338, 2015, doi: 10.1128/AEM.01985-15.

[267] F. Fernández-Cuenca *et al.*, "Reduced susceptibility to biocides in Acinetobacter baumannii: association with resistance to antimicrobials, epidemiological behaviour, biological cost and effect on the expression of genes encoding porins and efflux pumps," *J. Antimicrob. Chemother.*, vol. 70, no. 12, pp. 3222–3229, 2015, doi: 10.1093/jac/dkv262.

[268] V. E. Lee and A. J. O'Neill, "Potential for repurposing the personal care product preservatives bronopol and bronidox as broad-spectrum antibiofilm agents for topical application," *J. Antimicrob. Chemother.*, vol. 74, pp. 907–911, 2019, doi: 10.1093/jac/dky520.

[269] S. Lanjri *et al.*, "In vitro evaluation of the susceptibility of Acinetobacter baumannii isolates to antiseptics and disinfectants: comparison between clinical and environmental isolates," *Antimicrob. Resist. Infect. Control*, vol. 36, no. 6, pp. 1–7, 2017, doi: 10.1186/s13756-017-0195-y.

[270] E. Martró *et al.*, "Assessment of Acinetobacter baumannii susceptibility to antiseptics and disinfectants," *J. Hosp. Infect.*, vol. 55, pp. 39–46, 2003, doi: 10.1016/S0195-6701(03)00220-2.

[271] L. B. Rice, "Federal funding for the study of antimicrobial resistance in nosocomial pathogens: No ESKAPE," *J. Infect. Dis.*, vol. 197, no. 8, pp. 1079–1081, 2008, doi: 10.1086/533452.

[272] F. R. Cockerill *et al.*, *Methods for Dilution Antimicrobial Susceptibility Tests for Bacteria That Grow Aerobically ; Approved Standard — Ninth*, vol. 32, no. 2. CLSI, 2012.

[273] D. Kwaśniewska, Y. L. Chen, and D. Wieczorek, "Biological activity of quaternary ammonium salts and their derivatives," *Pathogens*, vol. 9, no. 6, pp. 1–12, 2020, doi: 10.3390/pathogens9060459.

[274] R. Bragg, A. Jansen, M. Coetzee, W. van der westhuizen, and C. Boucher, "Bacterial resistance to quaternary ammonium compounds (QAC) disinfectants," *Adv. Exp. Med. Biol.*, vol. 808, pp. 1–13, 2014, doi: 10.1007/978-81-322-1774-9_1.

[275] D. G. White and P. F. McDermott, "Biocides, drug resistance and microbial evolution," *Curr. Opin. Microbiol.*, vol. 4, no. 3, pp. 313–317, 2001, doi: 10.1016/S1369-5274(00)00209-5.

[276] H. Nikaido, "Prevention of Drug Access to Bacterial Targets : Permeability Barriers and Active Efflux," *Science (80-.).*, vol. 264, 1994.

[277] W. R. Bowman and R. J. Stretton, "Antimicrobial Activity of a Series of Halo-Nitro Compounds," *Antimicrob. Agents Chemother.*, vol. 2, no. 6, pp. 504–505, 1972.

[278] N. G. Clark, B. Croshaw, B. E. Leggetter, and D. F. Spooner, "Synthesis and Antimicrobial Activity of Aliphatic Nitro Compounds," *J. Med. Chem.*, vol. 17, no. 9, pp. 977–981, 1974.

[279] M. Ghannoum, M. Thomson, W. Bowman, and S. Al-Khalil, "Mode of Action of the Antimicrobial Compound 5-Bromo-5-nitro-1,3-dioxane (Bronidox)," *Folia Microbiol. (Praha).*, vol. 31, pp. 19–31, 1986.

[280] E. M. Fox, N. Leonard, and K. Jordan, "Physiological and Transcriptional Characterization of Persistent and Nonpersistent Listeria monocytogenes Isolates," *Appl. Environ. Microbiol.*, vol. 77, no. 18, pp. 6559–6569, 2011, doi: 10.1128/AEM.05529-11.

[281] S. Hernando-amado *et al.*, "Multidrug efflux pumps as main players in intrinsic and acquired resistance to antimicrobials," *Drug Resist. Updat.*, vol. 28, pp. 13–27, 2016, doi: 10.1016/j.drup.2016.06.007.

[282] C. J. Ioannou, G. W. Hanlon, and S. P. Denyer, "Action of Disinfectant Quaternary Ammonium Compounds against Staphylococcus aureus," *Antimicrob. Agents Chemother.*, vol. 51, pp. 296–306, 2007, doi: 10.1128/AAC.00375-06.

[283] P. Gilbert, D. Pemberton, and D. E. Wilkinson, "Synergism within polyhexamethylene biguanide biocide formulations," *J. Appl. Bacteriol.*, vol. 69, pp. 593–598, 1990.

[284] H. S. Bean and A. Das, "The absorption by Escherichia coli of phenols and their bactericidal activity," *J. Pharm. Pharmacol.*, vol. 18, pp. 107S-113S, 1966.

[285] M. D. Alcántar-Curiel *et al.*, "Multi-functional analysis of Klebsiella Pneumoniae fimbrial types in adherence and biofilm formation," *Virulence*, vol. 4, no. 2, pp. 129–138, 2013, doi: 10.4161/viru.22974.

[286] D. Gusnard and R. H. Kirschner, "Cell and organelle shrinkage during preparation for Scanning electron microscopy: effects of fixation, dehydration and critical point drying," *J. Microsc.*, vol. 110, no. 1, pp. 51–57, 1977.

[287] C. G. Golding, L. L. Lamboo, D. R. Beniac, and T. F. Booth, "The scanning electron microscope in microbiology and diagnosis of infectious disease," *Sci. Rep.*, 2016, doi: 10.1038/srep26516.

[288] C. Guilhen *et al.*, "Colonization and immune modulation properties of Klebsiella pneumoniae biofilm-dispersed cells," *npj Biofilms Microbiomes*, vol. 5, no. 1, 2019, doi: 10.1038/s41522-019-0098-1.

[289] R. Sharma *et al.*, "Polymyxin B in combination with meropenem against carbapenemase-producing Klebsiella pneumoniae: pharmacodynamics and morphological changes," *Int. J. Antimicrob. Agents*, vol. 49, no. 2, pp. 224–232, 2017, doi: 10.1016/j.ijantimicag.2016.10.025.

[290] T. Yoshimatsw and K.-I. Hiyama, "Mechanism of the Action of Didecyldimethylammonium chloride (DDAC) against Escherichia coli and Morphological Changes of the Cells," *Biocontrol Sci.*, vol. 12, no. 3, pp. 93–99, 2007.

[291] J. Judis, "Mechanism of Action of Phenolic Disinfectants VII: Factors affecting binding of phenol derivatives to Micrococcus lysodeikticus cells," *J. Pharm. Sci.*, vol. 55, no. 8, pp. 803–807, 1966.

[292] A. Ramírez Granillo, M. Gabriela Medina Canales, E. María Sánchez Espíndola, M. Angeles Martínez Rivera, V. Manuel Bautista de Lucio, and A. Verónica Rodríguez Tovar, "Antibiosis interaction of Staphylococccus aureus on Aspergillus fumigatus assessed in vitro by mixed biofilm formation," *BMC Microbiol.*, vol. 15, no. 33, 2015, doi: 10.1186/s12866-015-0363-2.

[293] C. M. Watters, T. Burton, D. K. Kirui, and N. J. Millenbaugh, "Enzymatic degradation of in vitro Staphylococcus aureus biofilms supplemented with human plasma," *Infect. Drug Resist.*, no. 9, pp. 71–78, 2016.

[294] C. I. Mawang, Y. Y. Lim, K. S. Ong, A. Muhamad, and S. M. Lee, "Identification of α -tocopherol as a bioactive component of Dicranopteris linearis with disrupting property against pre-formed biofilm of Staphylococcus aureus Identification of α -tocopherol as a bioactive component of Dicranopteris linearis with disrupt," *J. Appl. Microbiol.*, 2017, doi: 10.1111/jam.13578.

[295] A. Davies, M. Bentley, and B. S. Field, "Comparison of the Action of Vantocil, Cetrimide and Chlorhexidine on Escherichia coli and its Spheroplasts and the Protoplasts of Gram Positive Bacteria," *J. Appl. Bacteriol.*, vol. 31, no. 4, pp. 448–461, 1968, doi: 10.1111/j.1365-2672.1968.tb00394.x.

[296] B. M. A. El-Falaha, A. D. Russell, and J. R. Furr, "Effect of chlorhexidine diacetate and benzalkonium chloride on the viability of wild type and envelope mutants of Escherichia coli and Pseudomonas aeruginosa," *Lett. Appl. Microbiol.*, vol. 1, no. 1, pp. 21–24, 1985.

[297] J. Y. Maillard, "Bacterial target sites for biocide action," *J. Appl. Microbiol. Symp. Suppl.*, vol. 92, no. 1, pp. 16–27, 2002, doi: 10.1046/j.1365-2672.92.5s1.3.x.

[298] S. Angermüller and H. D. Fahimi, "Imidazole-buffered osmium tetroxide: an excellent stain for visualization of lipids in transmission electron microscopy," *Histochem. J.*, vol. 14, pp. 823–835, 1982.

[299] J. J. Bozzola and L. D. Russell, *Electron Microscopy, Principles and Techniques for Biologists*. 1992.

[300] M. R. J. Salton, "Lytic Agents, Cell Permeability, and Monolayer Penetrability," *J. Gen. Physiol.*, vol. 52, no. 1, pp. 227–252, 1968.

[301] D. J. Noel, C. W. Keevil, and S. A. Wilks, "Synergism versus Additivity: Defining the Interactions between Common Disinfectants," *MBio*, vol. 12, no. 5, 2021, doi: 10.1128/mbio.02281-21.

[302] European Patent Office, "European Patent Convention. Chapter 1 - Patentability," 2020. .

[303] A. L. Barry, W. A. Craig, H. Nadler, L. B. Reller, C. C. Sanders, and J. M. Swenson, *Methods for Determining Bactericidal Activity of Antimicrobial Agents, 1st Edition*. CLSI, 1999.

[304] M. A. H. Soudeiha, E. A. Dahdouh, E. Azar, D. K. Sarkis, and Z. Daoud, "In vitro evaluation of the colistin-carbapenem combination in clinical isolates of a. baumannii using the checkerboard, Etest, and time-kill curve Techniques," *Front. Cell. Infect. Microbiol.*, vol. 7, no. May, pp. 1–10, 2017, doi: 10.3389/fcimb.2017.00209.

[305] A. Oliva *et al.*, "In-vitro evaluation of different antimicrobial combinations with and without colistin against carbapenem-resistant Acinetobacter baumannii," *Molecules*, vol. 24, no. 5, pp. 1–12, 2019, doi: 10.3390/molecules24050886.

[306] R. Kheshti, B. Pourabbas, M. Mosayeb, and A. Vazin, "In vitro activity of colistin in

combination with various antimicrobials against Acinetobacter baumannii species, a report from South Iran.," *Infect. Drug Resist.*, vol. 2019, no. 12, pp. 129–135, 2018.

[307] E. A. Greene, V. Brunelle, G. E. Jenneman, and G. Voordouw, "Synergistic inhibition of microbial sulfide production by combinations of the metabolic inhibitor nitrite and biocides," *Appl. Environ. Microbiol.*, vol. 72, no. 12, pp. 7897–7901, 2006, doi: 10.1128/AEM.01526-06.

[308] H. E. Saito, J. R. Harp, and E. M. Fozo, "Enterococcus faecalis Responds to Individual Exogenous Fatty Acids Independently of Their Degree of Saturation or Chain Length," *Appl. Environ. Microbiol.*, vol. 84, no. 1, 2018.

[309] E. Mileykovskaya and W. Dowhan, "Role of membrane lipids in bacterial division-site selection," *Curr. Opin. Microbiol.*, vol. 8, pp. 135–142, 2005, doi: 10.1016/j.mib.2005.02.012.

[310] K. E. Weaver *et al.*, "Enterococcus faecalis Plasmid pAD1-Encoded Fst Toxin Affects Membrane Permeability and Alters Cellular Responses to Lantibiotics," *J. Bacteriol.*, vol. 185, no. 7, pp. 2169–2177, 2003, doi: 10.1128/JB.185.7.2169.

[311] R. B. Srivastava and R. E. M. Thompson, "Influence of bacterial cell age on phenol action," *Nature*, vol. 206, p. 216, 1965.

[312] R. B. Srivastava and R. E. M. Thompson, "Studies in the mechanism of action of phenol on Escherichia coli cells," *Br. J. Exp. Pathol.*, vol. 47, no. 3, pp. 315–323, 1966.

[313] U. S. F. and D. Administration, "Safety and Effectiveness of Health Care Antiseptics; Topical Antimicrobial Drug Products for Over-the-Counter Human Use. Final rule," *Fed. Regist.*, vol. 82, no. 242, pp. 60474–60503, 2017.

[314] U.S. Food and Drug Administration, "Letter from FDA CDER to Lonza America, Inc., American Cleaning Institute and Henkel North America regarding Review of Benzethonium Chloride," 2016. https://www.regulations.gov/document/FDA-1975-N-0012-0638 (accessed Feb. 26, 2021).

[315] U.S. Food and Drug Administration, "Letter from CDER FDA to American Cleaning Institute," 2017. https://www.regulations.gov/document/FDA-1975-N-0012-0731 (accessed Feb. 26, 2021).

[316] U.S. Food and Drug Administration, "Grant of Second Extension April 12_2018," 2018. https://www.regulations.gov/document/FDA-1975-N-0012-0735 (accessed Feb. 26, 2021).

[317] U.S. Food and Drug Administration, "FINAL Third Extension Deferral Letter," 2019. https://www.regulations.gov/document/FDA-1975-N-0012-0778 (accessed Feb. 26, 2021).

[318] U.S. Food and Drug Administration, "Letter from FDA CDER to Lonza America, Inc., American Cleaning Institute and Henkel North America regarding Review of Benzalkonium Chloride," 2020. https://www.regulations.gov/document/FDA-1975-N-0012-0639 (accessed Feb. 26, 2021).

[319] American Cleaning Institute, "Response from American Cleaning Institute to FDA CDER (re: Benzalkonium Chloride)." 2016, [Online]. Available: https://www.regulations.gov/document/FDA-1975-N-0012-0646.

[320] K. Drlica, "The mutant selection window and antimicrobial resistance," *J. Antimicrob.*

Chemother., vol. 52, no. 1, pp. 11–17, 2003, doi: 10.1093/jac/dkg269.

[321] J. F. Acar, "Antibiotic synergy and antagonism," *Med. Clin. North Am.*, vol. 84, no. 6, pp. 1391–1406, 2000, doi: 10.1016/S0025-7125(05)70294-7.

[322] I. M. Helander *et al.*, "Characterization of lipopolysaccharides of polymyxin-resistant and polymyxin-sensitive Klebsiella pneumoniae 03," *Eur. J. Biochem.*, vol. 237, pp. 272–278, 1996.

[323] L. N. Nielsen *et al.*, "Staphylococcus aureus but not Listeria monocytogenes adapt to triclosan and adaptation correlates with increased fabI expression and agr deficiency," *BMC Microbiol.*, vol. 13, no. 177, 2013, doi: 10.1186/1471-2180-13-177.

[324] S. Forbes, J. Latimer, A. Bazaid, and A. J. Mcbain, "Altered Competitive Fitness, Antimicrobial Susceptibility, and Cellular Morphology in a Triclosan-Induced Small-Colony Variant of Staphylococcus aureus," *Antimicrob. Agents Chemother.*, vol. 59, no. 8, pp. 4809–4816, 2015, doi: 10.1128/AAC.00352-15.

[325] R. Wesgate, P. Grasha, and J.-Y. Maillard, "Use of a predictive protocol to measure the antimicrobial resistance risks associated with biocidal product usage," *Am. J. Infect. Control*, vol. 44, no. 4, pp. 458–464, 2016, doi: 10.1016/j.ajic.2015.11.009.

[326] R. López-rojas, F. Fernández-cuenca, L. Serrano-rocha, and Á. Pascual, "In vitro activity of a polyhexanide-betaine solution against high-risk clones of multidrug-resistant nosocomial pathogens," *Enferm. Infecc. Microbiol. Clin.*, vol. 35, no. 1, pp. 12–19, 2017, doi: 10.1016/j.eimce.2017.01.004.

[327] W. Guo *et al.*, "Determining the resistance of carbapenem- resistant Klebsiella pneumoniae to common disinfectants and elucidating the underlying resistance mechanisms," *Pathog. Glob. Health*, vol. 109, no. 4, pp. 184–192, 2015, doi: 10.1179/2047773215Y.0000000022.

[328] Y. Zhang *et al.*, "Chlorhexidine exposure of clinical Klebsiella pneumoniae strains leads to acquired resistance to this disinfectant and to colistin," *Int. J. Antimicrob. Agents*, vol. 53, pp. 864–867, 2019, doi: 10.1016/j.ijantimicag.2019.02.012.

[329] Y. Chen *et al.*, "Determining the susceptibility of carbapenem resistant Klebsiella pneumoniae and Escherichia coli strains against common disinfectants at a tertiary hospital in China," *BMC Infect. Dis.*, vol. 20, no. 88, 2020.

[330] J. Morante *et al.*, "Tolerance to disinfectants (chlorhexidine and isopropanol) and its association with antibiotic resistance in clinically-related Klebsiella pneumoniae isolates," *Pathog. Glob. Health*, vol. 115, no. 1, pp. 53–60, 2021, doi: 10.1080/20477724.2020.1845479.

[331] R. Vijayakumar *et al.*, "Distribution of biocide resistant genes and biocides susceptibility in multidrug-resistant Klebsiella pneumoniae , Pseudomonas aeruginosa and Acinetobacter baumannii — A first report from the Kingdom of Saudi Arabia," *J. Infect. Public Health*, vol. 11, pp. 812–816, 2018, doi: 10.1016/j.jiph.2018.05.011.

[332] L. J. Bock, M. E. Wand, and J. M. Sutton, "Varying activity of chlorhexidine-based disinfectants against Klebsiella pneumoniae clinical isolates and adapted strains," *J. Hosp. Infect.*, vol. 93, no. 1, pp. 42–48, 2016, doi: 10.1016/j.jhin.2015.12.019.

[333] R. Gadea, M. Ángel Fuentes Fernández, R. Pérez Pulido, A. Gálvez, and E. Ortega, "Effects of exposure to quaternary-ammonium-based biocides on antimicrobial

susceptibility and tolerance to physical stresses in bacteria from organic foods," *Food Microbiol.*, vol. 63, pp. 58–71, 2017, doi: 10.1016/j.fm.2016.10.037.

[334] R. Bayston, W. Ashraf, and T. Smith, "Triclosan resistance in methicillin-resistant Staphylococcus aureus expressed as small colony variants : a novel mode of evasion of susceptibility to antiseptics," *J. Antimicrob. Chemother.*, vol. 59, pp. 848–853, 2007, doi: 10.1093/jac/dkm031.

[335] N. Singh and P. J. Yeh, "Suppressive drug combinations and their potential to combat antibiotic resistance," *J. Antibiot. (Tokyo).*, vol. 70, pp. 1033–1042, 2017, doi: 10.1038/ja.2017.102.

[336] Y. Sakagami, H. Yokoyama, H. Nishimura, Y. Ose, and T. Tashima, "Mechanism of Resistance to Benzalkonium Chloride by Pseudomonas aeruginosa," *Appl. Environ. Microbiol.*, vol. 55, no. 8, pp. 2036–2040, 1989.

[337] S. Ishikawa, Y. Matsumura, F. Yoshizako, and T. Tsuchido, "Characterization of a cationic surfactant-resistant mutant isolated spontaneously from Escherichia coli," *J. Appl. Microbiol.*, vol. 92, pp. 261–268, 2002.

[338] M. Ceragioli, M. Mols, R. Moezelaar, E. Ghelardi, S. Senesi, and T. Abee, "Comparative Transcriptomic and Phenotypic Analysis of the Responses of Bacillus cereus to Various Disinfectant Treatments," *Appl. Environ. Microbiol.*, vol. 76, no. 10, pp. 3352–3360, 2010, doi: 10.1128/AEM.03003-09.

[339] N. Nordholt, O. Kanaris, S. B. I. Schmidt, and F. Schreiber, "Persistence against benzalkonium chloride promotes rapid evolution of tolerance during periodic disinfection," *Nat. Commun.*, vol. 12, 2021, doi: 10.1038/s41467-021-27019-8.

[340] V. B. Srinivasan and G. Rajamohan, "KpnEF, a New Member of the Klebsiella pneumoniae Cell Envelope Stress Response Regulon, Is an SMR-Type Efflux Pump Involved in Broad-Spectrum Antimicrobial Resistance," *Antimicrob. Agents Chemother.*, vol. 57, no. 9, pp. 4449–4462, 2013, doi: 10.1128/AAC.02284-12.

[341] V. B. Srinivasan, B. B. Singh, N. Priyadarshi, and N. K. Chauhan, "Role of Novel Multidrug Efflux Pump Involved in Drug Resistance in Klebsiella pneumoniae," *PLoS One*, vol. 9, no. 5, 2014, doi: 10.1371/journal.pone.0096288.

[342] R. Gadea, M. Ángel Fuentes Fernández, R. Pérez Pulido, A. Gálvez, and E. Ortega, "Adaptive tolerance to phenolic biocides in bacteria from organic foods: Effects on antimicrobial susceptibility and tolerance to physical stresses," *Food Res. Int.*, vol. 85, pp. 131–143, 2016, doi: 10.1016/j.foodres.2016.04.033.

[343] M. Angel Fernández-fuentes, E. Ortega Morente, H. Abriouel, R. Pérez Pulido, and A. Gálvez, "Isolation and identification of bacteria from organic foods: Sensitivity to biocides and antibiotics," *Food Control*, vol. 26, pp. 73–78, 2012, doi: 10.1016/j.foodcont.2012.01.017.

[344] W. B. Hugo and I. Franklin, "Cellular Lipid and the Antistaphylococcal Activity of Phenols," *J. Gen. Microbiol.*, vol. 52, pp. 365–373, 1968.

[345] H. W. A, "The Mechanism of the Bacteriostatic Action of Tetrachlorosalicylanilide : a Membrane-active Antibacterial Compound," *J. Gen. Microbiol.*, vol. 50, pp. 441–458, 1968.

[346] P. Gilbert and M. R. W. Brown, "Influence of Growth Rate and Nutrient Limitation on the Gross Cellular Composition of Pseudomonas aeruginosa and Its Resistance to 3- and

4-Chlorophenol," vol. 133, no. 3, pp. 1066–1072, 1978.

[347] V. S. Brözel and T. E. Cloete, "Adaptation of Pseudomonas aeruginosa to 2,2'-methylenebis (4-chlorophenol)," *J. Appl. Bacteriol.*, vol. 74, pp. 94–99, 1993.

[348] B. Kouidhi *et al.*, "Antibacterial and resistance-modifying activities of thymoquinone against oral pathogens," *Ann. Clin. Microbiol. Antimicrob.*, vol. 10, no. 29, 2011, doi: 10.1186/1476-0711-10-29.

[349] E. O. Akinkunmi and A. Lamikanra, "Susceptibility of community associated methicillin resistant Staphylococcus aureus isolated from faeces to antiseptics," *J. Infect. Dev. Ctries.*, vol. 6, no. 4, 2012.

[350] G. He *et al.*, "Detection of benzalkonium chloride resistance in community environmental isolates of staphylococci," *J. Med. Microbiol.*, vol. 63, pp. 735–741, 2014, doi: 10.1099/jmm.0.073072-0.

[351] I. Morrissey *et al.*, "Evaluation of Epidemiological Cut-Off Values Indicates that Biocide Resistant Subpopulations Are Uncommon in Natural Isolates of Clinically-Relevant Microorganisms," *PLoS One*, vol. 9, no. 1, 2014, doi: 10.1371/journal.pone.0086669.

[352] A. Ramzi, B. Oumokhtar, Y. Ez zoubi, T. F. Mouatassem, M. Benboubker, and A. E. O. Lalami, "Evaluation of Antibacterial Activity of Three Quaternary Ammonium Disinfectants on Different Germs Isolated from the Hospital Environment," *Biomed Res. Int.*, vol. 2020, 2020.

[353] J. M. Benarroch and M. Asally, "The Microbiologist's Guide to Membrane Potential Dynamics," *Trends Microbiol.*, vol. 28, no. 4, pp. 304–314, 2020, doi: 10.1016/j.tim.2019.12.008.

[354] M. Feldgarden *et al.*, "AMRFinderPlus and the Reference Gene Catalog facilitate examination of the genomic links among antimicrobial resistance, stress response, and virulence," *Sci. Rep.*, vol. 11, no. 1, 2021, doi: 10.1038/s41598-021-91456-0.

[355] National Center for Biotechnology Information, "Klebsiella pneumoniae genome assembly 32868_D02," 2018. .

[356] R. S. Kaas, P. Leekitcharoenphon, F. M. Aarestrup, and O. Lund, "Solving the Problem of Comparing Whole Bacterial Genomes across Different Sequencing Platforms," *PLoS One*, vol. 9, no. 8, 2014, doi: 10.1371/journal.pone.0104984.

[357] A. Rambaut, "FigTree," 2018. .

[358] B. Mlecnik, J. Galon, and G. Bindea, "Comprehensive functional analysis of large lists of genes and proteins," *J. Proteomics*, vol. 171, 2018, doi: 10.1016/j.jprot.2017.03.016.

[359] P. Shannon *et al.*, "Cytoscape : A Software Environment for Integrated Models of Biomolecular Interaction Networks," *Genome Res.*, vol. 13, no. 11, pp. 2498–2504, 2003, doi: 10.1101/gr.1239303.metabolite.

[360] The UniProt Consortium, "UniProt: the universal protein knowledgebase in 2021," *Nucleic Acids Res.*, vol. 49, pp. d480–d489, 2021, doi: 10.1093/nar/gkaa1100.

[361] Y. Van de Peer, "Bioinformatics & Evolutionary Genomics. Venn diagram tool." .

[362] D. W. Huang, B. T. Sherman, and R. A. Lempicki, "Systematic and integrative analysis of large gene lists using DAVID bioinformatics resources," *Nat. Protoc.*, vol. 4, no. 1, pp. 44–57, 2009, doi: 10.1038/nprot.2008.211.

[363] B. T. Sherman *et al.*, "DAVID: a web server for functional enrichment analysis and functional annotation of gene lists (2021 update)," *Nucleic Acids Res.*, vol. 50, pp. 216–221, 2022.

[364] M. Kanehisa and S. Goto, "KEGG: Kyoto Encyclopedia of Genes and Genomes," *Nucleic Acids Res.*, vol. 28, no. 1, pp. 27–30, 2000.

[365] M. Kanehisa, "Toward understanding the origin and evolution of cellular organisms," *Protein Sci.*, vol. 28, no. 11, pp. 1947–1951, 2019, doi: 10.1002/pro.3715.

[366] M. Sangiovanni, I. Granata, A. S. Thind, and M. R. Guarracino, "From trash to treasure : detecting unexpected contamination in unmapped NGS data," *BMC Bioinformatics*, vol. 20, no. 168, 2019, doi: 10.1186/s12859-019-2684-x.

[367] A. W. Pightling, N. Petronella, and F. Pagotto, "Choice of Reference Sequence and Assembler for Alignment of Listeria monocytogenes Short-Read Sequence Data Greatly Influences Rates of Error in SNP Analyses," *PLoS One*, vol. 9, no. 8, 2014, doi: 10.1371/journal.pone.0104579.

[368] M. N. Price, P. S. Dehal, and A. P. Arkin, "FastTree: Computing Large Minimum Evolution Trees with Profiles instead of a Distance Matrix," *Mol. Biol. Evol.*, vol. 26, no. 7, pp. 1641–1650, 2009, doi: 10.1093/molbev/msp077.

[369] M. N. Price, P. S. Dehal, and A. P. Arkin, "FastTree 2 – Approximately Maximum-Likelihood Trees for Large Alignments," *PLoS One*, vol. 5, no. 3, 2010, doi: 10.1371/journal.pone.0009490.

[370] J. W. Mouton, "Combination Therapy as a Tool to Prevent Emergence of Bacterial Resistance," *Infection*, vol. 27, pp. 24–28, 1999.

[371] A. R. M. Coates, Y. Hu, J. Holt, and P. Yey, "Antibiotic combination therapy against resistant bacterial infections: synergy, rejuvenation and resistance reduction," *Expert Rev. Anti. Infect. Ther.*, vol. 18, no. 1, pp. 5–15, 2020, doi: 10.1080/14787210.2020.1705155.

[372] M. S. Trent, A. A. Ribeiro, S. Lin, R. J. Cotter, and C. R. H. Raetz, "An Inner Membrane Enzyme in Salmonella and Escherichia coli That Transfers 4-Amino-4-deoxy-L-arabinose to Lipid A," *J. Biol. Chem.*, vol. 276, no. 46, pp. 43122–43131, 2001, doi: 10.1074/jbc.M106961200.

[373] K. Nummila, I. Kilpelainen, U. Zahringer, M. Vaara, and I. M. Helander, "Lipopolysaccharides of polymyxin B-resistant mutants of Escherichia coli are extensively substituted by 2-aminoethyl pyrophosphate and contain aminoarabinose in lipid A," *Mol. Microbiol.*, vol. 16, no. 2, pp. 271–278, 1995.

[374] J. S. Gunn *et al.*, "PmrA–PmrB-regulated genes necessary for 4-aminoarabinose lipid A modification and polymyxin resistance," *Mol. Microbiol.*, vol. 27, no. 6, pp. 1171–1182, 1998.

[375] A. Y. Mitrophanov, M. W. Jewett, T. J. Hadley, and E. A. Groisman, "Evolution and Dynamics of Regulatory Architectures Controlling Polymyxin B Resistance in Enteric Bacteria," *PLOS Genet.*, vol. 4, no. 10, 2008, doi: 10.1371/journal.pgen.1000233.

[376] C. R. H. Raetz, M. C. Reynolds, M. S. Trent, and R. E. Bishop, "Lipid A modification systems in Gram-negative bacteria," *Annu. Rev. Biochem.*, vol. 76, pp. 295–329, 2007, doi: 10.1146/annurev.biochem.76.010307.145803.LIPID.

[377] J. Huang *et al.*, "Regulating polymyxin resistance in Gram-negative bacteria: Roles of two-

component systems PhoPQ and PmrAB," *Future Microbiol.*, vol. 15, no. 6, pp. 445–459, 2020, doi: 10.2217/fmb-2019-0322.

[378] A. Cannatelli *et al.*, "An allelic variant of the PmrB sensor kinase responsible for colistin resistance in an Escherichia coli strain of clinical origin," *Sci. Rep.*, vol. 7, 2017, doi: 10.1038/s41598-017-05167-6.

[379] C. Duvernay, L. Coulange, B. Dutilh, V. Dubois, C. Quentin, and C. Arpin, "Duplication of the chromosomal bla SHV-11 gene in a clinical hypermutable strain of Klebsiella pneumoniae," *Microbiology*, vol. 157, pp. 496–503, 2011, doi: 10.1099/mic.0.043885-0.

[380] F. W. Outten, C. E. Outten, J. Hale, and T. V O'Halloran, "Transcriptional Activation of an Escherichia coli Copper Efflux Regulon by the Chromosomal MerR Homologue, CueR," *J. Biol. Chem.*, vol. 275, no. 40, pp. 31024–31029, 2000, doi: 10.1074/jbc.M006508200.

[381] M. J. Choi and K. S. Ko, "Mutant prevention concentrations of colistin for Acinetobacter baumannii, pseudomonas aeruginosa and Klebsiella pneumoniae clinical isolates," *J. Antimicrob. Chemother.*, vol. 69, no. 1, pp. 275–277, 2014, doi: 10.1093/jac/dkt315.

[382] S. J. Kim and K. S. Ko, "Diverse genetic alterations responsible for post-exposure colistin resistance in populations of the same strain of Klebsiella pneumoniae," *Int. J. Antimicrob. Agents*, vol. 52, no. 3, pp. 425–429, 2018, doi: 10.1016/j.ijantimicag.2018.06.010.

[383] A. Boehm *et al.*, "Second messenger signalling governs Escherichia coli biofilm induction upon ribosomal stress," *Mol. Microbiol.*, vol. 72, no. 6, pp. 1500–1516, 2009, doi: 10.1111/j.1365-2958.2009.06739.x.

[384] C.-J. Huang, Z.-C. Wang, H.-Y. Huang, H.-D. Huang, and H.-L. Peng, "YjcC, a c-di-GMP Phosphodiesterase Protein , Regulates the Oxidative Stress Response and Virulence of Klebsiella pneumoniae CG43," *PLoS One*, vol. 8, no. 7, 2013, doi: 10.1371/journal.pone.0066740.

[385] N. Strempel, M. Nusser, A. Neidig, G. Brenner-weiss, and J. Overhage, "The Oxidative Stress Agent Hypochlorite Stimulates c-di-GMP Synthesis and Biofilm Formation in Pseudomonas aeruginosa," *Front. Microbiol.*, vol. 8, 2017, doi: 10.3389/fmicb.2017.02311.

[386] S. L. Chua *et al.*, "C-di-GMP regulates Pseudomonas aeruginosa stress response to tellurite during both planktonic and biofilm modes of growth," *Sci. Rep.*, vol. 5, 2015, doi: 10.1038/srep10052.

[387] C. Lin, T. Lin, C. Wu, L. Wan, C. Huang, and H.-L. Peng, "CRP-Cyclic AMP Regulates the Expression of Type 3 Fimbriae via Cyclic di-GMP in Klebsiella pneumoniae," *PLoS One*, vol. 11, no. 9, pp. 1–19, 2016, doi: 10.1371/journal.pone.0162884.

[388] Q. Ou *et al.*, "Involvement of cAMP receptor protein in biofilm formation , fimbria production, capsular polysaccharide biosynthesis and lethality in mouse of Klebsiella pneumoniae serotype K1 causing pyogenic liver abscess," *J. Med. Microbiol.*, vol. 66, 2017, doi: 10.1099/jmm.0.000391.

[389] N. S. D. Panjaitan, Y.-T. Horng, S. Cheng, W. Chung, and P.-C. Soo, "EtcABC , a Putative EII Complex , Regulates Type 3 Fimbriae via CRP-cAMP Signaling in Klebsiella pneumoniae," *Front. Microbiol.*, vol. 10, 2019, doi: 10.3389/fmicb.2019.01558.

[390] L. M. Meng, M. Kllstrup, and P. Nygaard, "Autoregulation of PurR repressor synthesis and involvement," *Eur. J. Biochem.*, vol. 187, pp. 373–379, 1990.

[391] S. P. Cohen, L. M. Mcmurry, D. C. Hooper, J. S. Wolfson, and S. B. Levy, "Cross-Resistance to Fluoroquinolones in Multiple- Antibiotic-Resistant (Mar) Escherichia coli Selected by Tetracycline or Chloramphenicol: Decreased Drug Accumulation Associated with Membrane Changes in Addition to OmpF Reduction," *Antimicrob. Agents Chemother.*, vol. 33, no. 8, pp. 1318–1325, 1989.

[392] H. Okusu, D. Ma, and H. Nikaido, "AcrAB Efflux Pump Plays a Major Role in the Antibiotic Resistance Phenotype of Escherichia coli Multiple- Antibiotic-Resistance (Mar) Mutants," *J. Bacteriol.*, vol. 178, no. 1, pp. 306–308, 1996.

[393] R. Aono, "Improvement of organic solvent tolerance level of Escherichia coli by overexpression of stress-responsive genes," *Extremophiles*, vol. 2, pp. 239–248, 1998.

[394] R. R. Ariza, S. P. Cohen, N. Bachhawat, S. B. Levy, and B. Demple, "Repressor Mutations in the marRAB Operon That Activate Oxidative Stress Genes and Multiple Antibiotic Resistance in Escherichia coli," *J. Bacteriol.*, vol. 176, no. 1, pp. 143–148, 1994.

[395] L. M. Mcmurry, M. Oethinger, and S. B. Levy, "Overexpression of marA, sod, or acrAB produces resistance to triclosan in laboratory and clinical strains of Escherichia coli," vol. 166, pp. 305–309, 1998.

[396] L. U. Magnusson, A. Farewell, and T. Nystro, "ppGpp: a global regulator in Escherichia coli," *Trends Microbiol.*, vol. 13, no. 5, pp. 236–242, 2005, doi: 10.1016/j.tim.2005.03.008.

[397] W. Gao *et al.*, "Two Novel Point Mutations in Clinical Staphylococcus aureus Reduce Linezolid Susceptibility and Switch on the Stringent Response to Promote Persistent Infection," *PLOS Pathog.*, vol. 6, no. 6, 2010, doi: 10.1371/journal.ppat.1000944.

[398] E. S. Honsa *et al.*, "RelA Mutant Enterococcus faecium with Multiantibiotic Tolerance Arising in an Immunocompromised Host," *MBio*, vol. 8, no. 1, 2017, doi: 10.1128/mBio.02124-16.Editor.

[399] C. Rensing, B. Fan, R. Sharma, B. Mitra, and B. P. Rosen, "CopA: An Escherichia coli Cu(I)-translocating P-type ATPase," *PNAS*, vol. 97, no. 2, pp. 652–656, 2000, doi: 10.1073/pnas.97.2.652.

[400] F. A. Martin, D. M. Posadas, M. C. Carrica, S. L. Cravero, D. O. Callaghan, and A. Zorreguieta, "Interplay between Two RND Systems Mediating Antimicrobial Resistance in Brucella suis," *J. Bacteriol.*, vol. 191, no. 8, pp. 2530–2540, 2009, doi: 10.1128/JB.01198-08.

[401] J. D. Helmann, Y. Wang, I. Mahler, and C. T. Walsh, "Homologous Metalloregulatory Proteins from Both Gram-Positive and Gram-Negative Bacteria Control Transcription of Mercury Resistance Operons," *J. Bacteriol.*, vol. 171, no. 1, pp. 222–229, 1989.

[402] E. S. Boyd and T. Barkay, "The mercury resistance operon: from an origin in a geothermal environment to an efficient detoxification machine," *Front. Microbiol.*, vol. 3, 2012, doi: 10.3389/fmicb.2012.00349.

[403] S. F. Altschul *et al.*, "Gapped BLAST and PSI-BLAST : a new generation of protein database search programs," *Nucleic Acids Res.*, vol. 25, no. 17, pp. 3389–3402, 1997.

[404] S. F. Altschul, J. C. Wootton, E. M. Gertz, R. Agarwala, A. Morgulis, and A. A. Scha, "Protein database searches using compositionally adjusted substitution matrices," *FEBS J.*, vol. 272, pp. 5101–5109, 2005, doi: 10.1111/j.1742-4658.2005.04945.x.

[405] M. Ashenafi, T. Ammosova, S. Nekhai, and W. M. Byrnes, "Purification and

Characterization of Aminoglycoside Phosphotransferase APH(6)-Id, a Streptomycin Inactivating Enzyme," *Mol. Cell. Biochem.*, vol. 387, pp. 207–216, 2014, doi: 10.1007/s11010-013-1886-1.Purification.

[406] J. Itou, Y. Eguchi, and R. Utsumi, "Molecular Mechanism of Transcriptional Cascade Initiated by the EvgS/EvgA System in Escherichia coli K-12," *Biosci. Biotechnol. Biochem.*, vol. 73, no. 4, pp. 870–878, 2009, doi: 10.1271/bbb.80795.

[407] H. S. Lee *et al.*, "Structural and Physiological Exploration of Salmonella Typhi YfdX Uncovers Its Dual Function in Bacterial Antibiotic Stress and Virulence," *Front. Microbiol.*, vol. 9, 2019, doi: 10.3389/fmicb.2018.03329.

[408] C. Liu *et al.*, "RcsB regulation of the YfdX-mediated acid stress response in Klebsiella pneumoniae," *PLoS One*, 2019.

[409] M. R. Fernando, H. Nanri, S. Yoshitake, K. Nagata-kuno, and S. Minakami, "Thioredoxin regenerates proteins inactivated by oxidative stress in endothelial cells," *Eur. J. Biochem.*, vol. 209, pp. 917–922, 1992.

[410] Y. Meyer, B. B. Buchanan, F. Vignols, and J. Reichheld, "Thioredoxins and Glutaredoxins: Unifying Elements in Redox Biology," *Annu. Rev.*, vol. 43, pp. 335–367, 2009, doi: 10.1146/annurev-genet-102108-134201.

[411] A. Krisko, T. Copic, T. Gabaldón, B. Lehner, and F. Supek, "Inferring gene function from evolutionary change in signatures of translation efficiency," *Genome Biol.*, vol. 15, 2014.

[412] G. I. Morozov *et al.*, "Flavin Reductase Contributes to Pneumococcal Virulence by Protecting from Oxidative Stress and Mediating Adhesion and Elicits Protection Against Pneumococcal Challenge," *Sci. Rep.*, vol. 8, no. 314, 2018, doi: 10.1038/s41598-017-18645-8.

[413] R. E. Williams, D. A. Rathbone, N. S. Scrutton, and N. C. Bruce, "Biotransformation of Explosives by the Old Yellow Enzyme Family of Flavoproteins," *Appl. Environ. Microbiol.*, vol. 70, no. 6, pp. 3566–3574, 2004, doi: 10.1128/AEM.70.6.3566.

[414] M. M. González-pérez, P. Van Dillewijn, R. Wittich, and J. L. Ramos, "Escherichia coli has multiple enzymes that attack TNT and release nitrogen for growth," *Environ. Microbiol.*, vol. 9, no. 6, pp. 1535–1540, 2007, doi: 10.1111/j.1462-2920.2007.01272.x.

[415] C. Lee, J. Shin, and C. Park, "Novel regulatory system nemRA–gloA for electrophile reduction in Escherichia coli K-12," *Mol. Microbiol.*, vol. 88, no. 2, pp. 395–412, 2013, doi: 10.1111/mmi.12192.

[416] N. Baranova and H. Nikaido, "The BaeSR Two-Component Regulatory System Activates Transcription of the yegMNOB (mdtABCD) Transporter Gene Cluster in Escherichia coli and Increases Its Resistance to Novobiocin and Deoxycholate," *J. Bacteriol.*, vol. 184, no. 15, pp. 4168–4176, 2002, doi: 10.1128/JB.184.15.4168.

[417] N. Paracini, E. Schneck, A. Imberty, and S. Micciulla, "Lipopolysaccharides at Solid and Liquid Interfaces : Models for Biophysical Studies of the Gram-negative Bacterial Outer Membrane," *Adv. Colloid Interface Sci.*, vol. 301, 2022, doi: 10.1016/j.cis.2022.102603.

[418] R. Albrecht and K. Zeth, "Structural Basis of Outer Membrane Protein Biogenesis in Bacteria," *J. Biol. Chem.*, vol. 286, no. 31, pp. 27792–27803, 2011, doi: 10.1074/jbc.M111.238931.

[419] B. A. Sampson, R. Misra, and S. A. Benson, "Identification and Characterization of a New Gene of Escherichia coli K-12 Involved in Outer Membrane Permeability," *Genetics*, vol. 122, no. 3, pp. 491–501, 1989.

[420] B. Kneidinger *et al.*, "Biosynthesis Pathway of ADP-L-glycero-β-D-manno-Heptose in Escherichia coli," *J. Bacteriol.*, vol. 184, no. 2, pp. 363–369, 2002, doi: 10.1128/JB.184.2.363.

[421] S. M. Moskowitz, R. K. Ernst, and S. I. Miller, "PmrAB, a Two-Component Regulatory System of Pseudomonas aeruginosa That Modulates Resistance to Cationic Antimicrobial Peptides and Addition of Aminoarabinose to Lipid A," *J. Bacteriol.*, vol. 186, no. 2, pp. 575–579, 2004, doi: 10.1128/JB.186.2.575.

[422] S. M. Moskowitz *et al.*, "PmrB Mutations Promote Polymyxin Resistance of Pseudomonas aeruginosa Isolated from Colistin-Treated," *Antimicrob. Agents Chemother.*, vol. 56, no. 2, pp. 1019–1030, 2011, doi: 10.1128/AAC.05829-11.

[423] A. Yan, Z. Guan, and C. R. H. Raetz, "An Undecaprenyl Phosphate-Aminoarabinose Flippase Required for Polymyxin Resistance in Escherichia coli * □," *J. Biol. Chem.*, vol. 282, no. 49, pp. 36077–36089, 2007, doi: 10.1074/jbc.M706172200.

[424] K. Linder and J. D. Oliver, "Membrane Fatty Acid and Virulence Changes in the Viable but Nonculturable State of Vibrio vulnificus," *Appl. Environ. Microbiol.*, vol. 55, no. 11, pp. 2837–2842, 1989.

[425] M. Shleeva, G. V Mukamolova, M. Young, H. D. Williams, and A. S. Kaprelyants, "Formation of 'non-culturable' cells of Mycobacterium smegmatis in stationary phase in response to growth under suboptimal conditions and their Rpf-mediated resuscitation," *Microbiology*, vol. 150, no. 6, pp. 1687–1697, 2004, doi: 10.1099/mic.0.26893-0.

[426] R. R. Colwell, "Viable but nonculturable bacteria: A survival strategy," *J. Infect. Chemother.*, vol. 6, pp. 121–125, 2000, doi: 10.1007/PL00012151.

[427] J. J. Byrd, H. Xu, and R. R. Colwell, "Viable but Nonculturable Bacteria in Drinking Water," *Appl. Environ. Microbiol.*, vol. 57, no. 3, pp. 875–878, 1991.

[428] R. S. Flannagan and D. E. Heinrichs, "A Fluorescence Based-Proliferation Assay for the Identification of Replicating Bacteria Within Host Cells," *Front. Microbiol.*, vol. 9, 2018, doi: 10.3389/fmicb.2018.03084.

[429] G. N. Caron and R. A. Badley, "Viability assessment of bacteria in mixed populations using flow cytometry," *J. Microsc.*, vol. 179, pp. 55–66, 1995.

[430] J. E. Ueckert, G. N. von Caron, A. P. Bos, and P. F. ter Steeg, "Flow cytometric analysis of Lactobacillus plantarum to monitor lag times, cell division and injury," *Lett. Appl. Microbiol.*, vol. 15, pp. 295–299, 1997.

[431] J. Roostalu, A. Jõers, H. Luidalepp, N. Kaldalu, and T. Tenson, "Cell division in Escherichia coli cultures monitored at single cell resolution," *BMC Microbiol.*, vol. 8, 2008, doi: 10.1186/1471-2180-8-68.

[432] S. G. Mohiuddin, P. Kavousi, and M. A. Orman, "Flow-cytometry analysis reveals persister resuscitation characteristics," *BMC Microbiol.*, vol. 20, 2020, doi: 10.1186/s12866-020-01888-3.

[433] F. H.-S. Wong *et al.*, "Determining the Development of Persisters in Extensively Drug-Resistant Acinetobacter baumannii upon Exposure to Polymyxin B-based Antibiotic

Combinations Using Flow Cytometry," *Antimicrob. Agents Chemother.*, vol. 64, no. 3, 2020.

[434] J. James, B. Yarnall, A. Koranteng, J. Gibson, T. Rahman, and D. A. Doyle, "Protein over-expression in Escherichia coli triggers adaptation analogous to antimicrobial resistance," *Microb. Cell Fact.*, vol. 20, no. 13, 2021, doi: 10.1186/s12934-020-01462-6.

[435] K. Yoshioka *et al.*, "A novel fluorescent derivative of glucose applicable to the assessment of glucose uptake activity of Escherichia coli," *Biochim. Biophys. Acta*, vol. 1289, pp. 5–9, 1996, doi: 10.1016/0304-4165(95)00153-0.

[436] K. Yoshioka *et al.*, "Intracellular Fate of 2-NBDG, a Fluorescent Probe for Glucose Uptake Activity, in Escherichia coli Cells," *Biosci. Biotechnol. Biochem.*, vol. 60, no. 11, pp. 1899–1901, 1996.

[437] D. Hoefel, W. L. Grooby, P. T. Monis, S. Andrews, and C. P. Saint, "A comparative study of carboxyfluorescein diacetate and carboxyfluorescein diacetate succinimidyl ester as indicators of bacterial activity," *J. Microbiol. Methods*, vol. 52, pp. 379–388, 2003.

[438] S. M. Stocks, "Mechanism and Use of the Commercially Available Viability Stain, BacLight," *Cytom. Part A*, vol. 61A, no. 2, pp. 189–195, 2004, doi: 10.1002/cyto.a.20069.

[439] J. Robertson, C. McGoverin, F. Vanholsbeeck, and S. Swift, "Optimisation of the Protocol for the LIVE/DEAD BacLight Bacterial Viability Kit for Rapid Determination of Bacterial Load," *Front. Microbiol.*, vol. 10, 2019, doi: 10.3389/fmicb.2019.00801.

[440] P. Stiefel, S. Schmidt-emrich, K. Maniura-weber, and Q. Ren, "Critical aspects of using bacterial cell viability assays with the fluorophores SYTO9 and propidium iodide," pp. 1–9, 2015, doi: 10.1186/s12866-015-0376-x.

[441] J. D. Oliver, F. Hite, D. McDougald, N. L. Andon, and L. M. Simpson, "Entry into, and resuscitation from, the viable but nonculturable state by Vibrio vulnificus in an estuarine environment," *Appl. Environ. Microbiol.*, vol. 61, no. 7, pp. 2624–2630, 1995, doi: 10.1128/aem.61.7.2624-2630.1995.

[442] F. D. A. Gonçalves and C. C. C. R. de Carvalho, "Phenotypic modifications in Staphylococcus aureus cells exposed to high concentrations of vancomycin and teicoplanin," *Front. Microbiol.*, vol. 7, 2016, doi: 10.3389/fmicb.2016.00013.

[443] T. Brauge, C. Faille, G. Leleu, C. Denis, A. Hanin, and G. Midelet, "Treatment with disinfectants may induce an increase in viable but non culturable populations of Listeria monocytogenes in biofilms formed in smoked salmon processing environments," *J. Food Microbiol.*, vol. 92, 2020, doi: 10.1016/j.fm.2020.103548.

[444] S. Speck *et al.*, "Borderline resistance to oxacillin in Staphylococcus aureus after treatment with sub-lethal sodium hypochlorite concentrations," *Heliyon*, vol. 6, 2020, doi: 10.1016/j.heliyon.2020.e04070.

[445] C. Stein *et al.*, "Three Dimensional Checkerboard Synergy Analysis of Colistin, Meropenem, Tigecycline against Multidrug-Resistant Clinical Klebsiella pneumonia Isolates," *PLoS One*, vol. 10, no. 6, 2015, doi: 10.1371/journal.pone.0126479.